Università degli Studi di Roma “La Sapienza”

Facoltà di Ingegneria

Dipartimento di Ingegneria Strutturale e Geotecnica

Dottorato di ricerca – XXI Ciclo

A probabilistic approach to Performance-Based Wind Engineering (PBWE)

Candidate: Francesco Petrini

Advisor: Prof. Franco Bontempi

Co-Advisor: Prof. Giuliano Augusti

Rome, March 2009

Dissertazione per il conseguimento del titolo di

Dottore di ricerca in Ingegneria delle strutture

Acknowledgments

First and foremost, I would like to thank Professor Franco Bontempi, my thesis advisor, for his support during the last four and a half years of our collaboration. He constantly shows me the way to understand the teaching profession and to improve my engineering profile.
I would also like to thank Professors Giuliano Augusti, my thesis co-advisor, and Professor Marcello Ciampoli for constantly providing their enthusiastic support and their scientific knowledge.
The suggestions by Professors Paolo Emilio Pinto and Paolo Franchin and by Engineers Enrico Sibilio, Flavio Paduano and Eva Luongo are gratefully acknowledged.
I would to thank my colleagues and friends: Stefania Arangio, Chiara Crosti, Luisa Giuliani, Fabio Giuliano, Konstantinos Gkoumas, Sauro Manenti and Luca Sgambi, who tolerated and helped me during these years.

INDEX

PART III: APPLICATIONS

INTRODUCTION

A great research effort has been spent in the last decades in studying the risks of engineered facilities and infrastructures due to natural and/or man-made phenomena and the way to reduce them. Considering risk requires to design under uncertainties, taking into account several hazards: wind storms, snowfalls, rainfalls, floods, landslides, earthquakes and - recently - terrorist attacks. All these events may occur frequently at their lower intensities and, while causing no apparent structural damage, result nevertheless in a degradation of the life time performance of the concerned facility.

These considerations have brought a substantial change in the engineers' vision of the design objectives: rather than ensuring the survival under given actions at a minimum cost in a deterministic context, the more recent design approaches aim at minimizing the total probabilistically defined "cost" throughout the facility lifetime (or, even better, at maximizing its "utility").

The international Codes of Practice, in particular Structural Design Codes, are being transformed in this direction: "old" Codes prescribed quantitative rules to be satisfied by the design, while "new" Codes state the performance(s) required from the structure and provide criteria and methods for verifying their achievement, and possibly "optimizing" the design.

This approach is in generally known as "Performance-Based Design (PBD)": many of the most advanced current researches in civil engineering are motivated by possible developments and extensions of PBD.

Structural Eurocodes (the corpus of Codes that is progressively being implemented throughout Europe) follow the performance approach. Indeed, the opening statement of EN 1990 "Basis for Structural Design", basic document for all Structural Eurocodes, defines the objectives to be achieved: "A structure shall be designed and executed in such a way that it will, during its intended life, with appropriate degrees of reliability and in an economical way: (i) sustain all actions and influences likely to occur during execution and use, and (ii) remain fit for the use for which it is required". In other words, EN 1990 correctly recognizes that the achievement of the set performance objectives cannot be guaranteed in deterministic terms but only in a probabilistic context ("with appropriate degrees of reliability"); recognizes, moreover, that these objectives are conditioned by economical restraints ("in a economical way").

PBD has been so far developed to be applied in Seismic Engineering [1-3]: however, extensions to other engineering branches already exist. A significant example is Performance-Based Blast Engineering that has received a great deal of attention in the USA after the recent terrorist attacks: indeed, property owners and insurance companies have begun to consider an increased asset a design that takes the consequences of possible blasts into account. Another field is Fire Engineering were the performances are strictly related with the maintaining of the structural stability under fire action. Another sector of great potential interest for PBD procedures is Wind Engineering [4]: indeed, the development of Performance-based Wind Engineering (PBWE) [5] is now an important objective of the wind engineering scientific community both for ordinary [6] and complex structures [7].
The main objective of a procedure for the PBWE is the accomplishment, in probabilistic terms, of the performances specific to the examined construction (no collapse, occupant safety, accessibility, full functionality, limited displacements or accelerations, etc.) for different “intensities” of the wind actions.

The objective of the present work is to give a contribution to the formulation and implementation of a procedure for the management of the Aeolian risk of the structures within the framework of Performance-Based Wind Engineering (PBWE). The whole process for risk management covers two aspects: (a) risk assessment and (b) decision analysis. In particular the present work will be focused on the step (a).
In general, a procedure of Aeolian risk assessment consists of intermediate steps aimed at:

1. defining the Aeolian hazard at the site, in terms of wind intensity and/or selected parameters of the wind speed field;
2. analyzing the structural response, mainly in the context of stochastic dynamics;
3. with a distinction between performances connected with safety and functionality or comfort, defining and evaluating the indicators of the structural damage (intended as the degradation of the relevant performance) caused by wind actions;
4. defining the decisional variables that are appropriate to quantify the performances required for the structure, in terms of consequences of damage (restoration costs, costs due to loss or deterioration of service, personal damages, alterations of users comfort, etc.);
5. evaluating the structural risk by the probabilistic characterization of the decision variables;

From an analytical and computational point of view, a variety of engineering techniques have to be implemented in performing the listed steps:

- in order to perform the step 1, a proper probabilistic model of the wind field is needed, this model has to be able in evaluating the extreme values for the wind intensity, represented as a stochastic process ([8]);
- in the step 2, the use of proper stochastic dynamic systems analysis concepts is needed, this can be done by using of analytical ([9]) or simulation techniques ([10]);
- finally, the step 5 implies the use of the reliability analysis tools ([11], [12]).
- obviously the wind effects evaluation implies the use of non-trivial resolution techniques in order to model fluid-structure interaction phenomena ([13]).

A typical example of probabilistic PBD approach based on computations is the equation proposed by the Pacific Earthquake Research Centre (PEER) for PB seismic design ([3]), that begin with the definition of a vector of decisional variables (DV) and their probabilistic description, e.g. by means of the PDF of its annual exceedance rate p(DV).

In the present work, starting from the PEER approach a probabilistic procedure for the application of PBD concepts to wind engineering is proposed; the procedure is successively applied for the PBWD of a long span suspension bridge.

The outlining of a general PBWE procedure implies some main steps as reported in Fig. 1:

- first of all, the structural typologies of interest have to be identified, and for these structures, the performance objectives and the performance levels have to be expressed in a qualitatively way by using of non-technical requirements;
- second, the performances defined at the previous step, have to be expressed in a quantitative and probabilistic way, for example by using of Limit States;
- third, a procedure has to be established for the performance evaluation and optimization, in particular the task of performance evaluation is tackled here. This will be done with referring to the approaches already existing for seismic engineering, and in particular with specific reference to the PEER approach. The aim is to specialze the approach for wind engineering problems.

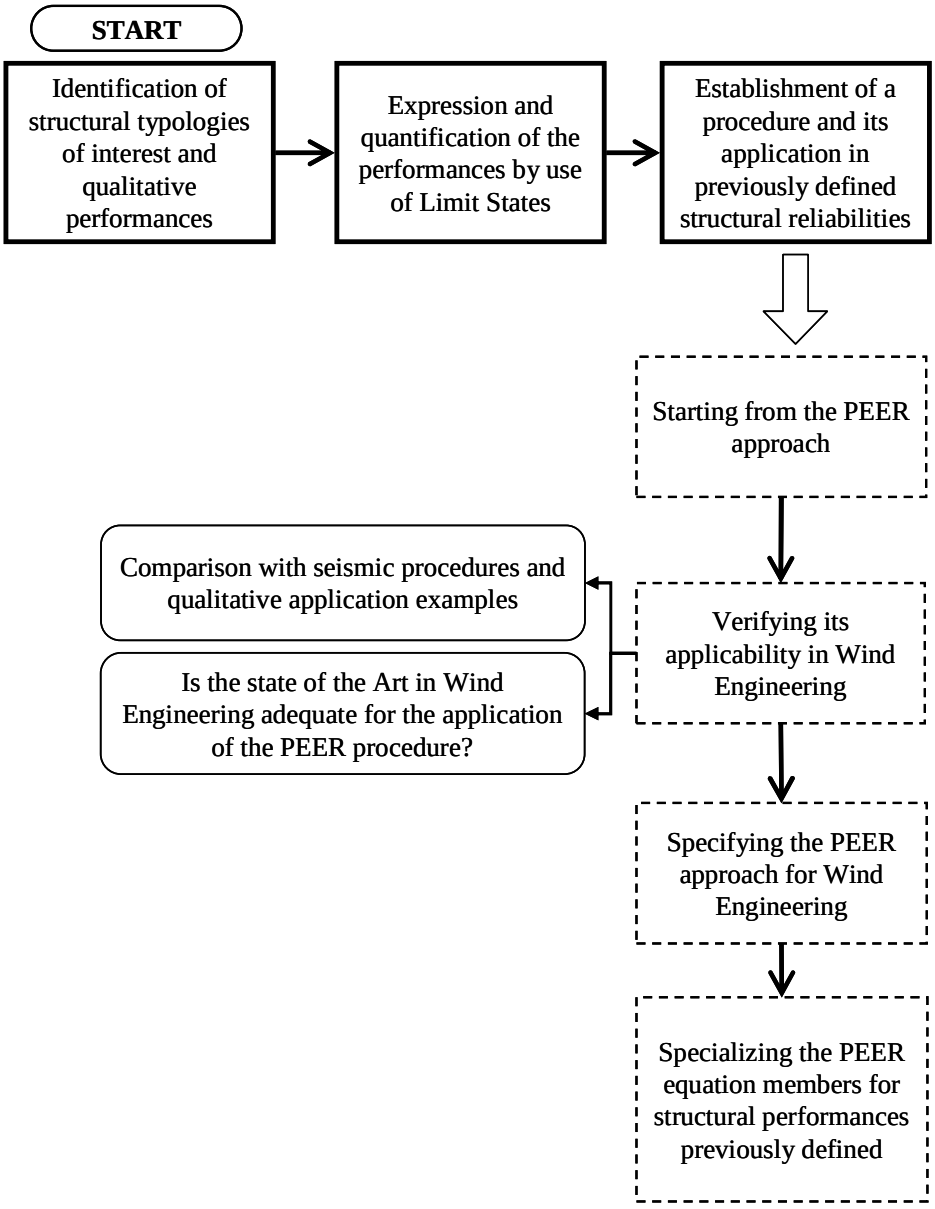

Fig. 1. Working plane.

Keywords: wind effects on structures, performance-based design, aeolian risk analysis, structural reliability, stochastic dynamics, probabilistic analysis.

Thesis outline.

The thesis is composed from three main parts:

- Part I (chapters 1 and 2): Basic concepts. This first part is dedicated to the explanation of the fundamental concepts related to the two engineering disciplines from the meeting of which the PBWE born; these are: the Wind Engineering (the subject of the chapter 1) and the PBE (the subject of the chapter 2).

- Part II (chapters 3 and 4): PBWE formulation. This second part is dedicated to the explanation of the proposed procedure, starting from the state of art in the PBWE, the PBWE procedure is conceptually and analytically formulated (chapter 3) and finally, the adopted implementation procedures are presented (chapter 4.
- Part III (chapter 5): PBWE application. In the last part of the thesis, the proposed PBWE procedure is applied to a long span suspension bridge and for an offshore wind turbine, some proposal for future developments are given.

Essential references list.

[1] Jalayer, F., Franchin, P. and Pinto, P.E. (2007). "A scalar damage measure for seismic reliability analysis of RC frames", Earthquake Engng. and Struct. Dyn., 36: 2059-2079.

[2] Ching, J., Porter, A.K. and Beck, J., (2004). Uncertainty propagation and feature selection for loss estimation in performance-based earthquake engineering, Report EERL 2004-02, Pasadena, California, United States. Available on line at http://peer.berkeley.edu/publications/peer_reports.html.

[3] Mitrani-Reiser, J. (2007). An ounce of prevention: probabilistic loss estimation for performance - based earthquake engineering, Report EERL 2007-01, Pasadena, California, United States. Available on line at http://peer.berkeley.edu/publications/peer_reports.html.

[4] Augusti, G. Borri, C. and Neumann, H.J. (2001). "Is Aeolian risk as significant as other environmental risks?", Reliability Engineering and System safety, Vol. 74, pp. 227-237.

[5] Augusti, G., Ciampoli, M., (2008), "Performance-Based Design in risk assessment and reduction", Probabilistic Engineering Mechanics, 23, 496-508.

[6] Ellingwood, B.R. Rosowsky, D.V., Li, Y. and Kim, J. H. (2004), "Fragility Assessment of Light-Frame Wood Construction Subjected to Wind and Earthquake Hazards", Journal of Structural Engineering, 130(12), 1921-1930.

[7] Bontempi, F. (2006), "Basis of Design and expected Performances for the Messina Strait Bridge". Proc. of the International Conference on Bridge Engineering – Challenges in the 21st Century, Hong Kong, 1-3 November, 2006.

.

[8] Carassale, L. and Solari, G. (2006). "Monte Carlo simulation of wind speed field on complex structures", J Wind Eng. Ind. Aerodyn. 94 (1) 323-339.

[9] Augusti, G. Baratta, A., Casciati, F., Probabilistic Methods in Structural Engineering, Chapman and Hall, 1984.

[10] Robert, C.P. and Casella, G., Monte Carlo statistical methods, Springer, New York, 2004.

[11] Ditevslen, O. and Madsen, H.O., Structural Reliability Methods, John Wiley & Sons Ltd, Chichester, 1996.

[12] Pinto, P.E., Giannini, R. and Franchin, P., Seismic reliability analysis methods, IUSS Press, Pavia, Italy, 2004.

[13] Bontempi, F., Malerba, P. and Giudici, M. (2000). "La Formulazione matriciale dei problemi aeroelastici di ponti sospesi e strallati" (in Italian), Studi e Ricerche-Politecnico di Milano 21.

PART I

BASIC CONCEPTS

Chapter 1

WIND ENGINEERING

In this chapter, some basic concepts in the wind engineering are reported. There is not intention to give an exhaustive literature review of the topic. The scope of this first part is to give some reminders concerning the concepts that will be assumed as known in the next sections.

1.1 Wind field

According to the definition given by Cermak in 1975, "Wind Engineering is best described as the rational treatment of interactions between wind in the atmospheric boundary layer and man and his works on the surface of earth".

1.1.1. Atmospheric circulation

Wind, or the motion of air with respect to the surface of the earth, is fundamentally caused by variable solar heating of the earth's atmosphere. It is initiated, in a more immediate sense, by differences of pressure between points of equal elevation. Such differences may be brought about by thermodynamic and mechanical phenomena that occur in the atmosphere non uniformly both in time and space. The energy required for the occurrence of these phenomena is provided by the sun in the form of radiated heat.

While the sun is the original source, the source of energy most directly influential upon the atmosphere is the surface of the earth. Indeed, the atmosphere is to a large extent transparent to the solar radiation incident over the earth, much in the same way as the glass roof of a greenhouse. That portion of the solar radiation that is not reflected or scattered back into space may therefore be assumed to be absorbed almost entirely by the earth. The earth, upon

being heated, will emit energy in the form of terrestrial radiation, the characteristic wave lengths of which are long (of the order of 10μ) compared to those of heat radiated by the sun. The atmosphere, which is largely transparent to solar but not to terrestrial radiation, absorbs the heat radiated by the earth and re-emits some of it toward the ground.

It will be recalled that the axis of rotation of the earth is inclined at approximately 66°30' to the plane of its orbit around the sun (plane of the ecliptic). Therefore, the average annual intensity of solar radiation and, consequently, the intensity of terrestrial radiation and the temperature of the atmosphere will be higher in the equatorial than in the polar regions.

Consequently, an atmospheric circulation would be developed that could be represented as in Fig, 1.1.

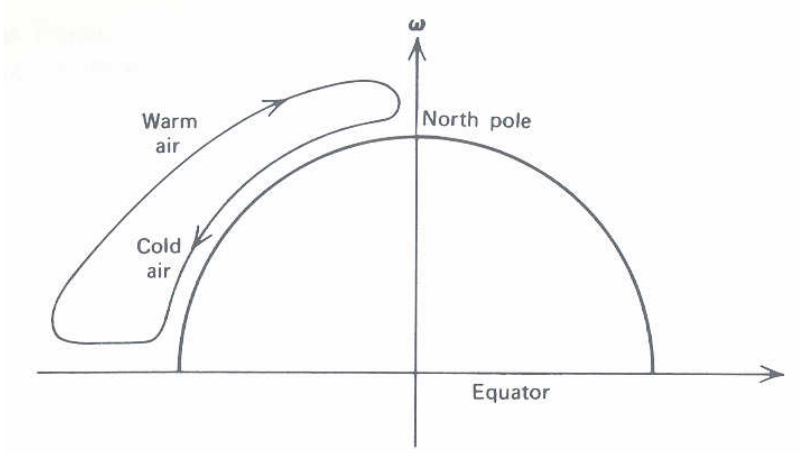

Fig. 1.1. Mono-cellular hemispheric circulation

In reality, the circulation of the atmosphere is vastly complicated by the factors neglected in the above model. In general the non-homogeneous distribution of the water masses generates two pressure macro bands: a sub-tropical (high pressure) band and a sub-polar (low pressure) one. This generates a tri-cellular hemispheric circulation (Fig. 1.2).

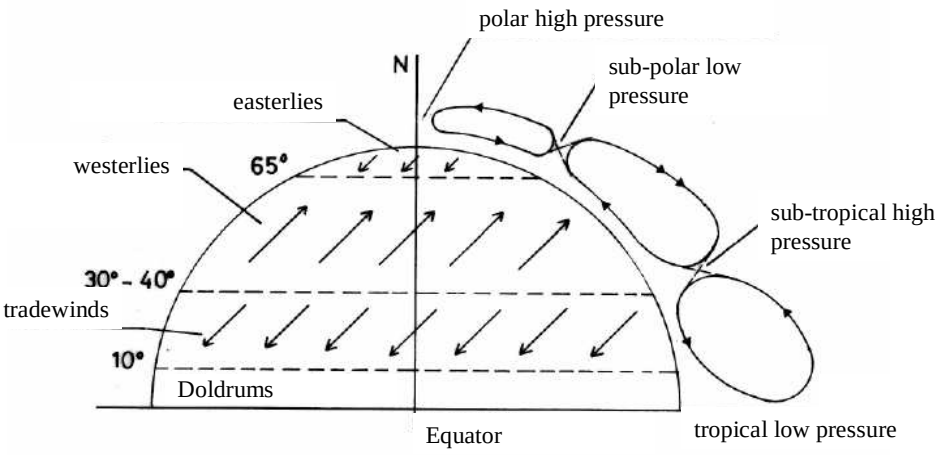

Fig. 1.2. Tri-cellular hemispheric circulation

1.1.2. Atmospheric boundary layer

As the earth's surface is approached, the frictional forces play an important role in the balance of forces on the moving air. The region of frictional influence is called the 'atmospheric boundary layer' and is similar in many respects to the turbulent boundary layer on a flat plate or airfoil at high wind speeds, for larger storms such as extra-tropical depressions, this zone extends up to 500 to 1000 m height. Figure 1.3 shows records of wind speeds recorded at three heights on a tall mast at Sale in southern Australia (as measured by sensitive cup anemometers, during a period of strong wind produced by gales from a synoptic depression) (Holmes, 2001), the records show the main characteristics of fully-developed 'boundary-1ayer' flow in the atmosphere:

• the increase of the average wind speed as the height increases

• the gusty or turbulent nature of the wind speed at all heights

• the broad range of frequencies in the gusts in the air flow

• there is some similarity in the patterns of gusts at all heights, especially for the more slowly changing gusts, or lower frequencies,

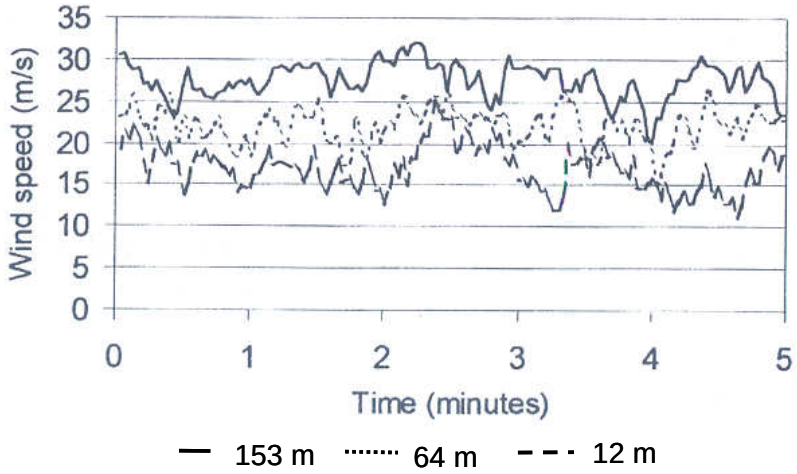

Fig. 1.3. Wind speed time histories.

The term 'boundary-layer' means the region of wind how affected by friction at the earth's surface, which can extend up to 1 km. The most used mathematical laws describing the variation of the mean wind speed inside the boundary layer are the so-called 'logarithmic-law' and 'power-law' described in the following.

Logarithmic-law. Consider the variation of the mean or time-averaged wind speed with height above the ground near the surface (say in the first 100-200 m - the height range of most structures). In strong wind conditions, the most accurate mathematical expression describing

the mean wind speed profile is the 'logarithmic law'. The logarithmic law was originally derived for the turbulent boundary layer on a flat plate by Prandtl; however it has been found to be valid in an unmodified form in strong wind conditions in the atmospheric boundary layer near the surface. It can be derived in a number of different ways. The following derivation is the simplest, and is a form of dimensional analysis. We postulate that the wind shear, i.e. the rate of change of mean wind speed *V* with height is a function of the following variables:

• the height above the ground, *z*

• the retarding force per unit area exerted by the ground surface on the flow known as the surface shear stress, τ_0

• the density of air, ρ.

Note that near the ground, the effect of the earth's rotation (Coriolis forces) is neglected. Also because of the turbulent flow, the effect of molecular viscosity can be neglected. Combining the wind shear with the above quantities, we can form a non-dimensional wind shear:

$$\frac{dV}{dz} \cdot z \cdot \sqrt{\frac{\rho}{\tau_0}} \tag{1.1}$$

$\sqrt{\tau_0 / \rho}$ has the dimensions of` velocity, and is known as the *friction velocity*, u_* (note that this is not a physical velocity). Then, since there are no other non-dimensional quantities involved

$$\frac{dV}{dz} \cdot \frac{z}{u_*} = \text{constant} = \frac{1}{k} \tag{1.2}$$

Integrating,

$$V(z) = \frac{u_*}{k} \cdot (\log_e z - \log_e z_0) = \frac{u_*}{k} \cdot \log_e \left(\frac{z}{z_0} \right) \tag{1.3}$$

where z_0 is a constant of integration, with the dimensions of length, known as the roughness lengths. Equation (1.3) is the usual form of the logarithmic law, k is known as *von Karman's constant*, and has been found experimentally to have a value of about 0.4. The roughness length z_0 is a measure of the roughness of the ground surface.

Another measure of the terrain roughness is the *surface drag coefficient K*

$$K = \frac{u_*}{V_{10}^2} \tag{1.4}$$

By combining eq.(1.2) and eq. (1.3) for *z*=10 m the relation between the roughness and the surface drag coefficient can be obtained

$$K = \left[\frac{k}{\log_e \left(\frac{10}{z_0} \right)} \right] \tag{1.5}$$

Power-law. The power law has no theoretical basis but is easily integrated over height, a convenient property when wishing to determine bending moments at the base of a tall structure, for example. To relate the mean wind speed at any height, z, with that at 10 m (V_{10}) (adjusted if necessary for rougher terrains, as described in the previous section), the power law can he written:

$$V(z) = V_{10} \cdot \left(\frac{z}{10} \right)^{\alpha} \tag{1.6}$$

The exponent, α, in equation (1.6) will change with the terrain roughness, and also with the height range, when matched to the logarithmic law, A relationship that can be used to relate the exponent to the roughness length, z_0, is as follows:

$$\alpha = \left(\frac{1}{\log_e (z_{ref} / z_0)} \right) \tag{1.7}$$

where z_{ref} is a reference height at which the two 'laws' are matched. z_{ref} may be taken as the average height in the range over which matching is required, or half the maximum height over which the matching is required. Figure 1.4 shows a matching of the two laws for a height range of 100 m, using equation (1.7), with z_{ref} taken as 50 m. It is clear the two relationships are extremely close, and that the power law is quite adequate for engineering purposes.

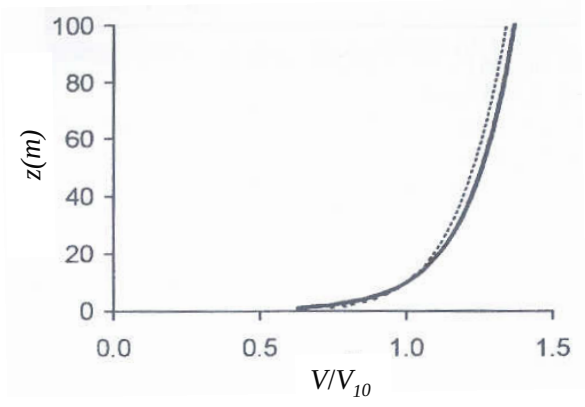

Fig. 1.4. Mean wind profile

1.1.3. Wind analytical representation

The wind flow moving inside the boundary layer crosses (in the ground surface proximity) both artificial and natural obstacles; this fact induces random fluctuations in the wind velocities.

Focusing on a long time period of observation, the power spectra of the wind speed $S_V(n)$ (where n is the frequency) is represented in Fig. 1.5; here two main harmonic contribution can be distinguish. The first one is associated with long period aeolian events (from about 1 hour to few months) and it is named *macro-meteorological peak*; this peak represent the recurrence of the aeolian storms. The second harmonic contribution is associated with short period aeolian events (from few seconds to about ten minutes) and is named *micro-meteorological peak*; this peak represent the turbulent fluctuation of the wind speed.

These considerations on the spectra $S_V(n)$ suggest the representation of the vectorial wind speed as the sum of a mean and turbulent part.

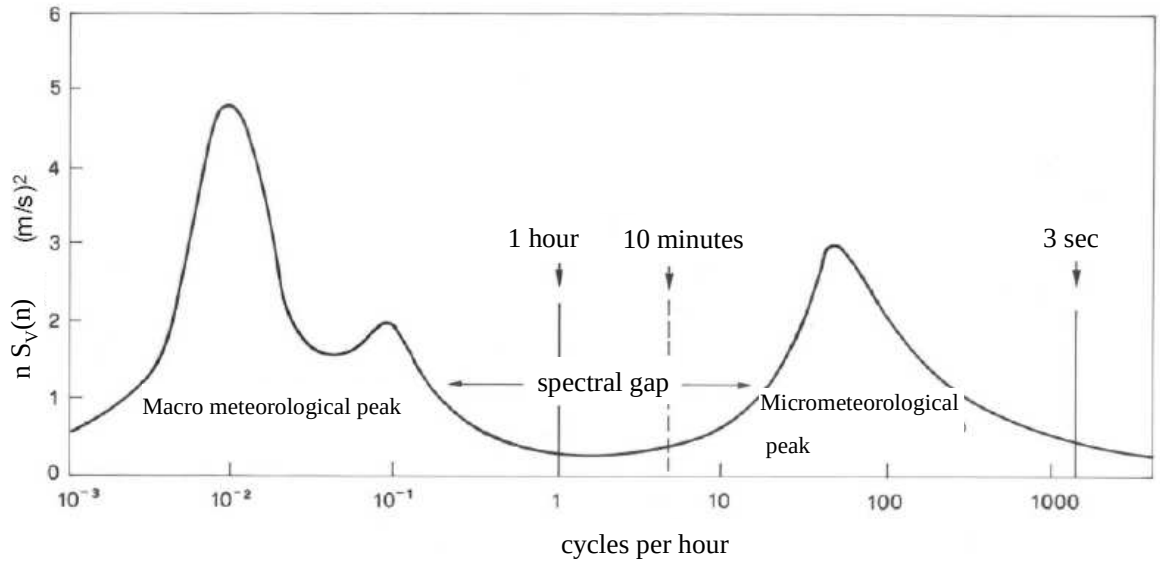

Fig. 1.5. Wind speed power spectra

A Cartesian three-dimensional coordinate system *(x,y,z)*, with origin at ground level and the z-axis oriented upward is adopted. Focusing on a short time period analysis the three components of the wind speed field $V_x(j)$, $V_y(j)$, $V_z(j)$ at each spatial point j (the variation with time is omitted for simplicity) can be expressed as the sum of a mean (time-invariant) value and a turbulent component $u(j)$, $v(j)$, $w(j)$ with mean value equal to zero.

Defining the *gradient height* z_g as the height above the ground delimiting the boundary layer, the generic wind speed profile is shown in Fig. 1.6

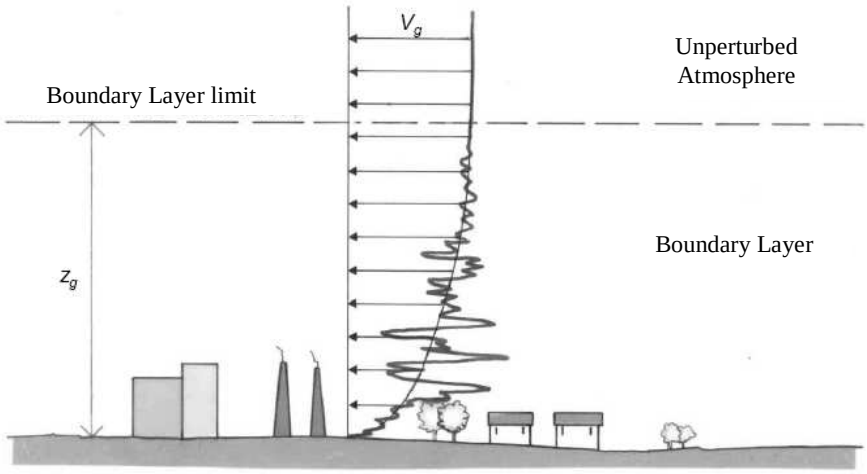

Fig. 1.6. Turbulent wind profile

Assuming that the mean value of the velocity is non zero only in y direction, the three components are given by:

$$V_x(j) = u(j); \quad V_y(j) = V_m(j) + v(j); \quad V_z(j) = w. \tag{1.8}$$

The mean velocity $V_m(j)$ can be determined by a database of values recorded at or near the site, and evaluated as the record average over a proper time interval (e.g. *10* minutes).

The variation of the mean velocity V_m with the height z over a horizontal surface of homogeneous roughness can be described, as usual, by the power law (equation (1.6)):

For long time period analyses V_{10} can be associated with a certain return period T_R by the expression:

$$V_{10,T_R}(z) = F_{V_{10},\max,1year}^{-1}\left(1 - \frac{1}{T_R}\right) \tag{1.9}$$

where $F_{10,max,1year}$ is the cumulated probability of the maximum annual ten minutes average velocity V_{10}, typically a Weibull distribution.

The turbulent components of the wind speed are modeled as zero-mean Gaussian ergodic independent processes; by a discretization of the spatial domain in N points representing the locations where the wind acts on the structure, adopting an Eulerian point of view, each Gaussian process is completely characterized by the power spectral density (PSD) matrix $[S]_i$, $(i = u, v, w)$. The diagonal terms $S_{ijij}(n, z)$ $(i = u, v, w$ and $j = 1,2,\ldots,N)$ of $[S]_i$ are given by the normalized half-side von Karman's power spectral density (Solari and Piccardo 2001):

$$\frac{nS_{ijij}(n,z)}{\sigma_i^2} = \frac{4n_i}{\left[1 + 70.8n_i^2(z)\right]^{5/6}} \tag{1.10}$$

where n is the current frequency (in *Hz*), z is the height (in m), σ_i^2 is the variance of the velocity fluctuations, given by (Solari and Piccardo 2001):

$$\sigma_i^2 = \left[6\text{-}1.1\arctan g\left(\log(z_0)+1.75\right)\right]u_*^2 \tag{1.11}$$

where u_* is the friction or shear velocity (in m/s), given by: $(0.006)^{1/2}\, V_m(z=10)$, $n_i(z)$ is a non-dimensional height dependent frequency given by:

$$n_i(z) = \frac{nL_i(z)}{V_m(z)} \tag{1.12}$$

The integral scale $L_i(z)$ of the turbulent component can be derived respectively *for i = u, v, w* according to the procedure given in ESDU (2001).

The out of diagonal terms $S_{ijik}(n, z)$ $(k = 1,2,\ldots,N)$ of $[S]_i$ are given by

$$S_{ijik}(n) = \sqrt{S_{ijij}(n)S_{ikik}(n)}\exp(-f_{jk}(n)) \tag{1.13}$$

In which

$$f_{jk}(n) = \frac{|n|\sqrt{C_z^2(z_j - z_k)^2}}{2\pi\left(V_m(z_j)+V_m(z_k)\right)} \tag{1.14}$$

where C_z represents the *decay coefficient*, which is inversely proportional to the spatial correlation of the process.

1.1.4. Mean wind probabilistic characterization

A statistical description of the wind speed field comprises three levels (Stømmer 2006): the long term variation of the mean wind speed (both in magnitude and direction), the short term single point time domain variation of the turbulence components, and finally, the short term spatial distribution of the turbulence components. A short indication on the last two have been presented in the previous section, in this section the long term variation of the mean wind speed is treated.

Mean velocity magnitude

Concerning the mean wind speed, as previously stated, the statistics are usually performed on the mean velocity at z=10m and averaged over a period of T=10 min.

Data from large population of annual observation may usually be fitted to a Weibull distribution, for which the cumulative and the density distribution functions are given by:

$$F_{V_{10}} = P(V_{10} \le V, \varphi) = 1 - \alpha(\varphi) \cdot \exp\left[-\left(\frac{V}{\beta(\varphi)} \right)^{\gamma(\varphi)} \right] \tag{1.15}$$

$$f_{V_{10}} = \frac{dF_{V_{10}}}{dV} = \frac{\alpha(\varphi) \cdot \gamma(\varphi)}{\beta(\varphi)} \cdot \left(\frac{V}{\beta(\varphi)} \right)^{\gamma(\varphi)-1} \exp\left[-\left(\frac{V}{\beta(\varphi)} \right)^{\gamma(\varphi)} \right] \tag{1.16}$$

Where φ is the main flow direction and α(φ) and β(φ) are parameters to be fitted to the relevant data.

The Weibull distribution is representative for observations which are derived from one year of measures. If one is interested in characterizing the mean wind speed during a period larger than one year, the best way to do this is the derivation of the annual maxima wind speed distribution. There are several methods to obtain this probabilistic distribution (Mann et al. 1998); here the so-called *periodical maximum method* is reported. Assuming that *n* records of the wind speed are available and that these observations are related with n periods of equal length (typically one year), the record of the maxima of each period (V_1^{max}, V_2^{max}, …., V_n^{max}) can be derived. It has been shown that these maxima have a probability distribution which is (asymptotically) a Gumbel type I distribution, for which the cumulative is a double exponential given from:

$$F_{V^{max}} = P(V^{max} \le V \mid \alpha, \beta) = exp\left(- exp\left[- \alpha \cdot (V - \beta) \right] \right) \tag{1.17}$$

where the parameters α and β can be evaluated as (Mann et al. 1998)

$$\alpha = \frac{ln\, 2}{2 \cdot b_1 - V^{max}_{mean}} \tag{1.18}$$

$$\beta = V^{max}_{mean} - \frac{\gamma}{\alpha} \tag{1.19}$$

in which V^{max}_{med} is the mean of the maximum values (V_1^{max}, V_2^{max}, …., V_n^{max}), γ is the Euler constant about equal to 0.577216 and

$$b_1 = \frac{1}{n} \sum_{i=1}^{n} \frac{i-1}{n-1} V_i^{max} \tag{1.20}$$

computed by sorting the maximum values (V_i^{max} with $i=1,\ldots,n$) in ascending order from the minimum (assigning $i=1$) to the maximum ($1=n$).

Mean velocity directionality

Wind effects on various structures and components depend not only on the magnitude of the wind speeds but on the associated wind directions as well. For this reason, knowledge of continuous joint probability distributions of extreme wind speeds and directions would be useful for design and code development purposes. However, so far no credible models for such distributions have been proposed in the literature.

In the absence of such models, wind effects and their probability distributions may be estimated in well behaved wind climates on the basis of information consisting of largest yearly wind speed data recorded for each octant over periods of 20 years, or longer.

There are important practical applications in which information is needed on the mono-variate probability distributions of the largest yearly wind speeds associated with each of the principal compass directions, and on the correlation coefficients for the largest yearly winds blowing from any two directions. In well-behaved climates the largest yearly wind speeds for any given direction are in most cases (though not always) adequately fitted by Type I distributions of the largest values. The correlation between wind speeds occurring in any two of the eight principal compass directions is in most cases weak. For example, the estimated correlation coefficients between wind speeds from directions i and j (i, j = l, 2, . . . , 8).

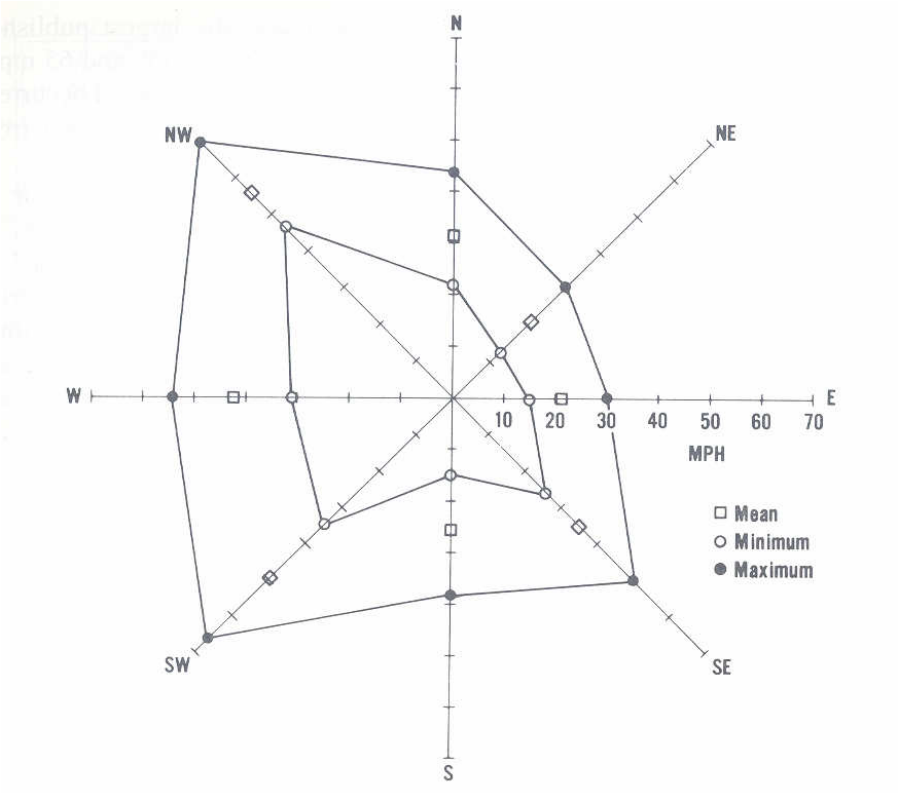

Fig. 1.7. Wind directional registrations

1.1.5. Wind interactions with other environmental agents

The wind in general can interact with the environment; because of this interaction the basic parameters of the analytical model adopted to describe the wind speed field can be changed in their values. This is the case for example of the wind acting on the sea

Over land the surface drag coefficient, *K* (Eq.1.5), is found to be nearly independent of mean wind speed. This is not the case over the ocean, where higher winds create higher waves, and hence higher surface drag coefficients. The relationship between *K* and V_m has been the subject of much study, and a large number of empirical relationships have been derived. In (Holmes 2001), a mean wind profile over the ocean is proposed, that implies that the roughness length, z_0, should be given by equation (1.21).

$$z_0 = \frac{a \cdot u_*^{\,2}}{g} \tag{1.21}$$

where g is the gravitational constant, and *a* is an empirical constant, equation (1.17), with the constant a lying between 0.01 and 0.02, is valid over a wide range of wind speeds. It is not valid at very low wind speeds, under aerodynamically smooth conditions, and also may not be valid at very high wind speeds, during which the air-sea surface experiences intensive wave breaking and spray.

Substituting for the surface drag coefficient, *K* from equation (1.5) into equation (1.21), equation (1.18) is obtained.

$$z_0 = \frac{a}{g}\left[\frac{k \cdot V_{10}}{\log_e(10/z_0)}\right] \tag{1.22}$$

The implicit nature of the relationship between z_0 (or K) and V_m, in equations (1.21) and (1.22) makes them difficult to apply, and several simpler forms have been suggested.

Garratt (1977) (Holmes, 2001) examined 21 large amount of experimental data and suggested a value for *a* of 0.0l44.

Furthermore the wind can changes the parameters used for the description of other environmental actions, this is also the case of the wind acting on the sea, that can generates an additional sea current ($Vcurr_{wind}$) which have to be taken into account in the offshore structures design. Following the IEC-61400-1 can be written

$$Vcurr_{wind} = 0.01 \cdot V_{1hour}(z = 10m) \tag{1.23}$$

where V_{1hour} is the mean wind speed averaged over a period of T=1 hour.

Finally, has been assessed that the wind and currents speeds are correlated in magnitudes and direction.

1.2 Aerodynamic

The Aerodynamic is the discipline that focuses on the effects of the relative motion between the fluids and solids. Its principal goals consist in assessing the fluid state variables in the solid proximity and in the evaluation of the mutual actions between the fluid and the solid.
By assuming that the generic structure subjected to wind actions experiments small displacements, the undeformed configuration can be assumed as the reference one; in this case the structural response (R) is not characterized from fluid-structure interaction effects and the mechanism of the structural response generation is represented from the chain shown in Fig. 1.8; here the aerodynamic forces are indicate by the symbol F_a.

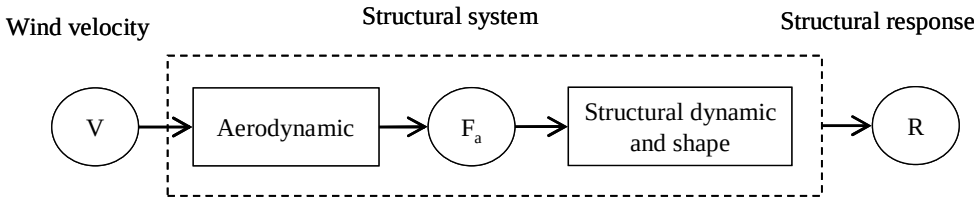

Fig. 1.8. Aerodynamic "chain".

1.6.1. Some basic definitions

In this section some basic definition concerning the fluid mechanics are reported. The section has to be intended as a very short reminder of the treated arguments and is not exhaustive of the focused matter.

Viscosity (Newtonian fluids). Consider a fluid between two parallel flat plates which are distant *h* each other as shown in Fig.1.8; experimental experiences shown that the fluid remains attached to the surfaces of both the upper and the bottom plates. If the upper plate moving in horizontal direction with a certain velocity *v*, and the lower one remain blocked, the velocity profile of the fluid particles is the one shown in Fig. 1.9.

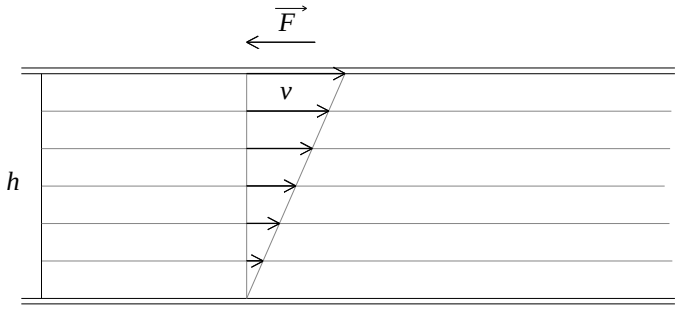

Fig.1.9. Viscous flow velocity profile

Because some fluid internal shear stresses are generated, a breaking force *F* acts on the moving plate; its magnitude is directly proportional to the contact surface *S* between the fluid and the plate following the relation:

$$F = \mu S \frac{v}{h} \tag{1.24}$$

in terms of tangential stresses:

$$\tau = \mu \frac{dv}{dh} \tag{1.25}$$

where μ is the *viscosity constant*. For an inviscid fluid results μ=0.

Flow curve: is a curve inside the fluid domain that, focusing on a cetrain instant t, is tangential to the flow velocity for each point.

Streamline. It is the path of a particle fluid.

The fluid flow is called *stationary* if the velocity components are time-independent.

The fluid flow is called *uniform* if the velocity components are the same in the whole domain.

Incompressible fluid. The compressibility β of a fluid is expressed by:

$$\beta = \frac{1}{\rho} \frac{d\rho}{dp} \tag{1.26}$$

And, for a moving fluid, it depends on the fluid velocity *V*. Defining the Mach number *M* as:

$$M = \frac{V}{V_{sound}} \tag{1.27}$$

A fluid is considered *incompressible* if during the motion results $M<0.3$.

Turbulence. A fluid flow is called turbulent if the streamline are not parallel (or similar) each other. In a turbulent flow, following the single particle motion (Lagrangian point of view), one can see the velocity changing both in magnitude and direction in a random way.

Reynolds number. Is defined as:

$$\mathrm{Re} = \frac{\rho V L}{\mu} \tag{1.28}$$

Where L represents a characteristic dimension of the physical problem under observation. Experimental observations show the existence of critic Reynolds number value Re_{crit} for which the flow is laminar for $\mathrm{Re}<\mathrm{Re}_{crit}$, and it becomes turbulent for $\mathrm{Re}>\mathrm{Re}_{crit}$. Re_{crit} is a characteristic of the specific physical problem.

Bernoulli equation. The region outside the boundary layer in the case of an airfoil, and the outer region of a bluff-body, can be approximated as regions of inviscid (zero viscosity) and irrotational (zero vorticity) flow. Here the pressure p, and the velocity V, in the case of incompressible fluid in stationary motion, are related by Bernoulli's equation

$$gz + \frac{p}{\rho} + \frac{V^2}{2} = \text{constant in time and along the trajectories} \tag{1.29}$$

Where ρ is the fluid mass density and g is the gravity acceleration.

1.2.1. Aerodynamic actions

Given a fluid flow with horizontal velocity V impacting on a rigid body, this generates an elementary aerodynamic force $\vec{f}$ acting on the body surface element dS. $\vec{f}$ has two vectorial components: the pressure $\vec{p}$ (orthogonal to dS) and the tangential stress $\vec{\tau}$ (parallel to dS). It results

$$\vec{f} = \vec{p} + \vec{\tau} \quad , \quad \left|\vec{f}\right| = \sqrt{\left(\left|\vec{p}\right|^2 + \left|\vec{\tau}\right|^2\right)} \tag{1.30}$$

the total aerodynamic force acting on the body is obtained by integration:

$$\vec{F} = \int_S \vec{f} dS \tag{1.31}$$

For a generic airfoil section having infinity length, if it is immersed in a fluid flow having velocity V_0 lying in the airfoil cross sectional plane, the aerodynamic force F lies in the same plane and is applied to a certain point called *centre of pressure*. The *centre of pressure* location depends on the flow attack angle α (Fig. 1.10).

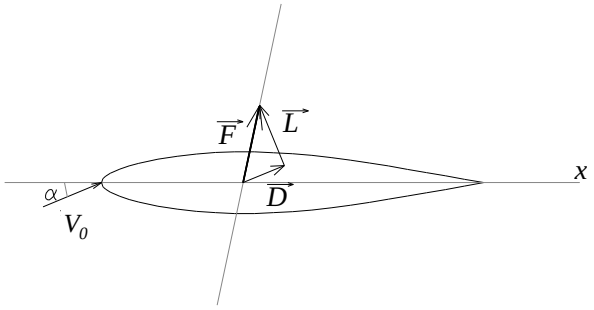

Fig 1.10. Aerodynamic actions

In engineering applications, it is usual to decompose the aerodynamic force in two components, the Drag (D) force, which is parallel to the mean flow velocity (V_0), and the Lift (L) force, which is orthogonal to the mean flow velocity. These forces generate a rotational moment M respect to each point which is non-coincident with the centre of pressure.

For viscous fluids, the presence of tangential stresses determines a non-zero drag force. The tangential stresses makes null the relative velocities of fluid particles attached to the body surface, these cause a slackening of the nearest flow layers; the flow velocity increases with the distance from the body surface once a certain distance *d* where the flow velocity is equal to the one of the impacting unperturbed flow. The physical region where this mechanism is developed is called *boundary layer*. The flow motion inside the boundary layer can be laminar or turbulent according to the *local Reynolds number* (Fig. 1.11).

Fig 1.11. Boundary layer: laminar (left) and turbulent (right).

A classical example is the flat plate, in which the characteristic dimension which appears in the (1.28) is the linear abscissa having its origin in the flow-body attack point and is directed through the flow direction, as shown in the Fig.1.12. The Reynolds number is given from:

$$\mathrm{Re} = \frac{\rho v L}{\mu} \tag{1.32}$$

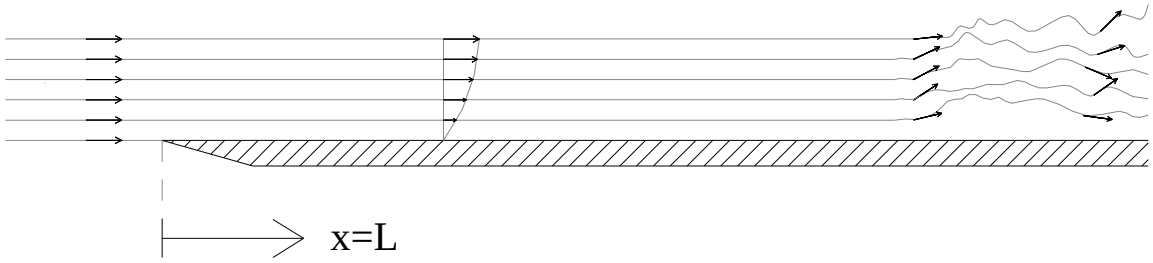

Fig.1.12. Laminar flow on a flat plate

Concerning the problem of the flat plate under an incident laminar flow, focusing the attention on a material flow portion which is located inside the boundary layer, starting from the attack point one can follow its motion (lagrangian point of view). It can be stated that the Re of the material flow portion increases in value (because L increases itself) since the Re attain a certain value named *critic Re number*, at this state the inertial forces overcome the viscous forces and the flow, which was laminar type, becomes turbulent. Due to the transition from laminar to turbulent flow, the boundary layer increases its thickness, this is principally due to the increasing of the viscous forces magnitude which is caused from the increasing of the mass transition from a substrate to another that is characteristic of a turbulent flow. Anyway a very thin *laminar sub-layer* is still present, and it is located at the base of the turbulent boundary layer, near the plate surface. The equations describing the flow motion inside the boundary layer, are generally really complex, and it is not the scope of the present work to discuss about them, anyway referring to the Fig. 1.13, the boundary layer thickness (δ) for the flat plate problem can be computed by the equation (1.33):

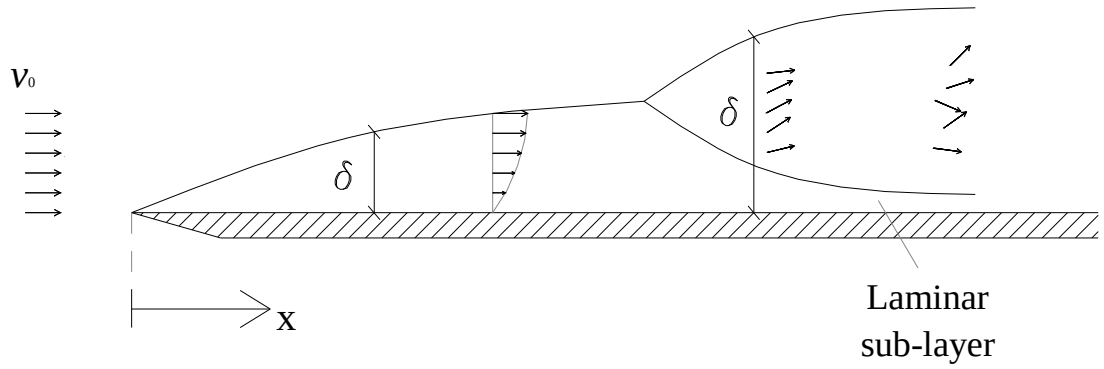

Fig.1.13: Boundary layer thickness.

$$\frac{\delta}{x} = C\sqrt{\frac{\mu x}{\rho V_0}} = C\frac{1}{\sqrt{\mathrm{Re}}} \qquad (1.33)$$

were *C* is a constant and the other symbols have the previously specified meaning.

Finally, concerning the practical resolution of the problems, the following important consideration can be stated: inside the boundary layer, due to the great differences between the various flow layers speed, non negligible viscous forces are generated, while outside the boundary layer, these differences are negligible and the flow can be approximately considered as laminar. Here, for example, the Bernoulli theorem (1.29) can be applied.

Consider now a cylinder body with circular base, having an infinite extension in the direction orthogonal to the paper, and consider an incident laminar viscous flow impacting on the cylinder with orthogonal speed V_0 as shown in the Fig. 1.14. The overpressure configurations $p-p_0$ (with p_0 equal to the hydrostatic flow pressure) is the one shown in the figure.

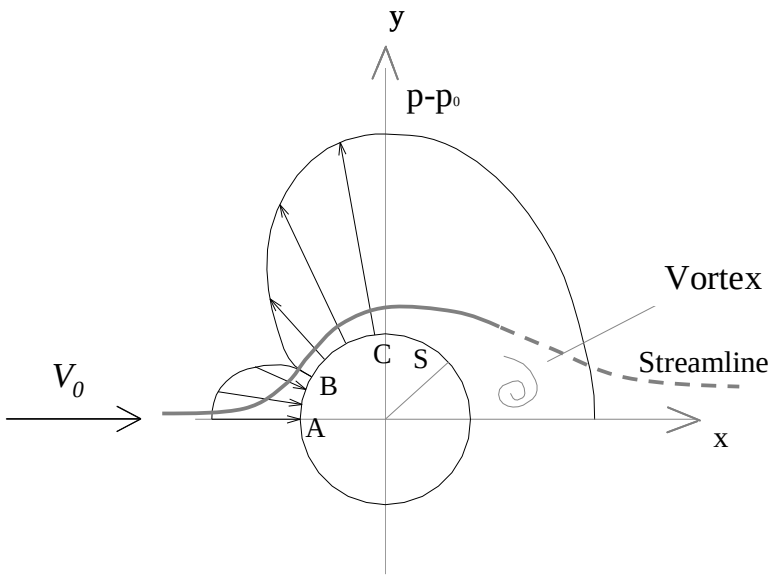

Fig.1.14. Pressures around a circular cylinder.

Referring to the Fig. 1.14, and proceeding from the point A (frontal stagnation point) following the flow on the upper part of the cylinder section it can be seen that: from A to B (inflection point of the streamlines) the overpressures are oriented toward the cylinder, in B the overpressures change their orientation and from B to C the overpressures are directed leaving from the cylinder, from C there is a recover of the pressures, which is not complete. Focusing on the particles speed, it can be seen that the flow particles located inside the boundary layer, due to the viscous forces, decrease their speed proceeding in their motion. Since the particles meet a pressures gradient which is opposite to the motion direction (from the C point), they may stop their motion and, successively, they can begins to move in opposite orientation with respect to the previous motion as shown in Fig. 1.15. This phenomenon is called *boundary layer detachment*. The opposite current which is born under the stream line starting from S (detachment point), can make a complete loop, forming some

vortexes behind the cylinder, and they can be dragged away from the mean current. So in the region behind the cylinder, some speeds directed toward the cylinder could be present, this region is called *wake*. The location of the point S depends on the Re of the incoming undisturbed flow before the impacted body, low Reynolds numbers generated a so called "large wake", high Reynolds numbers produce a so called "narrow wake" (Fig. 1.16).

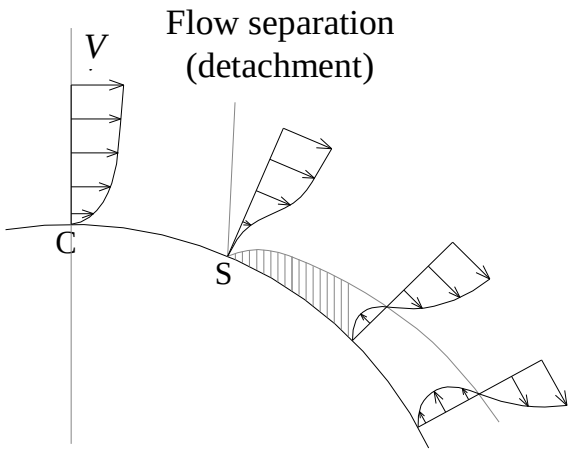

Fig. 1.15. Deatachment of the boundary layer.

The generated vortexes loose themselves in the wake, they rotate in a clockwise direction in the upper wake region and in an anticlockwise in the low wake region, as shown in Fig. 1.17.

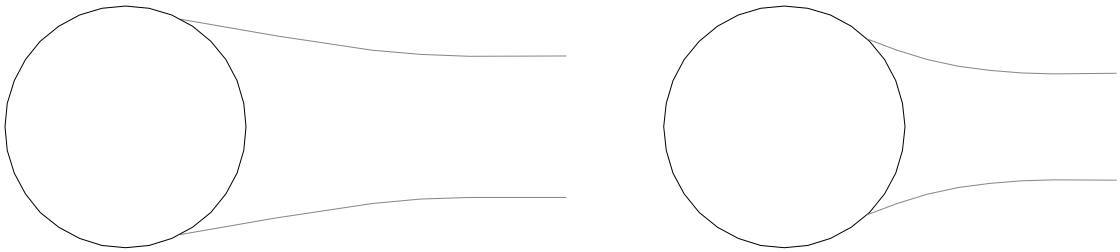

Fig. 1.16. Large wake and narrow wake.

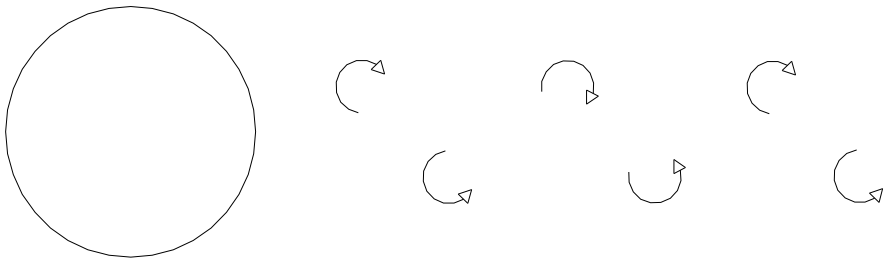

Fig. 1.17. Vortexes rotation

The presence of the wake makes the pressures field asymmetric with respect to the y-axis as shown in Fig.1.14, this makes the sum of the pressures around the body surface not equal to zero. This sum is called *shape drag* and is given from:

$$D_{shape} = \int_S p_x dS \tag{1.34}$$

Were p_x indicates the projection of the pressures with respect to the V_0 direction.

Together with the shape drag, a so called *friction drag* is generated, and given from:

$$D_{friction} = \int_S \tau_x dS \tag{1.35}$$

were τ_x represent the projection of the tangential stresses with respect to the V_0 direction, and they shown an high dependence from the Re of the incident undisturbed flow.

It is known that the last contribute to the drag shows an high dependence from the roughness of the invested body surface. This influence becomes appreciable since the surface irregularities are greater than the laminar substrate inside the boundary layer.

The total drag can be computed from the sum of the two previously introduced drags. Since both terms depends on the Re and the friction drag depends on the roughness too, it can be deduced that the shape of the body determines the detachment point location. In conclusion, the combination of the factors Re, roughness and body shape, determines the relative locations of the detachment point (S) and the transition point (T) (from point of the body surface from where the boundary layer switch from a laminar to a turbulent type). In general one can have the two situation that are shown in Fig. 1.18 and Fig. 1.19 corresponding with low Re and high Re respectively.

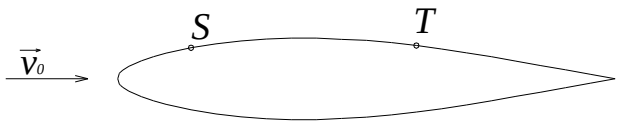

Fig. 1.18. Transition and detachment (low Re)

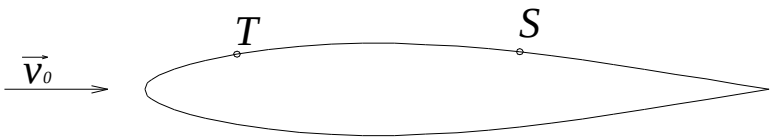

Fig. 1.19. Transition and detachment (high Re)

The problem of the cylinder in Fig.1.14 was symmetric with respect to the x-axis both for the body shape and for the incident flow speed configuration. In this case the lift is equal to zero, but if one of the previous two conditions is not realised, the lift assumes a finite value.

1.2.2. Aerodynamic coefficients

Consider two bodies which are similar from a geometric point of view (in the sense that they have the same shape but different dimensions), and consider that they are subjected to two inviscid, incompressible flows which are also similar from a geometric point of view (in the sense that they have the same orientation and the same Re whit respect to the impacted body but the densities, the speeds and the pressure fields are not the same ($|\vec{v}_{01}| \neq |\vec{v}_{02}|$, $\rho_1 \neq \rho_2$)), as shown in Fig.1.20.

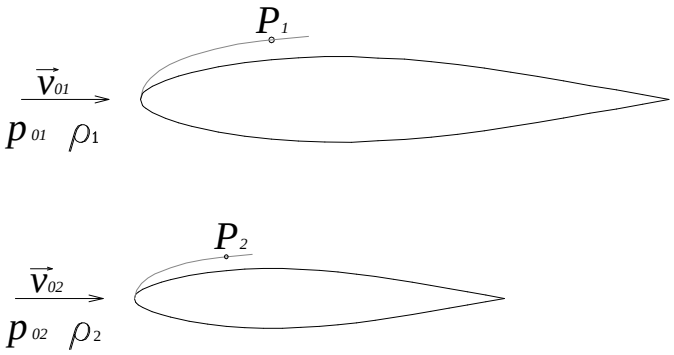

Fig. 1.20. Similar aerodynamic problems.

Consider two analogues points P_1 and P_2 located on the bounds of the two boundary layers which would be generated in the case of viscous flows. It can be stated that the speed ratios $\frac{|\vec{v}_{Pi}|}{|\vec{v}_{0i}|}$ (with i=1,2) computed for the two bodies is the same, namely:

$$\frac{|\vec{v}_{P1}|}{|\vec{v}_{01}|} = \frac{|\vec{v}_{P2}|}{|\vec{v}_{02}|} = k \tag{1.36}$$

Considering the two streamlines containing P_1 and P_2, one can applies the Bernoulli theorem, obtaining

$$\Delta p_1 = p_{P1} - p_{01} = \frac{1}{2}\rho_1\left(v_{01}{}^2 - v_{P1}{}^2\right) = \frac{1}{2}\rho_1 v_{01}{}^2\left(1-k^2\right) \tag{1.37}$$

$$\Delta p_2 = p_{P2} - p_{02} = \frac{1}{2}\rho_2\left(v_{02}{}^2 - v_{P2}{}^2\right) = \frac{1}{2}\rho_2 v_{02}{}^2\left(1-k^2\right) \tag{1.38}$$

were p_{0i} (with i=1,2) indicates the hydrostatic pressures. By dividing the last two equation each other

$$\frac{\Delta p_1}{\Delta p_2} = \frac{\frac{1}{2}\rho_1 v_{01}{}^2}{\frac{1}{2}\rho_2 v_{02}{}^2} \tag{1.39}$$

And multiplying for the unit of area, can be obtained

$$\frac{dF_{N1}}{dF_{N2}} = \frac{\Delta p_1 dS_1}{\Delta p_2 dS_2} = \frac{\frac{1}{2}\rho_1 v_{01}{}^2 dS_1}{\frac{1}{2}\rho_2 v_{02}{}^2 dS_2} \tag{1.40}$$

Which is the ratio between the two orthogonal elementary aerodynamic forces. By a surface integration the equation (1.41) can be obtained

$$\frac{F_{N1}}{F_{N2}} = \frac{\frac{1}{2}\rho_1 v_{01}{}^2 S_1}{\frac{1}{2}\rho_2 v_{02}{}^2 S_2} \tag{1.41}$$

The equation (1.41) allows to define a constant coefficient for similar bodies subjected to similar flows

$$C_N = \frac{F_{N1}}{\frac{1}{2}\rho_1 v_{01}{}^2 S_1} = \frac{F_{N2}}{\frac{1}{2}\rho_2 v_{02}{}^2 S_2} \tag{1.42}$$

the same considerations can be done for the aerodynamic tangential force generated from the resistance of an eventual viscosity, obtaining

$$C_T = \frac{F_{T1}}{\frac{1}{2}\rho_1 v_{01}{}^2 S_1} = \frac{F_{T2}}{\frac{1}{2}\rho_2 v_{02}{}^2 S_2} \tag{1.43}$$

Must be considered that, in the case of viscous fluids, the geometric similitude of the bodies and the flows is not sufficient, but the complete similitude of the aerodynamic fields is required. In the case of incompressible, viscous flows, this similitude is guaranteed from the equality between the Reynolds numbers.

With the same consideration, the following *aerodynamic coefficients* can be defined:

- Force aerodynamic coefficient (were F is considered the same of the equation (1.31)

$$C_F = \frac{F}{\frac{1}{2}\rho v_0{}^2 S} \tag{1.44}$$

- Lift aerodynamic coefficient

$$C_L = \frac{L}{\frac{1}{2}\rho v_0{}^2 S} \tag{1.45}$$

- Drag aerodynamic coefficient

$$C_D = \frac{D}{\frac{1}{2}\rho v_0{}^2 S} \tag{1.46}$$

- Moment aerodynamic coefficient

$$C_M = \frac{M}{\frac{1}{2}\rho v_0{}^2 Sl} \tag{1.47}$$

Were v_0 represents the undisturbed flow speed and S represents a surface defining the dimension of the bodies and l represent a characteristic body dimension; the factor $\frac{1}{2}\rho v_0{}^2$ is called kinetic pressure of the undisturbed pressure.

Finally it is important to define a punctual aerodynamic coefficient called pressure coefficient

$$C_P(P) = \frac{p_P - p_0}{\frac{1}{2}\rho v_0{}^2 S} \tag{1.48}$$

were p_P is the punctual pressure in the point P, and p_0 is the hydrostatic pressure.

1.2.3. Bluff body aerodynamic. Strouhal number

The sections of the aerodynamic bodies are usually classified with regard to the dimensional ratio *B/D*, were *B* indicates the section dimension in the flow direction, while *D* indicates the section dimension orthogonally to the flow direction. High values of the *B/D* ratio characterizes the so-called "bluff bodies", while low *B/D* ratios characterizes the so-called "streamline bodies". In the case of bluff bodies, a detachment of the flow can be usually appreciated in the boundary layer, if the body dimension *B* is sufficient, the flow can also reattach itself to the section proceeding in the motion. The detachment is caused by the high vorticity assumed by the flow particles during the body over crossing, which is due to sudden change in their motion direction after the impact with the body. This fact increases the flow turbulence and can cause the generation of some vortex in the flow (*vortex shedding*). On the other hand, in the relative motion of the generic fluid with respect to a streamlined body, it may be that the detachment does not arise, in this case the flow around the body remain laminar. The processes of both vortex generation and boundary layer detachment are highly influenced from the presence of live edges in the body section, which for example, is the mean reason for the turbulence in bridge decks wake. The phenomenon is schematized in Fig. 1.21.

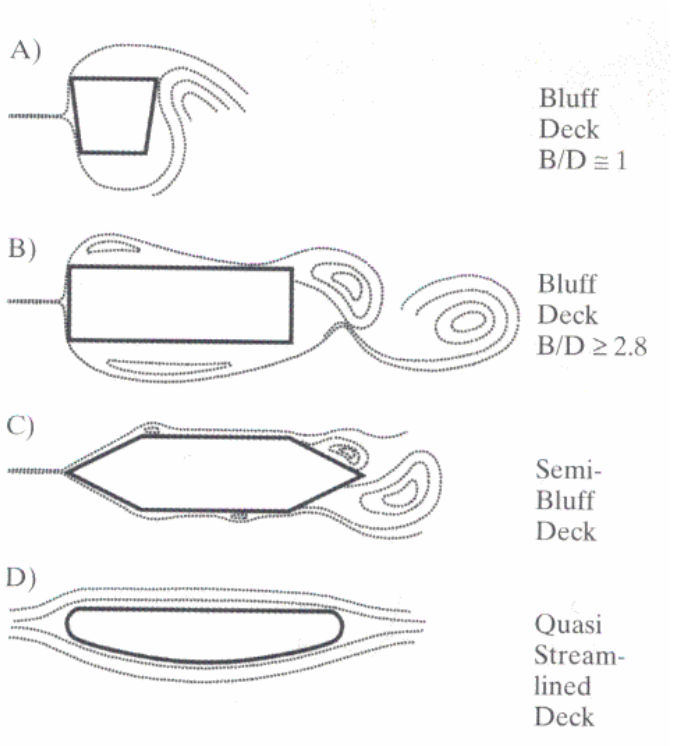

Fig. 1.21. Aerodynamic bridge decks sections (after Bruno and Khris 2003)

The vortex shedding is an important phenomenon that has to be considered in the suspension bridge design; when the vortex shedding happens, it is characterized by a certain frequency and consequently this oscillation frequency afflicts the aerodynamic actions, and in particular the Lift force. The Drag force, during the vortex shedding, shows an oscillation frequency that is double with respect to the Lift one (equal to the shedding frequency).

If the lift frequency meets one of the vertical oscillations deck frequency, the action can "lock" the motion, and the bridge can experiment important vertical deflections which became dangerous for the structure. This mechanism is characterized by a certain dimensionless number called "*Strouhal number*" given from

$$S = \frac{N_s D}{V_0} \tag{1.49}$$

were N_s represents the vortex shedding frequency, D represent a characteristic physical size for the structure (for example the width of the deck section) and V_0, as usual represent the incoming flow mean undisturbed speed.

1.3 Aeroelasticity

Aeroelasticity is the discipline concerned with the study of phenomena wherein aerodynamic forces and structural motions interact significantly.

A body immersed in a flow is subjected to surface pressures induced by that flow. If there is turbulence in the incident flow, this will be the source of time dependent surface pressures. Such stresses are also caused by flow fluctuations initiated by the body itself. Further, if the body moves or deforms appreciably under the induced surface forces, these deflections, changing as they do the boundary conditions of the flow, will affect the fluid forces which in turn will influence the deflections. Such forces are termed self-excited.

In this case the structural response (R) is characterized from fluid-structure interaction effects and the mechanism the structural response generation is represented from the chain shown in Fig. 1.22; here the self-excited forces generated from the fluid-structure interaction mechanism are indicate by the symbol F_{se}.

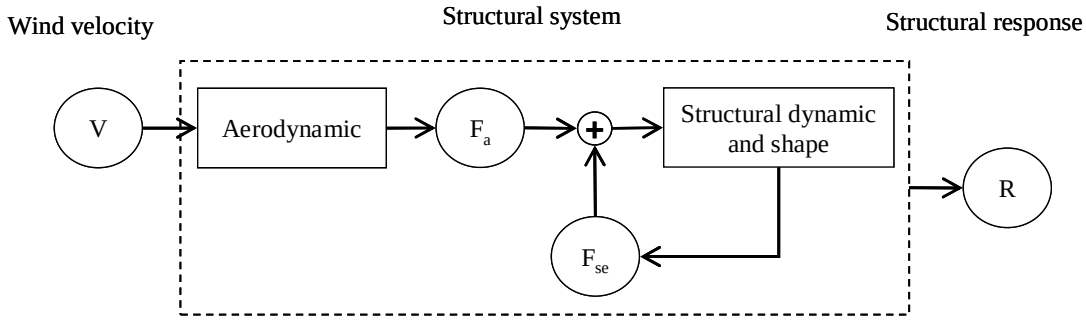

Fig. 1.22. Aeroelastic “chain”.

Under certain conditions, instability phenomena could arise for the structural system composed from the structure and the flow around the structure boundary. All aeroelastic instabilities involve self-excited forces that act upon the body as a consequence of its motion.

The topics dealt with in this paragraph include vortex shedding and the associated lock-in phenomena, torsional divergence, and flutter.

1.3.1. Vortex shedding

Dynamic instability very similar to a resonance. Some vortexes loose themselves in the wake behind the body. Such physic configuration generates an oscillation in aerodynamic forces, with a definite frequency. In a certain range of wind speed, the oscillation frequency of the forces “lock” the structural oscillations frequency and it governs the structural oscillation period.

It was seen in section 1.2.3 that under certain conditions a fixed bluff body sheds alternating vortices, whose primary frequency N_s is, according to the Strouhal relation,

$$\frac{N_s \cdot D}{V} = S \qquad (1.50)$$

where S depends upon body geometry and the Reynolds number, D is the across-wind dimension of the body, and V is the mean velocity of the uniform flow in which the body is immersed. The frequency N, is also that of the net primary forces acting transversely to the direction of V while the primary frequency of net forces acting in the flow direction will be $2N_s$. Actually the net force vector defined by the integral of instantaneous pressures over a given bluff body will vary in magnitude and direction with time in a fairly complex manner depending upon detailed body geometry and Reynolds number of the flow. Only the frequencies of its principal harmonics are given by N_s and $2N_s$.

If the body that instigates the vortex shedding is elastically supported or if it is subject to local contour deformation, it will deflect wholly or locally and, by this action, influence the local flow. Not many of the full range of possibilities latent in this situation have been studied in detail. Deformable steel shells have given rise to so-called ovalling oscillations under these conditions. Many examples of cross-wind rigid-contour oscillations have been noted; and in water flows important along-flow deflections have been observed.

Unless otherwise noted, it will be assumed in this section that the structure is a cylinder with a rigid surface, the oncoming flow has uniform mean velocity, the deflections of the body are the same throughout its length, the body is elastic and possesses mechanical damping in the across-wind direction, and it is rigidly constrained in the along-wind direction. Under the action of the vortices shed in its wake the cylinder will be driven periodically, but this driving will produce only small response unless the Strouhal frequency of alternating pressures approaches the natural across-flow mechanical frequency of the cylinder. Near this frequency greater body movement is elicited, and the body begins to interact strongly with the flow. It is experimentally observed at this point that body mechanical frequency controls the vortex-shedding phenomenon eyen when variations in flow velocity displace the nominal Strouhal frequency away from the natural mechanical frequency by a few percent.

This control of the phenomenon by the mechanical forces is commonly known as lock-in. In dynamical systems theory this phenomenon is referred to as synchronization. Observations show that during lock-in the amplitude of the oscillations attains some fraction, rarely exceeding half, of the across-wind dimension of the body. The effect of lock-in upon vortex shedding is represented in Fig. 1.23, which shows that in the lock-in region the vortex-

shedding frequency is constant rather than being a linear function of wind speed, as suggested by equation (1.50) (and as it in fact is outside the lock-in region).

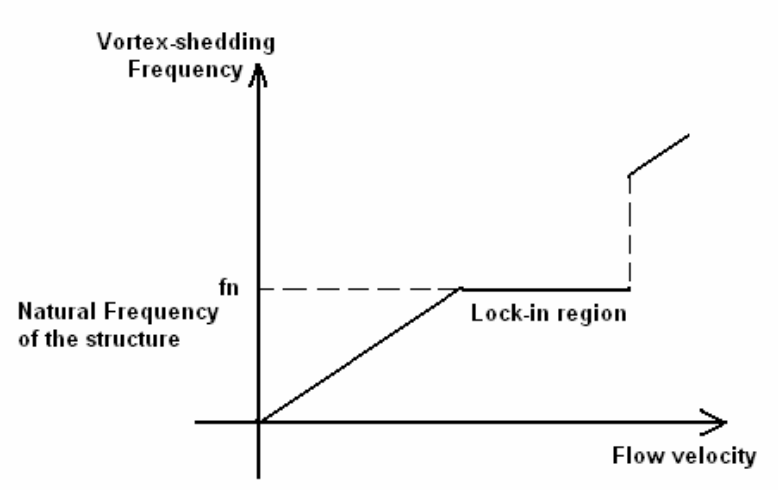

Fig. 1.23. Lock-in phenomenon.

Under the vortex shedding action, for a slender structure (like a cylinder having infinite length), in general for the lift force can be written:

$$L(t) = A_s \cdot \sin(2\pi \cdot n_s \cdot t)$$

Where A_s is opportune amplitude and n_s is the dominant shedding frequency, given by the Strouhal number (equation 1.50). When n_s (varying with V) becomes equal to the first transversal frequency $n_{1,L}$, the lock-in phenomenon arises, this wind incoming velocity is called *vortex shedding critical velocity* ($V^{VS}crit$).

The amplitude of the lock-in region represented in Fig. 1.23 depends on the so-called *Scruton number*

$$Sc = \frac{4\pi \cdot m \cdot \xi}{\rho \cdot D^2} \qquad (1.51)$$

Where m is the mass per unit of length (assumed punctual), D is the across-wind dimension of the body, and ξ is the damping factor of the first transversal structural mode of vibration.

The amplitude of the lock-in region decreases as the Scruton number increases, it can disappear for high Scruton numbers (Fig. 1.24).

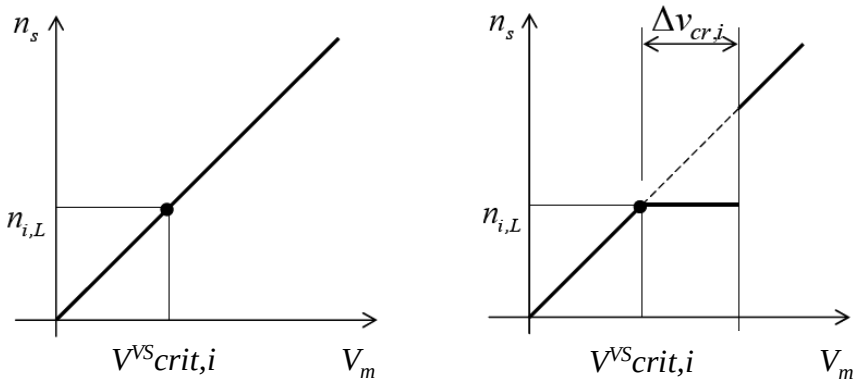

Fig. 1.24. Strouhal law: high *Sc* (left), small *Sc* (right).

1.3.2. Flutter

Typically, for suspension bridges, the most dangerous instability phenomenon is the so called "classical flutter": a dynamic instability in which two DOFs of the forced structural system are coupled: under opportune configurations (defined "critical") for the two frequencies and reciprocal phase angles, it makes the damping of the system become negative, and the structural oscillations increase in amplitude. For a suspension bridge, the two coupled DOFs are the vertical and the rotational ones for the deck section. As the vertical and, in particular, rotational motion frequency depend on the incident wind speed, when this velocity increases the frequencies come closer to each other until the "frequency coalescence"; during this interval of time the damping is positive. When the oscillation frequencies have the same value, and phase shifted of $\pi/2$, the damping of the system becomes zero and, if the wind speed increases, it becomes negative. The wind speed which corresponds to zero damping and incipient flutter is called *critical flutter wind speed* ($V^{FL}crit$).

The damping of the generic time oscillation can be estimated by identifying it with the exponential coefficient δ of the function $q(t) = \bar{q} \pm q_0 \cdot e^{-\delta \cdot t}$ (where $\bar{q}$ identifies the static equilibrium position), which envelopes the generic oscillation (see Fig. 1.25a): in damped ($V_m < V^{FL}crit$), critical ($V_m = V^{FL}crit$) and amplified ($V_m > V^{FL}crit$) oscillations, it results respectively $\delta >$, = or < to zero. In Fig. 1.25b, the amount of damping δ for various V_m is shown: here, δ represents the total damping of the structural system, which is sum of the structural (assumed constant in this case, and equal to 0.5%) and the aerodynamic one (computed as the analytical difference from the total damping and the structural one). The total damping curve grows when there is an increasing of the wind speed; at a certain value it changes its slope and begins to decrease until the intersection of abscissa axis. Such intersection represents the critical flutter velocity.

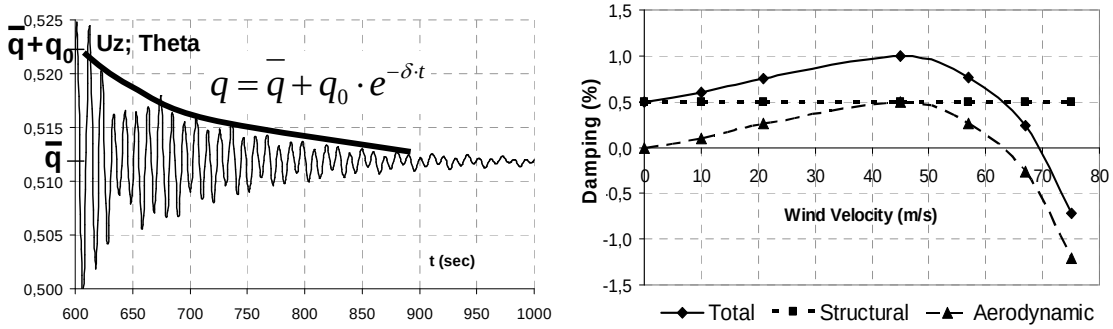

(a) (b)

Fig. 1.25. Aerodynamic damping: envelope of mid span oscillation ($V_m < V^{FL}crit$, $\delta>0$) to evaluate damping (a), damping on incident flow velocity (b)

1.3.3. Other aeroelastic phenomena

A short definition of other aeroelastic phenomena is reported follow

Torsional divergence. Static instability in which torsional moment due to aeroelastic forces, overcomes the elastic resistant moment of the body

Galloping. An asymmetry in the flow produces a vertical oscillation that generates oscillations in aerodynamic forces, which depends on body oscillations velocity and involves an aerodynamic damping, which is opposite to the structural damping. If aerodynamic damping is greater than the structural one, the motion may become unstable.

Buffeting. Motion under the action of time random variable forces both in intensity and direction. The buffeting phenomenon assumes aeroelastic importance in concomitance of other aeroelastic phenomena (like Flutter or Vortex shedding). A classic buffeting effect is the one generated by the intrinsic turbulence within the atmospheric boundary layer.

1.4 Wind actions on civil engineering structures

The wind actions on a generic surface, are determined by the configuration of punctual actions (pressure and tangential stresses), which are caused by the wind impact in the relative motion.

For a flexible body inside a wind flow, these stresses are determined by the flow configuration in the surface proximity zone, and so depend on the body motion: from a mechanic point of view, the couple of the flow and the body is a self-excited dynamic system.

By discredizing the body to a finite number of degrees of freedom (DOFs), the equation governing the body motion is the dynamic equilibrium equation:

$$\underline{\underline{M}} \cdot \underline{\ddot{q}} + \underline{\underline{C}} \cdot \underline{\dot{q}} + \underline{\underline{K}} \cdot \underline{q} = \underline{F}(body\ shape\ ; \underline{q}, \underline{\dot{q}}, \underline{\ddot{q}}; \underline{V}; t; \underline{n}) \tag{1.52}$$

where $\underline{\underline{M}}$, $\underline{\underline{C}}$ and $\underline{\underline{K}}$ are the mass matrix damping matrix and the stiffness matrix of the system, $\underline{q}, \underline{\dot{q}}, \underline{\ddot{q}}$ are the DOFs of the system and their first an second time derivates, $\underline{V}$ is the incident wind speed, t is the time and $\underline{n}$ is the oscillation frequencies vector of the system.

In general, inside the right hand member of the equation (1.52) there is an “self-excited” component of the aerodynamic forces which depends on body motion ($\underline{q}, \underline{\dot{q}}, \underline{\ddot{q}}$); in the case that the inertial terms, if compared with others, assume infinitesimal order, the equation (1.52) becomes a static equilibrium statement.

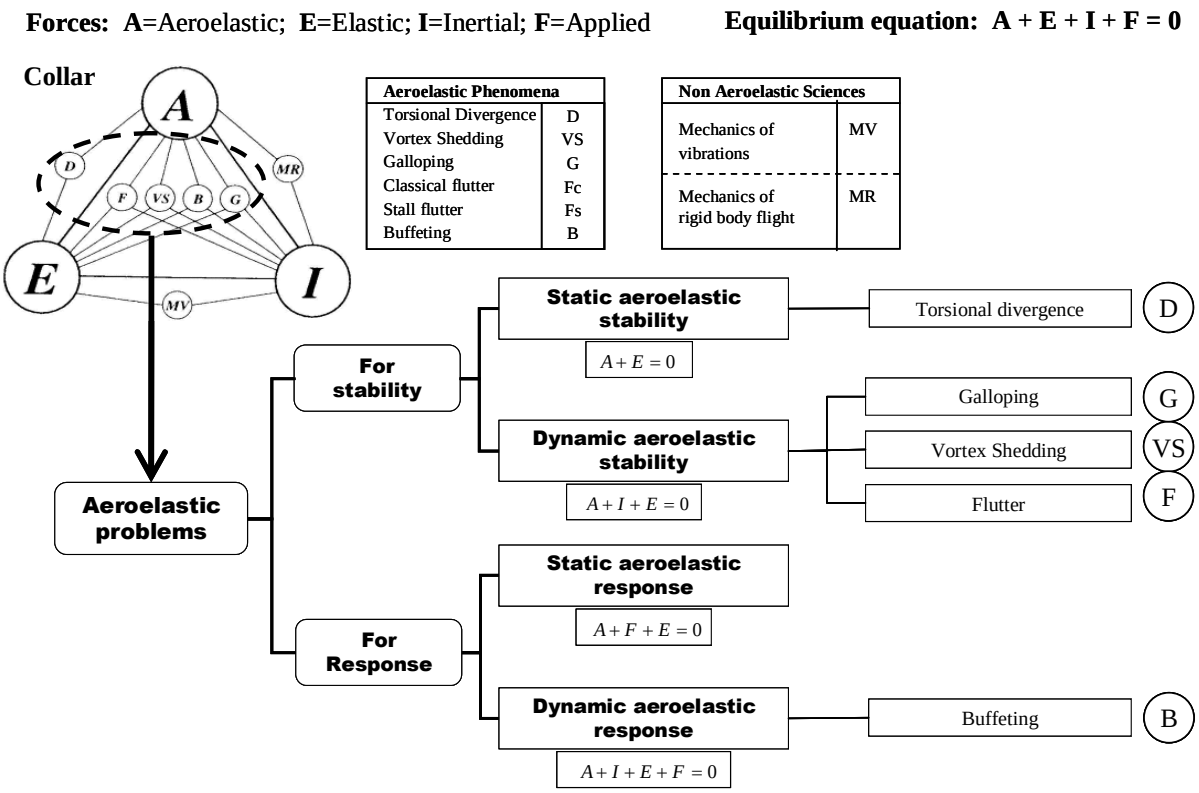

Fig. 1.27. Aeroelastic problems classification

A global picture of all the aeroelastic problems that can involve a structure is represented by the "Collar triangle", as shown in the upper side in Fig. 1.27: here, focusing on aeroelastic forces dependences, aeroelastic problems are classified in three categories:

1. Response problems, in which there is a dynamic equilibrium between the body and the wind forces, the expression of the forces does not contain DOFs dependent (self-excited) terms.

2. Stability problems, in which the interchanging energy between the body motion and the aeroelastic forces may produces a gradual and unlimited increment of the motion energy, leading to the dynamic equilibrium instability at "critical velocities". For these problems, the expression of the forces does not contain DOFs-independent terms.

3. Mixed (stability and response) problems, in which incident wind velocities are close to the critical velocities and the expression of the forces contains both DOFs-independent and self-excited terms.

In stability problems, the forces are usually transferred in the left side hand of the equation in order to obtain a homogeneous equation in which mass, damping, and stiffness matrices contain self-excited coefficients.

In what follows, the term *aeroelastic* will be used only in the case of stability or mixed problems, while in general the term *aerodynamic* will be used to describe the wind actions in facing with response problems.

Considering a generic structure under wind action, two principal approaches exist to solve the relative aerodynamic/aeroelastic problem:

1. Frequency domain approach, usual for instability problems, based on a modal combination to assess the structural response, is less reliable for structures with strong nonlinear nature.
2. Time domain approach, requiring a time integration of the equilibrium equation (1.52) of the structure subjected to wind loads, with large computational costs for structure with many DOFs.

In the last decades, referring to aeronautic engineering, civil engineers have developed many analytical theories to model wind effects on structures, and simplified approaches have been adopted to evaluate the aeroelastic terms, because of the very complex dependence above listed. Both frequency and time domain techniques to model aeroelastic forces, derive from wing theory (Theodorsen, 1931a, 1931b, 1935, Caracoglia and Jones, 2003).

Since the first applications of the present work regards a long span suspension bridge, in this section the most used aeroelastic theories developed in both time and frequency domain are presented referring to a generic suspension bridge deck section. The explanation of the aeroelastic theories will be made considering, under a general point of view, a mixed stability-response problem.

In the case of civil structures, two peculiar aspects have to be considered.

First, civil structures usually have so-called “semi-bluff” or “bluff” body shapes, opposite to wing or streamlined shapes. For example suspension bridges deck sections have well predictable points of flow detachments along the deck surfaces (“live edges”), where the turbulence of the flow is very high.

The second particular aspect is related to the intrinsic turbulent content of an incident wind flow, because these structures are located inside the atmospheric boundary layer. Furthermore a larger complexity and rotationally nature of the flow determines a larger “aerodynamic delay”, which is the transient effect due to the adjustment time of aerodynamic field, in consequence of a changing in body geometric configuration (i.e. rotation and displacements of a bridge deck). In order to take into account these effects, the so-called “memory terms”, which consider the influence of displacements history in the expression of the aeroelastic

forces, are introduced. These terms are usual implemented by integral expressions (Chen et al 2000).

1.4.1. Wind actions model in frequency domain

The uncertainties related to the above phenomena lead to the use of the experimental approach. In this sense, studies conduced by Scanlan and Tomko (1971), by Jain, Jones and Scanlan (1996), and resumed in Simiu and Scanlan (1996) conducted for bridge aeroelastic phenomena, had great relevance in wind engineering. Following Scanlan theory, the Self-Excited (SE) components of the aeroelastic forces are determined by a superposition of the effects, referring to the forces obtained by wind tunnel tests, acting on a sectional model of the deck that is moving in simple harmonic oscillations along three sectional DOFs (the rotational and the two translational ones). Referring to Fig. 1.28, it results for the Lift force

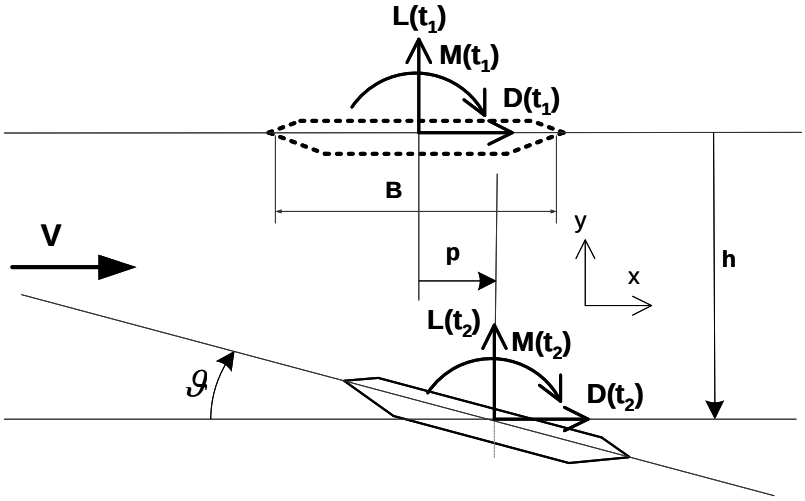

Fig. 1.28. Bridge deck section under horizontal wind flow

$$L_{SE}(p,\dot{p},h,\dot{h},\vartheta,\dot{\vartheta},k,\omega) =$$
$$= \frac{1}{2}\cdot\rho\cdot V^2\cdot B\cdot\left[\begin{array}{l} k\cdot H_1^*(k)\cdot\dfrac{\dot{h}}{V}+k\cdot H_2^*(k)\cdot\dfrac{B\cdot\dot{\vartheta}}{V}+k^2\cdot H_3^*(k)\cdot\vartheta+ \\ +k^2\cdot H_4^*\cdot\dfrac{h}{B}+k\cdot H_5^*(k)\cdot\dfrac{\dot{p}}{V}+k^2\cdot H_6^*(k)\cdot\dfrac{p}{B} \end{array}\right] \qquad (1.53)$$

where:

$k=\dfrac{\omega\cdot B}{V}=$ reduced frequency of the system, in simple harmonic motion

$H_i^*(k)=$ functions of the reduced frequency

$B=$ characteristic dimension of the bridge deck

$\omega =$ circular frequency of the system, in simple harmonic motion

$V =$ incident wind speed

The functions $H_i^*(k)$ are called "flutter derivatives" of the bridge deck, and are determined by wind tunnel tests, imposing simple harmonic motion to the deck model. In the equation (1.48), the lift self-excited action is expressed in a mixed time-frequency domain formulation, by operating the Fourier transformation one can express the actions completely in the frequency domain.

Analogous expressions of (1.53) can be written for drag force and moment.

1.4.2. Wind actions model in time domain

Expressions in time domain which consider the correct dependence of the actions from the involved parameters are not trivial to implement. Consequently in the last years simplified formulations for aeroelastic forces have been developed and improved. Referring to Fig. 1.29, where the problem is represented like a two-dimensional problem, horizontal and vertical components of absolute wind turbulent velocity $V_a(t)$, are considered as composed by mean components U, W, and fluctuant (or turbulent) components $u(t)$ e $w(t)$. The resulting absolute velocity is not horizontal, and has a time-varying instantaneous angle of incidence.

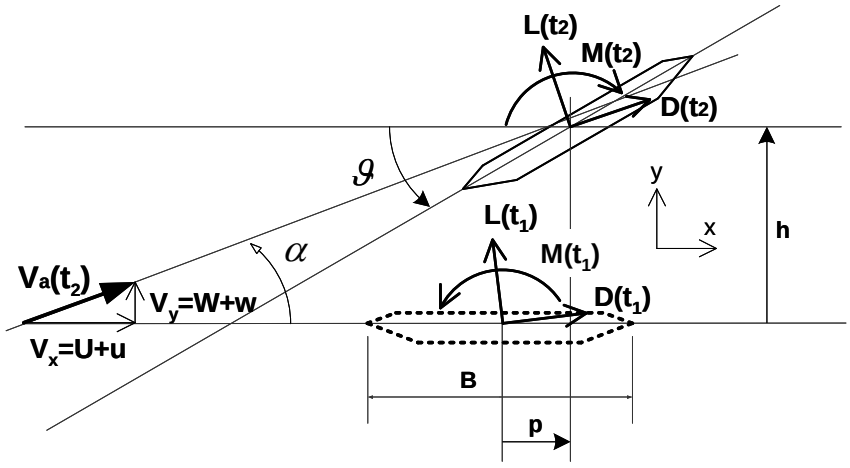

Fig. 1.29. Bridge deck section under turbulent wind action.

Adopting the general notation previously introduced (equation (1.52)), one has, for the system DOFs, $\underline{q}^T = [s \quad h \quad \vartheta]$. Moreover, the dependence of the forces from structural DOFs and their time derivatives can be generally expressed in matrix form as:

$$\underline{F}(\underline{q},\dot{\underline{q}},\ddot{\underline{q}};\underline{n}) = \underline{\underline{P}}(t,\underline{n})\cdot\ddot{\underline{q}} + \underline{\underline{Q}}(t,\underline{n})\cdot\dot{\underline{q}} + \underline{\underline{R}}(t,\underline{n})\cdot\underline{q} \qquad (1.54)$$

where the time dependence of DOFs has not been noticed: $\underline{\underline{P}}(t,\underline{n})$, $\underline{\underline{Q}}(t,\underline{n})$ and $\underline{\underline{R}}(t,\underline{n})$ represent in expression (1.54) coefficient matrices which, in the most general case, depends on time and on oscillation frequency of the system.

Non aeroelastic theory (NO).

This is a "zero level" aeroelastic theory: aeroelastic effects are not considered in the forces formulation but only the relative angle of incidence between wind and deck, change with time just in accordance with the turbulence of the incident wind. Adopting the small displacements hypothesis, (linearised Lift and Moment polar line), it results

$$\begin{aligned} D(t) &= \frac{1}{2}\rho \cdot |V_a(t)|^2 \cdot B \cdot c_D[\alpha(t)] \\ L(t) &= \frac{1}{2}\rho \cdot |V_a(t)|^2 \cdot B \cdot K_{L0} \cdot \alpha(t) \\ M(t) &= \frac{1}{2}\rho \cdot |V_a(t)|^2 \cdot B^2 \cdot K_{M0} \cdot \alpha(t) \end{aligned} \qquad (1.55)$$

where α is the angle of attack, c_D is Drag coefficient and K_{L0} , K_{M0} are the angular coefficients of Lift and Moment polar diagrams respectively.

Steady theory (ST).

This is a "first level" aeroelastic theory, where the relative angle of incidence between wind and deck, changes with time due to both the incident wind turbulence and the rotation (torsion) of the deck. Supposing that the bridge deck section rotates around a mean equilibrium position $\vartheta = \vartheta_0$, adopting the small displacements hypothesis (both Lift and Moment polar diagrams are linearised), the aerodynamic coefficients become

$$\begin{aligned} c_L(\gamma) &= c_L(\vartheta_0) + K_{L0} \cdot (\gamma - \vartheta_0) \\ c_M(\gamma) &= c_M(\vartheta_0) + K_{M0} \cdot (\gamma - \vartheta_0) \end{aligned} \qquad (1.56)$$

in which K_{L0} e K_{M0} are the angular coefficients of polar lines computed in $\vartheta = \vartheta_0$. Referring to Fig. 1.28 and defining $\gamma(t) = \alpha(t) - \vartheta(t)$, the aeroelastic forces are expressed as

$$D(t) = \frac{1}{2}\rho \cdot |V_a(t)|^2 \cdot B \cdot c_D[\gamma(t)]$$
$$L(t) = \frac{1}{2}\rho \cdot |V_a(t)|^2 \cdot B \cdot c_L[\gamma(t)] \qquad (1.57)$$
$$M(t) = \frac{1}{2}\rho \cdot |V_a(t)|^2 \cdot B^2 \cdot c_M[\gamma(t)]$$

Adopting the general formulation of equation (1.54), one can write

$$\underline{F} = \underline{F}(\underline{q}; t) = \underline{\underline{R}} \cdot \underline{q}(t) \qquad (1.58)$$

The steady theory has the appeal of simplicity; furthermore, in the case of non turbulent incident wind, it shows the fundamental mechanisms of a flutter stability problem (coalescence of frequency, influence of structural parameters, etc.). Nevertheless it implies many approximations, such as the neglecting of the dependence of aeroelastic forces on structural velocities, accelerations and oscillation frequency, and the linearization of the relation between aeroelastic forces and structural DOFs. Furthermore, the steady theory does not consider the aerodynamic delay, and utilizes static aerodynamic coefficients.

Quasi Steady theory (QS).

It is a "*second level*" aeroelastic theory: instantaneous aeroelastic forces acting on the structure are the same that act on the structure itself when it moves with constant translational and rotational velocities, equal to the real instantaneous ones. The main assumption consists in considering that the body (deck section) is motionless, together with the wind having velocities and directions equal to the instantaneous relative (wind-deck) ones: such assumption is represented in Fig. 1.30.

The coefficients of $\dot{\vartheta}$ (b_i, with $i = L, M$) should be derived experimentally by wind tunnel tests (Lazzari 2005); it can be derived also through the use of Computational Fluid Dynamic (CFD) techniques (Bruno and Khris 2003, Petrini et al. 2005).

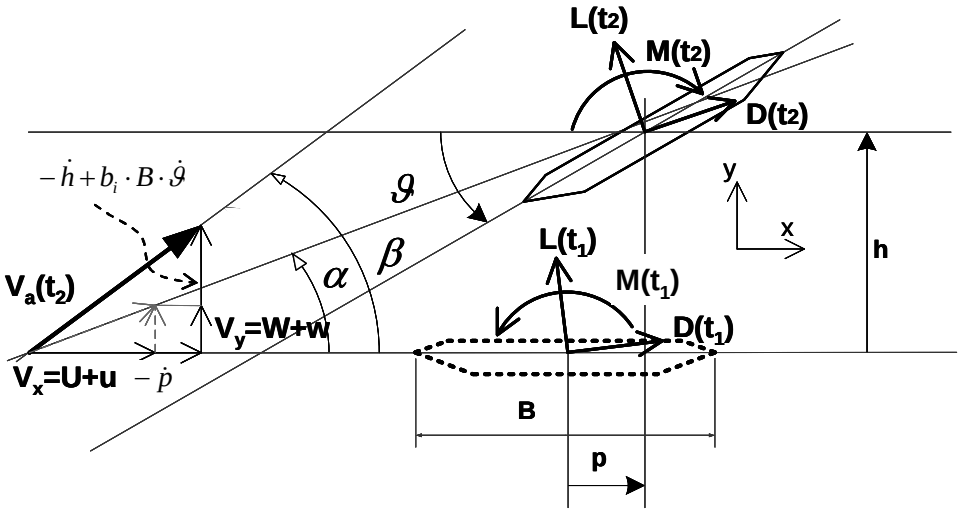

Fig. 1.30. Quasi steady theory assumption

Adopting the hypothesis of small displacements around the mean configuration, equations (1.56) are also valid and the expressions of aeroelastic forces are identical (in the form) to the steady theory ones, with $\beta_i(t) = arctg\left(\frac{V_y(t) - \dot{h} + b_i \cdot B \cdot \dot{\vartheta}(t)}{V_x - \dot{p}}\right)$ ($i = L, M$) in substitution of $\alpha(t)$:

$$
\begin{aligned}
D(t) &= \frac{1}{2}\rho \cdot \left|V_{aL}(t)\right|^2 \cdot B \cdot c_D\left[\gamma(t)\right] \\
L(t) &= \frac{1}{2}\rho \cdot \left|V_{aL}(t)\right|^2 \cdot B \cdot c_L\left[\gamma(t)\right] \\
M(t) &= \frac{1}{2}\rho \cdot \left|V_{aM}(t)\right|^2 \cdot B^2 \cdot c_M\left[\gamma(t)\right]
\end{aligned}
\qquad (1.59)
$$

where $\gamma_i(t) = \beta_i(t) - \vartheta(t)$ and $\left|V_{ai}(t)\right|^2 = \sqrt{\left(V_x - \dot{p}\right)^2 + \left(V_y - \dot{h} + b_i \cdot B \cdot \dot{\vartheta}\right)^2}$, i= L, M.

Adopting the general formulation of equation (1.54), one can write:

$$\underline{F} = \underline{F}(\underline{q}, \dot{\underline{q}}; t) = \underline{\underline{R}} \cdot \underline{q}(t) + \underline{\underline{Q}} \cdot \dot{\underline{q}}(t) \qquad (1.60)$$

The Quasi Steady theory can consider the dependences of aeroelastic forces from structural velocities ($\dot{p}, \dot{\theta}$), preserving also a relatively simple algorithmic implementation. Furthermore, the dependence from oscillation frequency is neglected, and the dependence of aeroelastic forces from the DOFs of the structure is linearised. The Quasi Steady theory does not consider the aerodynamic delay, utilizing static aerodynamic coefficients, with the

possible exception for the b_i coefficients (with $i = L, M$), whose value are dynamically assessed (Lazzari 2005).

Considering the expected low incidence of turbulent component on the self-excited forces, and neglecting the high order infinitesimal terms, it is possible to obtain (Lazzari 2005) more elegant and explicit expressions than the (1.54), in which static, self-excited and buffeting component are outlined and expressed separately.

Modified Quasi Steady theory (QSM).

In this "third level" aeroelastic theory, in respect to the QS theory, the only changes concern the aerodynamic coefficients for the Lift and the Moment, which become dynamic as measured by wind tunnel tests (Diana et al. 1995). Referring to Fig. 1.30, aeroelastic forces are expressed by the following expressions:

$$\begin{aligned} D(t) &= \frac{1}{2}\rho \cdot \left|V_{aL}(t)\right|^2 \cdot B \cdot c_D\left[\gamma(t)\right] \\ L(t) &= \frac{1}{2}\rho \cdot \left|V_{aL}(t)\right|^2 \cdot B \cdot c^*{}_L\left[\gamma(t)\right] \\ M(t) &= \frac{1}{2}\rho \cdot \left|V_{aM}(t)\right|^2 \cdot B^2 \cdot c^*{}_M\left[\gamma(t)\right] \end{aligned} \qquad (1.61)$$

where $\gamma_i(t)$, $\left|V_{ai}(t)\right|^2$ ($i = L, M$) and c_D, have the same meaning as the previous expressions included in QS theory. In the expressions (1.61), aerodynamic coefficients $c^*{}_L$ and $c^*{}_M$ are dynamic and they are computed like below:

$$\begin{aligned} c^*{}_L &= c_L(\vartheta_0) + \int_{\vartheta_0}^{\vartheta} K_L \, d\bar{\vartheta} \\ c^*{}_M &= c_M(\vartheta_0) + \int_{\vartheta_0}^{\vartheta} K_M \, d\bar{\vartheta} \end{aligned} \qquad (1.62)$$

where $c_L(\vartheta_0)$ e $c_M(\vartheta_0)$ are the static aerodynamic coefficients computed in the mean equilibrium configuration ($\vartheta = \vartheta_0$), and K_L, K_M are the "dynamic derivatives" computed like below:

$$\begin{aligned} K_L &= h_3 \cdot \left(\frac{\partial c_L}{\partial \vartheta}\right)_{\vartheta=\bar{\vartheta}} \\ K_M &= a_3 \cdot \left(\frac{\partial c_M}{\partial \vartheta}\right)_{\vartheta=\bar{\vartheta}} \end{aligned} \qquad (1.63)$$

where h_3 and a_3 are the Zasso's theory coefficients (Zasso 1996), assessed by dynamic wind tunnel tests. These coefficients are similar to the Scanlan's motion derivatives (1.53), and they depend both from the rotation deck angle and the "reduced wind speed" $V_{red} = V/(\omega \cdot B)$ (depending from ω, which is the motion frequency). For multi-degree of freedom structures (MDOFs), the motion frequency is a combination of overall mode shape frequencies, and for nonlinear structures it varies at every instant, depending on the state of structure. So the in advance computation of h_3 and a_3 is not practicable. To overcome this problem, in the QSM theory, the fundamental frequency of the structure is used to compute the reduced velocity $V_{red} = V/(\omega \cdot B)$ and the corresponding h_3 and a_3 coefficients. Therefore, the dependence of aeroelastic forces from the motion frequency is not considered.

Adopting the general formulation, one can write

$$\underline{F} = \underline{F}(\underline{q}, \dot{q}; t) = \underline{\underline{R}}(t) \cdot \underline{q}(t) + \underline{\underline{Q}}(t) \cdot \underline{\dot{q}}(t) \qquad (1.64)$$

the QSM theory has the attractive aspects of the QS theory (together with high analytic difficulty), and implements dynamic aerodynamic coefficients. Such coefficients take into account the nonlinearity of the response in respect to the wind angle of attack, taking also a partial consideration of the aerodynamic delay. Furthermore they do not consider the dependence of the forces from the oscillation motion frequency.

Theory of Aeroelastic Derivates in Time Domain (ADTD).

In this "fourth level" aeroelastic theory, the basic concept is very similar to the Wagner's indicial function theory (Chen et al. 2000). The self-excited component of aeroelastic forces is computed by a convolution integral:

$$\begin{aligned}
D_{SE}(t) &= \int_{-\infty}^{t} \left(I_{D_{SEh}}(t-\tau) \cdot h(\tau) + I_{D_{SEp}}(t-\tau) \cdot p(\tau) + I_{D_{SE\vartheta}}(t-\tau) \cdot \vartheta(\tau) \right) \cdot d\tau \\
L_{SE}(t) &= \int_{-\infty}^{t} \left(I_{L_{SEh}}(t-\tau) \cdot h(\tau) + I_{L_{SEp}}(t-\tau) \cdot p(\tau) + I_{L_{SE\vartheta}}(t-\tau) \cdot \vartheta(\tau) \right) \cdot d\tau \qquad (1.65) \\
M_{SE}(t) &= \int_{-\infty}^{t} \left(I_{M_{SEh}}(t-\tau) \cdot h(\tau) + I_{M_{SEp}}(t-\tau) \cdot p(\tau) + I_{M_{SE\vartheta}}(t-\tau) \cdot \vartheta(\tau) \right) \cdot d\tau
\end{aligned}$$

where $I_{i_{SEj}}$ (i=*D, L, M* and $j = p, h, \vartheta$) is the impulsive function of the self-excited force i which corresponds to the generic j-th DOF. Such function represents the aeroelastic force component *i* that acts on a body under a wind flow which has an impulsive motion along the j-th DOF. By a Fourier transformation of equations (1.65), and supposing that the motions

along the three DOFs are sinusoidal with the same oscillation frequency, by comparing equations (1.65) with equations (1.53), it is possible to obtain the relationships between the Fourier transform ($\overline{I_{i_{SEj}}}$) of $I_{i_{SEj}}$ (i=D, L, M and j= p, h, ϑ), and the Scanlan's flutter derivatives: if the Scanlan's flutter derivatives of lift, drag and moment are known then the functions $\overline{I_{i_{SEj}}}$ (Chen et al. 2000) can be obtained. Nevertheless the flutter derivatives are known only in discrete values of reduced frequency (k), and are made continuous in the frequency domain by the Roger's approximating function (Chen et al. 2000) that can replace the $\overline{I_{i_{SEj}}}$. Operating a changing of variable, the Roger's functions are transposed in Laplace's domain and, by the Laplace's inverse transformation, they are finally transposed in the time domain. Concerning, for example, the part of self-excited component of the Lift that depends on the sectional vertical DOF ($h(t)$), using this procedure one can obtain the following expression

$$L_{SEh}(t) = \frac{1}{2}\rho \cdot |V_a(t)|^2 \cdot B \cdot \left(a_1 \cdot h(t) + a_2 \cdot \frac{B}{|V_a|} \cdot \dot{h} + a_3 \cdot \frac{B^2}{|V_a|^2} \cdot \ddot{h} + \sum_{l=1}^{m} \phi_l(t) \right) \qquad (1.66)$$

where a_i coefficients and the sum extreme m are those previously defined (during the Roger's function generation phase), and $\phi_l(t)$ are the integral terms, which represent the "memory terms" of the force. The assessment of $\phi_l(t)$ functions needs the introduction of further m differential equations in the $\phi_l(t)$ and $h(t)$ functions.

Adopting the general formulation one can write

$$\underline{F}(\underline{q}, \underline{\dot{q}}, \underline{\ddot{q}}; n) = \underline{\underline{P}}(t, \underline{n}) \cdot \underline{\ddot{q}} + \underline{\underline{Q}}(t, \underline{n}) \cdot \underline{\dot{q}} + \underline{\underline{R}}(t, \underline{n}) \cdot \underline{q} \qquad (1.67)$$

From a conceptual point of view, such theory is the most complete among the time domain formulations: the dependences of aeroelastic forces on both the structural DOFs and the structural velocities and accelerations are implemented, and the dependence from the motion frequency is also considered. Furthermore the aerodynamic delay is quantified by Roger's formulas. Otherwise one can note a great increase in the analytical difficulties of the method in respect to the others.

1.5 State of the art in wind engineering

The research in wind engineering science can be subdivided in various fields as shown in Fig. 1.31, here two macro sectors are identified for the research topics: analytical/numerical wind engineering researches and experimental wind engineering researches. Since the present work falls in the first group, in the follow some proper references are mentioned concerning this topic. For what concerns the field of the structural performances under wind action, the state of the art will be reported in the next chapters.

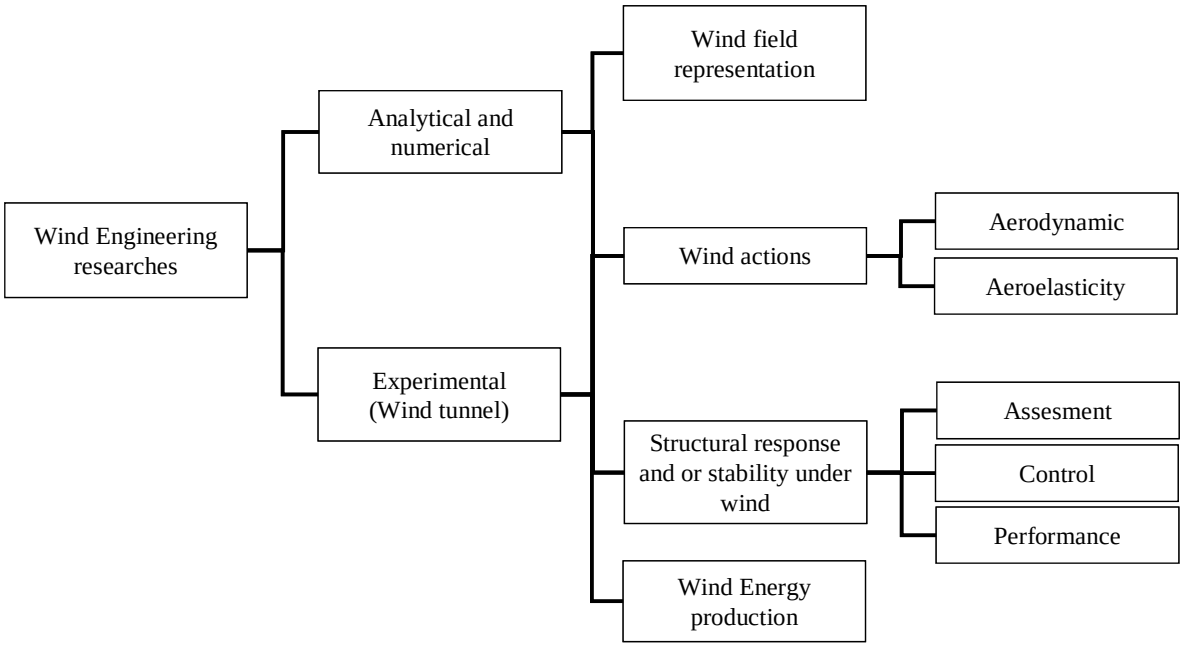

Fig. 1.31. Wind engineering research topics

— Analytical and numerical wind engineering research:

- **Wind field representation**: Carassale and Solari 2006, Di Paola and Gullo 2001, Deodatis 1996, ESDU 2001, Nielsen et al 2004, Rossi et al 2003, Shinozuka and Deodatis 1997.
- **Wind action modeling**: Caracoglia and Jones 2000, Ellingwood and Tekie 1999.
- **Structure under wind**
  - **Response assessment**: Chen et al 2000, Davenport 1998, Jain et al 1996, Kareem 1987, Solari and Piccardo 2001.
  - **Stability assessment**: Bontempi et al. 2000, Diana et al 1993, Lazzari 2005, Salvatori and Borri 2007, Zasso 1996.
  - **Vibration and instability control**
- **Wind energy production**

1.6 Standard and Codes

In the following list, some references are reported for what concerns the standards regarding the wind engineering.

Eurocodes

- Eurocode 1: Basis of design and actions on structures. Part 2-4: Wind actions, CEN, ENV 1991-2-4, 1994.
- Eurocode 1: Actions on structures - General actions. Part 1-4: Wind actions, CEN, EN 1991- 1-4, 2004.

Italian standards (in Italian)

- Ipotesi di carico sulle costruzioni, Circolare LL.PP. N. 4773, 8 giugno 1968.
- Criteri generali per la verifica della sicurezza delle costruzioni e dei carichi e sovraccarichi, D.M. 3 ottobre 1978.
- Ipotesi relative ai carichi e ai sovraccarichi ed ai criteri generali per la verifica di sicurezza delle costruzioni, Circolare LL.PP N. 18591, 9 novembre 1978.
- Aggiornamento delle norme tecniche relative ai "Criteri generali per la verifica della sicurezza delle costruzioni e dei carichi e sovraccarichi", D.M. 12 febbraio 1982.
- Istruzioni relative ai carichi e ai sovraccarichi ed ai criteri generali per la verifica di sicurezza delle costruzioni, Circolare LL.PP N. 22631, 24 maggio 1982.
- Norme tecniche relative ai "Criteri generali per la verifica di sicurezza delle costruzioni e dei carichi e sovraccarichi", D.M. 16 gennaio 1996.
- Istruzioni per l'applicazione delle "Norme tecniche relative ai criteri generali per la verifica di sicurezza delle costruzioni e dei carichi e sovraccarichi", di cui al decreto ministeriale 16 gennaio 1996, Circolare LL.PP. N. 156AA.GG./STC., 4 luglio 1996.
- Norme tecniche per le costruzioni, D.M. 23 settembre 2005.
- Norme tecniche per le costruzioni, D.M. 2008 e Circolare collegata.
- Ipotesi di carico sulle costruzioni, CNR-UNI 10012, 1964.
- Ipotesi di carico sulle costruzioni, CNR-UNI 10012, 1967.
- Azioni sulle costruzioni, Norme tecniche CNR, N. 10012/81, 1981.
- Istruzioni per la valutazione delle azioni sulle costruzioni, CNR 10012/85, 1985.
- Istruzioni per la valutazione delle azioni e degli effetti del vento sulle costruzioni, CNR-DT 207/2008, 2008.

Other standards and guidelines

- Recommendations for calculating the effects of wind on constructions, European Convention for Constructional Steelwork, ECCS, N. 52, 1987.
- Steel stacks, ASME STS-1-1992, The American Society of Mechanical Engineers, 1992.
- National Building Code of Canada, NRC-CNRC, 1995.
- Loading for buildings. Part 2: Code of practice for wind loads, British Standards Institution, BS 6399, Part 2, 1997.
- Model code for steel chimneys, CICIND, 1999.
- Structural design actions. Part 2: Wind actions, Australian / New Zealand Standard, AS/NZS 1170.2, 2002.
- Wind actions on structures, ISO TC 98/SC 3 N254, ISO/CD 4354 (documento di lavoro, 20.4.2005).
- AIJ Recommendations for loads on buildings, Architectural Institute of Japan, 2005.
- Minimum design loads for buildings and other structures, ASCE/SEI Standard N. 7-05, American Society of Civil Engineers, Structural Engineering Institute, 2005.
- Wind tunnel studies of buildings and structures. ASCE manuals and reports on engineering practice No. 67, Isyumov, N. (Ed.), Aerodynamics Committee, American Society of Civil Engineers, 1999.
- Environmental meteorology. Physical modelling of flow and dispersion processes in the atmospheric boundary layer. Application of wind tunnels, Verein Deutscher Ingenieure, VDI 3783, 2000.

1.7 Uncertainties in wind engineering

Wind engineering field is characterized by a great number of uncertainties affecting every aspect of the procedures or models adopted to face with the structural problems. This makes the "Aeolian risk quantification and reduction" a big issue of the field.

Following (Davenport 1998), assuming that a preliminary version of the structure has been developed, there are a series of steps that can be taken in the design process to achieve of safety against the wind:

1. identify the physical mechanisms generating the wind action;
2. define suitable models (whether physical, analytical or qualitative) for describing the wind field, the structure and the wind actions and for predicting the response;
3. define parameters for the models;
4. assess the uncertainties in the models and the parameters.

This last step is the basis of a consistent Aeolian risk analysis. This analysis includes, among others, a probabilistic performance evaluation analysis that, in particular, is the subject of the present work.

First of all, could be important to define the typologies and the source of uncertainties affecting the problem. From the definition of the problem uncertainties, the strategies follow in handling the various entities.

Is important to outline that, following the most possible coherent point of view, no one entity could be treated as deterministic, and the uncertainties affecting the various entities could not be univocally identified and defined. Nevertheless it is not the goal of this work to discuss about this philosophic aspect and a classical point of view will be adopted to treat the uncertain entities.

Among the enormous number of parameters characterizing a physical problem, Morgan and Hernion (1998) suggest that for reasons of both rationality and simplicity, only the so called "empirical parameters" should be treated as probabilistic entities; these are defined as "the measurable proprieties of the real-world system being modeled". In the case of wind engineering problems, some examples of empirical parameters are: the wind speed and turbulence, the structural damping and structural stiffness, the aerodynamic forces or coefficients etc.

The empirical parameters are defined separately from other quantities of the physical problem as for example the so called "defined constants", which comprise both the fundamental physical constants and the empirical parameters that can be measured or computed in such a way to reduce the uncertainties to a small degree. Examples of defined constant are: the

gravitational constant, the air density in a certain range of the air flow velocity, or mathematical constants such as π.

The uncertainties affecting the empirical parameters (called simply "parameters" in the following) have various origins, among which Morgan and Hernion (1998) consider:

- random error;
- subjective judgment and systematic error;
- linguistic imprecision;
- variability;
- randomness and unpredictability;
- disagreement;
- approximation.

Separately from previous, the last uncertainty origin is the modeling activity.

In the next chapters, a simplified classification will be adopted to formulate a probabilistic procedure for the performance assessment. In the following, referring to the basic concepts previously reported, the major uncertainties affecting the wind engineering physical parameters are listed.

Wind speed field characterization. As previously stated, the wind speed field has a stochastic nature. The major uncertainties involving in its characterization are related with the unpredictable nature of both the magnitude and the direction of the wind speed and turbulence; these are generated from the previously mentioned causes of variability and randomness and unpredictability.

Structural behavior characterization. Here the classical structural uncertainties are present, these concerns the structural mechanical behavior (strength, stiffness and damping, material characteristics, etc.), the structural geometry and the structural part relationship (stress transmission, coupling of parallel or serial stiffness and damping, etc.).

Mechanical wind-structure exchanges. The third basic source of uncertainties is related with the physical mechanisms (dynamic, aerodynamic and aeroelastic phenomena) which arise when the structure is immersed in the wind field. These are considered separately from the previous ones because they are generated from the exchange of energy between the wind and the structure. Following this point of view, it is evident that they are conditioned from the previous sources of uncertainties.

1.8 References

Bruno, L. and Khris, S. (2003). “The validity of 2D numerical simulations of vortical structures around a bridge deck”, Mathematical and Computer Modeling 37, 795- 828.

Carassale, L. and Solari, G. (2006). “Monte Carlo simulation of wind speed field on complex structures”, J Wind Eng. Ind. Aerodyn. 94 (1) 323-339.

Caracoglia, L., Jones, N.P. (2003). “Time domain vs. frequency domain characterization of aeroelastic forces for bridge deck section”, J Wind Eng. Ind. Aerodyn. 91, 371-402.

Chen, X., Matsumoto, M. and Kareem, A. (2000). “Time domain flutter and buffeting response analysis of bridges”, J. of Eng. Mechanics (January) 7- 16.

Davenport, A.G. (1998). “Probabilistic methods in wind engineering for long span bridges”, Proc. of the Int. Symp. on Advances in Bridge Aerodynamics, May 1998, Copenhagen, Denmark.

Deodatis G. (1996). "Simulation of ergodic multivariate stochastic processes", Journal of Engineering Mechanics, vol. 122, 778-787.

Di Paola M., Gullo I. (2001). "Digital generation of multivariate wind field processes", Probabilistic Engineering Mechanics, vol. 16, 1-10.

Diana, G., Bruni, S., Cigada, A. and Collina, A. (1993). “Turbulence effect on flutter velocity in long span suspended bridges”, J Wind Eng. Ind. Aerodyn. 48, 329-342.

Diana, G., Falco, M., Bruni, S.,Cigada, A., Larose, G.L., Damsgaard, A. and Collina, A. (1995). “Comparison between wind tunnel tests on a full aeroelastic model of the proposed bridge over Stretto di Messina and numerical results”, J Wind Eng. Ind. Aerodyn. 54/55, 101-113.

Ellingwood B.R. and Tekie P. B. (1999). “Wind load statistics for probability-based structural design”, J. Structural Engineering, Vol. 125, No. 4, pp. 453-463.

ESDU (Engineering Sciences Data Unit) (2001), Report N. 86010: “Characteristic of atmospheric turbulence near the ground. Part III: variations in space and time for strong winds (neutral atmosphere)”, http:// www.esdu.com.

Nielsen, M., Larsen, G. C., Mann, J., Ott, S., Hansen, K. S. and Pedersen, B. J., (2004). Wind Simulation for Extreme and Fatigue Loads, Risø Report 1437(EN), Risø National Laboratory, Roskilde, Denmark.

Holmes, J.D.. Wind loading of structures, Spoon Press, 2001.

Kareem, A., (1987). “Wind effects on structures: a probabilistic viewpoint”, Probabilistic Engineering Mechanics, 4(2), 166-200.

Jain, A., Jones, N.P. and Scanlan, R.H. (1996). “Coupled flutter and buffeting analysis of long-span bridges”, J. of Structural Engineering, ASCE, 122(7): 716-725.

Lazzari, M., Vitalini, R. V. and Saetta, A. V. (2004). “Aeroelastic forces and dynamic response of long-span bridges”, Int. J. Numer. Meth. Engng., 60, 1011- 1048.

Lazzari, M. (2005). “Time domain modeling of aeroelastic bridge decks: a comparative study and an application”, Int. J. Numer. Meth. Engng., 62, 1064- 1104.

Morgan, M. G. and Henrion, M., Uncertainty, Cambridge University Press, 1998.

Petrini, F., Giuliano, F. and Bontempi, F. (2005). “Modeling and simulations of aerodynamic in a long span suspension bridge”, Proceedings of the ninth International Conference on Structural Safety and Reliability, ICOSSAR ’05, Rome, Italy.

Salvatori, L. and Borri, C. (2007), “Frequency and time-domain methods for the numerical modeling of full-bridge aerolasticity”. Computer & Structures (85), 675-687.

Scanlan, R.H. and Tomko, J.J., (1971). “Airfoil and bridge deck flutter derivates”, J. of Eng. Mechanics Div. ASCE, Vol. 97, 1717-1737.

Shinozuka M., Deodatis G. (1997). "Simulation of stochastic processes and fields", Probabilistic Engineering Mechanics, vol. 12, no. 4, 203–207.

Simiu, E., Scanlan, R.H. Wind effects on structures, John Wiley e sons Inc., third edition 1996.

Solari, G. Piccardo, G. (2001). “Probabilistic 3-D turbulence modeling for gust buffeting of structures”, Probabilistic Engineering Mechanics, (16), 73–86.

Stømmer, E., Theory of Bridge Aerodynamics, Springer, New York, 2006.

Theodorsen, T., (1931 a). On the theory of wing section with particular reference to the lift distribution”, NACA Report No. 383.

Theodorsen, T., (1931 b). Theory of wing section of arbitrary shape, NACA Report No. 411.

Theodorsen, T., (1935). General theory of aerodynamic instability and the mechanism of flutter, NACA Report No. 496.

Zasso, A. (1996). “Flutter derivates: Advantages of a new representation convention”, J. Wind Eng. Ind. Aerodyn. 60, 35-47.

Chapter 2

PERFORMANCE-BASED ENGINEERING (PBE) AND PERFORMANCE-BASED DESIGN (PBD)

A definition of Performance Based Design (PBD) can be obtained by generalizing as follows the definition formulated by SEAOC1 with specific reference to seismic engineering (SEAOC 1995): "Performance-Based Engineering consists of those actions, including site selection, development of conceptual, preliminary and final design, construction and maintenance of a structure over its life, to ensure that it is capable of predictable and reliable performances. The life of a structure includes also its dismission and/or demolition. Each of the above actions can have significant impact on the ability of the structure to reliably reach desired performances".

Also the European Structural Codes (Eurocodes) refer to a performance-based approach. As a matter of fact, EN 1990 (CEN 2002), the fundamental document for all Structural Eurocodes, opens with a statement on the performance objectives to be aimed at: "A structure shall be designed and executed in such a way that it will, during its intended life, with appropriate degrees of reliability and in an economical way: (i) sustain all actions and influences likely to occur during execution and use, and (ii) remain fit for the use for which it is required".

2.1 The Performance-based Design (PBD) philosophy and comparison with the prescriptive approach

The content of the prescriptive approach is oriented to the description of how to reach the design targets how to build structures, which means may be employed: it is based on experience and the knowledge of what works well, and imposes specific prescriptions to prevent disasters.

For example, in the design of civil structures, a prescriptive approach makes sure to define all the loads applied and to verify that stresses and strains are within admissible levels; generally speaking, a prescriptive approach leads to an acceptable technical solution, being the margins of freedom quite limited, while a performance oriented approach states explicitly which are the performance requested, and eventually the levels to be guaranteed, giving more freedom to the designer, who can choose the optimum in a range of possible solutions.

As a consequence, the main advantages of a prescriptive approach are:

- the simplicity of the application for a designer;
- the easiness for any controller;
- the consolidation in the tradition and in the experience of specialists.

Yet it represents also an obstacle to innovation and to the design of structures of which there is no experience, and for which most of the prescriptions cannot be applied or even represent a non-sense. Furthermore, in a prescriptive context the proposal of alternative solutions creates procedural difficulties, for the need of demonstrating that the alternative solution is able to get equal performance levels, using equivalence criteria between non-homogeneous solutions.

Another disadvantage of prescriptive codes concern the difficulty for the international trade of construction products: at this regard the *World Trade Organization (WTO)* stated in the clause 28 of the "*Agreement on Technical Barriers to Trade*" (WTO 1997), that "*wherever opportune, the Members shall specify technical regulations based on product requirements in terms of performance rather than design or descriptive characteristics*". So the subscribers of this Agreement committed themselves to use the performance language in trade.

Generally speaking, the Performance-based Design, represents a modern, continuously growing and versatile option to overcome these difficulties. In a project, it makes sure of fixing directly the performance guideline required and moves, in the space of the free variables, using extensively the capabilities of materials and the composition of the sub-structures maximizing the possible levels of efficiency, if the capabilities of materials and technologies are demonstrated to be adequate for the targets with satisfactory levels of performance (safety, functionality, etc.).

A Performance-based Approach to the design requires a clear description of the requested performance, not related to the final specific technical solution, while the levels of performance could be expressed also in reliability terms to keep into account possible uncertainties. Consequently in this process a new relevance is given to the *Clients/Users*, who

pay for the work but must declare their needs, while the *Suppliers/Designers* have the task of offer a technical solution, including the estimated performance. The way of establishing, verifying and validating the performance is the open area of research.

The greater freedom for the designers, now free from many prescriptions, stimulates innovation but is paid in terms of need of a greater knowledge of the phenomena and, broadly speaking, implies an increase of responsibility.

In general, the final agreement between Designers and Users, established in the draft of the *Design Specification*, are a "mix" of prescriptive and performance statements: more performance-oriented the statements are, and more freedom the designer will have to provide different alternative solutions (Figure 2.1).

A low-level specification has a high prescriptive content, and gives low margins of freedom; for high-level of performance specification the designers' freedom grows but it is more difficult to establish universal criteria of evaluations.

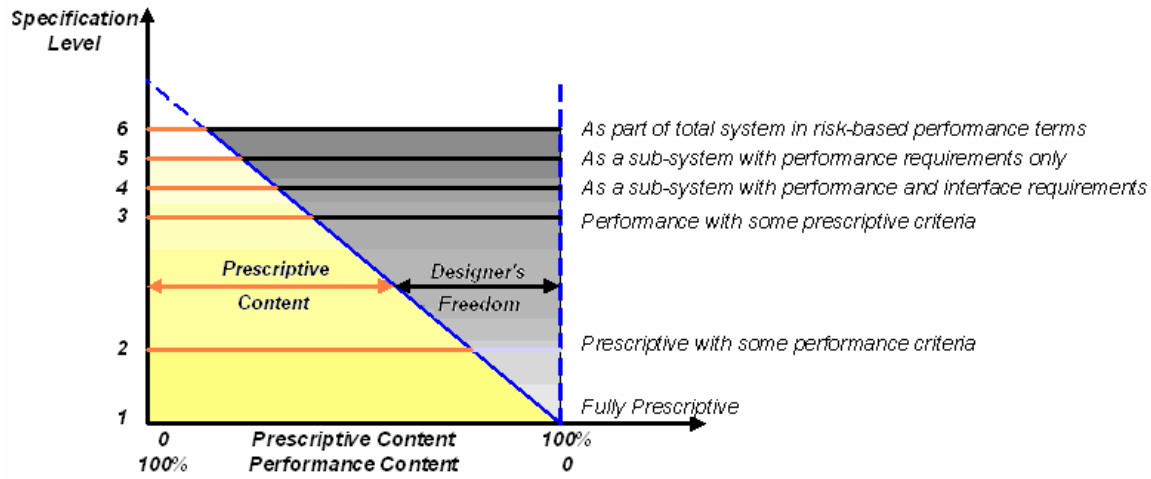

Fig. 2.1. Prescriptive vs Performance approach (Bontempi 2006).

If a product is considered as a matrix of components - *Parts* - and *Attributes*, the main difference between the traditional prescriptive approach and the performance oriented one can be summarized as in Fig. 2.2:

- following the prescriptive approach the components of the product are specified with an adequate level of description, leading to a product with certain attributes;
- following the performance approach only the requirements and the performance to be satisfied are fixed, and the absolute freedom to get them in different ways is left, with different combinations of constructive components (*Parts*). This focus on the

performance to be guaranteed extends the fields of the constructive technologies and areas of research.

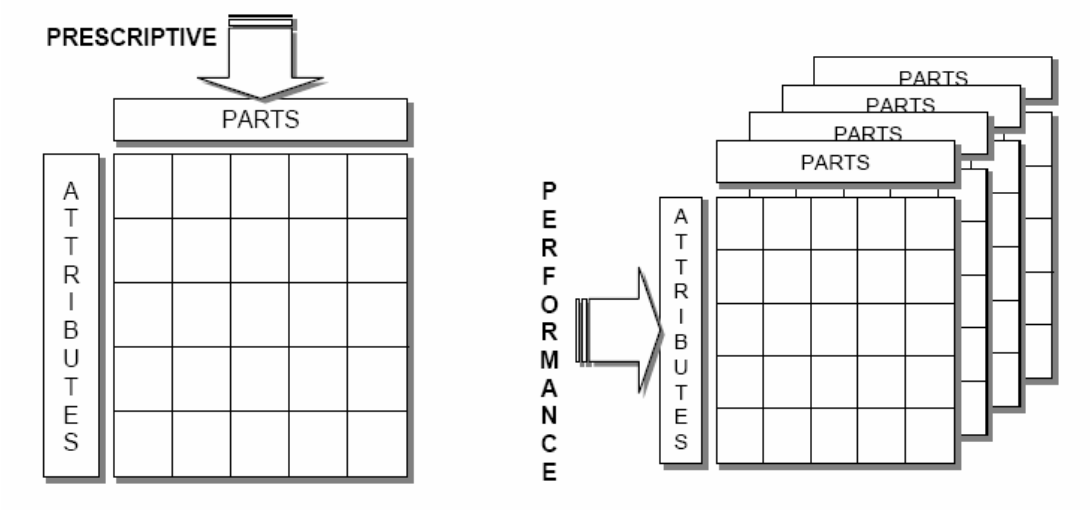

Fig. 2.2. Prescriptive vs Performance approach: Attribute Specifications and Parts (Foliente, 2000)

The expression *Performance-Based Design (PBD)* refers to a performance oriented approach, where:

- the design is conducted in way that the structural system can perform its functions with prefixed and acceptable margins of safety;
- the requested performance is a qualitative/quantitative measure of the efficiency of the system, when it is subjected to the actions and load during its service life.

The primary target of the PBD is the creation of a framework in which all the performance to be guaranteed are stated and the *Customers/Owners/Users* are previously informed, and take an active role, on the design, construction, overlooking steps and costs to get the expected performance levels. Such modern approach encourages the dialogue and the interaction between all the professional sub-systems involved in the process.
The performance approach requires that the satisfactions of the performance are certified, by experimental tests and numerical computations.

The Performance Approach, as it applies to building, is not new; it can be traced back thousands of years. King Hammurabi of Babylon, who reigned from 1955 to 1913 B.C., is credited for the first recorded building regulation. The Article 229 of the Hammurabi Code states: "*The builder has built a house for a man and his work is not strong and if the house he*

has built falls in and kills a householder, that builder shall be slain". King Hammurabi provided a performance statement, addressing structural safety entirely in terms of user requirements, did not state how to construct the building, and did not refer to building structure or building materials.

The modern development of Performance-based and objective-based codes starts in the seventies with the "Nordic Model" (NKB 1978): this model contains one of the key characteristics of the Performance approach, the dialog and the negotiation between the WHY + WHAT and the HOW, shown in the summary diagram of Fig. 2.3.

The goals and the user needs (WHY) are expressed by explicit functional statements and performance requirements (WHAT), and transformed in acceptable solutions (HOW) by the suppliers, who must demonstrate their technical validity.

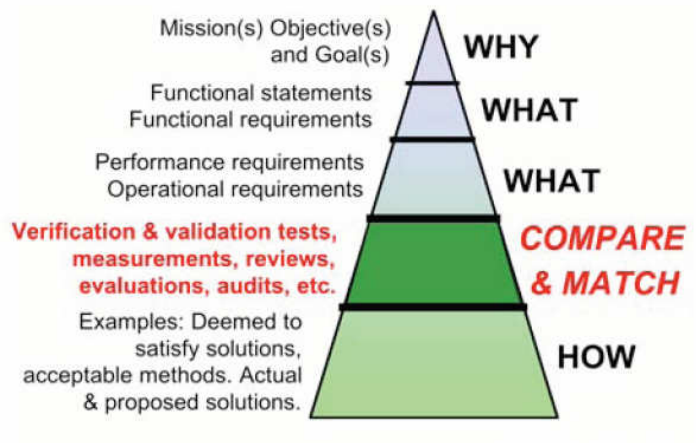

Fig. 2.3. The Nordic Model Approach for Design (Szigeti & Davis, 2005).

The targets and their hierarchy must be stated in a precise, unambiguous, measurable way, in form of attributes of the product, in order to define univocal criteria of choice for the alternative design solutions (Figure 2.4).

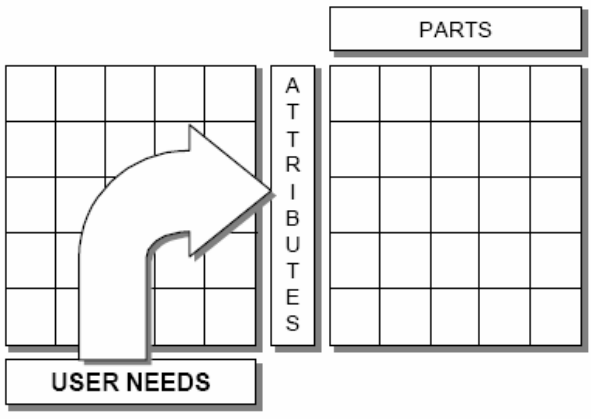

Fig. 2.4. Performance-based Design: Users' request and Specifications (Foliente, 2000).

The quantification of the expected performance levels must consider possible incomplete knowledge and require also the application of probabilistic methods, concerning the possible environmental interactions, the material uncertainties, the human factors. For innovative design this phase results particularly critical: there is generally a lack of information, and the judgement of experts already involved in similar works is desirable or even necessary.

Furthermore the definition of the performance requirements is generally done in the early stages of the design, when there is a lack of quality information for the process control. In this stage there is a lot of flexibility for process control. As the design-build process progresses, this flexibility decrease while more and more refined information become available (Fig. 2.5).

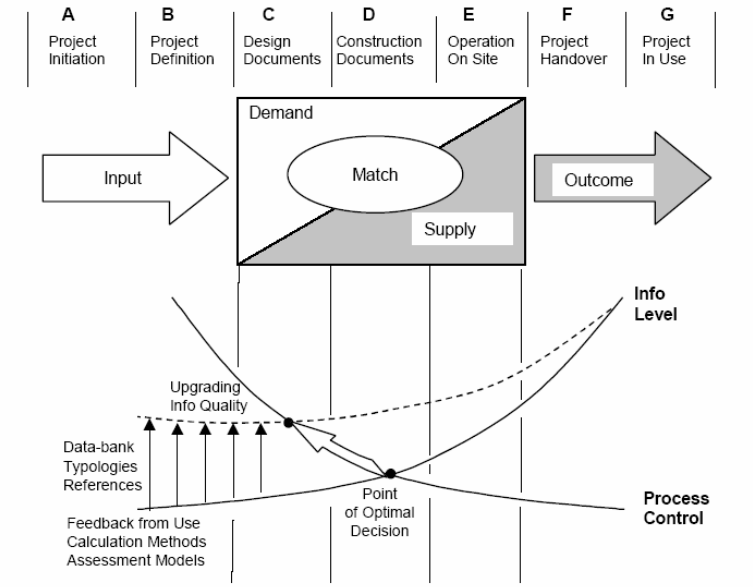

Fig. 2.5. Application of the Performance Approach in the Design Process (Ang and Wyatt, 1998).

The collection and management of the information is an important tool to optimize the performance levels of the product: a possible strategy consists of setting a database (*data-bank*) of information of similar products already realized and in service, of which also mathematical models are available.

2.1.1. Performance Decomposition and Dependability

The design and the construction of the object must be developed in such a way to get an optimum level of *Dependability*.

The term is used to describe the availability of performance and its influencing factors: reliability, performance, maintainability performance and maintenance support performance.

Dependability is generally used for general descriptions in non-quantitative terms and it is a time-related aspect of quality.

It can be considered, as a whole, by the complex of performance (*Attributes*) and its influencing factors (*Threats*) (Figure 2.6).

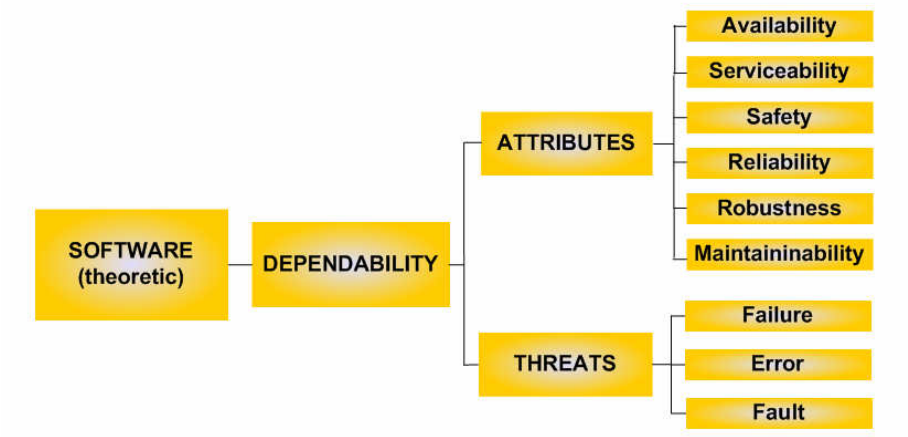

Fig. 2.6. Scheme of Performance Decomposition of a Structural System (Bontempi, Gkoumas, Arangio, 2008a).

The *Attributes* include the characteristics of the product as required by the Client. In particular the following performance (each corresponding to minimum levels expected, and with different hierarchic relevance in the decision process):

- *Availability*, which is the degree of effectiveness for the users;
- *Serviceability*, which is the degree of functionality performance of the system;
- *Safety*, which represent absence or tolerable levels of danger for humane life and environment;
- *Reliability*, which represents the ability of the system to perform Safety and Serviceability during time;
- *Robustness*, which is the capability of not being damaged by accidental loads, like fire, explosions, airplane impact or consequences of human error, to an extent disproportionate with the severity of the triggering event;
- *Maintainability*, which is the ease and the speed by which any activity related to the preservation and upgrade of the structure can be carried out on the system or its parts.

Each of the attribute defined for the product finds expression in a list of specific demands of expected performance.

The *Threats* for a system can be classified as:

- *Failure*, which is the system deviance from compliance with the system specifications for a specified period of time;
- *Errors*, which is an incorrect state of the system: it may be or may not be a possible cause of failure for the system;
- *Fault*, which is a defect and represents a potential cause of error, active or dormant: it can be due to natural causes (environment, materials, etc.) or to human-made causes (accidental or deliberated).

Concerning structures, the Attributes and the requirements are motivated by the following main aspects:

- the *Structural Serviceability*: Availability, Functionality, Comfort.
- the *Structural Safety*: Resistance, Stability, Rigidity, Ductility;
- the *Structural Robustness*;
- the *Durability*.

Structural Serviceability can be defined as the ability of the structure to satisfy the functional requests during the service life.

Structural Safety can be defined as the ability of the structure to guarantee the resistance requirements.

Structural Robustness can be defined as the ability of a structure to absorb proportional damage for exceptional and accidental cause (impact, fire, and explosion).

Durability can be defined as the ability of the structure to keep correctly in the time the previously seen qualities, if an opportune maintenance plane is provided.

The confidence on the fulfilment of these requirements must be supported by analytical results, obtained by reliable numerical models representing the behaviour of the structure *as designed* with an adequate degree of accuracy.

The computed performances offered by the structure are compared within *Limit States* corresponding on:

- *Service Limit States (SLE)* for Serviceability;
- *Ultimate Limit States (SLU)* for Safety;
- *Structural Integrity Limit States (SLIS)* for Robustness.

Limit States correspond to conditions beyond which the defined tasks are not satisfied.

2.1.2. Quantified Performance Criteria and Design

The satisfaction of the user requirements, transferred to Attributes for the structure, must be verified through performance criteria and analytical/numerical tools.

A *Performance Criterion* is an explicit statement of the features that a product must have to satisfy a certain performance (i.e. structural safety, fire resistance, thermal comfort, etc.).

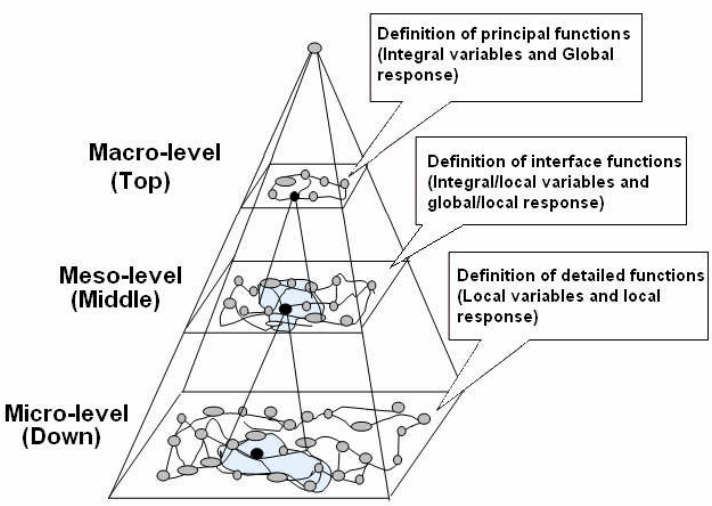

Fig. 2.7. Recursive Modeling: hierarchical layering (Bontempi, 2006).

When the Performance Criterion is expressed in quantitative form, a mathematical relation is written, relating the Performance and all the parameters that play a significant role.

- These statements can be deterministic (*Technology-Based Performance criteria*) or expressed in a probabilistic context (*Risk-Based Performance criteria*).

The formal expression of the Performance Criterion can be stated as follows:

$$\underline{R} = \underline{F}\left(\underline{x}_f, \underline{\bar{x}}_l, \underline{x}_r; \underline{\bar{E}}\right); \qquad R_i \geq \overline{R_i} \;\; \forall i \tag{2.1}$$

where $R = \left[R_1, R_2, ...R_i, ...R_n\right]^T$ is the vector of the performance established to be guaranteed;

$\underline{x}_f$ is the vector of the free variables of design;

$\underline{\bar{x}}_l$ is the vector of the locked variables of design (established);

$\underline{x}_r$ is the vector of the variables that vary within a defined interval: $x_{rj} \in \left[a_j, b_j\right]$;

$\underline{\bar{E}}$ represents the design environment;

$\overline{R_i}$ represents the minimum expected value for the i-th performance.

The vector of the Performance Functions $\underline{F} = [F_1, F_2, ...F_i, ...F_n]^T$ gathers accurately the functions that relate the performance of the system to the design variables: in general, these relations are nonlinear, affected by uncertainties and they identify different combinations of optimal variables for each performance controlled.

Possible solutions of the problem (Suppliers' solutions) are all the combinations of the design variables satisfying the stated equations.

The aspect remarking the difference between the Performance-based Approach and the traditional prescriptive one is that if the problem has no solutions, some release can be made for some range of the variables or in the expected performance (*negotiation*) to gain a possible solution. This negotiation process is identified, ordered and clarified to all the Stakeholders. When more than one solution is possible, since each performance identifies different optimal combinations of the design variables, an arbitrary (in some sense) establishment of hierarchies of the performance induces the final choice. This is the deep essence of design: a decision process, essentially rationally based but intrinsically and inescapably subjective, sometimes addressed as heuristically based.

2.2 Performance-based codes organization

In order to fix the basic aspects of the PBD, in this section the general scheme describing the performance-based codes organization as outlined by Rosowsky and Ellingwood (2002) is reported in Fig.2.8.

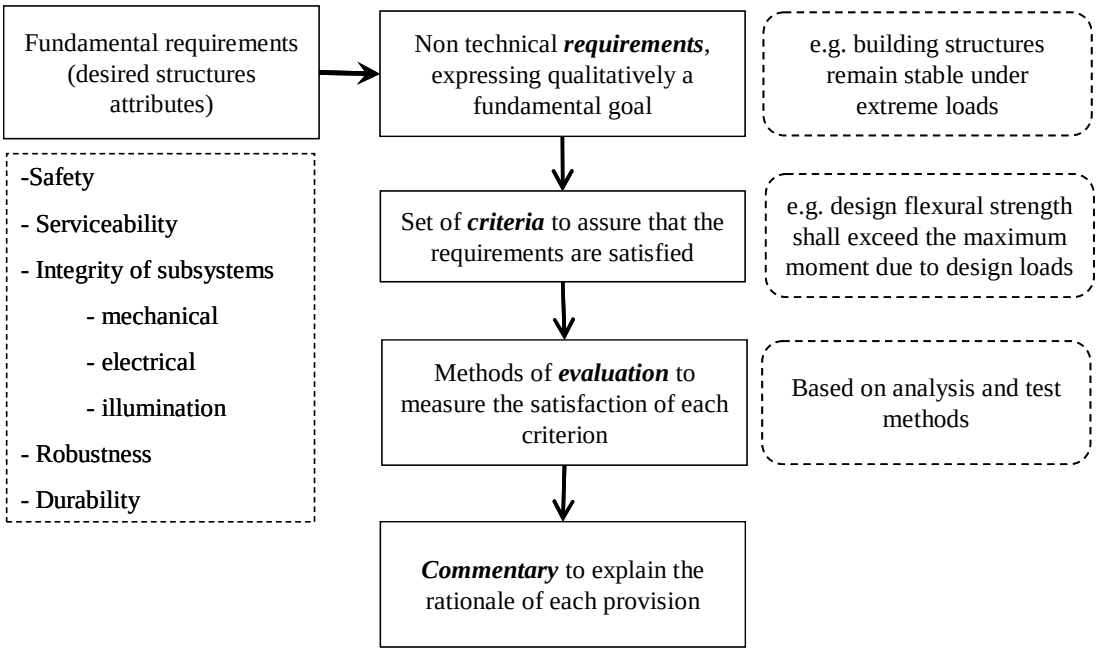

Fig.2.8. Performance-based codes organization.

2.3 Probabilistic approach in the PBD

The, EN1990 definition of the PBE, correctly recognizes that the achievement of the performance objectives cannot be guaranteed in deterministic terms, but must be put in a probabilistic framework ("with appropriate degrees of reliability"); recognizes, moreover, that these objectives are conditioned by economical restraints ("in an economical way").

As previously stated, the whole PBD process must follow a probabilistic approach since the satisfaction of the required performances and the analyses that should be carried out for evaluating them are affected by significant uncertainties (see section 1.7). Generally speaking, the uncertainties can spread their selves during the various design and/or analysis phases that are developed in cascade; an alignment of uncertainty sources could produce an unacceptable level of unquantifiable risk.

An amount of methods and procedures have been developed to govern or reduce the uncertainties affecting the structural engineering problems; the engineering field that deal with the modeling of uncertain systems response determination is called *reliability engineering* (Ditevslen and Madsen 1996, Der Kiureghian 1996, Lewis 1994, Franchin et al. 2002a and 2002b, Pinto et al. 2004, Franchin 2004).

In general in a probabilistic approach, the involved parameters describing the problem are treated as stochastic entities for which it is possible to define a certain probability distribution. The parameters can be subdivided in two main groups: the first describing the actions or the actions effects and the second describing the resistance or the capacity of the structure.

With reference to the Fig.2.8, for what concerns the design phase, the probabilistic approach is applied in the definition of proper *criteria* for the performance evaluation (step2) and in the development of “methods of evaluation to measure the satisfaction of each criterion” (step 3).

The most used method to perform the previous mentioned steps is the well known *semi-probabilistic limit states method;* here the performances are expressed in terms of overcoming probability of certain *limit states*, and the uncertainties are taken into account by using of the so called *Load and Resistance Factors* (LRF).

In the LRF design (LRFD) method, opportune factors (for which the magnitude is calibrated on the parameters statistics) multiplying the parameters are introduced in order to taking into account the uncertainties.

More evolutes approaches exist for the probabilistic PBD. Generally speaking, they are based on the stochastic system theory which is schematically represented in Fig.2.9: there are a certain number of stochastic input parameters θ_i (i=1,…,n) for the observed system, having

corresponding joint Probability Density Functions (PDFs) $q(\underline{\theta})$, where $\underline{\theta} \in R^n$ is the vector of uncertainties parameters, and the underline indicates a vector. The system can be represented by various deterministic models M_j (Input/output relations), each of them has a probability of occurrence $P(M_j)$ (with $\Sigma P(M_j)=1$) and, consequently, both output parameters and failure relations are probabilistic too.

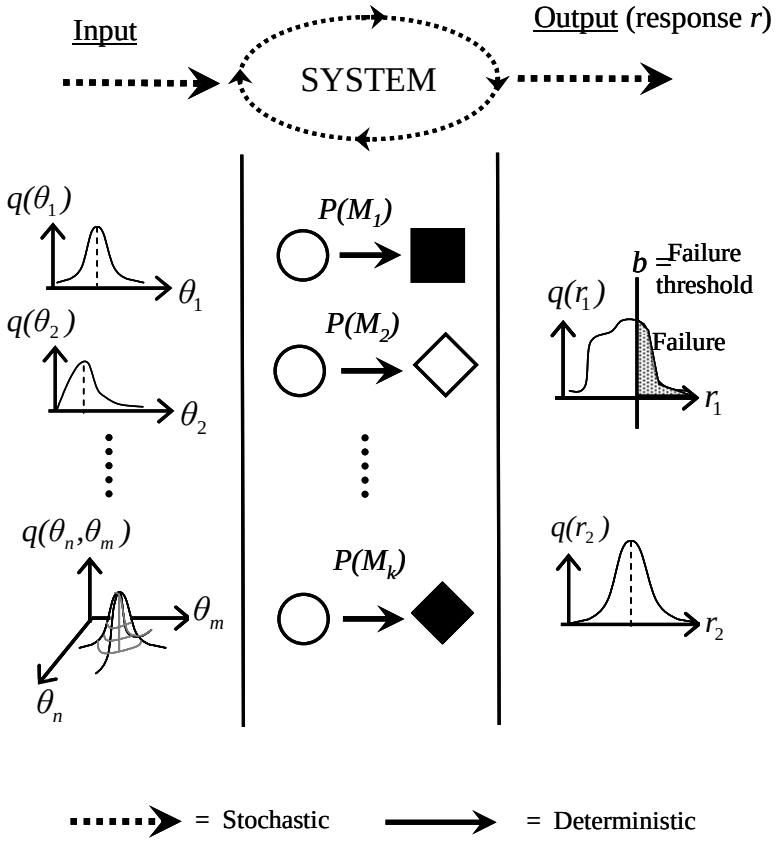

Fig.2.9. Stochastic system analysis

In the stochastic system analysis, the expected value J of a certain function (model) $h(\theta)$, can be computed by the probability integral:

$$J = E[h(\underline{\theta})] = \int h(\underline{\theta}) \cdot q(\underline{\theta}) \cdot d\underline{\theta} \qquad (2.2)$$

The occurrence probability of a certain value r^* for the response r is characterized by a probability

$$P(r = r^* | \underline{\theta}) \qquad (2.3)$$

which is conditioned to the values of the stochastic input parameters.

It is usual that inside the vector $\underline{\theta}$ there is some parameter describing the intensity measure of the stochastic loads acting on the structure (or system); great efforts have been spent in

seismic engineering in order to individuate a scalar parameter of the intensity measure (*IM*) that is *sufficient* and *efficient*, as reported in the next section. (Baker and Cornell 2006) .

2.3.1. Fragility curves

In the fully probabilistic approach to the PBD, design for specific level performance requires not only the connection between performance level and structural limit state (LS), but also a relation between the LS and the annual probability of occurrence (Rosowsky and Ellingwood 2002). The performance objective can be expressed as the *mean annual frequency of failure* (λ(LS)) where with *failure* it is intended the over crossing of the specific LS. It is desirable to express the LS by means of scalar threshold values (r_i*) for opportune response parameters (r_i) and describing the structural state by using of scalar demand-to-capacity ratios (e.g. for the limit state LS_i it is $Y_i = r_i / r_i$*). Under these assumptions, the mean annual frequency of failure for structure exposed to hazard can be expressed as

$$\lambda(LS_i) = \int_0^{\infty} P(Y_i > 1 \,|\, IM) \cdot dIM \qquad (2.4)$$

Where $P(Yi>1|IM)$ is the conditional probability of failure given *IM*, which is know as the *fragility curve*.

2.4 An example: Performance-based earthquake engineering by the PEER approach

Performance-based earthquake engineering (PBEE) is a methodology that incorporates desired performance levels into the earthquake design process. Performance in PBEE can be expressed in economic terms, or as elapsed downtime, or in terms of life and building safety objectives. These performance objectives are relevant to various types of stakeholders.

A number of studies have been developed in the field of the PBEE. Among others, in what follows it will be made particular reference to Jalayer et al (2007), Augusti and Ciampoli (2008), Mitrani-Reiser (2007), Kunnath (2007), Ching et al (2004), Ellingwood (2001), to explain the PBEE procedures.

2.4.1. Total Probability theorem

In the context of structural reliability it is useful to introduce the complementary Cumulative Distribution Function (CCDF), which denotes the probability that the random variable, for

example a response quantity, will *exceed* a certain value. The CCDF is herein denoted $G(x)$, so that $G(x^*)$ indicates the probability that the outcome of x will exceed x^*. In passing it is noted that the PDF is obtained by differentiation of the CDF or CCDF:

$$f(x) = dF(x)/dx = \left|dG(x)/dx\right| \tag{2.5}$$

Several of the rules of probability are applicable to random variables. Of particular interest in this study is the total probability theorem, which for events A, E_1, E_2, …, E_N reads

$$P(A) = \sum_{i=1}^{N} P(A|E_i) \cdot P(E_i) \tag{2.6}$$

where E_i represents a collection of mutually exclusive and collectively exhaustive events. In other words, none of the events E_i can happen simultaneously, and the probability of their union is equal to unity. The significance of equation (2.6) lies in the fact that knowledge of the conditional probabilities $P(A|E_i)$ and the individual probabilities $P(E_i)$ enables the computation of the unconditional probability $P(A)$. Translated into the domain of continuous random variables, the total probability theorem to obtain the CCDF of a random variable x is an integral of the form:

$$G(x) = \int_{-\infty}^{\infty} G(x|y) \cdot f(y) dy \tag{2.7}$$

where the integration is performed over the entire outcome range of the continuous random variable y, and the conditional CCDF $G(x \mid y)$ is interpreted as the CCDF of x given a certain outcome of y.

2.4.2. PEER performance-based framework

The Pacific Earthquake Engineering Research (PEER) center's approach, is a modular framework in accordance with the PBEE philosophy.

The PEER evaluation methodology is summarized in Fig. 2.10. The methodology comprises four distinct but related phases: *hazard analysis* that characterizes the seismicity at the site; *structural analysis* of a simulation model that yields the necessary force and deformation measures; *damage analysis* to enable transformation of response measures into physical states of damage; and *loss analysis* that relates the damage to a measure of performance.

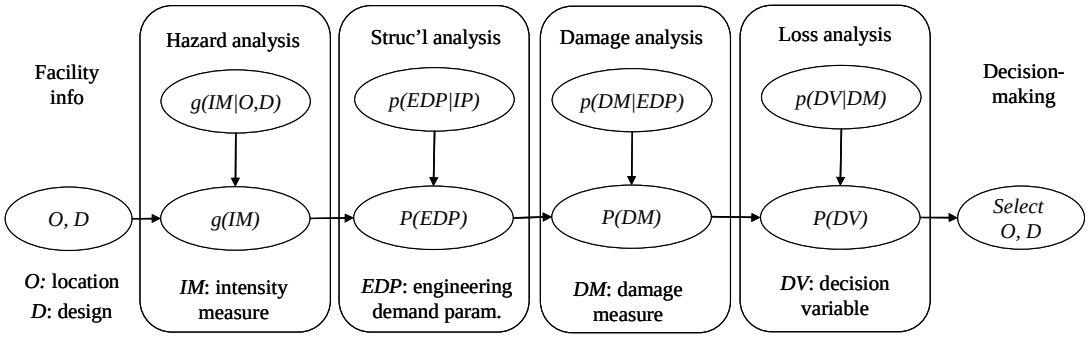

Fig. 2.10. PEER performance-based evaluation framework (after Kunnath 2007)

Figure 2.10 also introduces abbreviations to describe measures of intensity, response, damage, and loss estimates. These abbreviations described briefly in the following.

Intensity Measures (*IM*s). This denotes a measure of ground motion intensity. Several choices of this measure are possible: peak ground acceleration, spectral acceleration, and magnitude at some characteristic period of the structure. Recommendations have also been made to utilize a vector of *IM*s instead of simple scalar measures. Baker and Cornell (2004) proposed a method for determining an optimal vector of *IM*s for use in performance-based evaluation.

Engineering Demand Parameters (*EDP*s). Seismic demand needs to be characterized by a limited set of response measures that are referred to as *EDP*s. In the case of building structures, the displacement at the roof of the structure or the interstory drift ratio is a typical response measure that can be correlated with damage and performance. Other examples of demand parameters include: forces, stresses, strains, and cumulative measures such as plastic deformation and dissipated energy. For bridge structures a larger subset of response measures exists. Damage to bridges can result from movement of the foundation, substructure, or superstructure. Hence, in a realistic evaluation, it may be necessary to monitor a vector of *EDP*s. In the PEER framework, the measure of interest is the conditional probability p(*EDP*|*IM*).

Damage Measures (*DM*s). This refers to the conversion of response measures to quantifiable damage states. For bridge structures, possible damage states that can be identified during post-event bridge inspection include amount and degree of concrete spalling, buckling of longitudinal reinforcing bars, fracture of transverse reinforcement, and horizontal and vertical offsets at expansion joints. In the context of the PEER methodology, damage needs to be expressed as a fragility function for different response measures. Hence the outcome of a damage analysis will yield P(*DM*|*EDP*). It is clear that the damage measure relies on the

choice of the *EDP*. Once a fragility curve (cumulative distribution function) is established for a defined damage state and P(*EDP*) is computed, it becomes possible to estimate P(*DM*).

Decision Variables (*DV*s). It is expected that the performance of a structure is defined as a discrete or continuous function with realistic decision-making potential. Such a loss modelling measure is defined as a *DV* in the PEER framework. An example of a *DV* for building evaluation is mean annual loss, for bridges the critical *DV* is the likelihood of closure of the facility. In either case, the *DV*s must be correlated with damage measures (*DM*s) selected in the previous phase so that P(*DV*|*DM*) can be calculated. If the measured damage is conditioned on the intensity measure so that P(*DM*|*IM*) is obtained, it is feasible to assess performance for different hazard levels.

Equation (2.6) forms the basis for the PEER equation, in which the CCDF of a decision variable (*DV*) is computed based on knowledge of conditional probabilities involving the structural performance. In this framework, structural performance is specified in terms of structural response quantities, which have previously been classified as engineering demand parameters (*EDP*s) which, in turn, are functions of the ground motion intensity, or intensity measures (*IM*s). On the other hand, from an owner's or decision-maker's perspective, performance events must be defined in terms of the decision variables, *DV*s, which characterize the cost and/or risk associated with different structural performance outcomes, e.g., the costs of repair and loss of function of a bridge as a result of an earthquake. *DV*s in general depend on the state of the structure as characterized by a set of damage measures (*DM*s). For example, different levels of drift may be used as indicators of different levels of damage to a bridge or building. *DM*s in general are functions of *EDP*s. Thus, one can write *DV*(*DM*(*EDP*(*IM*))). Each of the relationships *DV*(*DM*), *DM*(*EDP*) and *EDP*(*IM*) is, ideally, a probabilistic model that produces a conditional probability. For instance, researchers that study damage models enables the computation of the conditional CCDF *G*(*DM*|*EDP*), that is, the probability that the damage will exceed a certain threshold *given* a certain value of the *EDP*. Some of these models are well developed, while others are subjects of current research within and outside PEER.

To understand the role of the total probability theorem in the development of the PEER equation, assume first that the PDF of the intensity measure, *f*(*IM*) is available (an extension to the mean annual frequency is presented below). The total probability theorem in the form of equation (2.6) is then applied to obtain the CCDF of the *EDP*:

$$G(EDP) = \int_0^\infty G(EDP|IM) \cdot f(IM) dIM \tag{2.8}$$

The corresponding PDF is obtained by differentiation: $f(EDP) = |\mathrm{d}G(EDP)/\mathrm{d}EDP|$. With knowledge of the PDF of the engineering demand parameter, the theorem is subsequently applied to obtain the probability distribution for the damage measure, and thereafter to obtain the probability distribution for the decision variable. The combination of all equations leads to the triple integral:

$$G(DV) = \int_0^\infty \int_0^\infty \int_0^\infty G(DV|DM) \cdot \left| \frac{dG(DM|EDP)}{dDM} \right| \cdot \left| \frac{dG(EDP|IM)}{dEDP} \right| \cdot f(IM) dIM \; dEDP \; dDM \tag{2.9}$$

Equation (2.9) is a variation of the PEER integral. However, in the above derivation it is assumed that *IM* is a random variable that represents the value of the intensity of the impending earthquake. Rather, in the PEER framework it is common to introduce a probabilistic occurrence model to describe the probability of occurrence of earthquakes of varying intensity. The Poisson process is the most frequently employed occurrence model in engineering practice. At each intensity level this process is uniquely defined by one parameter; the mean rate of occurrence, here denoted λ. If the time axis is in years, then λ is equal to the mean annual frequency. The mean rate λ as a function of *IM*, namely λ(*IM*), is interpreted as a seismic hazard curve, which is determined, e.g., by probabilistic seismic hazard analysis. Notably, λ(*IM*) is interpreted as a cumulative distribution function that is differentiated with respect to *IM* before replacing *f*(*IM*) in (2.9). Consequently, (2.9) is written as follows:

$$\lambda(DV) = \int_0^\infty \int_0^\infty \int_0^\infty G(DV|DM) \cdot |dG(DM|EDP)| \cdot |dG(EDP|IM)| \cdot |d\lambda(IM)| \tag{2.10}$$

In Equation (1.5), λ(*DV*) is the mean annual rate of a decision variable exceeding some threshold value *DV; DM* represents the damage measure; *EDP* is the selected engineering demand parameter (such as drift, plastic rotation, etc.); and *IM* represents the intensity measure. *dλ(IM)* is the differential of the mean annual frequency of exceeding the intensity measure (which for small values is equal to the annual probability of exceedance of the intensity measure). It is necessary to use the absolute value of this quantity because the derivative (slope of the hazard curve) is negative. The expression of the form *G(A|B)* is the complementary cumulative distribution function or the conditional probability that *A* exceeds a specified limit for a given value of *B*. The term of the form *dG(A|B)* is the derivative with respect to *A* of the conditional probability *G(A|B).* One useful partial result of equation (2.8)

results prior to the integration over $d\lambda(IM)$, which provides information about the variation of the $G(DV)$ as a function of IM. The advantage offered in expressing the methodology in the above format is that it lends itself to intermediate results of considerable value.
An important issue in probabilistic PBEE is the treatment of uncertainties that arise in each step of the process that can be identified as follow:

Facility definition. To define the facility one must know its location (latitude and longitude) and design, including site soils, substructure, structural and non structural components, jointly denoted by D. One creates an inventory of the damageable assemblies and identifies the engineering demand parameter — EDP, which might be story drift ratio, member force, etc. — that would cause damage to each assembly.
Hazard analysis. In the hazard analysis, one considers the seismic environment (nearby faults, their magnitude-frequency recurrence rates, mechanism, site distance, site conditions, etc.) and evaluates the seismic hazard at the facility considering D, to produce the seismic hazard, g[IM|D], where IM refers to the intensity measure. IM can be parameterized in any of a variety of terms, such as peak horizontal ground acceleration, Arias intensity, etc. It is common to use Sa(T1), the damped elastic spectral acceleration at the small-amplitude fundamental period of the structure, which is readily available by using software such as Frankel and Leyedecker (2001), adjusting to account for site classification such as by using Fa or Fv as appropriate from the 2000 International Building Code (International Code Council, 2000). In the present analysis, we use Sa(T1) for IM.
Structural analysis. In the structural analysis, the engineer creates a structural model of the facility in order to estimate the uncertain structural response, measured in terms of a vector of engineering demand parameters (EDP), conditioned on seismic excitation and design (p[EDP|IM,D]). EDPs can include internal member forces or local or global deformations, including ground failure (a partial list of EDPs in use by PEER is provided in Porter, 2006). The structural analysis typically takes the form of a series of nonlinear time-history structural analyses using a suite of strong-motion records that are scaled to have the specified IM. The structural model need not be deterministic some PEER analyses have included uncertainty in the mass, damping, and force-deformation characteristics of the model. The present study does so, as will be discussed later.
Damage analysis. EDP is then input to a set of fragility functions that model the probability of various levels of physical damage (expressed via damage measures, or DM), conditioned on structural response and design, p[DM|EDP,D]. Physical damage is not described at a

detailed level, but instead is defined relative to particular repair efforts required to restore the component to its undamaged state. Fragility functions currently in use give the probability of various levels of damage to individual beams, columns, non-structural partitions, or pieces of laboratory equipment, as functions of various internal member forces, story drift, etc. These functions are drawn from laboratory or field experience. For example, PEER has compiled a library of destructive tests of reinforced concrete columns (Mitrani-Reiser, 2007). The result of the damage analysis is a probabilistic vector of DM. Note that component damage may be correlated with structural characteristics of D, even conditioned on EDP.

Loss analysis. The last stage in the analysis is the probabilistic estimation of performance (parameterized via various decision variables, DV), conditioned on damage and design p[DV|DM,D]. Decision variables measure the seismic performance of the facility in terms of greatest interest to stakeholders, whether in dollars, deaths, downtime, or other metrics. Dollar losses can be estimated using standard construction-contracting principles, given the detailed damage state of the facility. Deaths can be estimated using empirical casualty estimates (Ching et al 2004).

Decision-making. The analysis produces estimates of the frequency with which various levels of DV are experienced, given the facility definition D. These frequencies can be used to inform a variety of risk-management decisions. For example, a common concern among insurers the need for reinsurance to deal with catastrophically high losses. Consequently, it is of interest to know the frequency with which future repair cost will exceed some ruin threshold, G[DV|R], where G[X|Y] refers to the frequency with which X is exceeded, conditioned on knowledge Y. For an individual facility exposed to seismic risk, one can calculate this ruin frequency as

$$G(R|D) = \int_{DV=R}^{\infty} G(DV|D) \cdot dDV \qquad (2.11)$$

Defining the problem of uncertainty propagation. Observe that DV can be viewed as a deterministic function of a number n of uncertain input variables. For example, if we are concerned with uncertain future repair costs, we can consider the hazard model as an uncertain parameter IM, the structural model as a set of one or more structural variables (SM), the fragility model as a set of uncertain capacities C, and the loss model as a set of unit repair costs (URC), etc, collectively denoted by X, i.e.,

$$DV = f(X) \qquad (2.12)$$

where X = {IM, SM, C, URC, …} $\in R^n$ contains all basic variables. The problem of uncertainty propagation under PEER's PBEE framework can be defined as follows: Given the moments or joint PDF of X (we will call it the X PDF), the goal is to determine the moments of DV or the probability that DV will exceed a threshold value (i.e. determine the PDF of DV).

Following the PEER methodology, the fragility function (equation (2.4)) is represented by the conditional probability of attaining a certain value of the damage *DM* given an intensity measure IM

$$fragility\ \ function = P(DM \mid IM) \tag{2.13}$$

2.5 References

Ang, G.K.I. and Wyatt, D.P. (1998). "The rolo of performance specification in the design agenda", Proceedings of the Design Agenda Conference, Brighton, UK, September 1-18.

Augusti, G., Ciampoli, M., (2008), "Performance-Based Design in risk assessment and reduction", Probabilistic Engineering Mechanics, 23, 496-508.

Baker, J. W., and C. A. Cornell., (2004). Choice of a vector of ground motion intensity measures for seismic demand hazard analysis. Proceedings of the 13th World Conference on Earthquake Engineering, Vancouver, Canada.

Bontempi, F. (2006), "Basis of Design and expected Performances for the Messina Strait Bridge". Proc. of the International Conference on Bridge Engineering – Challenges in the 21st Century, Hong Kong, 1-3 November, 2006.

Bontempi, F., Gkoumas, K. and Arangio, S. (2008a), "Systemic approach for the maintenance of complex structural systems". Structure and infrastructure engineering, vol. 4; pp. 77-94, ISSN: 1573-2479, doi: 10.1080/15732470601155235.

CEN (European Committee for Standardization) (2002): EN 1990 - Basis for Structural Design. Brussels, Belgium; 2002.

Ching, J., Porter, A.K. and Beck, J., (2004). Uncertainty propagation and feature selection for loss estimation in performance-based earthquake engineering, Report EERL 2004-02, Pasadena, California, United States. Available on line at http://peer.berkeley.edu/publications/peer_reports.html.

Der Kiureghian, A., (1996). "Structural reliability methods for seismic safety assessment: a review", Engineering Structures, 18(6), 412-424.

Ditevslen, O. and Madsen, H.O., Structural Reliability Methods, John Wiley & Sons Ltd, Chichester, 1996.

Ellingwood, B.R. (2001). "Earthquake risk assessment of buildings structures", Reliability Engineering and System Safety, 74, 251-262.

Foliente, G.C. (2000), "Developments in performance-based building codes and standards", Forest Products Journal, 50 (7/8), 91-109.

Franchin, P., Ditlevsen, O. and Der Kiureghian, A. (2002a), "Model correction factor method for reliability problems involving integrals of non-Gaussian random fields", Probabilistic Engineering Mechanics, Elsevier, Vol 17(2): 109-122.

Franchin, P., Lupoi, A. and Pinto P.E., (2002b), "Methods of seismic risk analysis: State-of-the-Art versus advanced State-of-the-Practice", Journal of Earthquake Engineering, Imperial College Press, Vol.(6) Special Issue 1: 131-155.

Franchin, P. (2004) "Reliability of uncertain inelastic structures under earthquake excitation" ASCE Journal of Engineering Mechanics Vol 130(2): 180-191.

Frankel, A. and E.V. Leyendecker, (2001). Uniform Hazard Response Spectra and Seismic Hazard Curves for the United States, Open-File Report, US Geological Survey, Menlo Park, CA

Jalayer, F., Franchin, P. and Pinto, P.E. (2007). "A scalar damage measure for seismic reliability analysis of RC frames", Earthquake Engng. and Struct. Dyn., 36: 2059-2079.

Lewis, E.E., Introduction to Reliability Engineering, John Wiley & Sons Ltd, New York, 1994 (2nd ed.)

Kunnath, S.K., (2007). Application of the PEER PBEE Methodology to the I-880 Viaduct, PEER Report 2006/10 (I-880 testbed committee). Available on line at http://peer.berkeley.edu/publications/peer_reports.html.

International Code Council, (2000). International Building Code 2000, International Conference of Building Officials, Withtier, CA.

Mitrani-Reiser, J. (2007). An ounce of prevention: probabilistic loss estimation for performance - based earthquake engineering, Report EERL 2007-01, Pasadena, California, United States. Available on line at http://peer.berkeley.edu/publications/peer_reports.html.

Pinto, P.E., Giannini, R. and Franchin, P., Seismic reliability analysis methods, IUSS Press, Pavia, Italy, 2004.

Porter, K.A., (2006). EDP List, Pacific Earthquake Engineering Research Center, Richmond, CA: www.peertestbeds.net/Crosscutting.htm

Rosowski, D.V. and Ellingwood, B.R., (2002). "Performance-Based Engineering of wood frame housing: Fragility Analysis methodology", Journal of Structural Engineering, 128(1), 32-38.

SEAOC (1995). Vision 2000 - A Framework for Performance Based Design. Vol. I-III, Structural Engineers Association of California, Sacramento, CA.

Szigeti, F. and Davis, G. (2005). Performance Based Building: Conceptual Framework. EUR21990 Final Report, available online at http://www.pebbu.nl

PART II

PBWE FORMULATION

Chapter 3

PROBABILISTIC PERFORMANCE BASED WIND ENGINEERING (PBWE) APPROACH

This section is dedicated to the analytical formulation of the PBWE procedure, after a short report on the state of the art in the field, a classification of the wind effects on the different structural typologies is made and a definition of some limit states under wind action is proposed; after that, a wind engineering uncertainties classification and an hypothesis on their propagation are proposed, these two will drive the formal probabilistic formulation of the problem, which is subsequently developed.

In order to introduce this chapter, a briefly history of the wind engineering is reported. One of the best historical short introductions has been given from Solari and Augusti (1998) in a special issue of the scientific journal *Meccanica* (http://www.springerlink.com/content/102958/) and reported below:

> *According to the definition given by Cermak in 1975, "Wind Engineering is best described as the rational treatment of interactions between wind in the atmospheric boundary layer and man and his works on the surface of earth".*
>
> *It is said that Chinese already used wind mills from 4000 B.C. Many have maintained that wind science first appeared in the city of Kahun in Egypt, founded by King Sosostris II round 2000 B.C., where the poorer quarters sheltered the richer quarters from the hot desert wind. Somebody holds that wind study was born when anemological instruments where invented. Several scholars locate this moment between the first and the second century B.C., when a windvanewas placed on the Tower of the Winds in Athens. Others say that the crucial innovation was Leonardo da Vinci's anemometer.*
>
> *Many authors place the dawn of wind engineering with the first experiments with winds. In this regard, some quote Robin's invention, in 1746, of the rotating arm to measure the resistance of projectiles and optimize their shape. Others speak of the first wind tunnel built*

by Wenham towards the end of the 19th century. Somebody remembers the full-scale pressure measurements carried out by Baker in 1884 during the building of the Forth Bridge. Someone else recognizes the father of this science in Gustave Eiffel, because of the measures he took on his tower between 1889 and 1894.

Some aerodynamic scientists attribute their origins to Vogt's intuitions in 1860 on the flight of the albatros. Irminger is considered another precursor of the discipline due to the tests he carried out in 1893 at the Copenhagen gas-works. Someone considers the first boundary layer wind tunnel realized by Bailey in 1943 at the National Physical Laboratory of Teddington as the turning point of the new science. Others opt for Martin Jensen and his 1958 model law as the onset of experimental wind engineering.

Also the origin of studies concerning wind-excited response of structures is not so sure. But a turning point was certainly the episode of the Tacoma Narrows bridge in 1940. Soon after its opening on 1st July, this very slender suspension bridge showed repeatedly significant oscillations at wind speeds much lower than the design speed. Thus, when on 7th Novembre the oscillations begun increasing to worrying amplitudes, the traffic was immediately shut and no casualty occurred when the bridge collapsed some hours later, while an amateur cameraman recorded what is still the most impressive film of a disastrous collapse of a man-made structure. Cinema and television have shown hundreds of times the film of the Tacoma Bridge, so that it is now familiar also to laymen. However, the specialists cannot forget that the film was the in vivo experimental evidence which inspired and supported the studies that allowed the great fluid dynamist Von Kàrmàn to explain the collapse. A few years before, Von Kàrmàn had discovered the phenomenon of vortex shedding, and Lord Rayleigh acknowledged the discovery by indicating that it was vortex shedding which activated the legendary aeloian Harps. Von Kàrmàn understood that the Tacoma bridge was the victim of another aeroelastic phenomenon, still unknown to structural engineers but already much feared by designers of aeroplanes: flutter. And other disasters of the past, like the collapse of the suspended Brighton Pier in the middle of the 19th Century, where attributed to the same phenomenon.

Since 1940, the knowledge of the wind response of structures has developed greatly, thanks to many researches. However, the fundamental step probably occurred in 1961, when Alan Garnett Davenport published his fundamental paper in the Proceedings of the Institution of Civil Engineers. What is certain is that the study of the actions and effects of wind on built-up and natural environment is today, in the engineering panorama, one of the most relevant and pressing lines of research because of the importance and variety of the scientific, technological and technical problems it concerns.

Drawing its principles from several disciplines like physics of the atmosphere and fluid mechanics, meteorology and micro-meteorology, urban planning, architecture and

bioclimatic studies, aerodynamics and aeronautics, civil, environmental, energy and mechanical engineering, physiology and psychology, wind engineering develops autonomous concepts and methods which are applied in all sorts of contexts. It deals with forecasting and mitigating damage caused by storms, which alone are responsible for over 80% of the human casualties and economic losses that the world suffers from natural events, with the representation and measure of the wind and its related meteorological phenomena, the forecasting of weather and climatology, the aerodynamics of constructions and vehicles, wind tunnel experiments, the computer simulation of the flow fields and of actions of wind on bluff bodies, the wind behavior of all constructions, in particular towers, skyscrapers, bridges, large roofs and all structures whose safety depend on wind, the diffusion of atmospheric pollutants, the quality of air and environmental protection, the use of wind energy and the choice of sites for wind turbines, the land planning in terms of wind problems.

The scientific management of this sector is entrusted to the International Association for Wind Engineering (IAWE), founded in 1975 through the action of the Steering Committee for the International Study Group on Wind Effects on Buildings and Structures. IAWE has the primary purposes of liaising with national and international organizations working in similar fields and convening every four years the International Conferences on Wind Engineering (ICWEs) (Teddington 1963, Ottawa 1967, Tokyo 1971, London 1975, Fort Collins 1979, Gold Coast and Auckland 1983, Aachen 1987, London Ontario 1991, New Delhi 1995, Copenhagen 1999). Together with the Journal of Wind Engineering and Industrial Aerodynamics, formerly Journal of Industrial Aerodynamics since 1975, ICWEs trace the fundamental steps of the subject and reveal its rapid evolution.

The International Association for Wind Engineering is divided into three regions – the European and African Region, the American Region and the Asia-Pacific Region – whose activities are co-ordinated by regional chairmen. These manage relations between the different associations or national groups and plan the scientific initiatives of their area, first of all the Regional Conferences which take place in the mid-year between two world conferences. After the conference held in Guernsey, U.K., in 1993, 2 EACWE was the second official conference of the IAWE European and African Region. It will be followed by 3 EACWE in Eindhoven, in 2001.

Italy, although blessed by a mild climate, has not remained behind in the recent developments of wind engineering. The growing interest in the fieldwas recognized in 1988 with the foundation of the Italian National Association for Wind Engineering (ANIV). ANIV catalyzes the activities of Italian e searchers and engineers operating in this sector promoting, among other initiatives, a National Conference every second year (Firenze 1990, Capri 1992, Roma 1994, Trieste 1996, Perugia 1998) whose national and international relevance has grown steadily. The relevance of Italy in the world panorama of Wind Engineering is proved by the

significant papers published, the co-ordination of major European projects, the chairmanship of the IAWE European and African Region since 1995 and of 2 EACWE in 1997, the editorial role within "Wind and Structures", a new international journal published from 1998, the relevant contribution given to Italian, European and American standards dealing with wind actions and effects on structures, and the recently built and actively operative boundary layer wind tunnel in Prato" (extracted from Augusti and Solari 1998).

3.1 State of the art in the PBWE

The performances of a structure are defined regarding to many types of risks which are not limited to collapses and heavy damages but involve serviceability, comfort of the users, preservation of cultural or historical values, etc.

In the past, the Aeolian one has not been consider a significant risk in comparison of other environmental risks (seismic, floods, etc.), but in the last decades some studies (see for example Augusti et al. 2001) showed that the problems caused by winds cannot be neglected in a rational planning of our structure construction inside the environment. Furthermore, the progress in construction techniques has caused an increasing in the sensitivity of modern structures to the wind action.

For these reasons, a modern approach to wind engineering problems should consider performance aspects as a base for design procedures.

A generalized Performance-Based approach has not yet delineated for wind engineering problems.

Many studies have been conducted on the under-wind structural performances assessment, among others: Unanwa et al. (2000) developed a procedure to asses the wind damage band for the hurricane damage prediction focusing on low and medium rise buildings, Ellingwood et al. (2004) developed a procedure for the fragility assessment of light-frame wood construction subject to hurricanes, Khanduri and Morrow (2003) studied the vulnerability of buildings to windstorms, Garciano et al. (2005) developed a procedure for the assessment of some performances of wind turbines subject to typhoons, Pastò and de Grenet (2005) gave indications on the probability of occurrence of certain wind-induced risks for bridges, Pagnini (2005) focused the attention on the reliability of structures with uncertainty parameters under wind action, recently Zhang et al. (2008) defined the probability density functions for basic random parameters of a wind field and proposed a procedure for the reliability assessment of tall buildings and Norton (2007) proposed a systematic approach to evaluate performances under wind action. Very recently, Augusti and Ciampoli (2008) shown the validity of the

Performance-Based Design as a strategy for the Aeolian risk assessment, and van de Lindt and Dao (2009) proposed a procedure for the PBWE of wood-framed buildings based on the fragility assessment related to five different performance levels.

In Italy, after a very preliminary introduction (Paulotto et al., 2004), initial steps in the PBWE direction have been performed within a research project sponsored by the Ministry of University and Research (Bartoli et al. eds., 2006), named PERBACCO project, with specific reference to tall buildings. In the PERBACCO report volume, Augusti and Ciampoli (2006) introduced the use of the PEER equation (Porter 2003) in PBWE procedures; later Sibilio and Ciampoli (2007) studied the performance of a footbridge subject to turbulent wind by using of advanced Monte Carlo techniques; very recently Petrini et al. (2008) have proposed a modified seismic risk assessment procedure for the study of the fatigue damage to the hangers of a long span suspension bridge under wind action.

3.2 Sensitivity of different structural typologies to the wind effects

For the scope of this work, it is worth noting the essential differences between dynamic response of structures to wind and earthquake. The main differences between the excitation forces due to these two natural phenomena are:

- Earthquakes are of much shorter duration than windstorms (with the possible exception of the passage of a tornado), and are thus treated as transient loadings.
- The predominant frequencies of the earthquake ground motions are typically 10 - 50 times those of the frequencies in fully-developed windstorms. This means that structures will be affected in different ways. e.g. buildings in a certain height range may not experience significant dynamic response to wind loadings, but may be prone to earthquake excitation.
- The earthquake ground motions will appear as fully-correlated equivalent forces acting over the height of a tall structure. However, the eddy structure in windstorms results in partially-correlated wind forces acting over the height of the structure. Vortex-shedding forces on a slender structure also are not full correlated over the height.

The comparison of the wind and the earthquake spectra (Fig. 3.1) can also give an idea of the structural typologies which are sensitive to each environmental action; in particular, one can appreciate the variety of frequencies composing the wind spectra. Nevertheless the figure is representative only of such a problems in which the fluid-structure interaction effects are not relevant (response problems). In fact, when an aeroelastic phenomenon arise, in the major cases it does not depend on the wind frequency content.

The various aerodynamic and aeroelastic phenomena described in the previous chapters are related to the specific structural typologies subjected to the wind action.

For example, the vortex shedding phenomena is typically relevant for high rise tubular structures (like chimneys or piles) and for bridges decks or cables. The galloping phenomenon is characteristic of coupled transmission cables. The flutter and the torsional divergence can arise in particular for suspension bridge. The buffeting phenomenon can be relevant for whole typologies of structures due to the large frequency content of the wind spectrum.

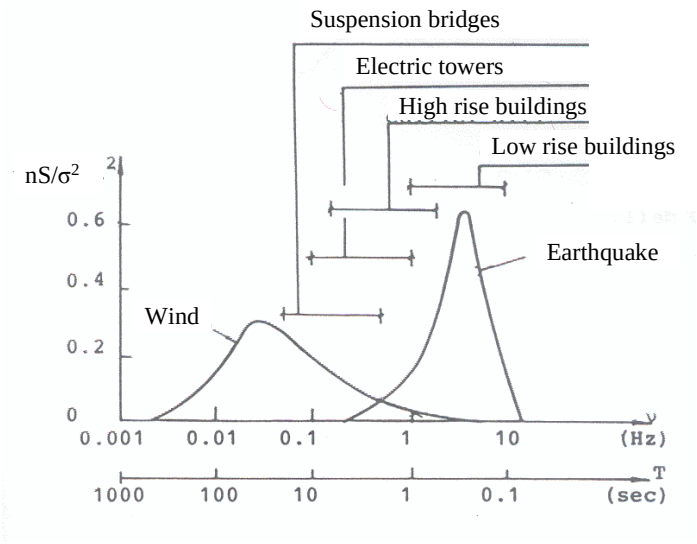

Fig. 3.1. Wind and earthquake spectra (after Faravelli, 1998).

The high variety of both the wind sensitive structures and the involved phenomena gives an idea of the complexity in defining a general procedure for the performance-based wind engineering.

3.2.1. **The wind engineering in the actual analysis process**

In the design of ordinary structures (Fig. 3.2), the structural response under wind action is evaluated in order to check that some requirements (say performances), which in general are not specifically related with the wind effects, will be satisfied. This goal is usually achieved by maintaining the design inside certain canonical features (e.g. adopting a well known shape for a bridge deck section depending on the span), and repeating the checks if some changes are made with respect to the previous design configurations (due for example to the optimization of some seismic performance).

In other words the improvement of the structural performances under wind action rarely drives the structural optimization process, and the wind is considered simply as a variable action that has to be considered in the limit states load combinations following a semi-probabilistic characterization (e.g. using the LRFD method).

Under this philosophy, no standardized under-wind performances have been defined for the different structural typologies, and general standardized fully probabilistic approaches which are outlined with specifically regard to the wind engineering don’t exist yet.

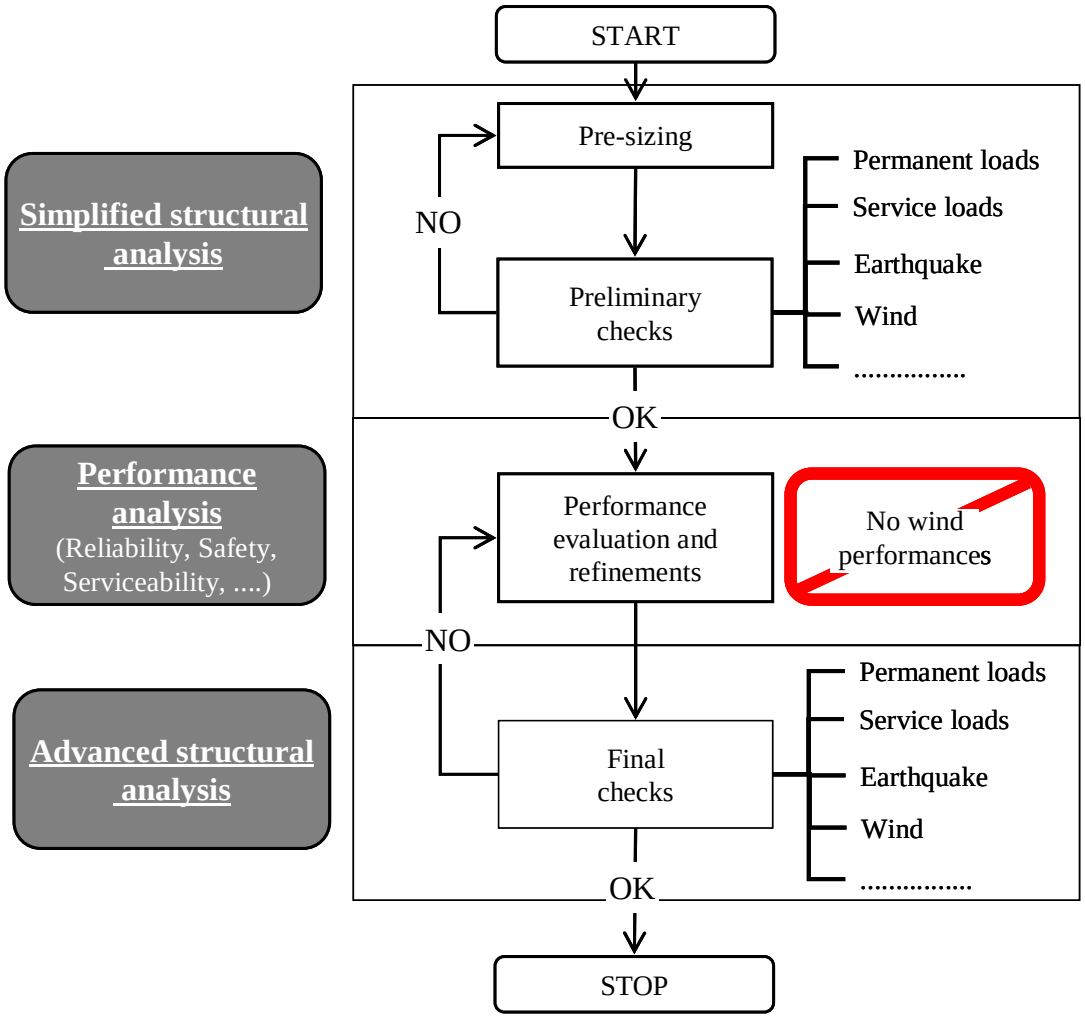

Fig. 3.2. Wind engineering in the design process

A main objective of the research in the field of the PBWE is to give to the designers a robust framework to conduct the so called *performance analysis* (Fig. 3.3).

In terms of Standards, a first step toward the PBWD has been done from the recent Italian guideline CNR-DT 107/2008 (CNR 2008) which, for example, defines some specific requirements for the structures under wind action in order to avoid the arising of certain characteristic wind instability phenomena. Nevertheless, this orientation is basically given by furnishing deterministic tools for the performance analysis (as described in Fig.3.4 following the *deterministic analysis* branch).

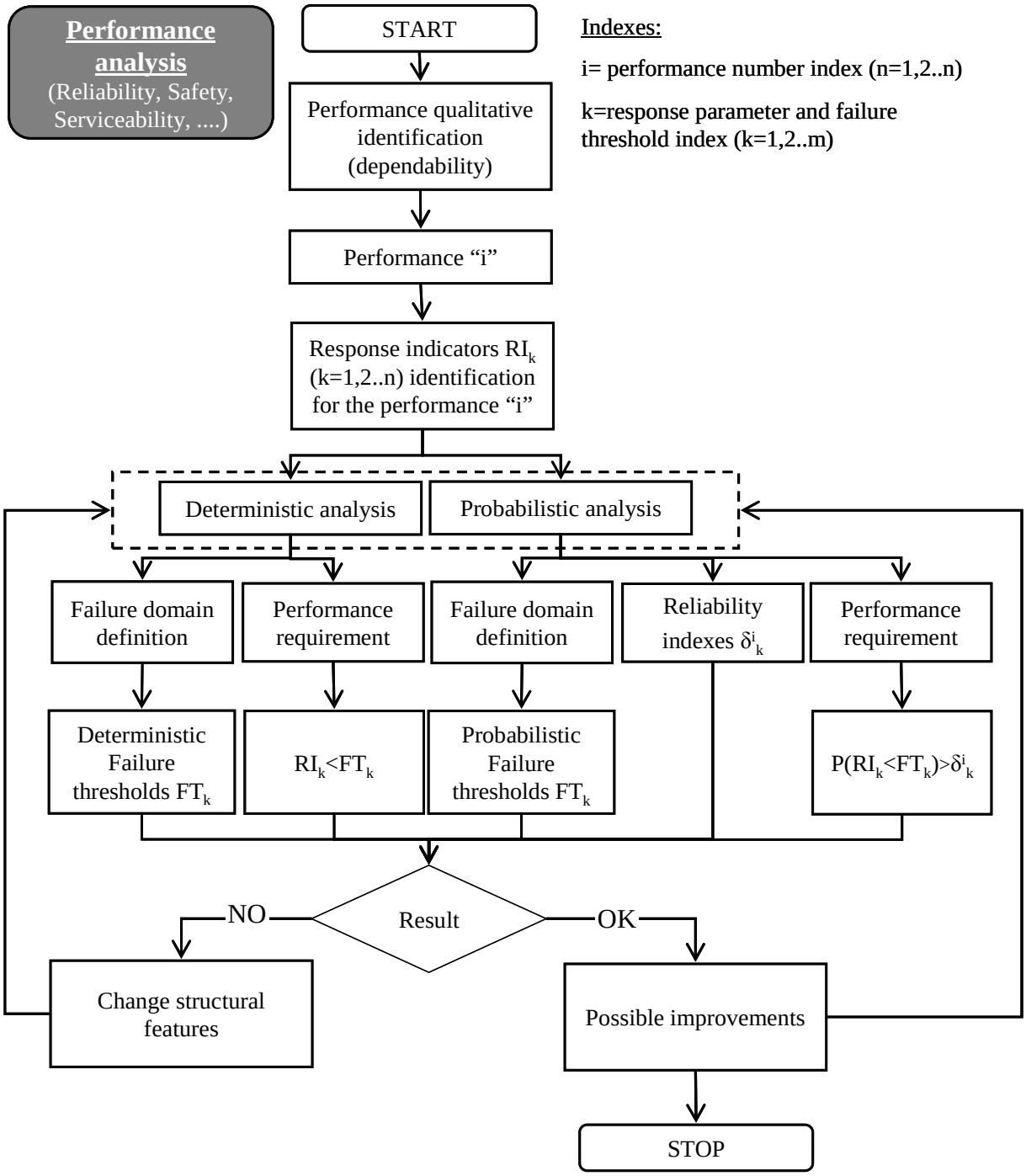

Fig. 3.3. Performance analysis

3.3 Performances of wind exposed structures

As previously stated (section 3.2), different classes of structures are prone to different wind effects. In order to give a general classification of the structural performances under wind action, two main performance levels will be defined:

1. *high level performances*: related with the serviceability of the structures or with the users comfort, this level of performances has to be maintained in the most wind storm cases. The high level performances are analytically expressed by using of Service Limit States (SLS). The lack of low level performances could be achieved mainly in the cases of:
   - a1 excessive deformations and distortions that can limit usage, efficiency and aspect of the structure (*SLS-D, loss of comfort serviceability limit state*);
   - b1 excessive deformations and distortions that can compromise the efficiency and aspect of non-structural elements, installations, machinery (*SLS-U, usage serviceability limit state)*;
   - c1 excessive vibrations that can compromise the usage of the structure (*SLS-V, vibration serviceability limit state*).
2. *low level performances*: related to the safety of the structure's users or to the maintainability of the structural integrity during its life cycle. The low level performances are analytically expressed by using of Ultimate Limit States (ULS). The lack of low level performances could be achieved mainly in the cases of:
   - a2 reach of the maximum strength capacity of structural components (*ULS-C, collapse ultimate limit stat*e);
   - b2 instability of structure or structural components (*ULS-I, instability ultimate limit state*).
   - c2 fatigue failure in members and joints (*ULS-F, fatigue ultimate limit state*).

For high performance levels related with comfort, it is necessary to define the terms "unacceptable discomfort". As reported in (Simiu and Scanlan 2006), the notion of unacceptable discomfort may be defined in the following way: "in any given design situation various degrees of wind-induced discomfort may be expected to occur with certain frequencies that depend upon the degrees of discomfort, the features of the design and the wind climate at the location in question; the discomfort is unacceptable if any of these frequencies is judged to be too high". Statements specifying maximum acceptable mean frequencies of occurrence for various degree of discomfort are known as discomfort criteria.

For high performance levels related with usage serviceability, the various serviceability criteria are strongly correlated with the type of structure, and they are generally expressed as function of structural displacements and their time derivates. The overcoming of some serviceability limit states it is usually due to the buffeting caused from the atmospheric turbulence or from the arising of Vortex Shedding phenomena.

Concerning the low performances level, the overcoming of ultimate limit states it is usually due to response phenomena under extreme wind condition (like the buffeting caused from the atmospheric turbulence for high wind velocities) or to the arising of some instability phenomenon (like flutter or torsional divergence).

In order to develop a PBWE framework, some performance requirements are here defined for different typologies of wind-sensitive structures, these are synthetically reported in tables 3.1 (low performance levels) and 3.2 (high performance level).

Tables 3.1 and 3.2. Performances of wind exposed structures

	ULS - C	**ULS - F**	**ULS - I**
Tall buildings	BU - strength		
Low-rise buildings	BU – strength cladding		
Bridges	BU - strength	VS – cables decks	FL - flutter
Long-span structures			FL - Instability
Chimneys	BU - strength	VS - Joints	
Antennas	BU - strength	VS - Joints	

	SLS - D	**SLS - U**	**SLS - V**
Tall buildings	BU – VS discomfort		
Low-rise buildings	BU – VS vibrations		
Bridges	BU – VS vibrations		BU – VS Excessive vibrations
Long-span structures			FL - Instability
Chimneys			VS Excessive vibrations
Antennas		BU – VS Transmission parameters	

ULS – I= instability ULS ULS – C= collapse ULS ULS – F= Fatigue ULS
SLS – D= Discomfort SLS – U = availability SLS SLS – V= Vibrations SLS
BU= buffeting VS= Vortex shedding FL= Flutter

Uncertainty parameters

As previously stated, the problem of performance-based design of structures under wind action has to be faced in a probabilistic terms. The first step in a probabilistic analysis is to evaluate the type of uncertainties involved in the problem. In wind engineering problems there are many uncertainties that have various origins, and they can influence the structural response in different manners. Various papers have been written on the topic, among others: Kareem 1987, Solari 1997, Davenport 1995 and 1998, Mann et al 1998, Minciarelli et al. 2001, Nielsen et al. 2004, Pagnini 2005, Zhang et al. 2008.

In the present work, a classification for the uncertainties and their propagation is proposed, this is represented in Fig. 3.4, which can give a general picture of the problem; following the wind course when it impacts on a structure, one can distinguish two zones:

- *environment zone*: it is the physical region which is sufficiently close to the structure in order to assume the same wind-site parameters of the structure, but far enough to neglect the flow field perturbations (in terms of particle's trajectories, pressure field, etc.) induced by the presence of the structure itself. In the environment zone, the wind flow can interact with other environmental agents, changing in its own basic parameters. A typical example of such an interaction is the one between wind and wave in offshore sites. The environment zone propagates both its physical phenomena and its uncertainties in the subsequent regions;
- *exchange zone*: it is the physical region just attached to the structure. In the exchange zone, the structural and the wind field configurations are strictly correlated. Here, the structural system and the wind field experience the mechanical interchange (aerodynamic and aeroelastic phenomena) from which the wind actions arise. In the exchange zone, some non-environmental solicitations are present; they may change the dynamic or aerodynamic characteristics of the original structure. So the wind actions are generated considering this structural sub-system (original structure plus non-environmental solicitations) instead of regarding to the original structure itself. A typical example for this interaction is given from the bridge-train interaction; the train transit can change both dynamic and aerodynamic characteristic of the bridge. By definition, the exchange zone cannot propagate both its physical phenomena and its uncertainties in the environment zone.

Referring to this general picture, it is important to define the typologies and the source of uncertainties affecting the problem. Starting from the definition of the problem uncertainties, the strategies in handling the various uncertainties can be chosen.

Here, concerning the wind engineering problems, a simplified and classical classification is adopted for the uncertainties. Three basic typologies of uncertainties are considered, depending on the source; these are:

- *aleatoric uncertainties*, arising from the unpredictable nature of both the magnitude and the direction of the wind speed and turbulence;
- *epistemic uncertainties*, deriving from both the insufficient information and errors in measuring the previously mentioned parameters;
- *model uncertainties*, deriving from the approximations in our models.

In the environment zone, the *aleatoric* uncertainties have a great relevance; they affect the magnitude of the basic wind-site parameters. In the environment zone the *epistemic* uncertainties are also present. The *model* uncertainties are surely relevant: regarding to wind model, for example, considering the turbulent wind speed field like a Gaussian stochastic process, an uncertainty related to the hypothesis of gaussianity is introduced. The uncertainty parameters of the environment zone will be called *basic parameters* ($\underline{\alpha}$).

In the exchange zone, for the subject of this study, the sources of the aleatoric uncertainties are not considered as relevant as those of the environmental zone; this assumption has two reasons: first, there is not propagation from the exchanged from environment side, second the main scope is to consider the propagation of environmental uncertainties in the structural response. So the aleatoric uncertainties considered in the exchange zone are those caused from the environment zone-aleatoric uncertainties propagation.

In the exchanged zone it is important to subdivide the parameters affected by the uncertainties in two main groups:

- *derived parameters* ($\underline{\beta}$), are those that vary in a significant manner according to the environmental parameters; so they are subjected to a lot of propagated-uncertainties from environment zone. An example is given by the aerodynamic coefficients of a bridge section, because they are very sensitive with respect to the mean velocity of incoming wind;
- *independent parameters* ($\underline{\gamma}$), are those which have a relatively low variation when the environment zone parameters vary their selves. An example is given by the elastic module of the structural materials.

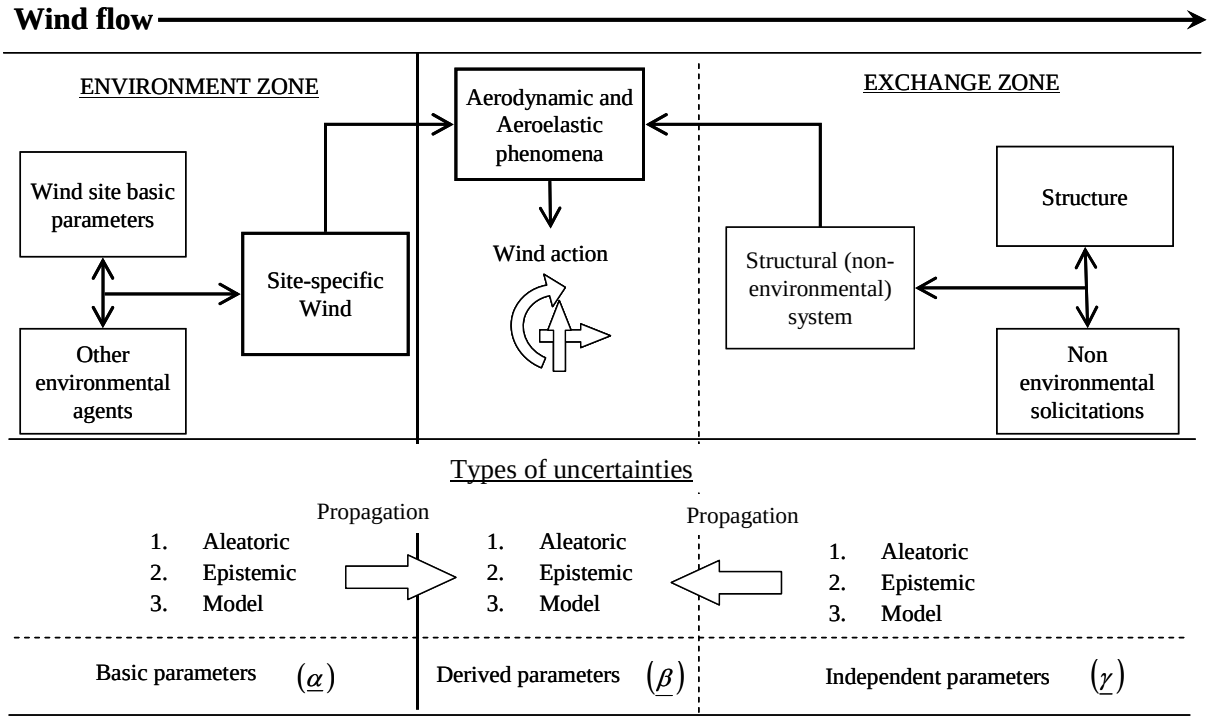

Fig. 3.4. Wind engineering uncertainties.

According to the adopted assumption, the parameters $\underline{\alpha}$ and $\underline{\gamma}$ can be considered as uncorrelated and, they are not affected by the uncertainty propagation coming from the parameters $\underline{\beta}$, while the parameters $\underline{\beta}$ are subjected from the propagation of both $\underline{\alpha}$ and $\underline{\gamma}$ parameters; it can be written:

$$P(\underline{\alpha}|\underline{\beta}) = P(\underline{\alpha}|\underline{\gamma}) = P(\underline{\alpha}) \tag{3.1}$$

$$P(\underline{\gamma}|\underline{\beta}) = P(\underline{\gamma}|\underline{\alpha}) = P(\underline{\gamma}) \tag{3.2}$$

which state the independence of both $\underline{\alpha}$ and $\underline{\gamma}$ parameters.

Retrieving the general rules of the conditional probability, concerning three events *A*,*B* and *C*:

$$P(A,B|C) = \frac{P(A,B,C)}{P(C)} = P(A|B,C)\cdot P(B|C) \tag{3.3}$$

from which:

$$P(A,B,C) = P(A|B,C)\cdot P(B|C)\cdot P(C) \tag{3.4}$$

this, together with the (3.1) or (3.2), can be applied to the introduced parameters obtaining:

$$P(\underline{\alpha},\underline{\beta},\underline{\gamma}) = P(\underline{\beta}|\underline{\alpha},\underline{\gamma})\cdot P(\underline{\alpha}|\underline{\gamma})\cdot P(\underline{\gamma}) = P(\underline{\beta}|\underline{\alpha},\underline{\gamma})\cdot P(\underline{\alpha})\cdot P(\underline{\gamma}) \tag{3.5}$$

3.4 Proposed PBWE procedure

The starting point of the performance assessment procedure proposed here is the total probability theorem (section 2.4.1), which for events A, E_1, E_2, …, E_N reads

$$P(A) = \sum_{i=1}^{N} P(A|E_i) \cdot P(E_i) \tag{3.6}$$

Where, as previously stated, E_i represents a collection of mutually exclusive and collectively exhaustive events. Using the equation (3.6), starting from the knowledge of the conditional probabilities $P(A|E_i)$ and the individual probabilities $P(E_i)$, the unconditional probability $P(A)$ can be computed. Translated into the domain of continuous random variables, the total probability theorem can be used to obtain the CCDF of a random variable x is an integral of the form:

$$G(x) = \int_{-\infty}^{\infty} G(x|y) \cdot f(y) dy \tag{3.7}$$

where the integration is performed over the entire outcome range of the continuous random variable y, and the conditional CCDF $G(x \mid y)$ is interpreted as the CCDF of x given a certain outcome of y; in other words $G(x|y)$ is it the probability that the stochastic variable X will be greater or equal than x when Y (uncertain parameter conditioning the X values) it is greater or equal than y, namely

$$G(x|y) = P[X \geq x | Y = y] \tag{3.8}$$

If there is a vector of uncertain independent parameters ($\underline{\theta}$) instead of a single parameter Y, the equation (3.4) becomes

$$G(x) = \int_{-\infty}^{\infty} G(x|\underline{\theta}) \cdot f(\underline{\theta}) d\underline{\theta} \tag{3.9}$$

Adopting the uncertain parameters vector fragmented as in the previous section,

$$\underline{\theta} = \begin{bmatrix} \underline{\alpha} \\ \underline{\beta} \\ \underline{\gamma} \end{bmatrix} \tag{3.10}$$

and substituting X with a stochastic vector $\underline{R}$ containing a set of parameters describing the response of the structure subjected to the uncertain wind action, the (3.9) becomes

$$G(\underline{R}^*) = \int_{-\infty}^{\infty} G(\underline{R}^* | \underline{\alpha}, \underline{\beta}, \underline{\gamma}) \cdot f(\underline{\alpha}, \underline{\beta}, \underline{\gamma}) \cdot d\underline{\alpha} \cdot d\underline{\beta} \cdot d\underline{\gamma} \tag{3.11}$$

that, with the (3.5) (written in terms of probability density functions), becomes

$$G(\underline{R}^*) = P\left[\underline{R} \geq \underline{R}^*\right] = \int_{-\infty}^{\infty} G(\underline{R}^* \left| \underline{\alpha}, \underline{\beta}, \underline{\gamma}\right) \cdot f(\underline{\beta} \left| \underline{\alpha}, \underline{\gamma}\right) \cdot f(\underline{\alpha}) \cdot f(\underline{\gamma}) \cdot d\underline{\alpha} \cdot d\underline{\beta} \cdot d\underline{\gamma} \qquad (3.12)$$

The equation (3.12) represents a probabilistic relation between the stochastic parameters of the problem.

By defining the failure as the lack of achievement of a certain performance under wind action, the integral (3.12) can be used to compute the probability of failure. This can be done by identifying the performance with an the acceptable value of the occurrence $G(\underline{R})$ of exceeding a threshold value $\underline{R}^*$ or, better, expressing the occurrence as the mean annual rate λ of a response $\underline{R}$ exceeding some threshold value $\underline{R}^*$, that for a scalar response parameter can be expressed as

$$\lambda(R^*) = P\left[R \geq R^*\right] = \int_{-\infty}^{\infty} G(R^* \left| \underline{\alpha}, \underline{\beta}, \underline{\gamma}\right) \cdot f(\underline{\beta} \left| \underline{\alpha}, \underline{\gamma}\right) \cdot f(\underline{\alpha}) \cdot f(\underline{\gamma}) \cdot d\underline{\alpha} \cdot d\underline{\beta} \cdot d\underline{\gamma} \qquad (3.13)$$

Recalling the PEER equation:

$$\lambda(DV) = \int_{-\infty}^{+\infty} P(DV \left| DM\right) \cdot P(DM \left| EDP\right) \cdot P(EDP \left| IM\right) \cdot g(IM) \cdot dDM \cdot dEDP \cdot dIM \qquad (3.14)$$

the equation (3.13) can be rewritten adopting the PEER notation as follow

$$\lambda(EDP) = \int_{-\infty}^{\infty} P(EDP \left| \underline{IM}, \underline{IP}, \underline{\gamma}\right) \cdot g(\underline{IP} \left| \underline{IM}, \underline{\gamma}\right) \cdot g(\underline{IM}) \cdot g(\underline{\gamma}) \cdot d\underline{IM} \cdot d\underline{IP} \cdot d\underline{\gamma} \qquad (3.15)$$

where the basic parameters $\underline{\alpha}$ have been assumed as a vectorial Intensity Measure $\underline{IM}$, derived parameters $\underline{\beta}$ have been called $\underline{IP}$ (Interaction Parameters), the other symbols have the meaning specified in the previous sections, finally $g(\underline{IP} \left| \underline{IM}, \underline{\gamma}\right)$ is the joint probability density function of the IPs.

The (3.15) can be viewed as a probabilistic risk-assessing equation similar to a partial PEER approach in which the damage analysis (introducing *DM*) and the loss analysis (introducing *DV*) are not included.

Focusing on the derived parameters $\underline{\beta}$, in the (3.15) these have been called interaction parameters $\underline{IP}$ because, from the proposed wind engineering uncertainties classification (previous section), can be stated that these type of parameters are the ones that regulate the aerodynamic or the aeroelastic phenomena determining the mechanical exchanges between

the wind flow and the structural system. Under this philosophy, the $\underline{IP}$ vector can be fragmented as follows

$$\underline{IP} = \begin{bmatrix} {}_{AD}\underline{IP} \\ {}_{AE}\underline{IP} \end{bmatrix} \tag{3.16}$$

where ${}_{AD}\underline{IP}$ represents the sub-vector of the aerodynamic stochastic parameters, ${}_{AE}\underline{IP}$ represents the sub-vector of the aeroelastic stochastic parameters. Examples of the ${}_{AD}\underline{IP}$ are the aerodynamic coefficient describing the polar lines, while examples of the ${}_{AE}\underline{IP}$ are the flutter derivates or the Strouhal number.

Concerning the so called *independent (or structural) parameters* ($\underline{\gamma}$), these are classically interpreted as the parameters defining the structural characteristics (geometry, materials, stiffness, damping, etc.). It is usual to neglect the uncertainties related to these parameters, this assumption is founded on the reducibility of these uncertainties by experimental tests. Obviously, these uncertainties becomes more important as the structure becomes more complex; probably, for the interests of the present work, the most important uncertainty is the one affecting structural damping, which could be propagated in the structural response especially in presence of aeroelastic phenomena.

A more complete extension of the PEER to the PBWE is given by:

$$\begin{aligned} &\lambda(DV) = \\ &= \int_{-\infty}^{\infty} P(DV|DM) \cdot P(DM|EDP) \cdot P(EDP|\underline{IM},\underline{IP},\underline{\gamma}) \cdot g(\underline{IP}|\underline{IM},\underline{\gamma}) \cdot g(\underline{IM}) \cdot g(\underline{\gamma}) \cdot \\ &\cdot dDM \cdot dEDP \cdot d\underline{IM} \cdot d\underline{IP} \cdot d\underline{\gamma} \end{aligned} \tag{3.17}$$

Under these assumptions, a diagram similar to the PEER flowchart (Fig.2.10) can be defined for the proposed PBWE procedure; the two flowcharts are compared in Fig. 3.5 (where the independent parameters $\underline{\gamma}$ have been neglected).

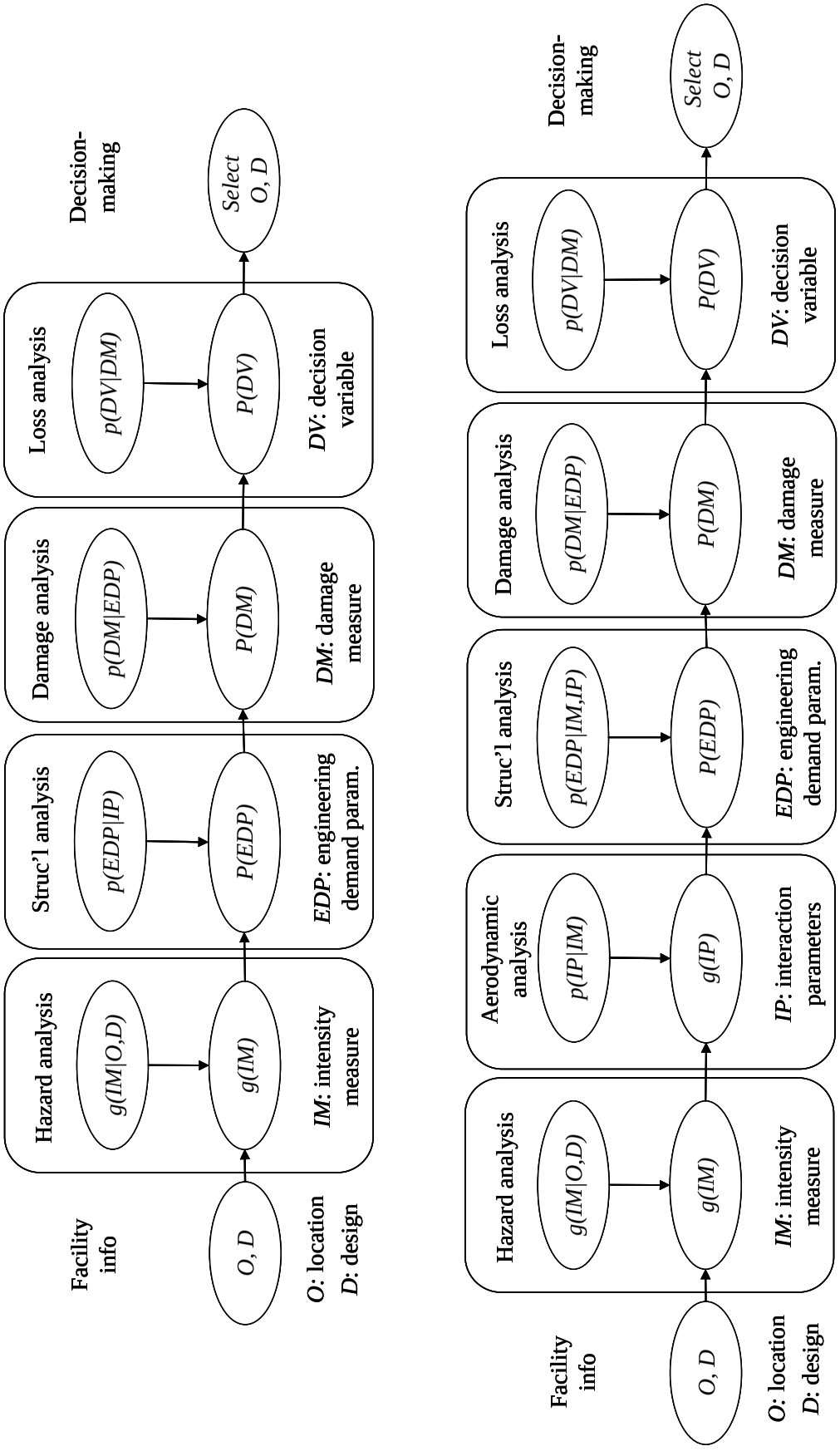

Fig. 3.5. Comparison between the PEER (left) and the PBWE (right).

Referring to the Fig. 3.5, can be noted that, with respect to the PEER approach, one more step has been introduced: the *Aerodynamic analysis*, which consists in the probabilistic characterization of the previously introduced interaction parameters. This part of the procedure can be done either by using wind tunnels tests or CFD techniques (Bruno and Khris 2003, Petrini et al 2005, Morghenthal 2006). In particular the probabilistic dependence of the *IPs* from the *IM* has to be assessed.

A simplified procedure can be obtained by using a proper *EDP* to characterize both levels of damage and the structural performance, by this way it results: first, the damage measure DM is identified by the *EDP* magnitude, and second, the performance can be expressed by using a Limit State (*LS*) function that depends on the *EDP(=DM)*. The choice of the limit state and its relation with the *EDPs* depends on several factors, such as the construction type, the structural model, the method of analysis. Adopting the simplified procedure, neglecting the uncertainties affecting the independent parameters $\underline{\gamma}$ and considering that the derived parameters $\underline{\beta}(=\underline{IP})$ are probabilistically independent from the $\underline{\alpha}(=\underline{IM})$ parameters, and finally identifying the performance requirement with an acceptable value of the mean annual frequency $\lambda(LS)$ of exceeding the limit state LS of the structure, the (3.17) can be expressed as

$$\lambda(LS) = \int\int\int P(LS|EDP) \cdot P(EDP|\underline{IM},\underline{IP}) \cdot g(\underline{IM}) \cdot g(\underline{IP}) \cdot dEDP \cdot d\underline{IM} \cdot d\underline{IP} \tag{3.18}$$

were $P(LS|EDP)$ is the conditional probability of overcoming *LS* given *EDP*. Concerning the LS function, a deterministic relation between the *EDPs* can be chosen; consequently the probabilistic response can be synthesized by the probability distribution of the *EDPs*, namely

$$\lambda(EDP) = \int\int P(EDP|\underline{IM},\underline{IP}) \cdot g(\underline{IM}) \cdot g(\underline{IP}) \cdot d\underline{IM} \cdot d\underline{IP} \tag{3.19}$$

from which $\lambda(LS)$ can be computed by the previously mentioned deterministic relation.
There are several methods to compute the integrals of the PBWE, among which Monte Carlo method seems to be the more suitable for nonlinear problems.

3.4.1. Intensity measure IM

Consider an ideal wind engineering problem (Fig. 3.6) in which a wind speed laminar profile becomes turbulent before the structure of interest because of the crossing of both artificial and natural structures (site roughness).

As previously stated, the parameters affected by significant aleatoric uncertainty are located in the environment zone. For the considered problem they can be identified in:

- *wind mean velocity;*
- *wind mean direction;*
- *turbulence intensity.*

Following the wind analytical model presented in previous sections, from equations (1.2) and (1.6) follows that the mean velocity V_m depends both on the site 10 meters height mean wind speed V_{10} and on the roughness z_0. On the other hand, from equations (1.6), (1.10), (1.11) and (1.12), it is clear that also the turbulence intensity depends on the roughness z_0 and on the site 10 meters height mean wind speed V_{10}.

Adopting this wind analytical model the three basic wind site parameters (defining the wind field inside the site) of the environment zone could be identified, which are:

- *10 meters height mean wind speed;*
- *roughness;*
- *mean wind speed direction.*

These will be considered the basic parameters that are affected by the uncertainties.

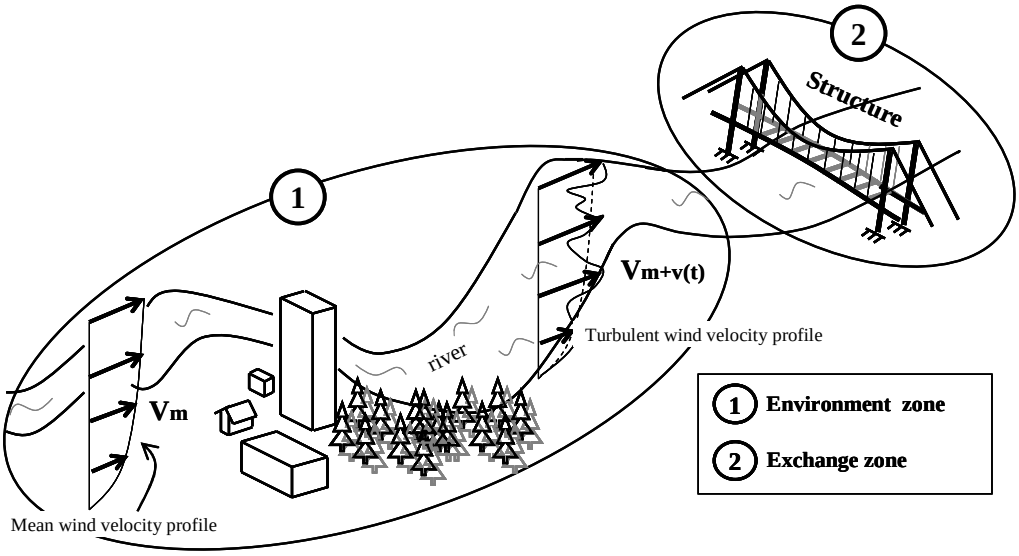

Fig.3.6. An ideal wind engineering problem.

3.4.2. Interaction parameters IPs

Concerning the exchange zone, here the main uncertainties affecting the wind actions values are related with the uncertainties on the aerodynamic and aeroelastic parameters of the structures. These parameters could be viewed as structural parameters, so they could be

considered as other parameters like the material elastic modulus, the structural damping, etc. Nevertheless, as previously stated, the aerodynamic and aeroelastic parameters are certainly subjected to the aleatoric uncertainties propagation from the environment zone. If the uncertainties affecting the structural response due to the environment variability have to be evaluated, the aerodynamic parameters uncertainties becomes of great relevance. Examples of these parameters are given by:

- *aerodynamic polar lines;*
- *aeroelastic derivates;*
- *dimensionless wind numbers (e.g., Strouhal number).*

In the following applications (chapter n°5) both the aerodynamic polar lines and the Strouhal number will be considered as stochastic Interaction Parameters.

3.5 References

Augusti, G. Borri, C. and Neumann, H.J. (2001). "Is Aeloian risk as significant as other environmental risks?", Reliability Engineering and System safety, Vol. 74, pp. 227-237.

Augusti, G. and Ciampoli, M., (2006), "First steps towards Performance-based Wind Engineering", in Performance of Wind Exposed Structures: Results of the PERBACCO project (G. Bartoli, F. Ricciardelli, A. Saetta, V. Sepe eds.), Firenze University Press, 13-20.

Augusti, G. and Ciampoli, M., (2008), "Performance-Based Design in risk assessment and reduction", Probabilistic Engineering Mechanics, 23, 496-508.

Bartoli, G., Ricciardelli, F., Saetta, A., Sepe, V. (eds.) (2006). "Performance of Wind Exposed Structures: Results of the PERBACCO Project", Firenze University Press, Italy.

Bruno, L. and Khris, S. (2003). "The validity of 2D numerical simulations of vortical structures around a bridge deck", Mathematical and Computer Modeling 37, 795- 828.

Davenport, A.G. (1995). "How we can simplify and generalize wind load?", J Wind Eng. Ind. Aerodyn. 54/55, 657-669.

Davenport, A.G. (1998). "Probabilistic methods in wind engineering for long span bridges", Proc. of the Int. Symp. on Advances in Bridge Aerodynamics, May 1998, Copenhagen, Denmark.

Lungu, D., Rackwitz, R., (2001), "Joint Committee on Structural Safety – Probabilistic Model Code, Part 2: Loads", http://www.jcss.ethz.ch/.

Nielsen, M., Larsen, G. C., Mann, J., Ott, S., Hansen, K. S. and Pedersen, B. J., (2004). Wind Simulation for Extreme and Fatigue Loads, Risø Report 1437(EN), Risø National Laboratory, Roskilde, Denmark.

Kareem, A., (1987). "Wind effects on structures: a probabilistic viewpoint", Probabilistic Engineering Mechanics, 4(2), 166-200.

Khanduri, A.C. and Morrow, G.C. (2003), "Vulnerability of buildings to windstorms and insurance loss estimation", Journal of Wind Engineering and Industrial Aerodynamics, (91), 455-467.

Mann, J., Kristensen, L. and Jensen, N.O., (1998). "Uncertainties of extreme winds, spectra and coherence", Proc. of the Int. Symp. on Advances in Bridge Aerodynamics, May 1998, Copenhagen, Denmark.

Minciarelli, F., Gioffrè, M., Mircea, G. and Simiu, E., (2001). "Estimates of extreme wind effects and wind load factors: influence of knowledge uncertainties", Probabilistic Engineering Mechanics, 16, 331-340.

Norton, T.R. (2007), "Performance-Based vulnerability analysis of wind-excited tall buildings", Ph.D. Thesis, Florida Agricultural and Mechanical University FAMU-FSU, College of Engineering.

Pagnini, L. (2005), "The reliability of structures with uncertain parameters excited by the wind", Proceedings of the ninth International Conference on Structural Safety And Reliability, ICOSSAR '05, Rome, Italy.

Paulotto, C., Augusti, G. and Ciampoli, M. (2004). "Some proposals for a first step towards a Performance Based Wind Engineering", Proc. IFED-International Forum in Engineering Decision Making, Stoos, CH. www.ifed.ethz.ch

Petrini, F., Bontempi, F. and Ciampoli, M. (2008), "Performance-based wind engineering as a tool for the design of the hangers in a suspension bridge", Proc. Fouth International ASRANet colloquium, Athens, Greece.

Sibilio, E. and Ciampoli, M. (2007). "Performance-Based wind design for footbridges: evaluation of pedestrian comfort", Proc. Tenth International Conference on Applications of Statistics and Probability in Civil Engineering ICASP10, Tokyo, Japan; abstract 561-562; paper in CDRom.

Solari, G. Piccardo, G. (2001). "Probabilistic 3-D turbulence modeling for gust buffeting of structures", Probabilistic Engineering Mechanics, (16), 73–86.

Solari, G. (1997). "Wind-excited response of structures with uncertain parameters", Probabilistic Engineering Mechanics,12 (2), 75–87.

Solari, G. and Augusti, G. (1998). "Wind engineering: a short introduction", Meccanica, 33: 215-217.

van de Lindt, J. W. and Dao, T. N. (2009), "Performance-Based Wind Engineering for Wood-Frame Buildings", Journal of Structural Engineering, 135(2), 169-177.

Zhang, X. and Zhang, R.R. (2001). "Actual ground-exposure determination and its influences in structural analysis and design", J Wind Eng. Ind. Aerodyn, Vol. 89, pp. 973-985.

Zhang, L., Jie, L. and Peng, Y, (2008), "Dynamic response and reliability analysis of tall buildings subject to wind loading", Journal of Wind Engineering and Industrial Aerodynamics, (96), 25-40.

Chapter 4

NUMERICAL PROCEDURES

In this section, the numerical issues related to the computational procedures adopted in the subsequent PBWE applications are discussed.

4.1. Wind field numerical simulation

The numerical simulation of turbulent wind speed time histories it is now a widely used tool in the study of structures under the wind action, especially in the case of structures having a non linear behavior for which the time domain approach is more reliable than the frequency one.

This has been one of the main topics of wind engineering during the last decades, both the hypotheses of stationary mean component and gaussian turbulent component of the wind speed are commonly used (Deodatis, 1996; Shinozuka and Deodatis, 1997; Carassale and Solari 2006), even if some studies on the non-gaussian simulation (see for example Nielsen et al, 2004) shown that the fatigue damage due to turbulent wind could be underestimated by using the hypothesis of Gaussian wind fields. In the present work the Gaussian hypothesis is adopted.

Various numerical simulation techniques exist for the generation of stochastic process realizations (Schuëller (ed.), 1997, Schüeller, 2006), in wind engineering problems the most used techniques are based on the harmonic signals superposition with random phases, also called Weighted Amplitude Wave Superposition (W.A.W.S.) methods; they are based on the decomposition of the Power Spectral Density matrix (Chapter 1) for the harmonic weights computation.

During last two decades, another simulation technique has been adopted for wind engineering problems: it implies the use of autoregressive (AR) or moving average autoregressive (ARMA) methods (Samaras et al 1985, Di Paola and Gullo, 2001); these methods are based on the reproduction of certain time histories matching the correlation matrix (Appendix A2) of the stochastic process that one wants to reproduce; finally, the two generation methods have been compared in a number of paper (e.g. Rossi et al 2003 or Ubertini and Giuliano 2008).
Concerning the W.A.W.S. method, two techniques are mainly used for the PSD matrix decomposition: the Cholesky decomposition (see for example Deodatis, 1996) and the so called Proper Orthogonal Decomposition (P.O.D.) (Di Paola, 1998, Carassale and Solari, 2006).

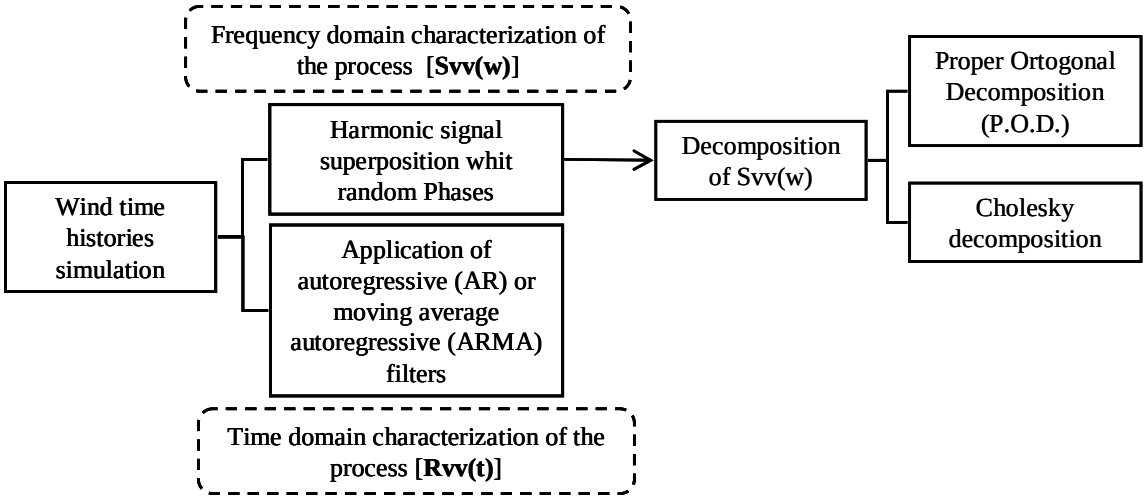

Fig. 4.1. Most used wind time histories simulation methods

Since a crucial point in the wind time histories generation concerns the computational effort, which becomes remarkable in the case of multivariate processes, starting from its early formulation in order to obtain a better computational efficiency, the W.A.W.S. method has been refined in various literature papers. The use of the Fast Fourier Transform (FFT) technique can dramatically improve the simulation algorithm efficiency (Deodatis, 1996), the interpolation techniques can be applied to improving the computational efficiency in computing the superposed harmonic waves (Carassale and Solari, 2006), the spatial correlations can be considered equal to zero for high distances between the wind domain generation points (Cao et al, 2000).
In this work, the W.A.W.S. methods have been adopted for the wind field simulation, and a comparison between the two PSD matrix decomposition techniques has been done in what follows.

4.1.1. Simplified hypotheses

At the top of procedure, some basic hypotheses are fixed:

- The wind speed is modeled as the sum of two components (as stated in the first chapter). A Cartesian three-dimensional coordinate system *(x,y,z)*, with origin at ground level and the z-axis oriented upward is adopted, here results

$$\vec{V}(x,y,z;t) = \vec{V}_m(z) + \vec{V}_t(x,y,z;t) \tag{4.1}$$

$$\vec{V}_t(x,y,z;t) = u(x,y,z;t)\cdot\hat{i} + v(x,y,z;t)\cdot\hat{j} + w(x,y,z;t)\cdot\hat{k} \tag{4.2}$$

  where V_m and V_t are the mean and the turbulent component of the wind speed, *i*, *j* and *k* are the axis unitary vectors and *u*, *v*, *w* are the three scalar turbulent components of the wind speed.

- $\vec{V}_t(x,y,z;t)$ is modeled as a zero-mean Gaussian stochastic process, for which only the second-order stochastic moments are not zero.

- According with Eq. (4.1) and (4.2), $\vec{V}_t(x,y,z;t)$ is a three-variate (3V) (having three components), four-dimensional (4D) (depending on four deterministic parameters) stochastic process. It will be indicated as [3V – 4D].

  - assuming that the three stochastic components *u*, *v*, *w* are statistically independent each other, one can switch from a [3V – 4D] process to three [1V – 4D] processes:

$$[3V - 4D] \rightarrow 3\cdot[1V - 4D]$$

  - by a discretization of the spatial domain in N points representing the locations where the wind acts on the structure and adopting an Eulerian point of view, each turbulent component *u*, *v*, *w* can be viewed as a stochastic vector having as generic component l_m (*l=u, v, w* and *m=1,2,..,*N) the stochastic wind component associated with the particular point $P(x_P, y_P, z_P)$ that is one of the N points representing the wind domain. Each vector component is a stochastic [1V – 1D] process (representing the single component of the turbulent wind speed in the particular location, depending on the single deterministic parameter *t* (the time)) that is correlated with the other components of the same vector. By this way one can switch from three [1V – 4D] processes to three [NV – 1D] each one represented from the stochastic vector modeling the single turbulent component *u*, *v* or *w*:

$$3\cdot[1V - 4D] \rightarrow 3\cdot[NV - 1D]$$

the last passage, let to simulate three distinct N-variate mono-dimensional stochastic processes.

- Making the hypothesis of stationary process for each turbulent component, the second order stochastic moments (statistical correlations) depend from a single scalar parameter $\tau_{ij} = t_i - t_j$, representing a certain time interval.

Under the previous assumptions it results that the single turbulent component *u*, *v* or *w* it is completely characterized by the PSD matrix $[S]_i$, *(i = u, v, w)* as previously described in chapter 1, the matrix dimension is *NxN* and the matrix elements are given by the Eq. (1.10) and (1.13).

4.1.2. W.A.W.S. methods

The steps of the wind time histories numerical generations are summarized below.

a. Wind field spatial discretization, defining N point of interest for the time history simulation. Typically in structural engineering the discretizing points are chosen as the structural points in which the wind actions will be computed for the subsequent structural analysis.
b. Fixing the generated wind time history duration T_{wind}.
c. Time axes discretization by defining the generation time step Δt (and the consequent number the time step $N_t = T_{wind}/\Delta t$).
d. Definition of the generation circular frequency range ($[\omega_{min}, \omega_{max}]$); the fundamental circular frequencies of each superposed simple harmonic will be contained inside the range. Usually the range is defined as $[0,\omega_{cut}]$, where ω_{cut} is the so called *cut-off circular frequency*.
e. Frequency axes discretization by defining the generation circular frequency step $\Delta\omega$ (and the consequent number the discretizing frequencies step $N_\omega = \omega_{cut} / \Delta\omega$).

In the steps from *b* to *e*, four independent parameters have to be chosen. The using of the FFT technique to improve the algorithm efficiency imposes the condition $N_t = N_\omega$.

Furthermore, well known relationships between the previous defined parameter have to be satisfied in order to obtain a good simulation result:

$$T_{wind} \leq \frac{2\pi}{d\omega} \tag{4.3}$$

$$\Delta t \leq \frac{2\pi}{8\omega_{cut}} \tag{4.4}$$

The (4.3) assures that the generated signal will be periodic with frequency $n<1/T_{wind}$ and the (4.4) assures that the simple harmonic component having the upper frequency of the range can be fitted at list by eight time domain points.

With these positions, a number of N_ω PSD matrices $[S]_i$, $(i = u, v, w)$ are computed for each turbulent component generation (Fig. 4.2).

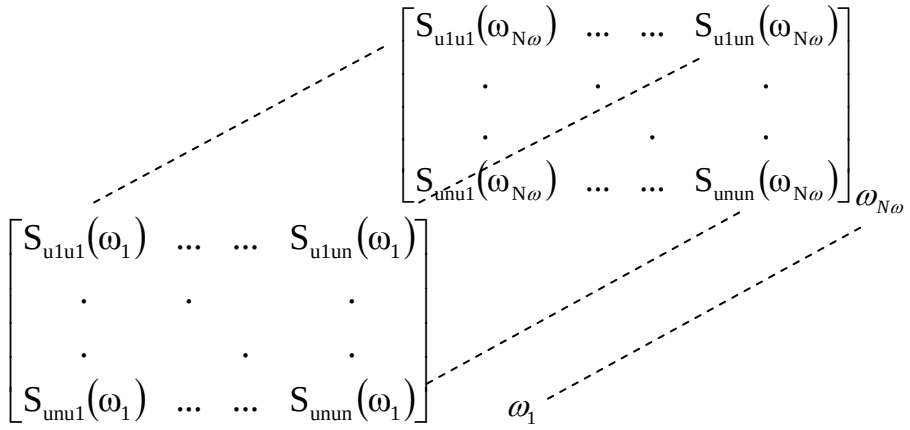

Fig. 4.2. Schematic projection of the PSD matrix on the frequency domain.

The successive steps of the generation procedure are:

f. PSD matrix decomposition (Cholesky or P.O.D.).

g. Generation formula .

Concerning the step f., the Cholesky decomposition of the generic PSD matrix is given by

$$\underline{\underline{S}}(\omega) = \underline{\underline{H}}(\omega) \cdot \underline{\underline{H}}^{T*}(\omega) \tag{4.5}$$

where the superscript T represents the transpose operation and $\underline{\underline{H}}(\omega)$ is a lower triangular matrix having the same dimension of $\underline{\underline{S}}(\omega)$.

In the case of Cholesky decomposition the generation formula (step g) is given by:

$$V_{t\,ij}(t) = \sqrt{2 \cdot \Delta\omega} \cdot \sum_{m=1}^{j} \sum_{l=1}^{N_\omega} \left| H_{jm}(\omega_{ml}) \right| \cdot \cos(\omega_{ml} \cdot t - \theta_{jm}(\omega_{ml}) + \Phi_{ml}) \qquad \begin{matrix} k = x, y, z \\ j = 1,2,\dots, N \end{matrix} \tag{4.6}$$

where $V_{t\,ij}(t)$ is the time history of the turbulent component velocity i (i=u, v, w) at location j where j indicates one of the N points discretizing the wind field, the Φ_{11}, Φ_{21},…, Φ_{1l} are sequences of independent random phase angles, uniformly distributed over the interval [0,2π], and $H_{jm}(\omega_{ml})$ is the element of the matrix $\underline{\underline{H}}(\omega)$ and $\theta_{jm}(\omega_{ml})$ is the phase angle of the element $H_{jm}(\omega_{ml})$ given from

$$\theta_{jm}(\omega) = \tan^{-1}\left\{\frac{\mathrm{Im}\left[H_{jm}(\omega)\right]}{\mathrm{Re}\left[H_{jm}(\omega)\right]}\right\} \tag{4.7}$$

in the (4.6), the ω_{ml} are the circular frequencies discretizing the frequency axes in the range previously defined at the step *d.*, that can be written as

$$\omega_{ml} = (l-1)\cdot \Delta\omega + \frac{m}{n}\cdot \Delta\omega \tag{4.8}$$

The P.O.D. decomposition is obtained by finding the eigenvectors and eigenvalues of the PSD matrix

$$\underline{\underline{Y}}^{T}(\omega)\cdot \underline{\underline{S}}(\omega)\cdot \underline{\underline{Y}}(\omega) = \underline{\underline{\Lambda}}(\omega) \tag{4.9}$$

where the superscript *T* represents the transpose operation, $\underline{\underline{Y}}(\omega)$ is the eigenvectors matrix and $\underline{\underline{\Lambda}}(\omega)$ is the diagonal eigenvalues matrix, both $\underline{\underline{Y}}(\omega)$ and $\underline{\underline{\Lambda}}(\omega)$ have the same dimension of $\underline{\underline{S}}(\omega)$.

In the case of P.O.D. decomposition the generation formula is given by:

$$\underline{V_{t\,i}}(t) = \sum_{j=1}^{N} \underline{Y}_j(t) \qquad i = u, v, w \tag{4.10}$$

where $\underline{V_{t\,i}}(t)$ is the N dimensional vector containing the time histories of the turbulent component velocity i (i=u, v, w) at different locations discretizing the wind field, the $\underline{Y}_j(t)$ are stochastic processes given by

$$\underline{Y}_j(t) = 2\sum_{k=1}^{N_\omega} \underline{\psi}_j(\omega_k)\cdot\sqrt{\Lambda_j(\omega)\cdot\Delta\omega}\cdot\left(R_k^{(j)}\cdot\cos(\omega_k t) - I_k^{(j)}\cdot\sin(\omega_k t)\right) \qquad j = 1,2,...,N \tag{4.11}$$

where $\underline{\psi}_j(\mathrm{t})$ is the eigenvector j, $\Lambda_j(\omega)$ is the eigenvalues j, $\mathrm{R_k}$ and $\mathrm{I_k}$ are Gaussian random numbers with zero mean value and unit variance, ω_k is the current generation frequency given by ω_k=$k\Delta\omega$.

As previously stated, the FFT technique can be adopted to improve the generation algorithm. It consists in writing the harmonic functions of the generation formulas (4.6) and (4.11) by using of the complex notation and recognizing that the internal sum operators can be computed by using of the FFT technique; this permits to reduce the number of total sum operators (Deodatis, 1996, Carassale and Solari, 2006). Another efficient technique in reducing the computational effort, has been proposed in the case of P.O.D. decomposition technique from Carassale and Solari (2006); it consists in the computation of a reduced

number of eigenvectors corresponding to opportune frequencies, and in the successive computing of the others by the interpolation techniques.

4.1.3. Numerical example: comparison of the W.A.W.S. methods

The generation techniques presented in the previous section have been implemented on a simple benchmark problem: two [3V – 1D] processes representing the along wind (*u* component) and across wind (*v* component) turbulent wind velocities have been generated. The three generation spatial points are located in the *z-x* plane at different altitude as shown in Fig. 4.3. The generation parameters are reported in Table 4.1.

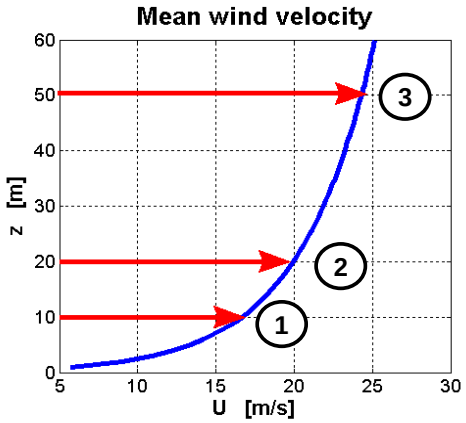

Fig. 4.3. Generation points.

Table 4.1.

Points location	z_1*=10 m;* z_2*=20 m;* z_3*=50 m;*
Mean wind velocities	V_1*=17 m/s;* V_2*=20 m/s;* V_3*=24 m/s;*
Roughness length	z_0*=0.2 m*
Generated wind time history duration	T_{wind}*=600 s*
Generation time step	Δt*=0.1 s*
Generation circular frequency step	$\Delta\omega$*=*
Cut-off circular frequency	ω_{cut}*=30 rad/s*
Cut-off frequency	n_{cut}*=9.55 Hz*

The algorithm has been developed using MATLAB ® (http://www.mathworks.com/), and both the Cholesky and the P.O.D. decomposition have been implemented, concerning the last one, efficiency improvement techniques have been successively used to optimize the simulation efforts.

In Fig. 4.4 the typical Power spectral densities of the wind speed stochastic process that want to be simulated by time histories generation is shown, these are computed by the equation (1.10).

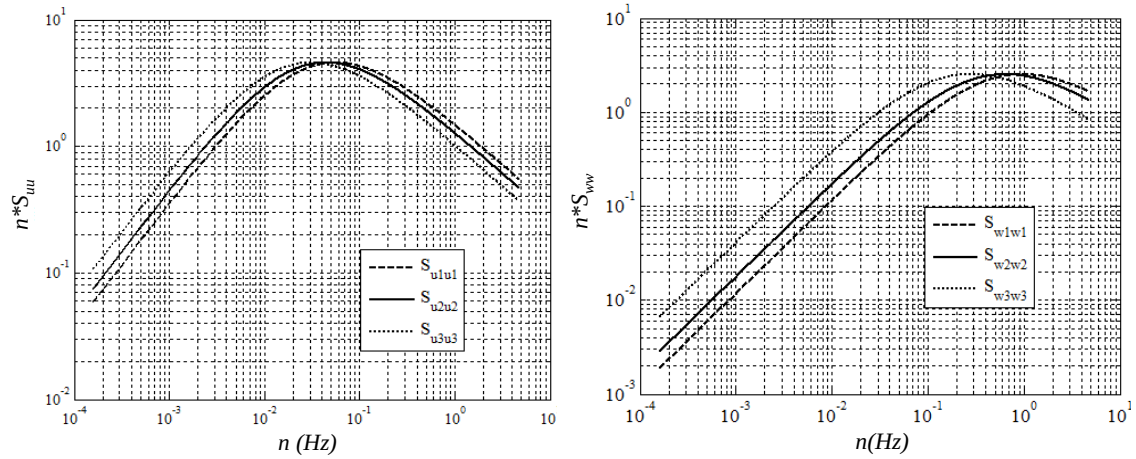

Fig. 4.4. Power spectral densities (auto-spectra functions) of the wind speed stochastic process. Along wind (left) across wind (right).

First, the Cholesky (CHO) and the POD techniques have been applied without any improvement technique, in Fig. 4.5 the turbulent wind time histories are shown for the point number 2. In Fig. 5.6 the three eigenvalues of the along-wind PSD matrix are shown versus the frequency, it is possible to appreciate that they decrease rapidly after a certain frequency value. The compatibility of the generated time history spectra with the stochastic process have to be checked. This is done in Fig. 4.8 and 4.9 for the auto-spectra. Also the autocorrelations of the generated time histories have been computed and compared (Fig.4.9 and 4.10) to the theoretical (from original stochastic process) ones. The comparisons shown that both adopted methods give reliable results in generating wind speed time histories.

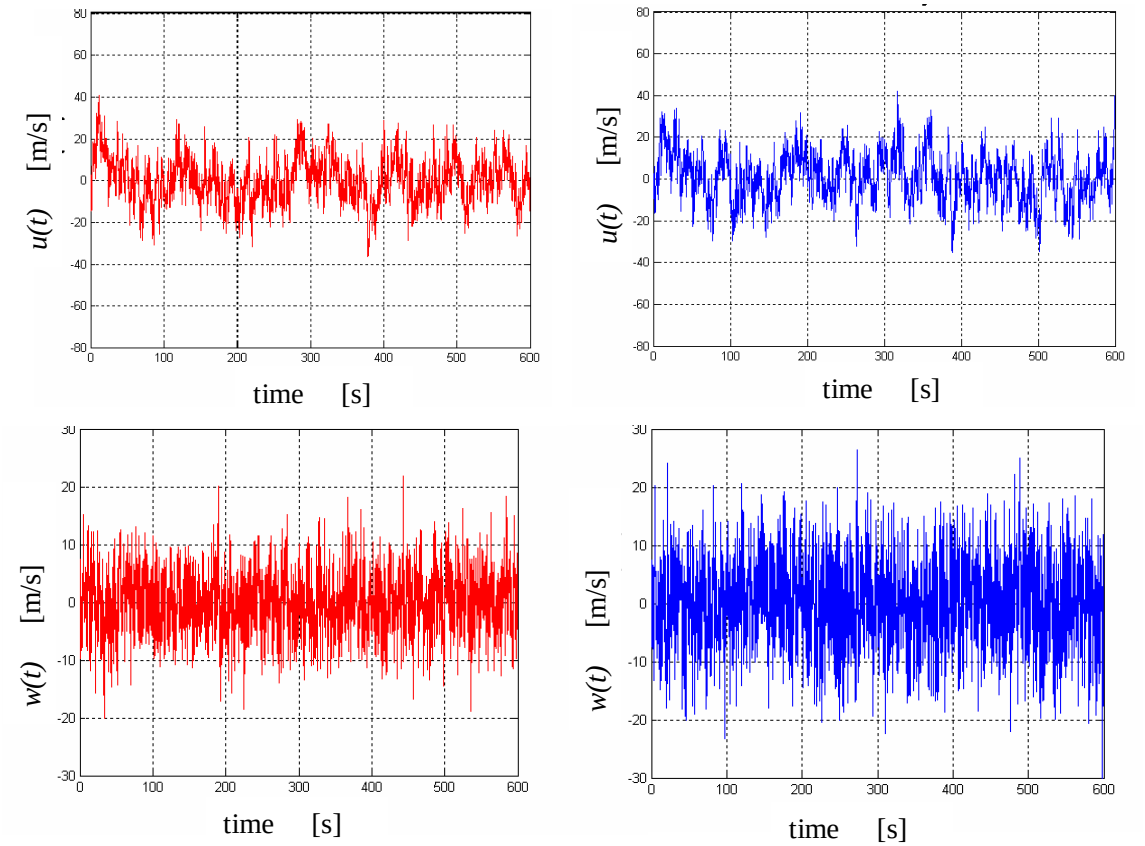

Fig. 4.5. Generated turbulent wind time histories at point No.2: along wind (up), across wind (down); POD (left), CHO (right).

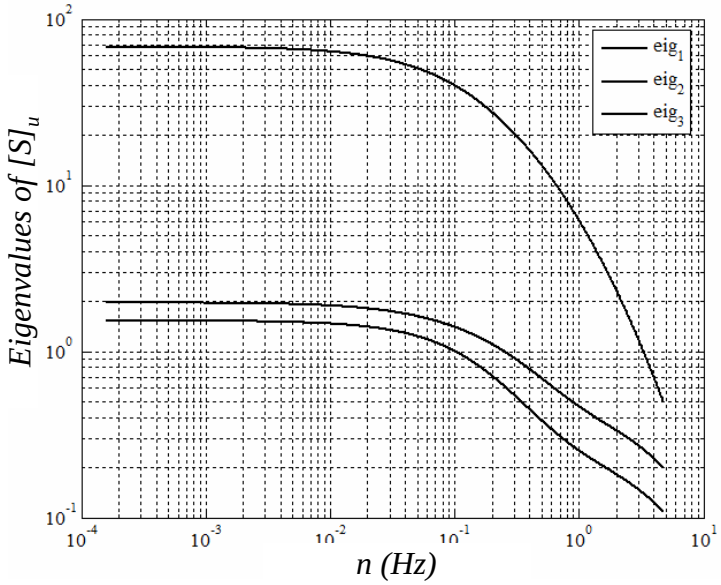

Fig. 4.6. First three eigenvalues of the along wind PSD matrix vs frequency .

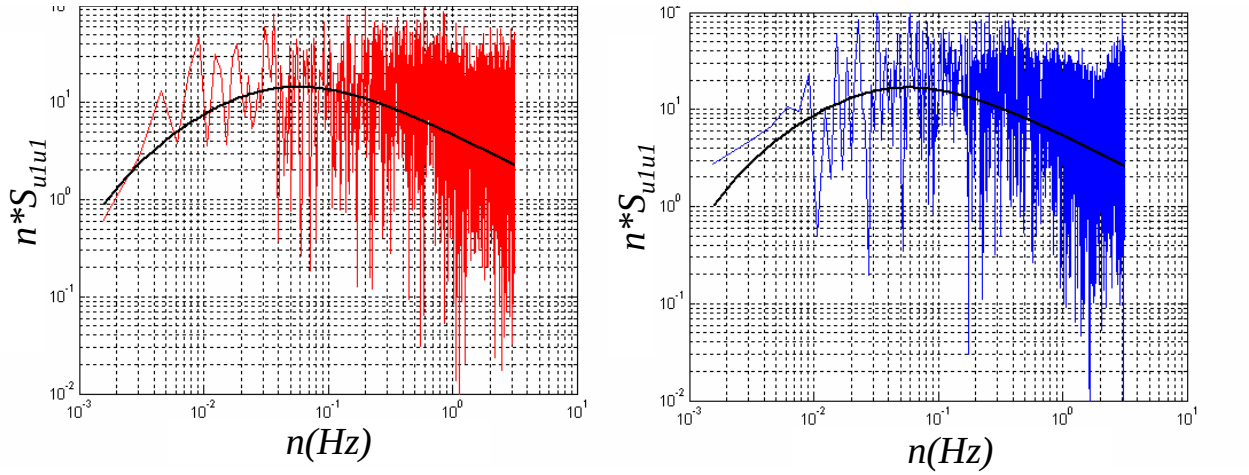

(a)

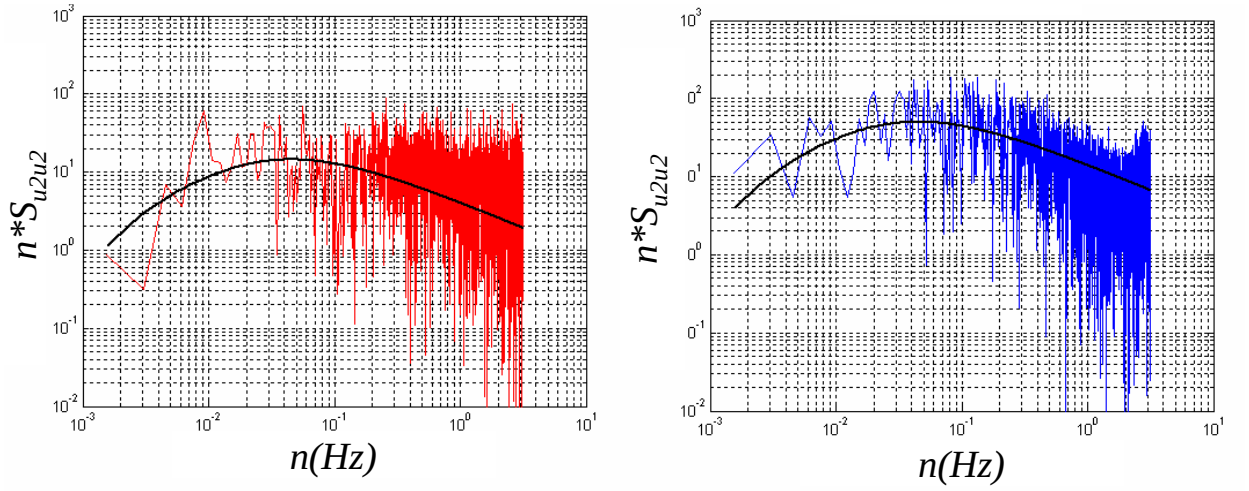

(b)

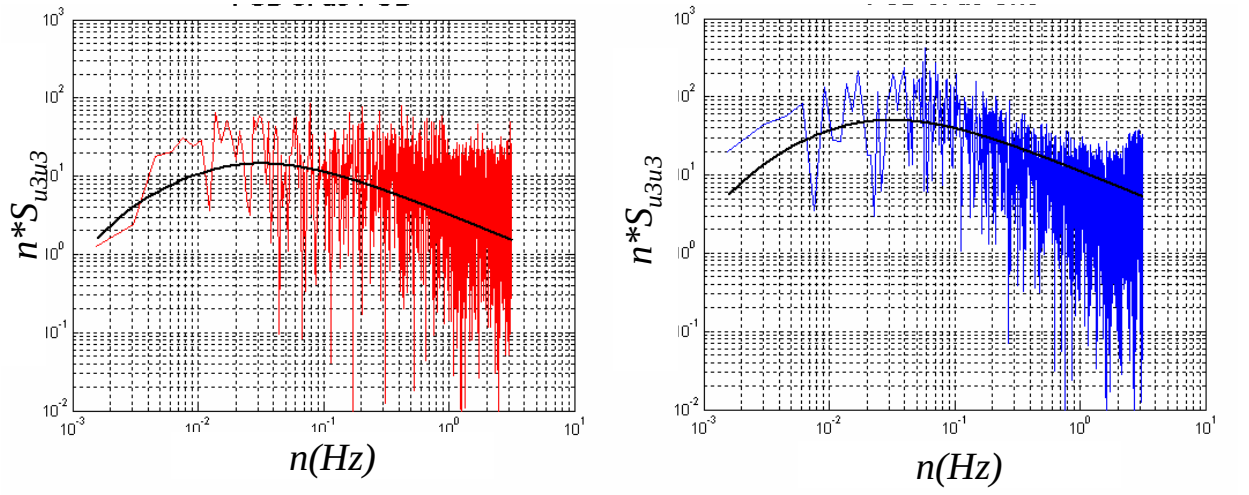

(c)

Fig. 4.7. PSD functions of the generated turbulent along wind time histories: point No.1 (a), point No.2 (b), point No.3 (c); POD (left), CHO (right).

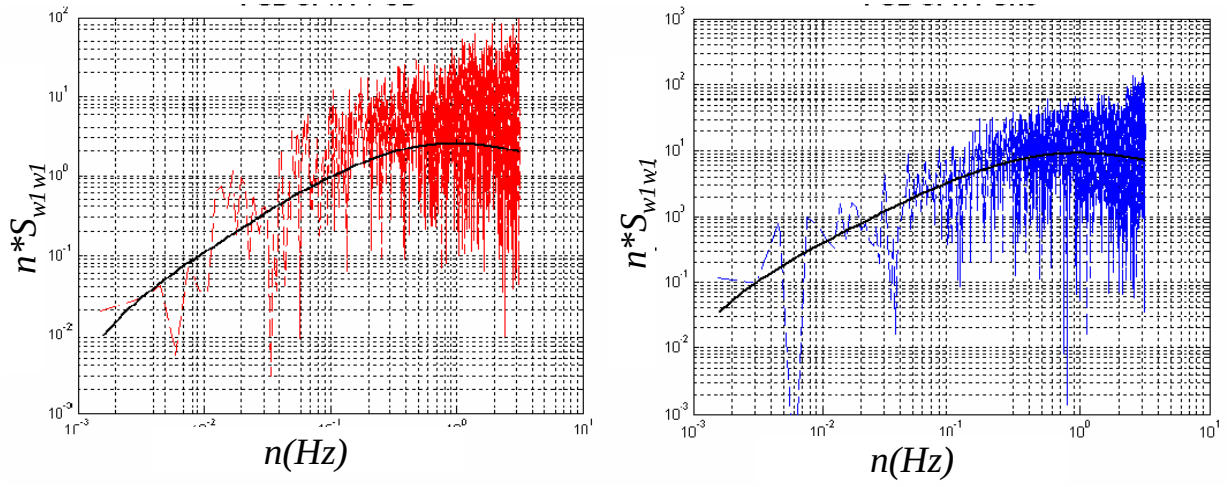

(a)

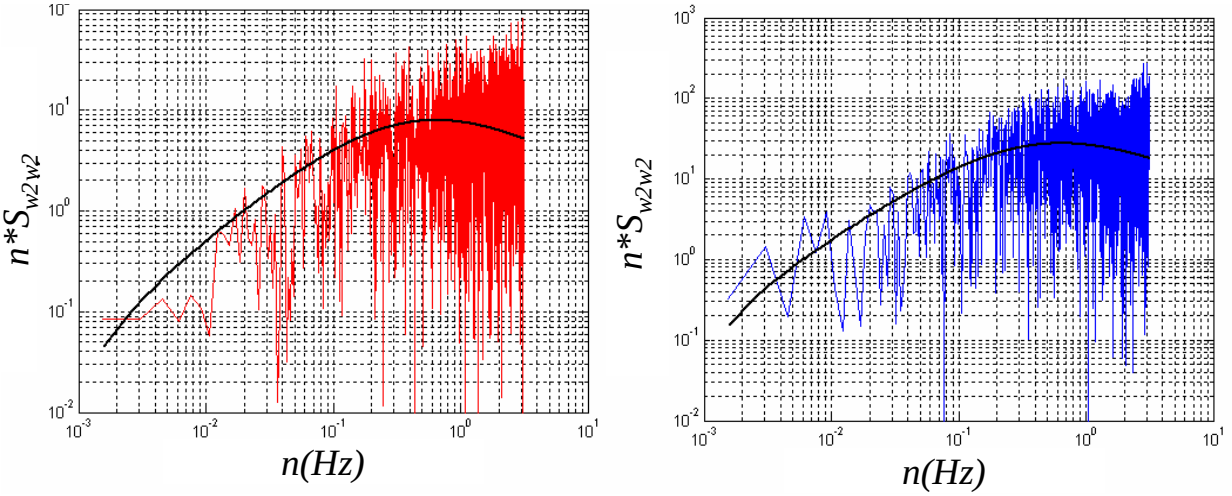

(b)

Fig. 4.8. PSD functions of the generated turbulent across wind time histories: point No.1 (a), point No.2 (b); POD (left), CHO (right).

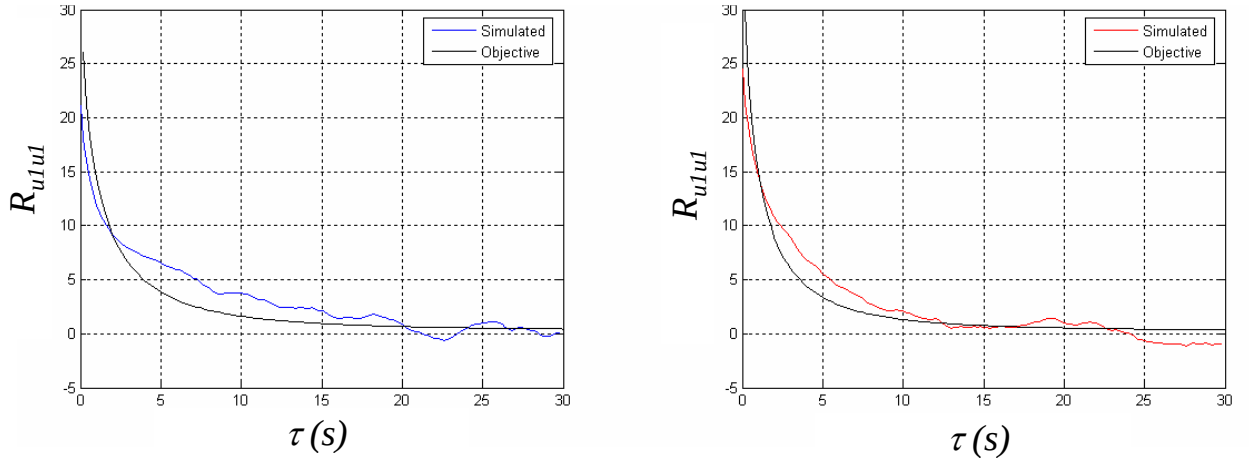

(a)

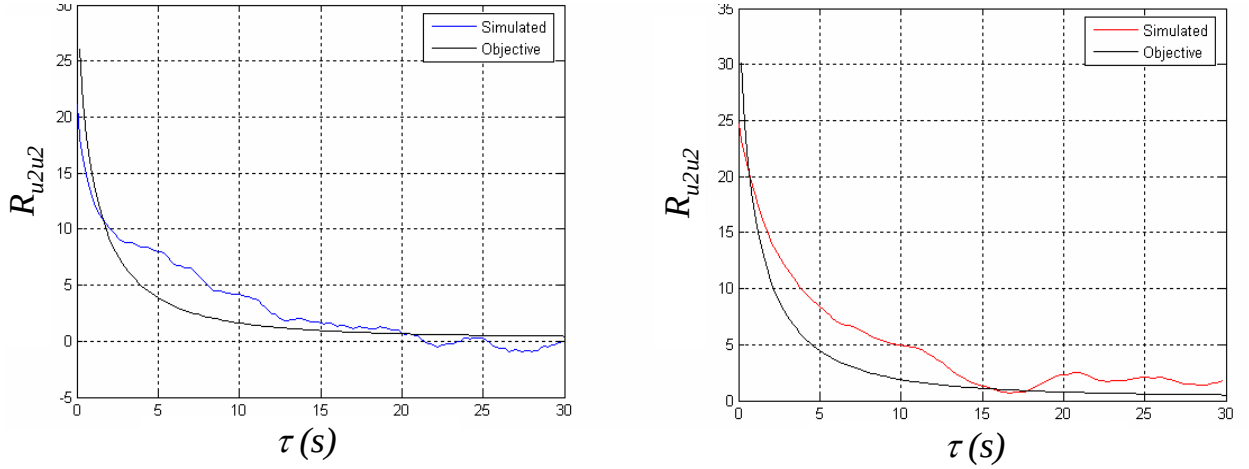

(b)

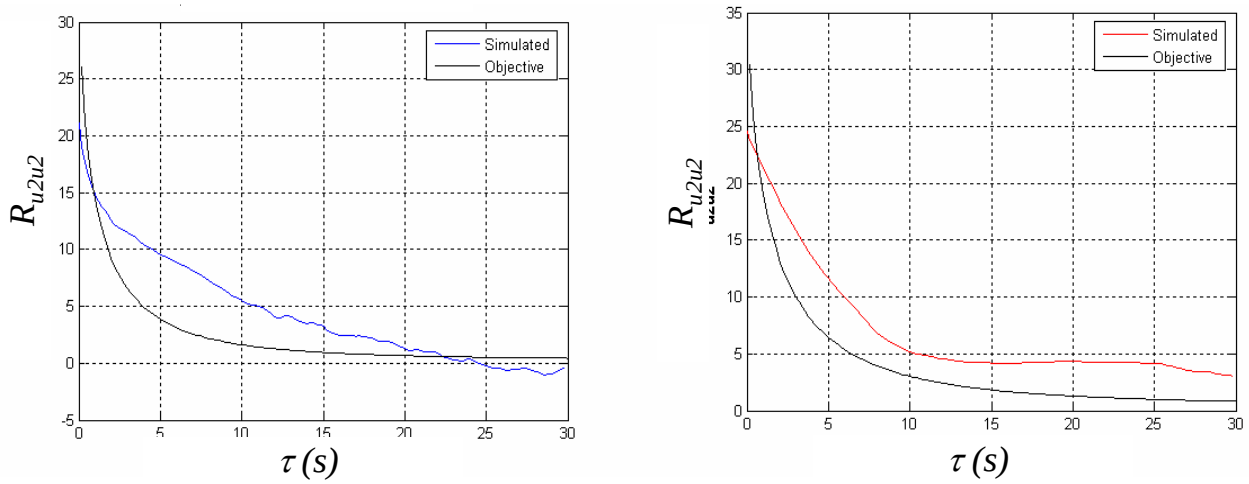

(c)

Fig. 4.9. Autocorrelation functions of the generated turbulent along wind time histories: point No.1 (a), point No.2 (b), point No.3 (c); POD (left), CHO (right).

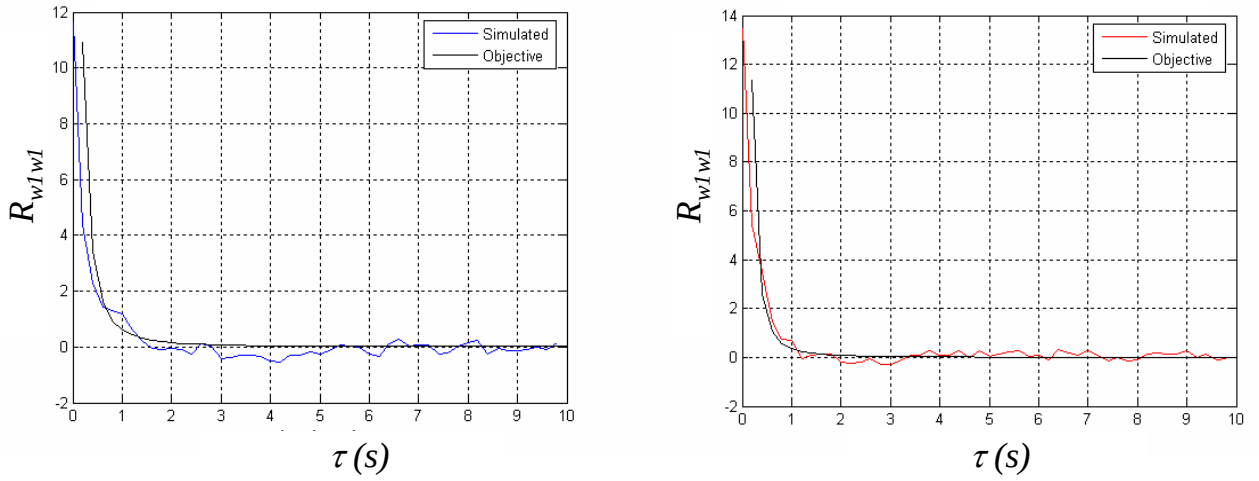

(a)

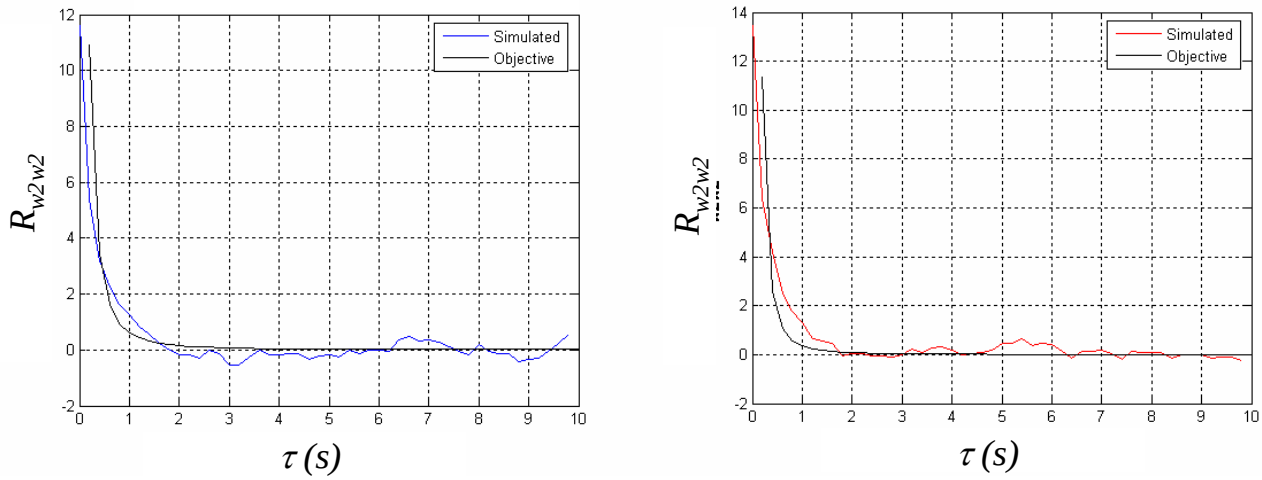

(b)

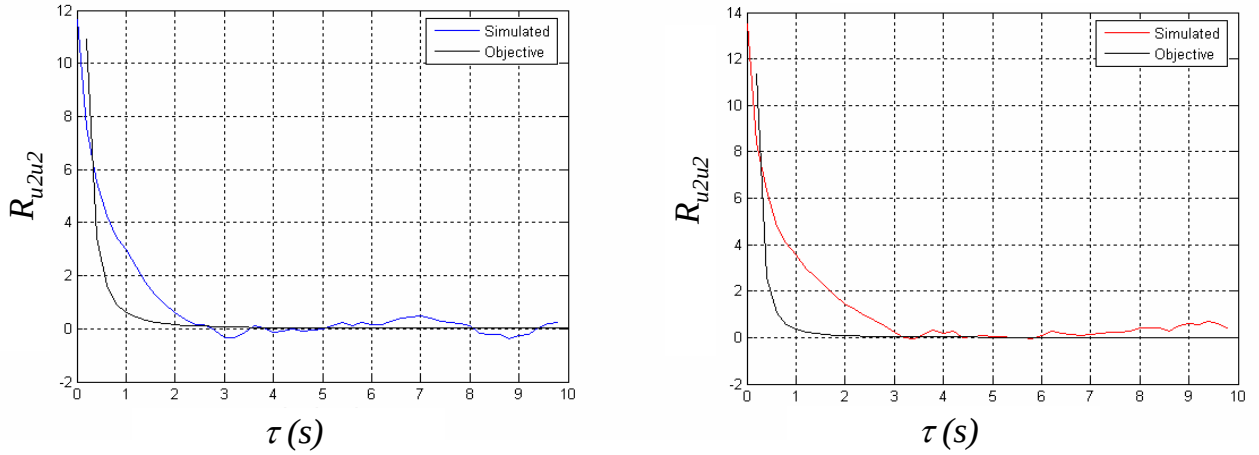

(c)

Fig. 4.10. Autocorrelation functions of the generated turbulent across wind time histories: point No.1 (a), point No.2 (b), point No.3 (c); POD (left), CHO (right).

Efficiency improvement techniques have been implemented in the P.O.D. generation algorithm in order to minimizing the computational efforts. In this case the generation spatial domain (Fig. 4.11) is referred to the long span suspension bridge subject of the successive application. There are a total of 27 generation points, both along and across wind components are generated, ant the generated wind time history duration T_{wind} it is 3600 seconds.

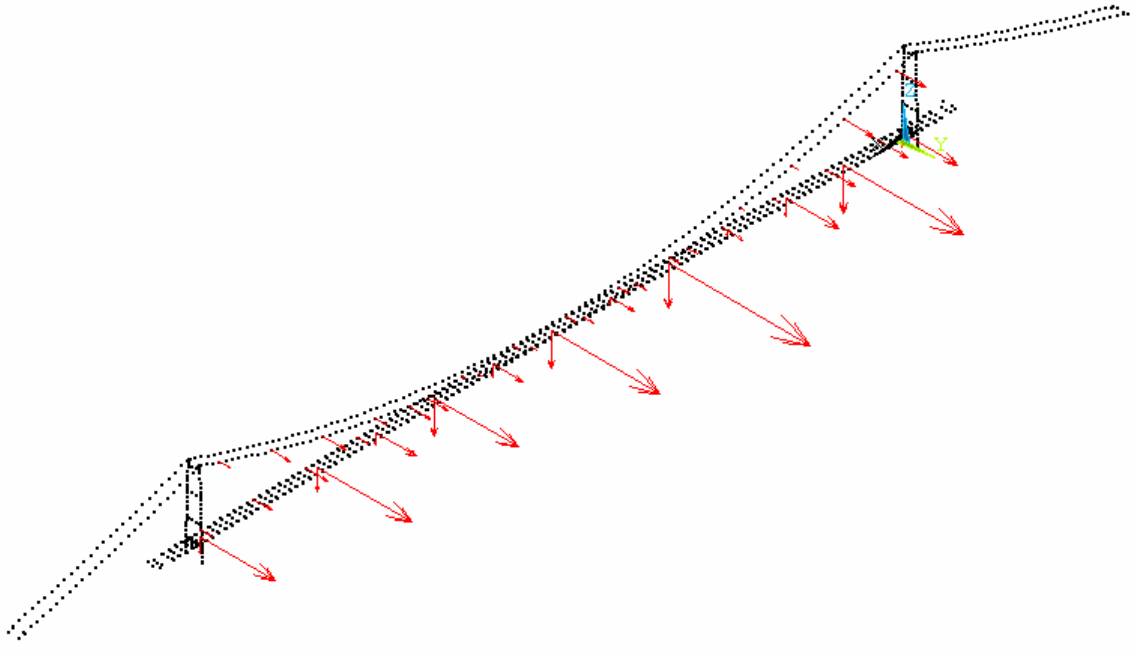

Fig. 4.11. Generation domain for a long span suspension bridge

The table 4.1 shows the amount of the generation time, required with a 32-bit Intel Core Duo processor (2.0 GHz, 6 MB L2 cache).

Table 4.1. Comparison of simulation time adopting improving technique

	Analysis time [sec]	**Analysis time [Hours]**	**Analysis time [Ratio]**
POD	77868	21.63	1.521
POD + FFT	63328	17.59	1.237
POD + interpolation	71110	19.75	1.389
POD + FFT + Interpolation	51195	14.22	1

From the table it is clear that, by adopting the improving efficiency techniques, until the 50% of the computational time can be saved.

4.2. Wind response and stability analysis

The designer's intent in considering the action of wind is to define the risks of key responses critical to satisfactory performance. These responses can embrace a wide variety of structural actions including resultant forces, bending moments and stresses at critical sections of members, cable tensions, as well as displacements and accelerations. The form of such responses is illustrated in Fig. 4.12; following Davenport (1995) and (1998) they can, generally speaking be broken in three main components

- a mean, time average response r_m;
- a background response, r_B varying slowly and irregular with time;
- resonant responses r_{R1}, r_{R2}, …., r_{Rm}, oscillating with varying amplitudes at the natural frequencies of the structures.

The peak response r^P can be written as

$$r^P = r_m + g \cdot \sqrt{r_B{}^2 + \sum_i r_{Ri}{}^2} \qquad (4.12)$$

where g is the statistical peak factor, usually in the range 3-4, while $r_B{}^2$ and $r_{Ri}{}^2$ is the mean square values of the background and i^{th} mode resonant response. The values of the mean square responses can be related to the portions of the power spectrum response which, combined, constitute the total variance of the response Fig.4.13.

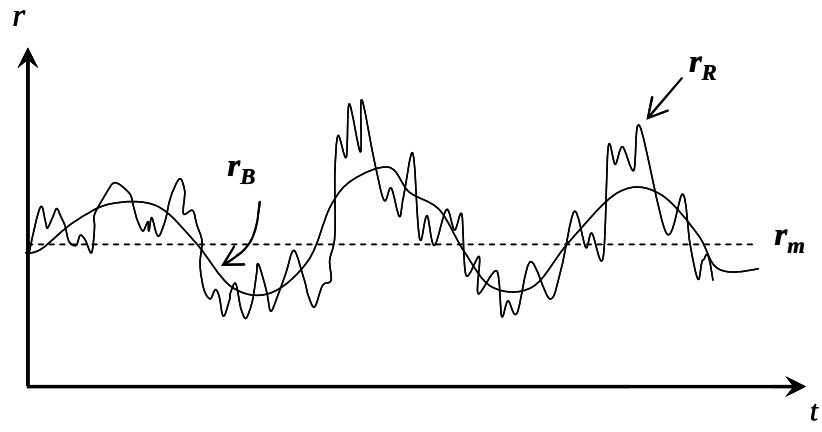

Fig. 4.12. Structural response to the wind action: r_m time average response, r_B background response, r_R resonant responses.

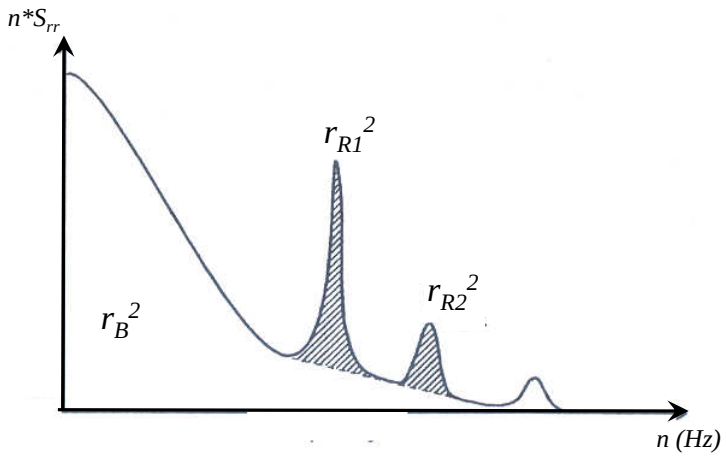

Fig. 4.13. Variance of the structural response.

The background response, made up largely of low-frequency contributions below the lowest natural frequency of vibration, is the largest contributor in Figure 4.13, and, in fact, is usually the dominant contribution in the case of along-wind loading. Resonant contributions become more and more significant, and will eventually dominate, as structures become taller or longer in relation to their width, and their natural frequencies become lower and lower.

As previously stated (chapter 1), the structural analysis can be conducted both in frequency and in time domain, the last one is widely adopted in the case of structures having a marked non-linear behavior.

4.2.1. Frequency domain for response

In this section the frequency domain analysis will be presented with reference to the classical Davenport method (1962). Taken a Single Degree Of Freedom (SDOF) punctual system, consider the along-wind response; the structure will be considered having small geometrical dimension *A* (like a punctual body in the limit), the fluid-structure interaction effects are considered negligible. This example is reasonable representative of a structure consisting of a large mass supported by a column of low mass, such as a wind turbine on a monopile support. The schematized structure is represented in Fig. 4.14.

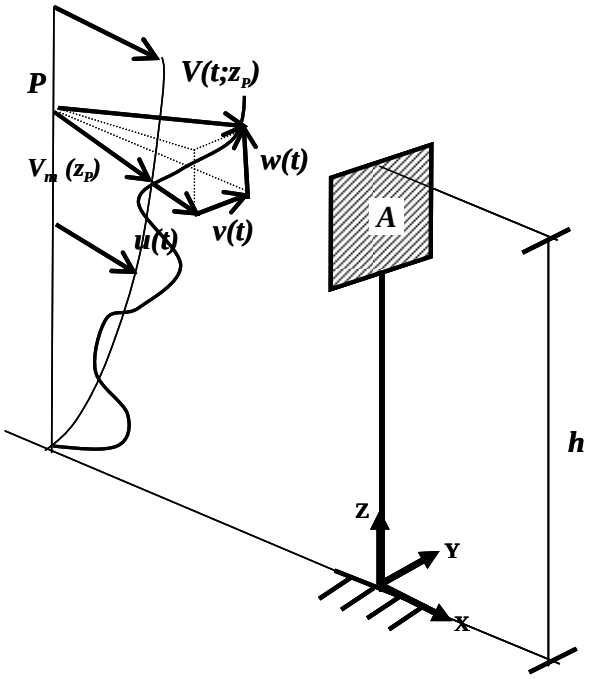

Fig. 4.14. Example problem.

Defining the along-wind aerodynamic action (drag force) by using the pressure coefficient, it results:

$$D(t) = D_m(t) + D_t(t) = \frac{1}{2}\rho \cdot c_P \cdot \int_A \left[V_{mx} + u(t)\right]^2 \cdot dA =$$
$$= \frac{1}{2}\rho x \int_A \left[{V_{mx}}^2 + 2u(t)\cdot V_{mx} + u(t)^2\right]\cdot c_P \cdot dA \cong \frac{1}{2}\rho \cdot c_D \cdot \int_A \left[{V_{mx}}^2 + 2u(t)\cdot V_{mx}\right]\cdot dA \quad (4.13)$$

where D_m and D_t are the mean and turbulent components respectly, c_D is the aerodynamic drag coefficient, $u(t)^2$ has been considered negligible (for normal or low turbulence intensity values), hence it results

$$D_m(t) = \frac{1}{2}\rho \cdot c_D \cdot A \cdot {V_{mx}}^2 \quad (4.14)$$

$$D_t(t) = \rho \cdot c_D \int_A \left[u(t)\cdot V_{mx}\right]\cdot dA \quad (4.15)$$

Since the turbulent wind speed is modeled as a Gaussian stationary process, the D_t aerodynamic force there will be also a stationary process. Introducing the vector $\underline{\xi}$=[x y z] defining the position of the generic spatial point in a Cartesian three dimensional coordinate system (see Fig.4.14), the correlation function of the D_t process can be written as

$$R_{D_t 1 D_t 2} = (\rho \cdot c_D \cdot V_{mx})^2 \int_A \int_A E\left[u(\underline{\xi_1}, t), u(\underline{\xi_2}, t+\tau)\right] \cdot dA \cdot dA = \\ = (\rho \cdot c_D \cdot V_{mx})^2 \int_A \int_A R_{uu}(\xi_1, \xi_2, \tau) \cdot dA \cdot dA \tag{4.16}$$

by applying the Fourier transformation at the (4.16), the PSD of the D_t process can be written as

$$S_{D_t 1 D_t 2}(\underline{\xi_1}, \underline{\xi_2}, \omega) = (\rho \cdot c_D \cdot V_{mx})^2 \int_A \int_A S_{u1u2}(\underline{\xi_1}, \underline{\xi_2}, \omega) \cdot dA \cdot dA \tag{4.17}$$

referring to the equation (1.13), in terms of circular frequencies, one can writes

$$S_{u1u2}(\omega) = \sqrt{S_{u1u1}(\omega) S_{u2u2}(\omega)} \exp(-f_{12}(\omega)) \tag{4.18}$$

In which $f_{12}(\omega)$ is given from (see equation (1.14))

$$f_{12}(\omega) = \frac{|\omega| \sqrt{C_z^2 (z_1 - z_2)^2}}{2\pi (V_m(z_1) + V_m(z_2))} \tag{4.19}$$

in general it is

$$f(\underline{\xi_1}, \underline{\xi_2}, \omega) = \frac{|\omega| \sqrt{C_z^2 (\underline{\xi_1} - \underline{\xi_2})^2}}{2\pi (V_m(\underline{\xi_1}) + V_m(\underline{\xi_2}))} \tag{4.20}$$

where C_z represents the *decay coefficient*. By neglecting the turbulence variation with the space, on the top of the structure ($\underline{\xi_1}, \underline{\xi_2} = h$, see Fig. 4.14), the (4.17) can be written as

$$S_{D_t D_t}(h, \omega) = (\rho \cdot c_D \cdot V_{mx})^2 \cdot S_{uu}(h, \omega) \cdot \frac{1}{A^2} \int_A \int_A \exp\left(- f(\underline{\xi_1}, \underline{\xi_2}, \omega)\right) \cdot dA \cdot dA = \\ = (\rho \cdot c_D \cdot V_{mx})^2 \cdot S_{uu}(h, \omega) \cdot \chi^2(\omega) \tag{4.21}$$

where

$$\chi^2(\omega) = \frac{1}{A^2} \int_A \int_A \exp\left(- f(\underline{\xi_1}, \underline{\xi_2}, \omega)\right) \cdot dA \cdot dA \tag{4.22}$$

is called *aerodynamic admittance*.

The PSD of the turbulent response can be computed as

$$S_{r_t r_t}(h, \omega) = |H(\omega)|^2 \cdot S_{D_t D_t}(h, \omega) = (\rho \cdot c_D \cdot V_{mx})^2 \cdot |H(\omega)|^2 \cdot S_{uu}(h, \omega) \cdot \chi^2(\omega) \tag{4.23}$$

where $|H(\omega)|^2$ is the well known *mechanical admittance* of the structure given from

$$|H(\omega)|^2 = \frac{1}{m^2 \cdot {\omega_0}^2} \cdot \frac{1}{\left[\left(1 - \frac{\omega^2}{{\omega_0}^2}\right)^2 + 4\nu^2 \cdot \left(\frac{\omega}{\omega_0}\right)^2\right]} \tag{4.24}$$

Where m is the structural mass, ω_0 is the undamped fundamental circular frequency of the structure, ω is the actual circular frequency, and ν is the ratio of the damping coefficient *c* to the critical damping.

To obtain the mean square of the fluctuating response, the (4.23) is integrated over all frequencies

$$\sigma_{r_t}(h)^2 = \int_0^\infty S_{D_t D_t}(h,\omega)\cdot d\omega = \left(\rho \cdot c_D \cdot V_{mx}\right)^2 \cdot \int_0^\infty \left|H(\omega)\right|^2 \cdot S_{uu}(h,\omega)\cdot \chi^2(\omega)\cdot d\omega \qquad (4.25)$$

this can be approximated by two components, *B* and *R*, representing the *background* and *resonant parts* respectively, as below

$$\sigma_{r_t}(h) = \sigma_u(h)^2 \cdot \left(\rho \cdot c_D \cdot V_{mx}\right)^2 \cdot \int_0^\infty \left|H(\omega)\right|^2 \cdot \frac{S_{uu}(h,\omega)}{\sigma_u(h)^2}\cdot \chi^2(\omega)\cdot d\omega \cong \qquad (4.26)$$

$$= \sigma_u(h)^2 \cdot \left(\rho \cdot c_D \cdot V_{mx}\right)^2 \cdot \left[B + R\right]$$

where

$$B = \int_0^\infty \frac{S_{uu}(h,\omega)}{\sigma_u(h)^2}\cdot \chi^2(\omega)\cdot d\omega \qquad (4.27)$$

$$R = \chi^2(\omega_1)\cdot \frac{S_{uu}(h,\omega_1)}{\sigma_u(h)^2}\int_0^\infty \left|H(\omega)\right|^2 \cdot d\omega \qquad (4.28)$$

where ω_1 is the first natural frequency of the system (in this case it is the unique frequency), the two components are shown in Fig.4.15.

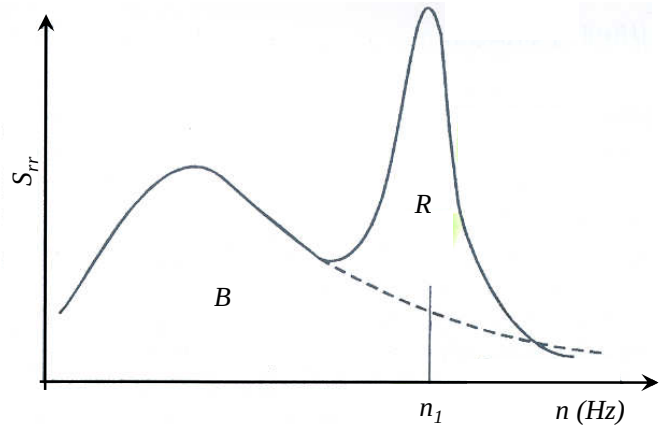

Fig.4.15. Background and resonant parts of the response.

The frequency domain approach for the response problem is synthesized in Fig. 4.16 (Davenport 1963).

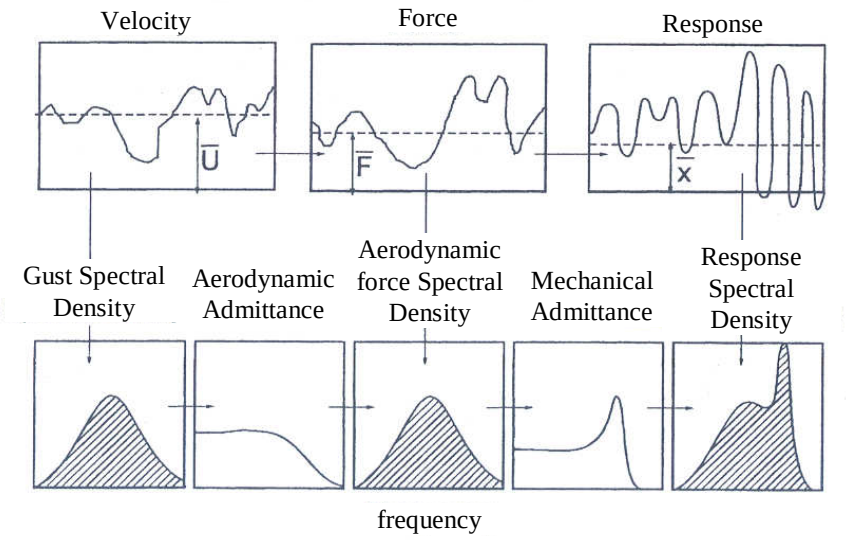

Fig. 4.16. Frequency domain approach (after Davenport 1963)

The peak structural response is then computed as

$$r^{p}(h) = r_m + g_r \cdot \sigma_r(h) \tag{4.29}$$

where the medium response r_m is given from

$$r_m = \frac{1}{K_r} D_m = \frac{\rho \cdot V_m^{\,2} \cdot c_D \cdot A}{2K_r} \tag{4.30}$$

in which K_r is the along-wind stiffness of the structure. In the (4.29), g_r is the *peak factor* of the response, which depends on the time interval for which the maximum value is calculated, and on the frequency range of the response.

The along-wind response of structures has a probability distribution which is closely Gaussian. For this case, Davenport (1964) derived the following expression for the peak factor:

$$g_r = \sqrt{2\log_e(\eta \cdot T_{wind})} + \frac{0.577}{\sqrt{2\log_e(\eta \cdot T_{wind})}} \tag{4.31}$$

where η is the "cycling rate" of effective frequency for the response: this is often conservatively taken as the natural frequency, n_1. T_{wind} is the time interval over which the maximum value is required.

4.2.2. Time domain analysis for response

Time domain approaches allow to consider directly the structural nonlinear effects and this is relevant for certain types of structures, like long span suspension bridges. Furthermore,

because the time domain analyses outputs are merely the time histories of specific variables, it is the most convenient approach in response problems.

The analysis in the time domain consists in a time integration that involves the time step updating of kinematic parameters and acting forces.

Usually the computational efforts required to carry out a time domain analysis for the response investigation is greater than the one required from the frequency analysis; besides the former requires the numerical simulation of the wind field in order to compute the wind action. As previously stated (chapter 1), if the interaction phenomena have to be investigated (stability or mixed response-stability problems), it is not trivial to implement in time domain expressions which are able to consider the variety of physical aspects involved in the interaction. Usually the analytical model contains integral terms, for which the time integration is a big issue. Simplified formulations have shown to be capable to reproduce the response of a non linear structure. In what follow the previously introduced (chapter 1) aeroelastic theories are applied to a response analysis of a long span suspension bridge. The bridge is described in the successive applications (chapter 6) for the PBWE methodology refinement. A detailed description of the bridge and the FE model is reported in chapter 6, the main suspended span of the bridge is 3300m long.

The analyses have been conducted considering a turbulent wind. Time histories of the wind speed field have been generated numerically by the previously introduced W.A.W.S. method with the POD decomposition technique, the wind field has been discretized by a total of 175 points representing both the bridge deck and the suspended cables, and the wind simulation time T_{wind} was 3000 seconds long. The analysis has been conducted by using the Non aeroelastic (NO), Steady (ST), Quasi Steady (QS), Modified Quasi Steady (QSM) aeroelastic theories, in order to compare the influence of the various simplified hypotheses.

In Fig. 4.17, the time oscillations along the three sectional DOFs of the deck mass centre, at bridge midspan, computed by the QS theory and corresponding to an incident turbulent flow having a mean velocity of 45 m/s, are represented. Every displacement time history has been characterized from a statistic point of view by the frequency probability density (including the 5% and 95% fractile values), and by the histogram representing the overcoming frequencies.

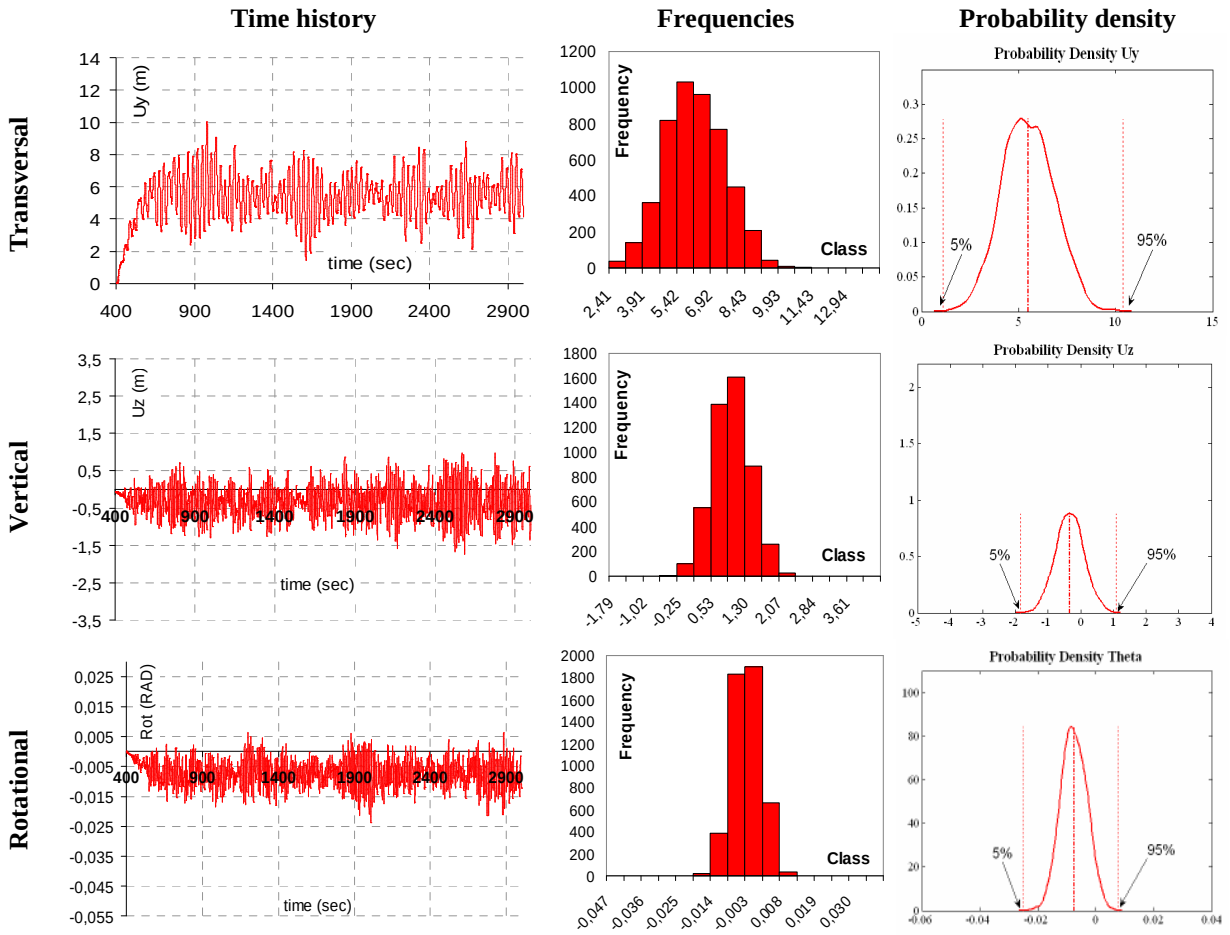

Fig. 4.17

In Fig. 4.18 the results obtained by the various aeroelastic theories are resumed and also the computed and experimental mean values are represented.

In general, one can note that by increasing the complexity of the aeroelastic forces representation (following the succession NO, ST, QS, QSM), both the maximum amplitude of the oscillations and the variance of computed time history decrease. Regarding this tendency an exception is represented from the rotation of the deck around own longitudinal axis, which in QSM results is greater (both in amplitude and in dispersion) than that obtained by QS.

One can note that NO results are a similar to those of ST results, and QS results are similar to the QSM ones. Concerning the mean values, the similitude of the results for couples of formulations (NO-ST, QS-QSM) is confirmed.

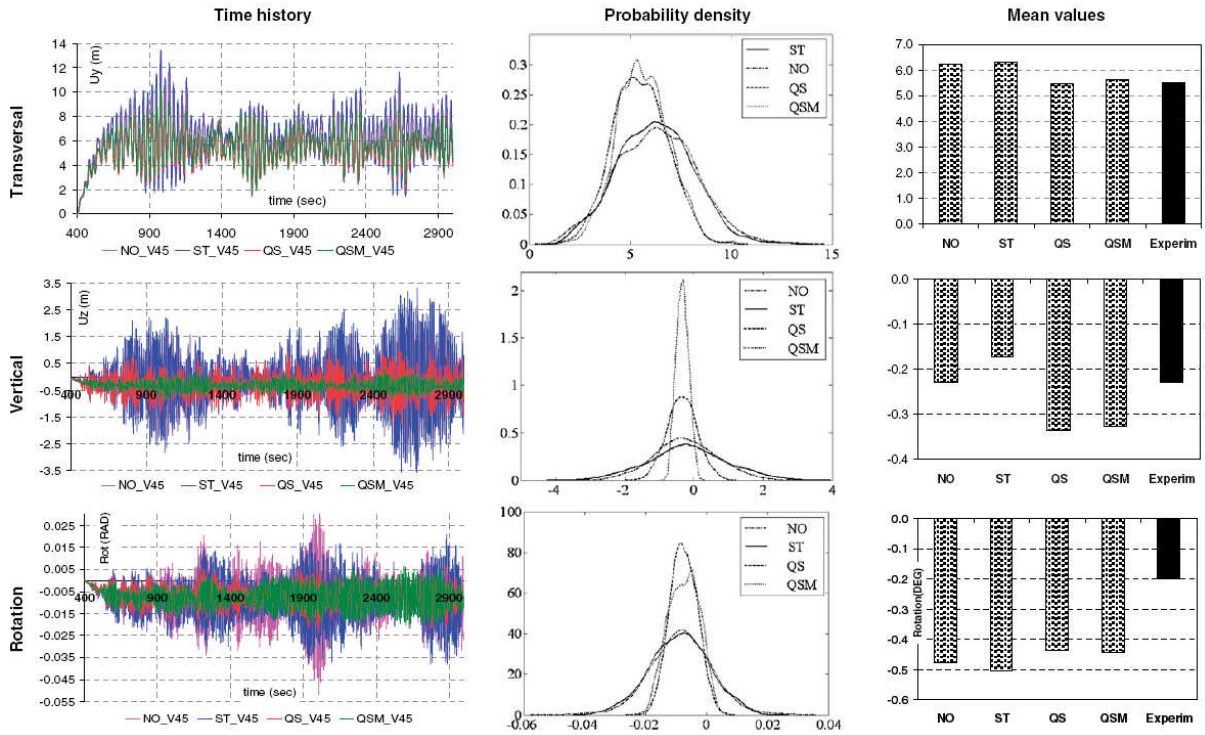

Fig. 4.18

In Fig. 4.19, time envelopes of the transversal and vertical deck displacements under turbulent flow are represented. Envelopes confirm the tendency previous evidenced by the time histories of midspan displacements: increasing the complexity of the aeroelastic forces representation, the envelopes decrease. Also in terms of envelopes, the similitude of the results for couples of formulations (NO-ST, QS-QSM) is confirmed. Among the examined formulations, the ST is the more sensitive to the increase of mean wind speed.

Similar diagrams have been computed concerning velocities and accelerations of the deck: in Fig. 4.20 the time envelopes of these kinematic entities are represented for the wind mean velocity of 45 m/s. The deck accelerations, in particular, have a great relevance in the bridge performance table: they have to maintain themselves under an imposed limit to ensure the safety during the transit of the trains.

Also in the velocities and in the accelerations envelopes, there is a decrease when the complexities of the formulations increase, and the results are similar by couple of formulations (NO-ST, QS-QSM).

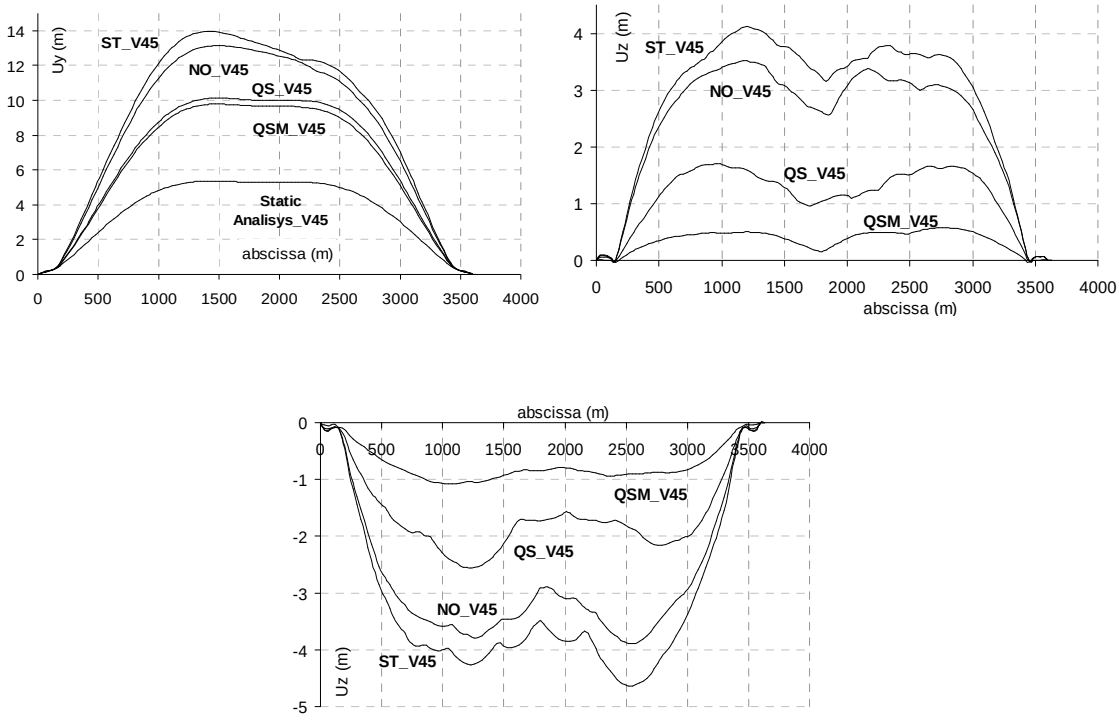

Fig. 4.19

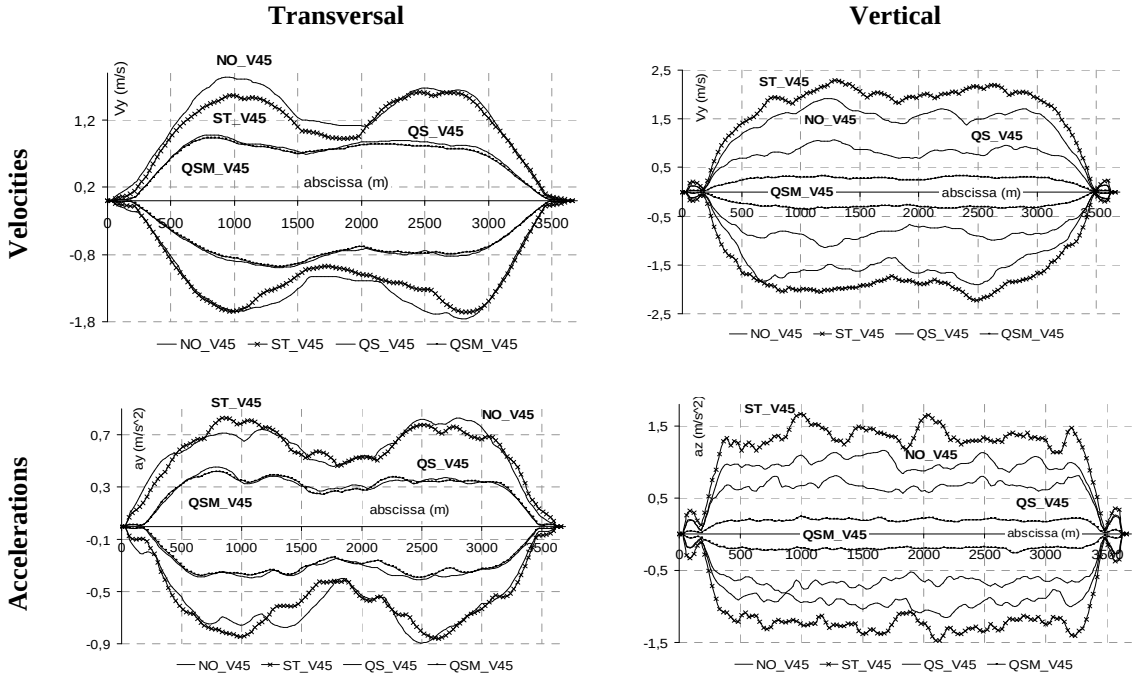

Fig. 4.20

4.2.3. Stability analysis

Frequently the study of the structural stability under the wind action can be reduced to an eigenvalues analysis (Bontempi et al. 2000). In this section an example of this methodology is shown with regard to the flutter analysis of a bridge structure.

The methodology will be explained with reference to the simplified 2 D.O.F. model shown in Fig. 4.21, following the reference (Borri and Costa, 2004).

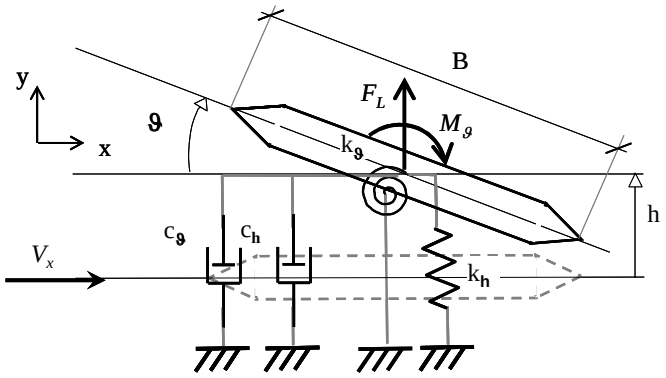

Fig. 4.21. Two-dimensional model for the stability analysis

Quasi steady approximation

Considering the simplified 2 D.O.F. model shown in Fig. 4.21, the effective angle of attack previously introduced is now given from:

$$\gamma_i(t) = \vartheta(t) - arctg\left(\frac{\dot{h}(t) + b_i \cdot B \cdot \dot{\vartheta}(t)}{V_x}\right) \qquad (4.32)$$

The following assumption are adopted:

bi = 1/2 were i = L,M due to the hypothesis that the physical phenomenon is governed from the interaction at the attack point; $\dot{h}$ e $\dot{\vartheta}$ sufficiently small in order to approximate the angles with their tangent.

The general equations (chapter 1) become:

$$\gamma(t) = \vartheta(t) - \frac{\dot{h}(t) + B/2 \cdot \dot{\vartheta}(t)}{V_x} \qquad (4.33)$$

$$V_{ai}(t) \approx V_x$$

Aerodynamic actions expression

$$F_L(h,\dot{h},\vartheta,\dot{\vartheta}) = \frac{1}{2}\rho V^2 B c_L(\gamma) = \frac{1}{2}\rho V^2 B c_L(h,\dot{h},\vartheta,\dot{\vartheta}) = \\ = \frac{1}{2}\rho V^2 B\left[c_L(\gamma=0) + K_{L0}\gamma\right] \tag{4.34}$$

$$M_\vartheta(h,\dot{h},\vartheta,\dot{\vartheta}) = \frac{1}{2}\rho V^2 B^2 c_M(\gamma) = \frac{1}{2}\rho V^2 B^2 c_M(h,\dot{h},\vartheta,\dot{\vartheta}) = \\ = \frac{1}{2}\rho V^2 B^2\left[c_M(\gamma=0) + K_{M0}\gamma\right] \tag{4.35}$$

Were K_{L0} and K_{M0} are the aerodynamic polar slopes ϑ=0.

Assuming that c_L(g=*0)=0* and c_M*(*g=*0)=0* it results:

$$F_L(h,\dot{h},\vartheta,\dot{\vartheta}) = \frac{1}{2}\rho V^2 B K_{L0}\left(\vartheta - \frac{\dot{h} - \frac{B}{2}\dot{\vartheta}}{V}\right) \tag{4.36}$$

$$M_\vartheta(h,\dot{h},\vartheta,\dot{\vartheta}) = \frac{1}{2}\rho V^2 B^2 K_{M0}\left(\vartheta - \frac{\dot{h} - \frac{B}{2}\dot{\vartheta}}{V}\right) \tag{4.37}$$

Equilibrium equations

$$m_h \cdot \ddot{h}(t) + c_h \cdot \dot{h}(t) + k_h \cdot h(t) = F_L\left(h,\dot{h},\vartheta,\dot{\vartheta};t\right) \tag{4.38}$$

$$I_\vartheta \cdot \ddot{\vartheta}(t) + c_\vartheta \cdot \dot{\vartheta}(t) + k_\vartheta \cdot \vartheta(t) = M_\vartheta\left(h,\dot{h},\vartheta,\dot{\vartheta};t\right) \tag{4.39}$$

by substituting the equations (4.36) and (4.37) in the equations (4.38) and (4.39) and omitting the variation with time:

$$m_h \cdot \ddot{h} + \left(c_h + \frac{1}{2}\rho \cdot V^2 \cdot B \cdot K_{L0}\right)\cdot \dot{h} + k_h \cdot h + \\ + \frac{1}{4}\rho \cdot V \cdot B^2 \cdot K_{L0} \cdot \dot{\vartheta} - \frac{1}{2}\rho \cdot V^2 \cdot B \cdot K_{L0} \cdot \vartheta = 0 \tag{4.40}$$

$$I_\vartheta \cdot \ddot{\vartheta} + \left(c_\vartheta + \frac{1}{4}\rho \cdot V \cdot B^3 \cdot K_{M0}\right)\cdot \dot{\vartheta} + \left(k_\vartheta - \frac{1}{2}\rho \cdot V^2 \cdot B^2 \cdot K_{M0}\right)\cdot \vartheta + \\ + \frac{1}{4}\rho \cdot V \cdot B^2 \cdot K_{L0} \cdot \dot{\vartheta} + \frac{1}{2}\rho \cdot V \cdot B^2 \cdot K_{M0} \cdot \dot{h} = 0 \tag{4.41}$$

the previous equations can be rewritten as a four dimensional system of equation as follows

$$\begin{cases} \dot{h} = \dot{h} \\ \dot{\vartheta} = \dot{\vartheta} \\ \ddot{h} = -\omega_h{}^2 \cdot h + \dfrac{1}{2}\dfrac{\rho}{m_h} \cdot V^2 \cdot B \cdot K_{L0} \cdot \vartheta - \left(\dfrac{c_h}{m_h} + \dfrac{1}{2}\dfrac{\rho}{m_h} \cdot V^2 \cdot B \cdot K_{L0} \right) \cdot \dot{h} - \dfrac{1}{4}\dfrac{\rho}{m_h} \cdot V \cdot B^2 \cdot K_{L0} \cdot \dot{\vartheta} \\ \ddot{\vartheta} = \left(-\omega_\vartheta{}^2 + \dfrac{1}{2}\dfrac{\rho}{I_\vartheta} \cdot V^2 \cdot B^2 \cdot K_{M0} \right) \cdot \vartheta - \dfrac{1}{2}\dfrac{\rho}{I_\vartheta} \cdot V \cdot B^2 \cdot K_{M0} \cdot \dot{h} - \left(\dfrac{c_\vartheta}{I_\vartheta} + \dfrac{1}{4}\dfrac{\rho}{I_\vartheta} \cdot V \cdot B^3 \cdot K_{M0} \right) \cdot \dot{\vartheta} \end{cases} \tag{4.42}$$

and in a canonical matrix form

$$\underline{\dot{\gamma}} = \underline{\underline{M}} \cdot \underline{\gamma} \tag{4.43}$$

where

$$\underline{\gamma} = \begin{bmatrix} h \\ \vartheta \\ \dot{h} \\ \dot{\vartheta} \end{bmatrix} \qquad \text{and} \qquad \underline{\underline{M}} = \begin{bmatrix} 0 & 0 & 1 & 0 \\ 0 & 0 & 0 & 1 \\ A & C & D & E \\ 0 & F & G & H \end{bmatrix}$$

$$A = -\omega_h{}^2;$$

$$C = \frac{1}{2}\frac{\rho}{m_h} \cdot V^2 \cdot B \cdot K_{L0};$$

$$D = -\left(\frac{c_h}{m_h} + \frac{1}{2}\frac{\rho}{m_h} \cdot V^2 \cdot B \cdot K_{L0} \right);$$

$$E = -\frac{1}{4}\frac{\rho}{m_h} \cdot V \cdot B^2 \cdot K_{L0};$$

$$F = \left(-\omega_\vartheta{}^2 + \frac{1}{2}\frac{\rho}{I_\vartheta} \cdot V^2 \cdot B^2 \cdot K_{M0} \right);$$

$$G = -\frac{1}{2}\frac{\rho}{I_\vartheta} \cdot V \cdot B^2 \cdot K_{M0};$$

$$H = -\left(\frac{c_\vartheta}{I_\vartheta} + \frac{1}{4}\frac{\rho}{I_\vartheta} \cdot V \cdot B^3 \cdot K_{M0} \right).$$

Since the equilibrium equations are written in the form (4.43), the flutter instability corresponds with the analytical instability called Hopf Bifurcation (Sedaghat et al 2001). This arise when, varying a scalar parameter (the wind speed V in the flutter case), which there is a couple of complex conjugate eigenvalues for the coefficient matrix, for switch the sign of the

real part becomes nil and, successively, change its sign (from negative to positive), doing so the two complex conjugate eigenvalues cross the imaginary axis (see Fig. 4.22).

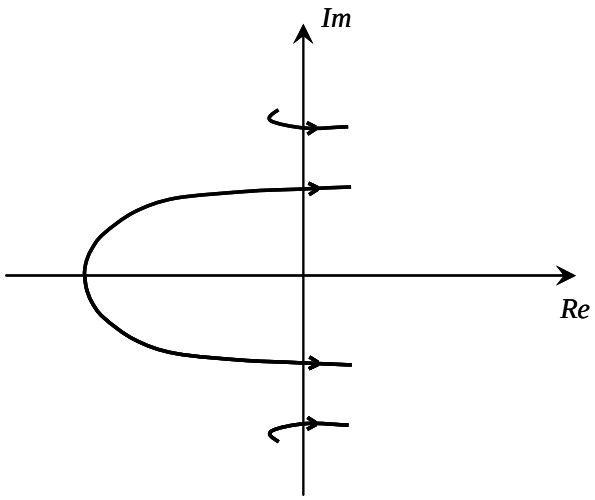

Fig. 4.22. Roofs plane flutter representation.

4.3.

4.4. References

Bontempi, F., Malerba, P. and Giudici, M. (2000). “La Formulazione matriciale dei problemi aeroelastici di ponti sospesi e strallati” (in Italian), Studi e Ricerche-Politecnico di Milano 21.

Borri, C. and Costa, C., (2004). “Quasi-steady analysis of a two-dimensional bridge deck element”, Computer & Structures, (82), 993-1006.

Cao ,Y., Xiang, H. and Zhou, Y. 2000. Simulation of Stochastic Wind speed Field on Long-Span Bridges. Journal of Engineering Mechanics 126(1): 1-6.

Di Paola M., Gullo I. (2001). "Digital generation of multivariate wind field processes", Probabilistic Engineering Mechanics, vol. 16, 1-10.

Davenport, A.G. (1995). “How we can simplify and generalize wind load?”, J Wind Eng. Ind. Aerodyn. 54/55, 657-669.

Davenport, A.G. (1998). “Probabilistic methods in wind engineering for long span bridges”, Proc. of the Int. Symp. on Advances in Bridge Aerodynamics, May 1998, Copenhagen, Denmark.

Deodatis G. (1996). "Simulation of ergodic multivariate stochastic processes", Journal of Engineering Mechanics, vol. 122, 778-787.

Holmes, J.D.. Wind loading of structures, Spoon Press, 2001.

Nielsen, M., Larsen, G. C., Mann, J., Ott, S., Hansen, K. S. and Pedersen, B. J., (2004). Wind Simulation for Extreme and Fatigue Loads, Risø Report 1437(EN), Risø National Laboratory, Roskilde, Denmark.

Rossi, R., Lazzari, M. and Vitaliani R. (2003). "Wind field simulation for structural engineering purposes", International Journal of Numerical Methods in Engineering, vol. 61, 738-763.

Samaras E., Shinozuka M., Tsurui A. (1985). "ARMA representation of random processes", Journal of Engineering Mechanics, vol. 111, 449–461.

Schuëller G.I. (ed.) (1997). "A state-of-the-art report on computational stochastic mechanics", Probabilistic Engineering Mechanics, vol. 12, n. 4, 197-321.

Schüeller, G.I. (2006). “Developments in stochastic structural mechanics”, Archive of Applied Mechanics vol. 75 No. 10-12/October 2006.

Shinozuka M., Deodatis G. (1997). "Simulation of stochastic processes and fields", Probabilistic Engineering Mechanics, vol. 12, no. 4, 203–207.

Sedaghat, A., Cooper, J., Leung, A.Y.T. and Wright, J.R. (2001). “Estimation of the Hopf bifurcation point for aeroelastic systems”, Journal of Sound and Vibration, 248 (1), 31-42.

Ubertini F., Giuliano F. (2008). "A comparative study on efficiency and accuracy of Gaussian wind simulation methods", Journal of Wind Engineering and Industrial Aerodynamics, submitted for publication.

PART III

APPLICATIONS

Chapter 5

APPLICATIONS

In this chapter the proposed PBWE procedure is tested and applied with regard to two case study structures: a long span suspension bridge (section 5.1) and an Offshore Wind Turbine (OWT) (section 5.2). In the first case, with the aim to validate the proposed modifies to the basic PEER procedure, after the application of the original PEER procedure, numerical analyses have been carried out to assess the importance of the additional parameters proposed in equation (3.17) with respect to the (2.10). In the second application, the proposed PBWE procedure implementing the proposed additional parameters considering the peculiar aspects of the wind engineering problem is applied. Here the relative importance of the various stochastic parameters is assessed by a preliminary sensitivity analysis.
In what follow, the ANSYS © Finite Element computational code has been adopted to conduct the structural analyses, while the evaluation of the stochastic parameters statistics and the random samples generation has been made by the MATLAB © computational code.

5.1. PBWE for a long span suspension bridge

For the validation of the proposed PBWE procedure (eq. (3.16)), a case study long span suspension bridge has been taken under consideration. The main span of the bridge is 3300 m long, while the total length of the deck, 60m wide, is 3666m (including the side spans). The deck is formed by three box sections, the outer ones for the roadways and the central one for

the railway. The roadway deck has three lanes for each carriageway (two driving lanes and one emergency lane), each 3,75m wide, while the railway section has two tracks.

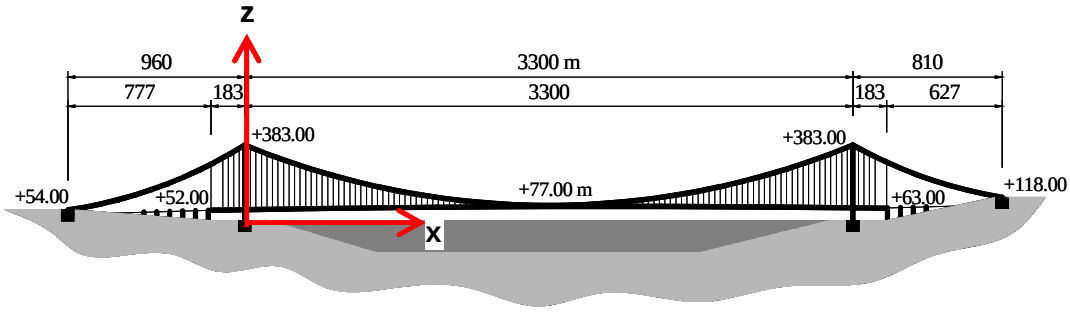

Fig. 5.1. Case study bridge profile.

5.1.1. Structural performance under wind actions and numerical models

For the bridge under the wind action, the required performances are classified and subdivided in two main levels:

- high level performances: related with the serviceability of the bridge, this level of performances has to be maintained in the most wind storm cases. The high level performances are analytically expressed by using of Service Limit States (SLS);
- low level performances: related to the safety of the structure's users or to the maintainability of the structural integrity during its life cycle. The low level performances are analytically expressed by using of Ultimate Limit States (ULS).

In the present work, examples of these two performance levels have been considered: concerning the high level performance problem, the serviceability of the bridge under wind action has been investigated; concerning the high level performance problem, both the aeroelastic stability of the bridge against the flutter and the fatigue resistance of the secondary suspension system (hangers) during the life cycle have been considered. Focusing on the simplified form of the procedure (equation (3.16)), its starting point concerns the analytical formulation of the failure criteria by using proper limit states functions, which express the failure (in the sense that a certain performance will not be satisfied by the system) in terms of proper EDPs. In sake of simplicity, the best choice for these functions is to adopt scalar relations, so in general one has a failure threshold that have not to be overcome by the EDP value. Concerning the high level performance (serviceability) problem, examples of relevant EDPs are: deck translational and rotational accelerations, deck rotational velocities, deck torsion (rotation of the deck section in its plane) which could generate an excessive

misalignment between the binary lines, and more others. In the present paper three EDPs have been considered for the serviceability. The EDPs have been identified as the maximum values (along the deck and during the wind storm) of certain motion parameters. These are: the vertical deck section acceleration (V_{ert} acc), the rotational deck section velocity (Rot vel) and the acceleration of the deck section along the longitudinal axis of the bridge (x-axis) (Long acc max); these EDPs are referred to the center of mass of the deck section. Two sub-levels of performances can be identified for the serviceability problem: the complete serviceability (train and vehicles transit) or the partial serviceability (only train transit), these two sub-levels are identified by different failure thresholds. Concerning the low level performance problem, in particular with regard to the flutter problem, the damping of a significant displacement time history (for example the mid span vertical displacement) is assumed as relevant EDP; as it becomes negative, the flutter instability arise. For what concern the fatigue problem, obviously the damage in the most vulnerable hanger is assumed as the relevant EDP, as it becomes equal to unity, the hanger experiments the fatigue collapse. Considering the specific performance, the failure is achieved when the value of the respective EDP overcomes the failure threshold value during the wind storm. Both performances description and failure criteria adopted in this paper are resumed in Tab.5.1.

Tab. 5.1. Performances table.

	Name	Performance	EDPs	Failure threshold
Service Limit State (SLS)	Se1_BU-SLS-1	Complete serviceability (roadway and railway traffic) under atmospheric Buffeting (BU)	*Rot vel max v_{rot} **Long acc max a_{l_max} ***Vert acc max a_{v_max}	v_{rot}=0.04 RAD/s a_{l_max}=2.5 m/s^2 a_{v_max}=0.9 m/s^2
	Se2_BU-SLS-2	Partial serviceability (railway traffic) under atmospheric Buffeting (BU)		v_{rot}=0.043 RAD/s a_{l_max}=2.5 m/s^2 a_{v_max}=1.1 m/s^2
Ultimate Limit State (ULS)	FL-ULS	Maintaining of the structural integrity (avoid the flutter) for Vm $\leq$ 57 m/s or during the whole Life Cycle (200 years)	****Total damping δ	$\delta = 0$
	Ftg_BU-ULS (response)	Fatigue resistance (of the hangers) During the whole Life Cycle (200 years)	*****Total fatigue damage in the hanger D_{ftg}	$D_{ftg} \leq 1$

* max rotational velocity of the deck section during the wind storm
** max longitudinal acceleration of the deck section during the wind storm
*** max vertical acceleration of the deck section during the wind storm
**** sum of structural and aerodynamic damping of the deck section during the wind storm
***** cumulate damage (during life cycle) in the most damaged hanger

5.1.2. Numerical analysis description

Numerical analyses are conducted in time domain by using of a complete 3D Finite Elements model of the bridge shown in Fig. 5.2. For the developed transient step by step analyses, a Newmark time integration scheme has been adopted, in which geometric non linearity has been considered.

The incident turbulent wind speed time histories have been generated numerically like components of a multivariate, multidimensional Gaussian stationary stochastic process; the Weighted Amplitude Wave Superposition method (W.A.W.S.) and Proper Orthogonal Decomposition (P.O.D.) of the PSD matrix (see chapter 5) are adopted. Starting from the wind speed time histories, computing the acting forces by use of aeroelastic theories is possible (Petrini et al. 2007, Salvatori and Borri 2007) as described in chapter 1. In the case of low level performance instability problem (FL-SLU problem) the wind flow has been modeled as non turbulent.

The probabilistic characterization of the response has been obtained by using Monte Carlo technique.

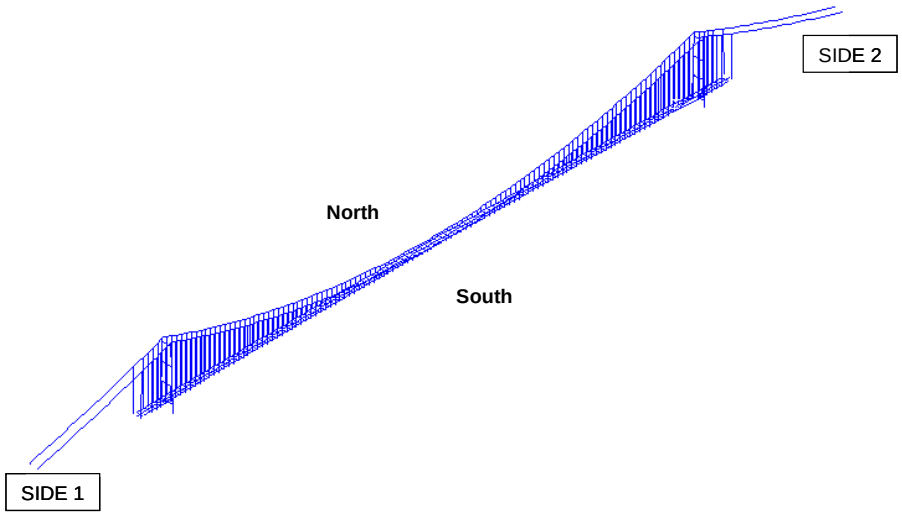

Fig. 5.2. 3D FE model of the bridge.

5.1.3. Application of the PEER original procedure

First of all, the PEER procedure (2.11) has been applied in its simplified form. Keeping the simplified hypotheses that had lead to the (5.15) it results from the equation (2.11):

$$\lambda(EDP) = \int\int P(EDP|IM) \cdot g(IM) \cdot dIM \tag{5.1}$$

By this way, IPs have not been modeled as stochastic variables, and one scalar parameter has been considered representative for the stochastic IM; this is the 10 meters height mean wind speed (V_{10}), that is assumed as stochastic, having a Weibull annual PDF given by:

$$P(V_{10}) = 1 - exp\left[-\frac{1}{2}\left(\frac{V_{10}}{\sigma} \right)^{k} \right] \tag{5.2}$$

with the parameters σ and k set respectively equal to 6.02 m/s and 2.02 on the basis of wind measures database for the structural site. Starting from the V_{10}, the Vm at the bridge deck medium height (77 m) can be computed by the equation (1.6). In the following the incident mean wind speed at the deck medium height V_m(z = 77 m) has been considered the IM parameter.

5.1.3.1.High level performance problem

A set of 500 samples has been extracted from the considered probability distribution function (Fig. 5.4), for each one of the samples ten-minute wind speed time history sample has been generated according with the analytical model and the generation technique before introduced. The generation domain is composed from a total o 27 spatial point (on both bridge deck and suspension cables, see Fig. 5.10), both along wind (parallel to y-axis, transversal to the deck) and an across wind (parallel to z-axis, vertical direction in the deck cross-sectional plane) turbulent wind velocities are considered. Each wind speed time history sample leads (by the structural analysis), to a sample of the EDPs; starting from the resulting 500 samples, the annual probability distribution and the annual probability of overcoming a certain failure threshold can be obtained for each EDP. In computing the wind actions the QS aeroelastic theory has been adopted (see chapter 1). The procedure is shown in Fig 5.5.

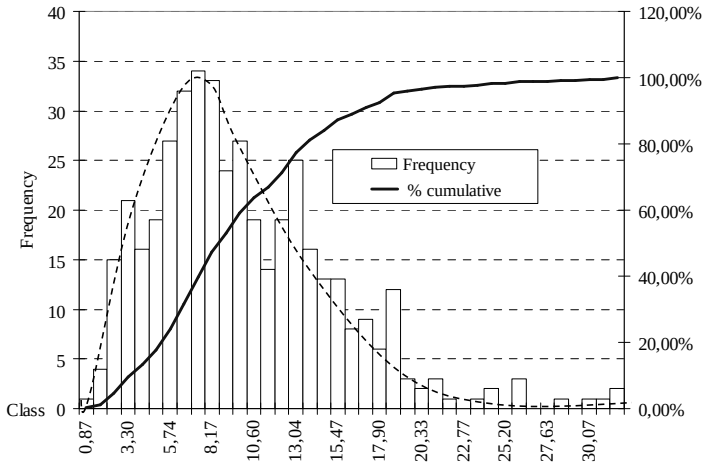

Fig. 5.3. IM sampling.

In Fig. 5.5, 5.6 and 5.7 the populations of the response EDPs and their histogram characterization (occurrence frequencies) are shown, along with the corresponding failure thresholds.

From figure 5.6 it can be seen that the EDP number 2 (Long acc max) is not dangerous for the considered performance.

The computed quantities λ(EDP) are represented in Fig. 5.6. Because these are related with an annual probability distribution function for the IM, the resultant occurrences are referred to an annual period of service for the structure. From the annual probability of occurrence curves (Fig. 5.8 and 5.9), by fixing a failure threshold for an EDP (abscissa values), the annual probability of that failure typology (referring to that specific EDP) can be identified in the corresponding λ(EDP).

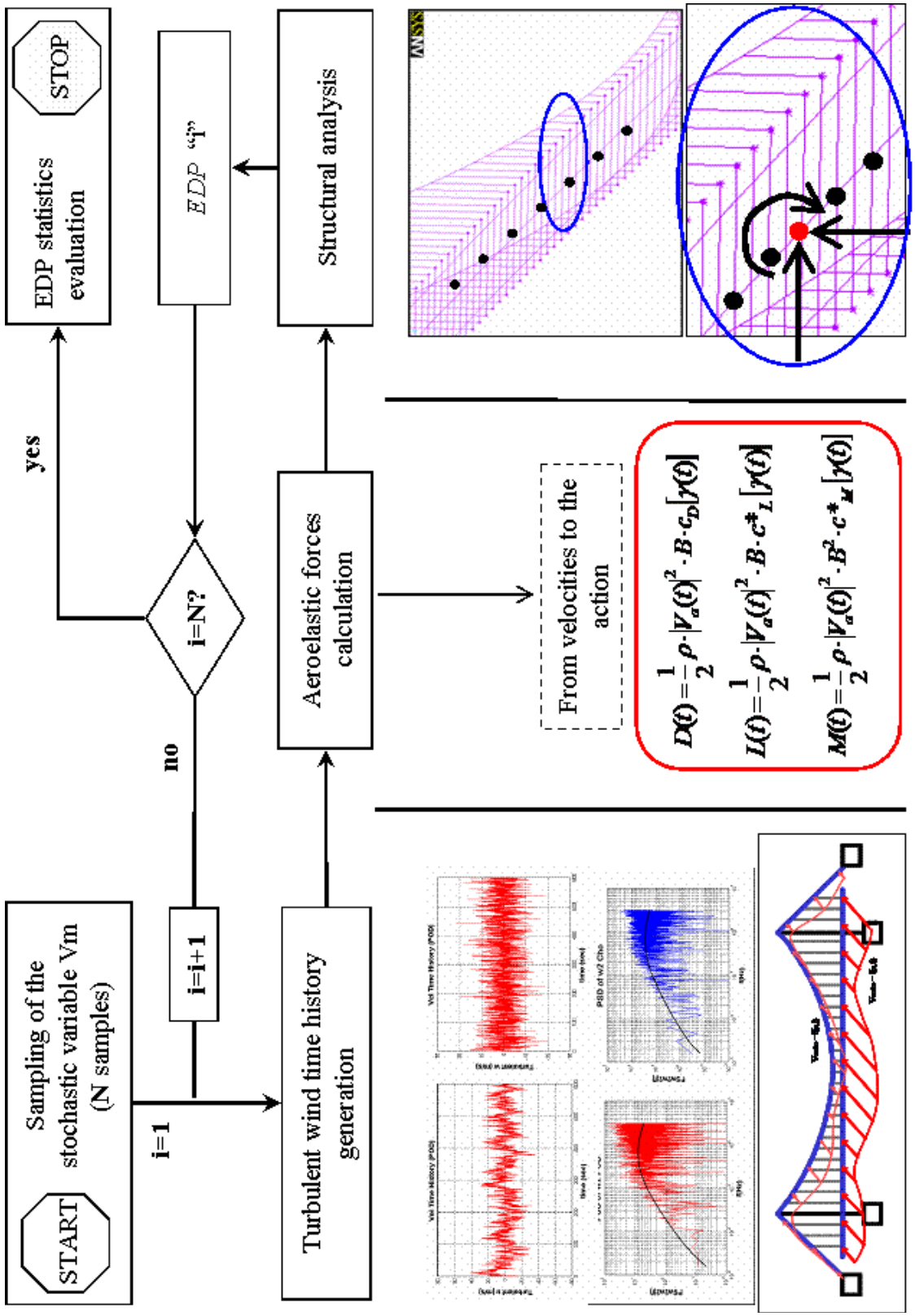

Fig. 5.4. Analysis flowchart.

In table 5.2 the annual failure probabilities computed for each failure type corresponding to the previous specified thresholds (Tab. 5.1) are summarized, here the annual total probability of failure, computed as the union of the singles failure typologies, is also reported for the considered SLS.

To asses the Se_BU-SLS bridge performance, the acceptability of the total failure probabilities have to be judged.

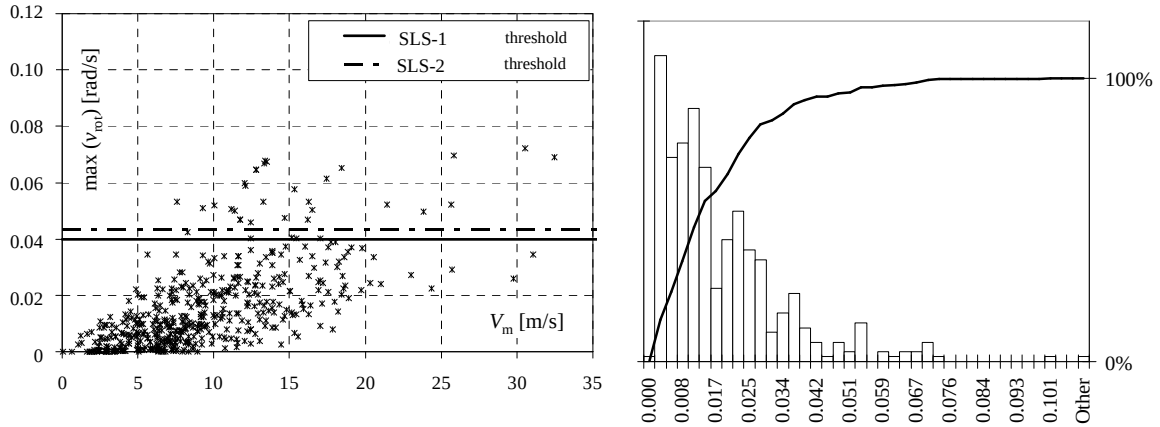

Fig. 5.5. EDP 1: Rot vel max. Population (left), occurrence frequencies (right).

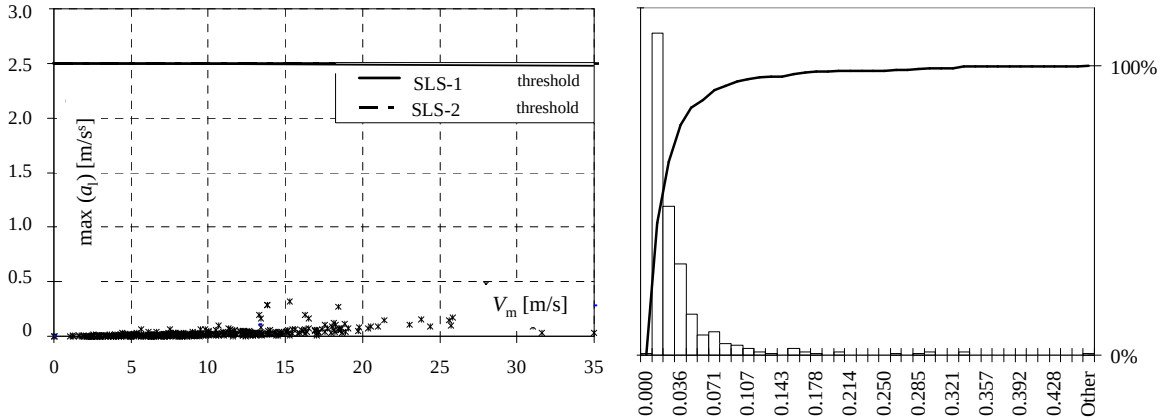

Fig. 5.6. EDP 2: Long acc max. Population (left), occurrence frequencies (right).

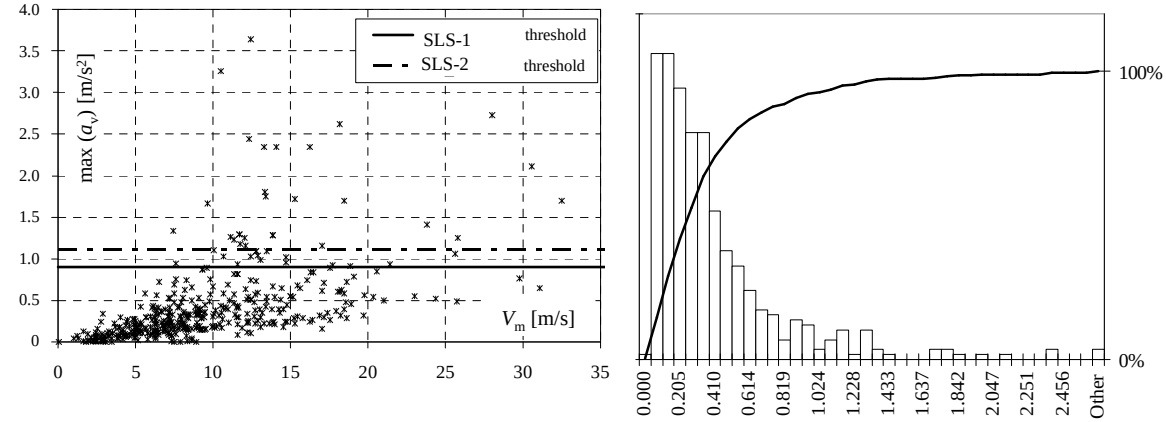

Fig. 5.7. EDP 3: Vert acc max. Population (left), occurrence frequencies (right).

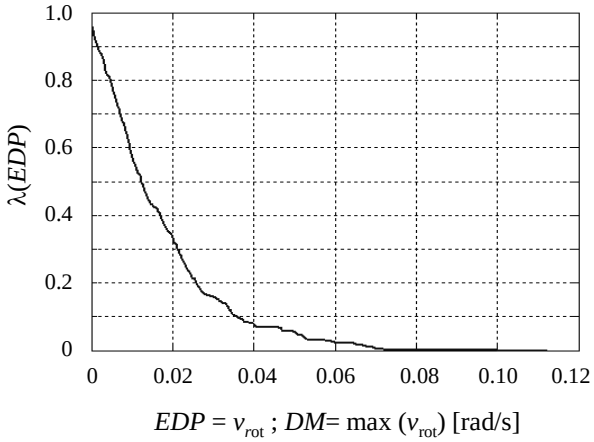

Fig. 5.8. EDP 1: Rot vel max annual occurrence.

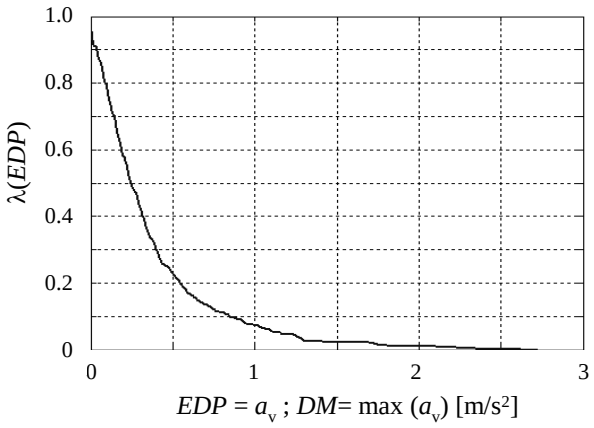

Fig. 5.8. EDP 2: Vert acc max annual occurrence.

Tab. 5.2. Failure probabilities

	Name and problem type	Failure typology	Failure typology probability	Total failure probability (union event)
Service Limit State (SLS)	Se1_BU-SLS	$v_{rot} \geq 0.04$ RAD/s	0.081775701	0,112149533
		$a_{l\_max} \geq 2.5$ m/s^2	0	
		$a_{v\_max} \geq 0.9$ m/s^2	0.091121495	
	Se2_BU-SLS	$v_{rot} \geq 0.043$ RAD/s	0.070093458	0,08411215
		$a_{l\_max} \geq 2.5$ m/s^2	0	
		$a_{v\_max} \geq 1.1$ m/s^2	0.056074766	

The fragility functions P(*EDPi*|*IM*) for the two dangerous *EDP*'s have been computed with a procedure similar to the one reported in (Jalayer et al. 2007); the performance indicators Y_i have been introduced, defined as

$$Y_i = \frac{EDPi}{EDPi^*} \quad \text{(i=1,2,3)} \tag{5.3}$$

where EDP_i^* is it the threshold value for the performance evaluation relatively to the *EDP* number *i*, by using the performance indicators, one can state that the threshold value for the generic Y_i is $Y_i^*=1$.

Under these assumptions it is possible to write the fragility functions as follow:

$$P(EDP_i \geq EDP_i^* \,|\, IM) = P(Y_i \geq 1 \,|\, IM) = P(IM \geq IM^{Y_i=1}) \tag{5.4}$$

where $IM^{Yi}=1$ is the value of *IM* for which results Y_i =1; assuming that $IM^{Yi}=1$ is a stochastic variable described by a Lognormal distribution with median $\eta_{IM^{Y_i=1}}$ and fractional standard deviation $\xi_{IM^{Y_i=1}}$. The fragility function can be computed by the assessing of the parameters $\eta_{IM^{Y_i=1}}$ and $\xi_{IM^{Y_i=1}}$. This can be done in various manners, in particular if the structural behavior is linear, the statistical distribution of $IM^{Yi}=1$ can be found by a simple linear interpolation of the *EDPi* samples derived from the Monte Carlo analysis as shown in Fig. 5.9.

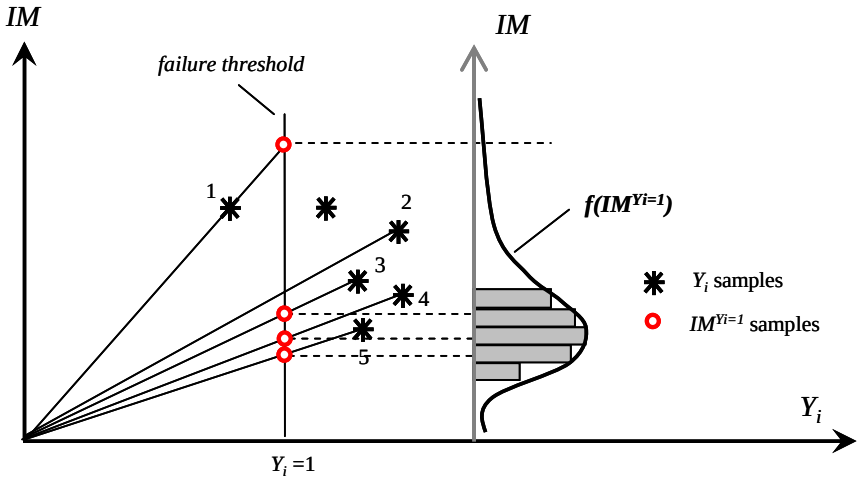

Fig. 5.9. Extrapolation of the $IM^{Y_i=1}$ probability distribution in the case of linear response.

Since the response of the case study structure it is non linear for the presence of geometric second order effects, the statistical parameters for the $IM^{Y_i=1}$ distribution function are derived by defining a *failure interval* (instead of a *failure threshold*) around the failure threshold as shown in Fig. 5.10 and 5.11 (red stripe around the value Y_i =1). The samples of *IM* producing some Y_i that falls in the failure interval, are taken as a samples of $IM^{Y_i=1}$, which are used to

evaluate $\eta_{IM^{Y_i=1}}$ and $\xi_{IM^{Y_i=1}}$; in the present case, the amplitude of the failure interval has been set equal to 0.2.

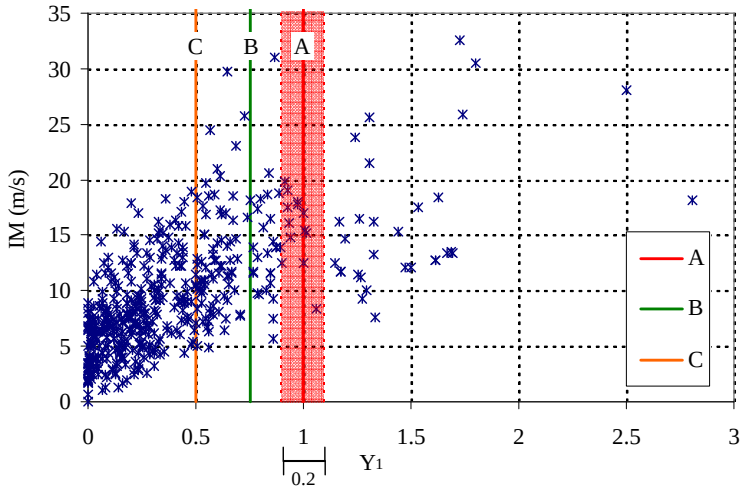

Fig. 5.10. Y_1 population, failure threshold for different performance levels and failure range.

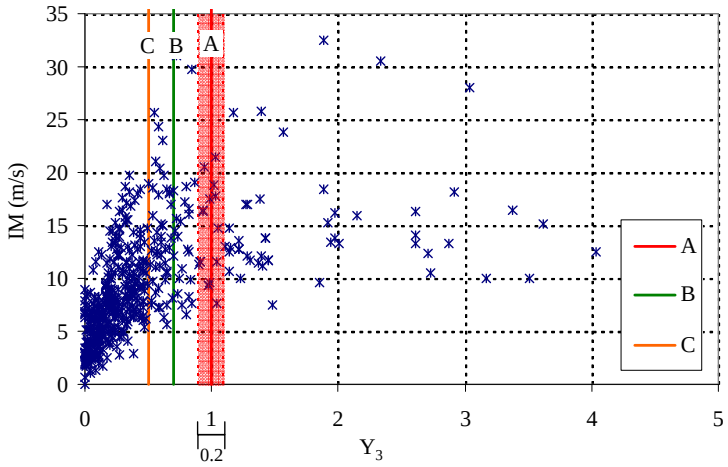

Fig. 5.11. Y_3 population, failure threshold for different performance levels and failure range.

For the EDPs numbers 1 and 3, three fragility curves have been computed, in correspondence with three failure thresholds (or system states) A, B, C, as shown in Fig. 5.10 and 5.11 and resumed in table 5.3, the state A coincides with the Se1_BU-SLS previously defined (see Tab.5.1).

Tab. 5.3. Performances table.

***EDP* No**	**Failure thresholds**		
	A (=Se1_BU-SLS)	**B**	**C**
1 (EDP_1*)	EDP_1* $_{(A)}$ = 0.04 RAD/s	0.03 RAD/s	0.02 RAD/s
2 (EDP_2*)	EDP_2* $_{(A)}$= 0.9 m/s^2	0.63 m/s^2	0.45 m/s^2
Y_i*= EDP_i* $_{(A)}$ / EDP_i* (i =1, 3)	1	0.75	0.5

The resultant fragility curves for the two *EDP*s are shown in Fig. 5.12 and 5.13. The comparison for the fragility curves relatively to the two *EDP*s is shown in Fig. 5.14 for the Se1_BU-SLS performance level (threshold A), it is clear that the EDP_3 is the most dangerous for low *IM*s while the EDP_1 is the most dangerous for high *IM*s.

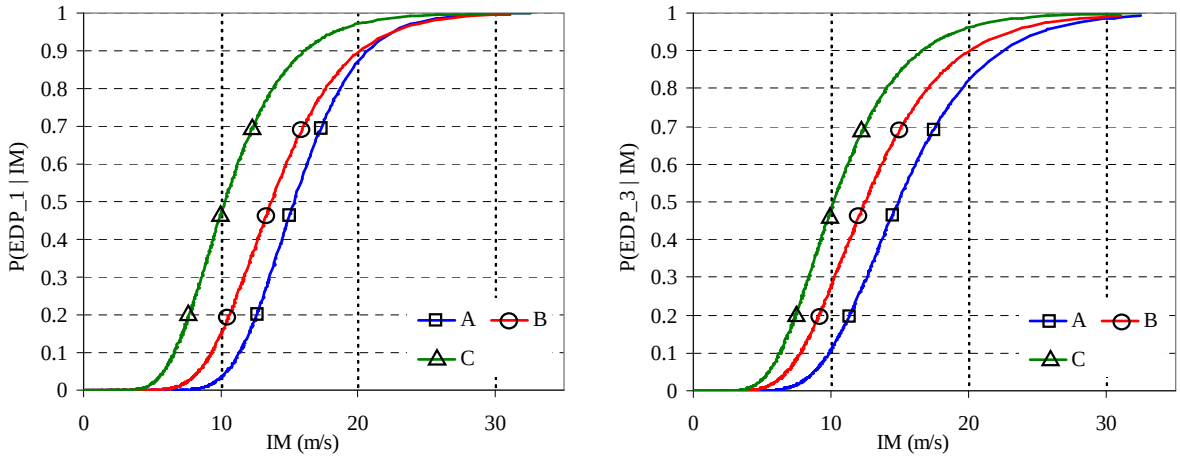

Fig. 5.12. EDP 1 and EDP 3: Fragility curves.

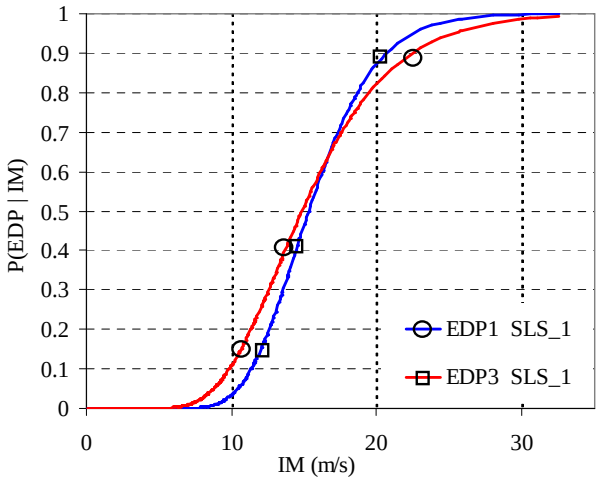

Fig. 5.13. Se1_BU-SLS performance level, comparison between fragility curves.

Finally, the fragility curves related with the union event of the two *EDPs* has been computed in Fig. 5.12 and 5.13. The population of the union event has been obtained from the samples of the two *EDPs* by selecting, for each sample IM_k (k=1,2,…N where N is the total number of samples adopted for the MC analysis), the value within the two *EDPs* which produces the values of Y_i that is located nearest to the unity, consequently will result

$$Y_{U(k)} = Y_{i(k)} \quad nearest\ to\ 1 \qquad (i=1,3)\ \text{ for each } IM_k \tag{5.5}$$

where U stands for "Union event". In Fig. 5.14 the population of performance indicators Y_U is shown and in Fig. 5.15 the Se1_BU-SLS fragility curve of the union event is reported In Fig. 5.15 superposed to the two "single-event" fragility curves.

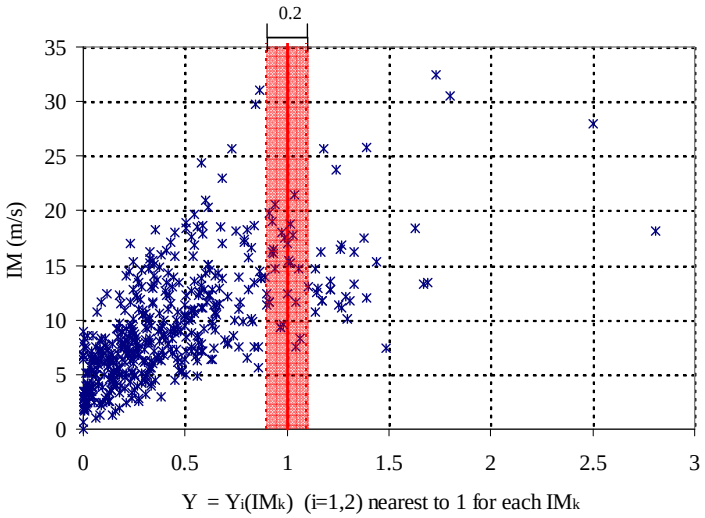

Fig. 5.14. Y_U population, and failure range.

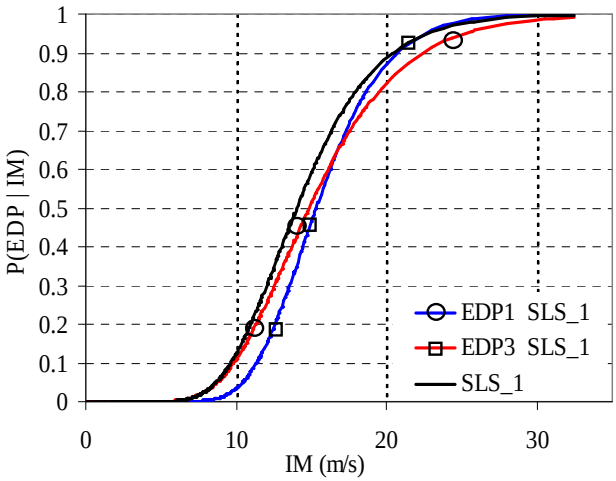

Fig. 5.15. Se1_BU-SLS performance level, comparison between fragility curves.

To asses the Se_BU-SLS bridge performance, the acceptability of the total failure probabilities have to be judged.

5.1.3.2.Low level performance problem: Flutter instability

Typically, for suspension bridges, the most dangerous instability phenomenon is the so called "classical flutter": a dynamic instability in which two DOFs of the forced structural system are coupled: under opportune configurations (defined "critical") for the two frequencies and reciprocal phase angles, it makes the damping of the system become negative, and the structural oscillations increase in amplitude. For a suspension bridge, the two coupled DOFs are the vertical and the rotational ones for the deck section. As the vertical and, in particular, rotational motion frequency depend on the incident wind speed, when this velocity increases the frequencies come closer to each other until the "frequency coalescence"; during this interval of time the damping is positive. When the oscillation frequencies have the same value, and phase shifted of $\pi/2$, the damping of the system becomes zero and, if the wind speed increases, it becomes negative. The wind speed which corresponds to zero damping and incipient flutter is called "critical wind speed" (Vcrit).
As previously stated, for this performance, the wind flow has been modeled as non turbulent, so only the mean wind speed component Vm is present. Adopting, in the polar lines, showed in Fig. 7a, by means of a step by step time domain analysis and the well known Quasi Steady (QS) theory for the aeroelastic forces computing, the critical velocity has been assessed to be equal to 70 m/s.
The damping of the generic time oscillation can be estimated by identifying it with the exponential coefficient δ of the function $q(t) = \bar{q} \pm q_0 \cdot e^{-\delta \cdot t}$ (were $\bar{q}$ identifies the static equilibrium position), which envelopes the generic oscillation (see Fig. 8a): in damped (Vm<Vcrit), critical (Vm=Vcrit) and amplified (Vm>Vcrit) oscillations, it results respectively δ >, = or < to zero. In Fig. 8b, the amount of damping δ for various Vm is shown: here, δ represents the total damping of the structural system, which is sum of the structural (assumed constant and equal to 0.5%) and the aerodynamic one (computed as the analytical difference from the total damping and the structural one). The total damping curve grows when there is an increasing of the wind speed; at a certain value it changes its slope and

begins to decrease until the intersection of abscissa axis. Such intersection represents the critical flutter velocity.

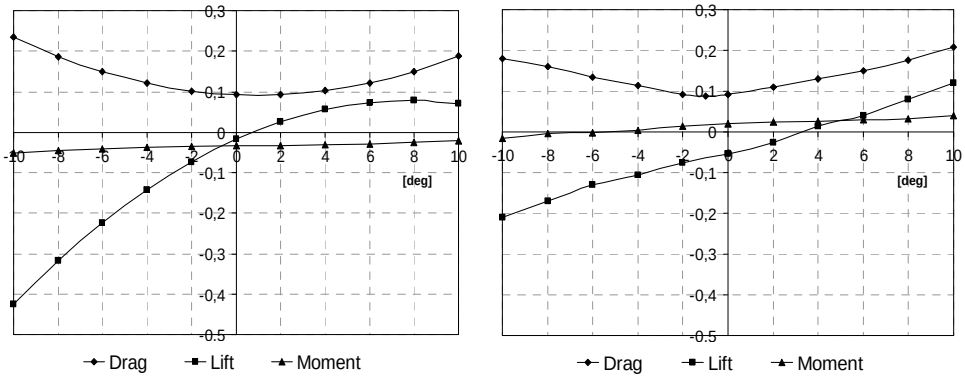

Fig. 5.16. Polar lines: type A (left), type B (right).

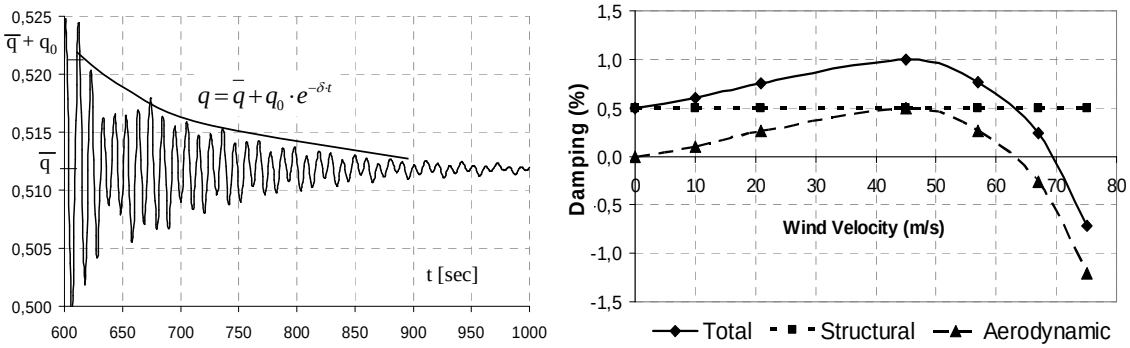

Fig. 5.17. Aerodynamic damping: envelope of mid span oscillation (Vm<Vcrit δ>0) to evaluate damping (left), damping on incident flow velocity (right)

The oscillations in the phase plane (rotation and vertical displacement) and the time projections (3-D graphics) of the plane are shown in Fig. 5.18. In such diagrams, the oscillations become pseudo-circular curves, which implode in a single point (final configuration) when $V_m < V^{FL}crit$, or they stabilize themselves along a circular curve of constant amplitude when $V_m = V^{FL}crit$ (after a transient initial period with different amplitude oscillations), or they explode like a divergent spiral when $Vm > V^{FL}crit$.

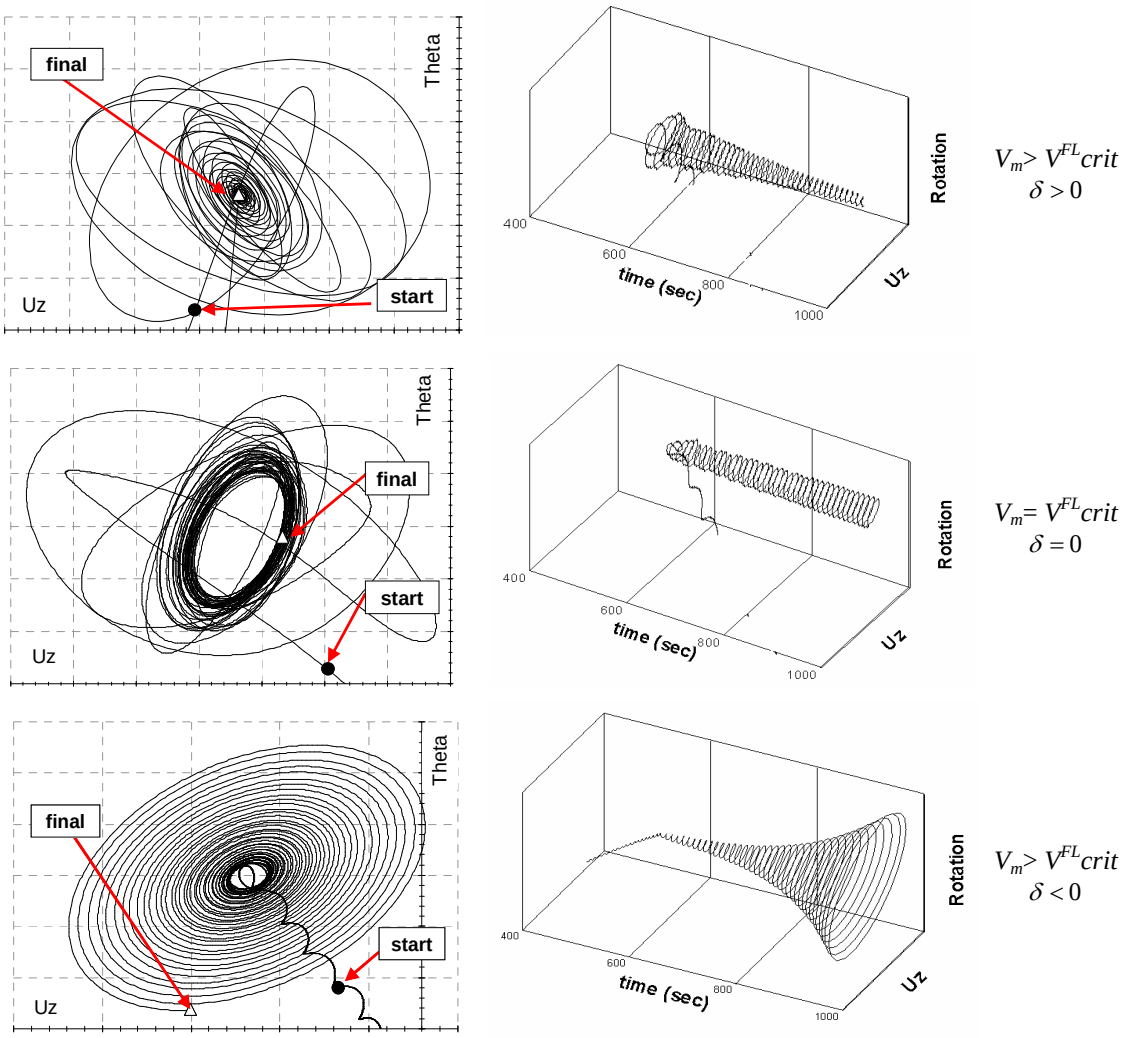

Fig. 5.18. Damped, critical and amplified oscillations for midspan of the deck (phases plane representation)

In this case, to asses the λ(EDP) and the probability of failure corresponding to the fixed failure threshold (see Tab. 5.1) one can proceed as in the previous presented high performance problem. Because the probability of failure in this case will be very small, a great number of samples are required to compute it by classical Monte Carlo methods. In the case study, taking advantage to the additional performance specification that the flutter has not to arise when $V_m \leq 57$ m/s, one can states that the examined low level performance is achieved. Nevertheless, by assuming the mean wind speed as a single intensity measure, and stating that the flutter critical velocity is a deterministic parameter, the failure probability can be easily computed from the distribution probability of the IM. Adopting the annual PDF of IM, one obtains the annual probability of failure, since the request of performance (see table 5.1) is

referred to the whole structural life cycle, the annual extreme values distribution referred to a return period of 200 years (see section 1.1.4) must be adopted for the IM.

With reference to the section 1.1.4, from the equation (1.17) the failure probability is given by

$$P(V^{\max} \geq V^{FL}crit \mid \alpha, \beta) = 1 - F_{V^{\max}}(V^{FL}crit) = 1 - \exp\left(-\exp\left[-\alpha \cdot (V - \beta)\right]\right) \quad (5.6)$$

Where α and β depends on the local wind specific statistics, in the present case has been assumed α= 0.227 and β= 45.037, the resultant CCDF (=1-CDF) is shown in Fig.5.19.

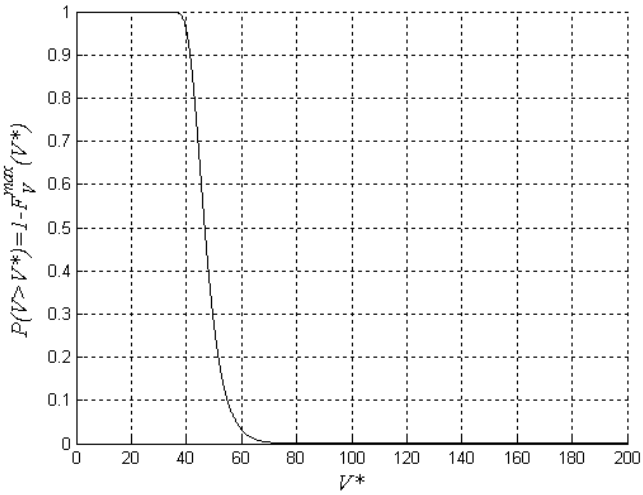

Fig. 5.19. Extreme wind speed probability

In the case study structure it results $V^{FL}crit$= 70 m/s and $P(V^{max} \geq V^{FL}crit)$=0.0034.

5.1.3.3.Low level performance problem: Fatigue of the secondary suspension system

Wind and traffic induced vibrations are the main causes of fatigue damage in the cables and hangers of suspension bridges. Cause of the high flexibility and reduced weight (in relation of the whole dimension of the structure), suspension cable system of these types of bridges can experiment a great number of tension-cycles with significant amplitude during their life-cycle. In the present work the fatigue problem regarding hangers of the bridge is treated. These members are subjected to axial fatigue effect that can be faced with simplified damage laws and fatigue curves referring to axial experimental data.

Concerning wind fatigue damage, several authors have done studies to assess fatigue behavior of structures (Repetto & Solari 2002 and 2007, Aprile & Benedetti 2000) and cables (e.g. Cluni et al. 2007) under wind action. Because of wind stochastic nature, the problem has to be treated in a probabilistic way. The fatigue damage is correlated with the mean wind speed magnitude (Ubertini & Bontempi 2008), which is a stochastic variable having an annual Weilbull probability density function. Consequently, each parameter which can describe adequately the response of the structure will be a stochastic variable too.

The fatigue damage induced by traffic is different in the different members of suspension bridges, depending on the stress rate induced by the transit of the vehicles: in the members which experience low excursions of the stress rate in respect the permanent load, such as the main cables, the expected fatigue damage is low, especially in the case of long span bridges, for which the permanent load is very high. Vice versa, hangers, deck and secondary components have high change in the stress during the transit of vehicles, and so they are prone to be damaged and substituted several times during the service life of the bridge.

The third aspect of discussion, concerning the subject of the study, is the interaction mechanism between train and wind. First, there is an aerodynamic interaction caused from the local changes in aerodynamic forces due to the train presence on the bridge deck (Petrini et al. 2005). This effect increase in importance when the geometrical dimension ratios between train and structure (length of the train vs length of the span, height and width of the train vs height and width of the deck section) increase. The second interaction mechanism concerns the structural dynamic behavior, it can be significant in the case of large deflection of the bridge. Third interaction mechanism concerns the fatigue damage interaction: the sum of damages due to wind and train is not equal to the damage caused from train transit when the structure is subjected to the wind action.

The fatigue damage due to the train transit has been evaluated considering two different typologies of train (see Table 5.4): a freight train, with a length of 750 m and a weight of 8,8 ton/m, and a passenger train, with a length of 390 m and a weight of 2,44 ton/m.
The number and frequency of trains have been evaluated with reference to a period of one year, considering the transit of three passenger trains and one freight train every hour, for 18 hours every day, 6 days every week, and 50 weeks every year. Therefore, the cumulative fatigue damage has been evaluated taking into account the transit of 16200 passenger trains and 8100 freight trains per year.
Real load scenarios are generally more complex, because various trains can cross the bridge at different speed at the same time, moving in the same or in opposite directions. However, for the sake of simplicity, the effects of different train running on the bridge at the same time and with different velocities have not been considered.
The same damage accumulation law has been considered for both wind and train transit. The life cycle of the structure has been set equal to 200 years.
In the case of stochastic fatigue analysis under wind action, referring to expression (2.2), reported below

$$J = E[h(\underline{\theta})] = \int h(\underline{\theta}) \cdot q(\underline{\theta}) \cdot d\underline{\theta} \qquad (5.7)\ ((2.2))$$

the output is the fatigue damage, and a function $h(\theta)$ is represented by a damage accumulation law (in the present case the Palmgreen-Miner law). The expected value of $h(\theta)$ is the mean damage caused by the wind speed magnitude probability distribution. Using Monte Carlo method doing N analyses, the total damage is the sum of the damages caused from each one of the N analyses, and it becomes a deterministic parameter (associated with the number N), instead of that a distribution of probability.
Due to the complexity of the structure, preliminary analyses have been carried out to assess the sensitivity to fatigue damage of the hangers located in various positions along the span (Petrini et al 2008).
The examined hangers are shown in Figure 5.20, while examples of the time histories of the axial force in a vulnerable hanger are reported in Figure 5.21.
The results of the preliminary analyses are summarized in Figure 5.22, where the fatigue damages due to wind actions (evaluated as the average of the values obtained by 5 analyses under time histories generated by considering a mean wind speed equal 15 m/s) and to the transit of one freight train are reported. It is evident that the hangers located near the tower are

more sensitive to the effects of wind actions, while the hangers located near midspan are more sensitive to the effects of train transit.

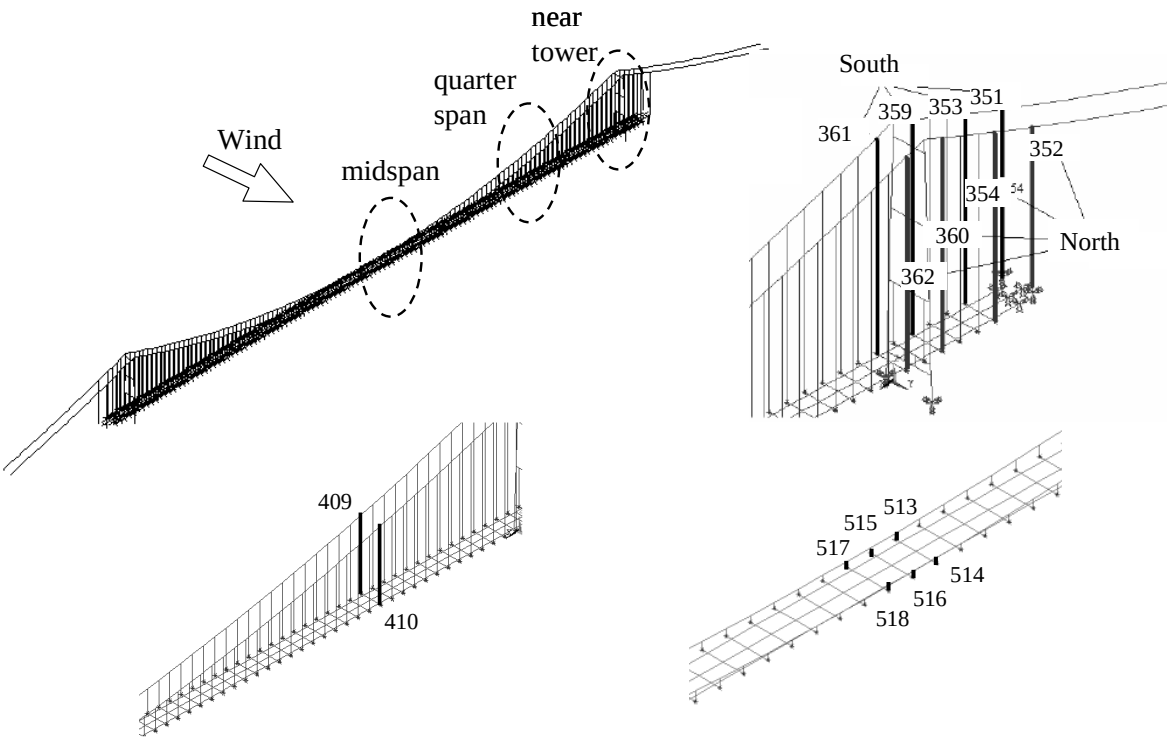

Figure 5.20. Hangers considered in the vulnerability assessment

The vulnerability assessment has been carried out with reference to the hanger N. 352, the most vulnerable to wind action.

To estimate the fatigue damage due to wind action, a Monte Carlo simulation has been carried out (500 samples). The rainflow counting method has been adopted; the cumulative damage has been evaluated according to the Palmgren-Miner law. Reference has been made to the fatigue strength curve for direct stress ranges (detail category 160 N/mm2) given in (CEN 2003).

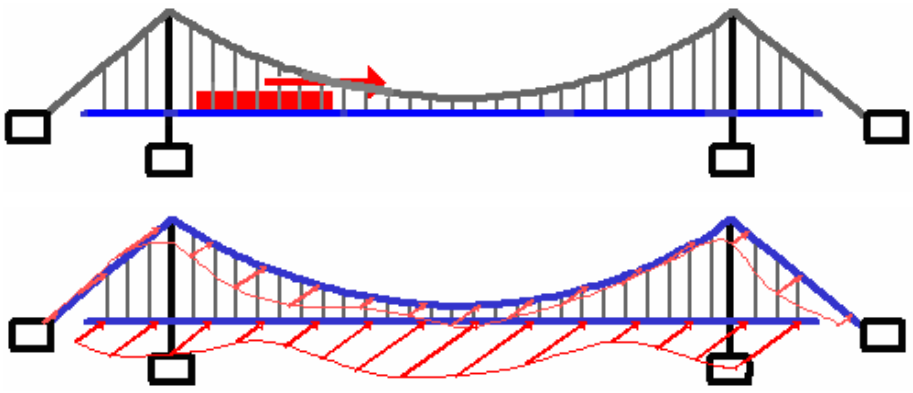

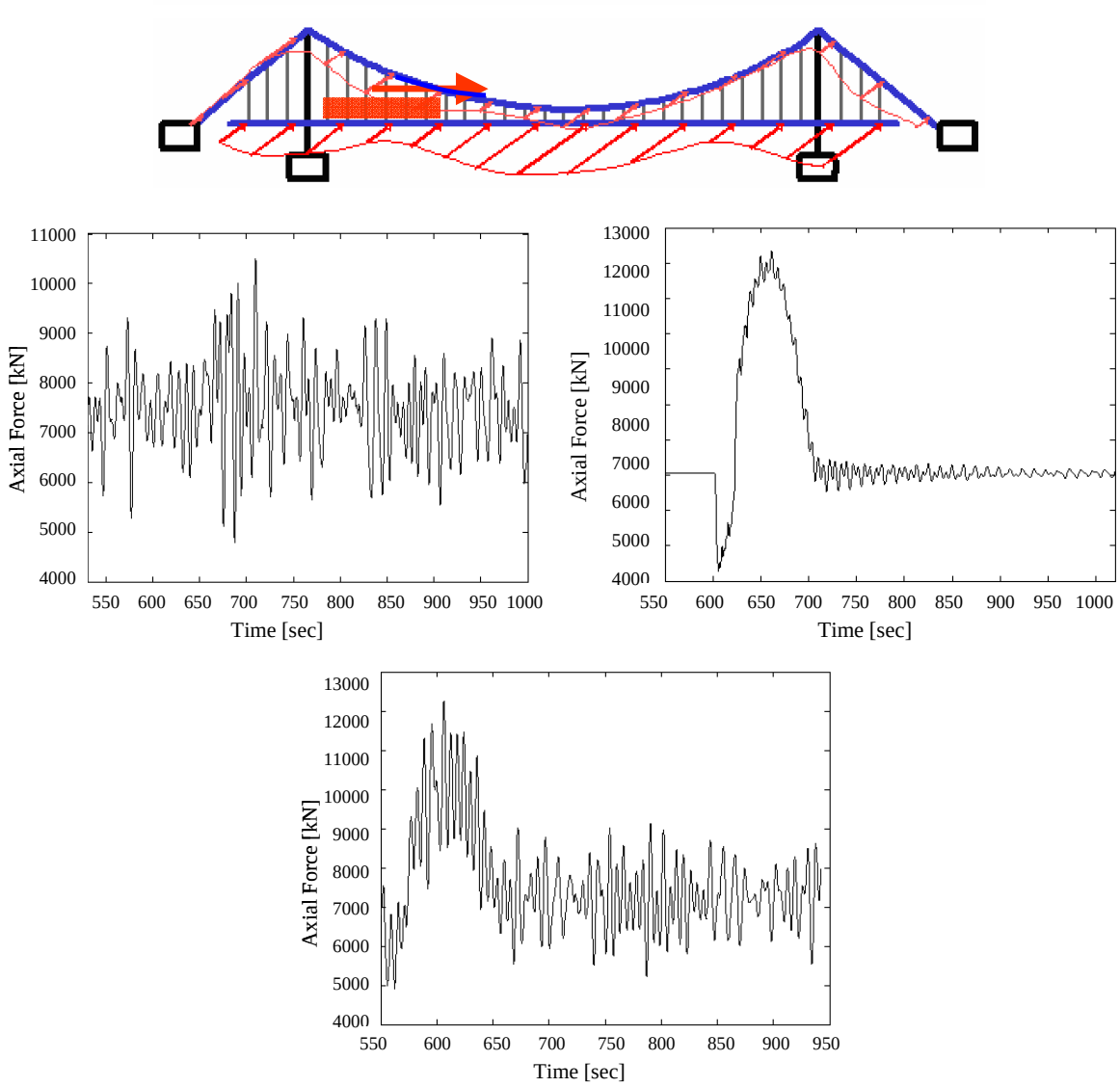

Fig. 5.21. Time histories of the axial force in hanger N. 352 due to: wind action (upper-left); freight train transit (upper-right); wind action and train transit (bottom);

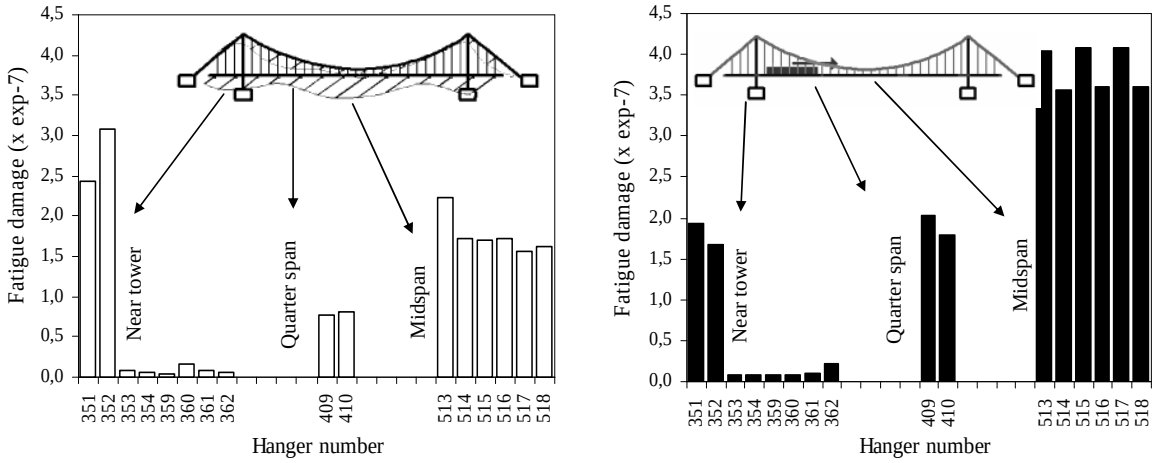

Fig. 5.22. Fatigue damages due to (left) wind actions (Vm = 15 m/s) and (right) transit of freight train in the examined hangers.

The values of the fatigue damage to hanger N. 352 are reported in Figure 5.23 as a function of the mean wind speed. Damage increases more than linearly as the mean value of the velocity increases.

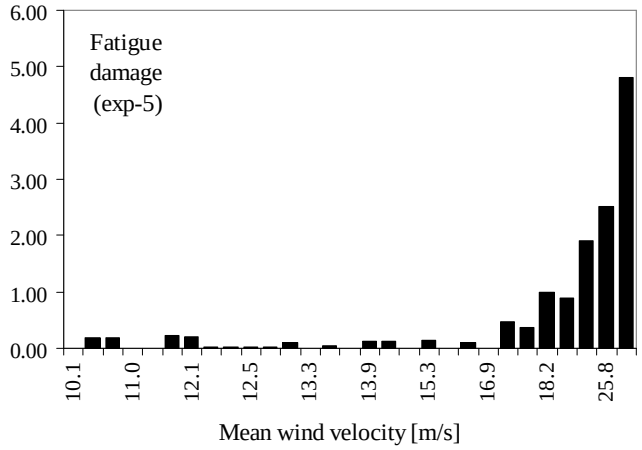

Fig. 5.23. Fatigue damage to hanger N. 352 due to wind action

With the aim to validate the proposed modifies to the basic PEER procedure, numerical analyses have been carried out to assess the importance of the additional parameters proposed The sum of values reported in Figure. 5.23 have also been assumed as representative of the annual damage to hanger N. 352; therefore, the fatigue life under wind action is higher than 2000 years (the threshold value assumed in design). The assumed approximation is certainly rough, but not essential to illustrate the application of the procedure of PBWE.

The values of the fatigue damage due to the train transit in hangers N. 517 and N. 352 are reported in Table 5.4.

Table 5.4. Characteristics of the considered trains and fatigue damage corresponding to one transit

	Train type	
	freight	passenger
Length [m]	750	390
Weight [ton/m]	8,80	2,44
Velocity [Km/h]	135	250
Damage to hanger 517 (more sensitive to train transit)	3,072E-07	8,200E-08
Damage to hanger 352 (more sensitive to wind actions)	1,67E-07	3,90E-08
Total annual transits	16200	8100

In Table 5.5 the total annual fatigue damages due to train transit are reported, together with the corresponding fatigue life (in years) for hanger N. 517, the most sensitive to damage due to train transit, and hanger N. 352.

Table 5.5. Life-cycle damage in critic hangers due to train transit and corresponding fatigue life.

Hanger number	Total annual damage due to train transit	Fatigue Life [years]
517	0,005641	177,2786
352	0,003021	330,9834

As concerns the procedure of PBWE, the results reported in Figure 5.24 have been elaborated to obtain a relation between the considered EDP (the fatigue damage due to wind action) and the assumed IM (the mean wind speed).
The evaluated EDP-IM relation is depicted in Figure 5.24; the probability density functions of IM and EDP are reported in Figures 5.25. The probability density function of EDP has been derived by the conditional probability density function corresponding to the relation EDP-IM shown in Figure 5.25.

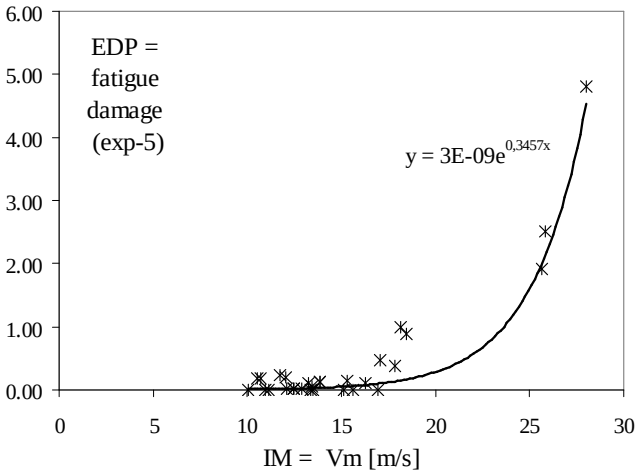

Figure 5.24. Relation between the fatigue damage due to wind (the assumed EDP) and the mean wind speed (the assumed IM)

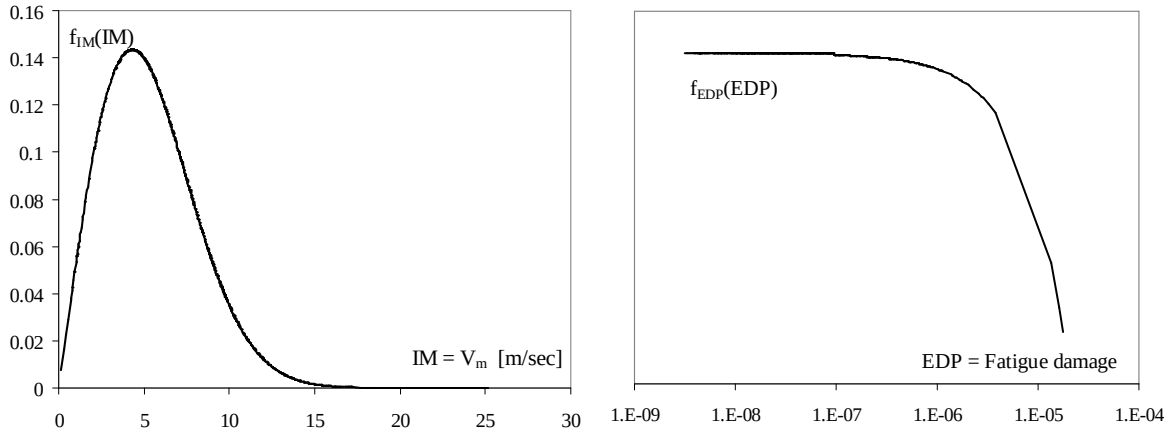

Figure 5.25. Probability density functions of IM (left) and EDP (right).

As previously stated the train transit modifies the structural dynamic properties and influence the structural response to wind. Therefore some attention has to be given to the assessment of the effects of the interaction mechanisms between the fatigue damages due to train transit and wind action. Three aspects have to be considered.

First, the aerodynamic forces are influenced by the transit of trains; this effect is more significant if the ratios between the dimensions of the train and the structure (length of train vs length of span; height and width of train vs height and width of deck section) increase. However, this effect is not relevant in the example case.

The second interaction mechanism is related to the second order effects, which can be significant in case of train transit. This effect has been considered in developed calculations.

The third interaction mechanism is directly related to the interaction between fatigue due to wind and fatigue due to train transit: simply, the sum of fatigue damages due to wind and train is not equal to the damage evaluated by considering both causes of fatigue.

This effect has been tentatively considered by running a limited number of analyses. The results are reported in Figure 5.26, where the damages to different hangers due to wind, train transit and train transit under wind action are reported.

Reference has been made to a lower detail category (36 N/mm2) in order to have comparable damages due to train transit and wind. From these preliminary results, it appears that the fatigue damage due to both train transit and wind action is lower than the sum of damages resulting from these causes if considered separately.

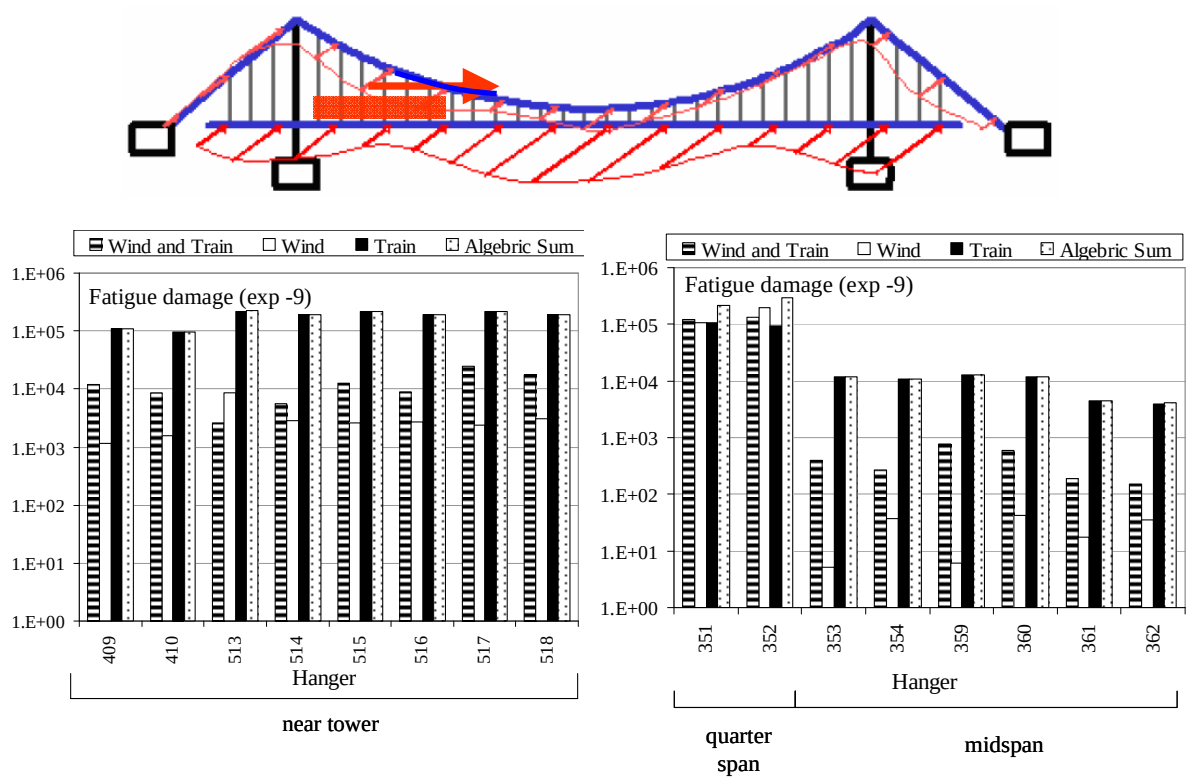

Figure 5.26. Axial fatigue damage to hangers due to wind and train transit acting separately or interacting

5.1.4. Analyses for the validation of the proposed PBWE procedure

With the aim to validate the proposed modifies to the basic PEER procedure, numerical analyses have been carried out to assess the importance of the additional parameters proposed in equation (3.17) with respect to the (2.10).

5.1.4.1.Importance of the roughness inside a vectorial Intensity Measure (IM)

The importance of the roughness has been investigated: 100 samples have been generated for the mean wind speed Vm(z = 77 m), and these have been used to perform three distinct Monte Carlo analyses, changing the value of the roughness, which assumes the values z0= 0.05, z0= 0.1 and z0= 0.2 respectively. Focusing on the EDP1 (Rot vel max), three occurrence curves λ(EDP) have been computed and they are represented in Fig. 5.27, since the three probability curves differs significantly each other, the importance of the roughness as intensity measure it is evident.

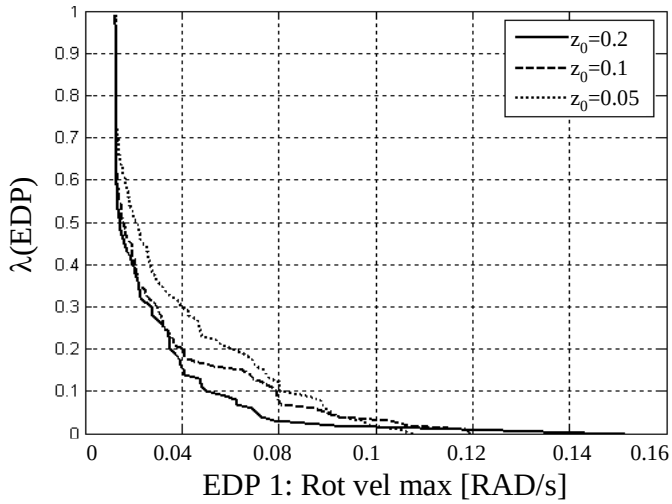

Fig. 5.27. Importance of the roughness as intensity measure

As in the high performance problem related to the bridge serviceability, the influence of the uncertainty affecting the roughness (z_0) values has been evaluated also for the fatigue problem. The EDP-IM relation that is shown in Fig. 5.23 for the case of z_0=0.1, has been investigated also for z_0=0.05 and z_0=0.2; similar EDP-IM relations has been derived as shown in fig. 5.28.

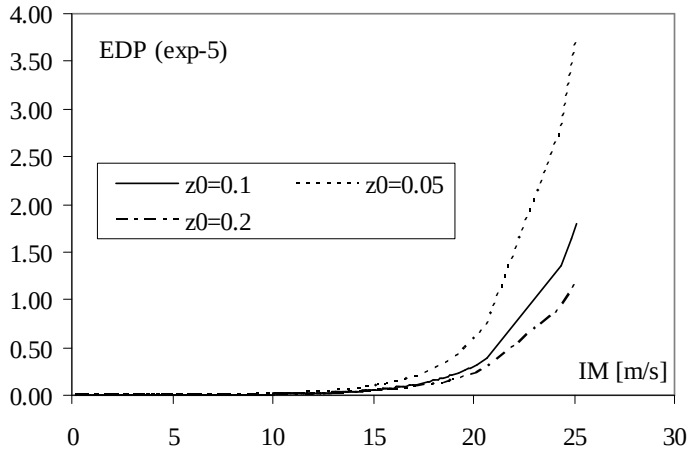

Figure 5.28. Probability of fatigue damage due to wind as a function of the mean wind speed - vulnerability curve of hanger N. 352

The PDFs for the fatigue damage due to the wind action in the critic hanger (N.352) corresponding to the three roughness values are shown in Fig. 5.29; as from the Fig. 5.27, it is clear that the uncertainty affecting the roughness value plays an important role in the probabilistic performance assessment.

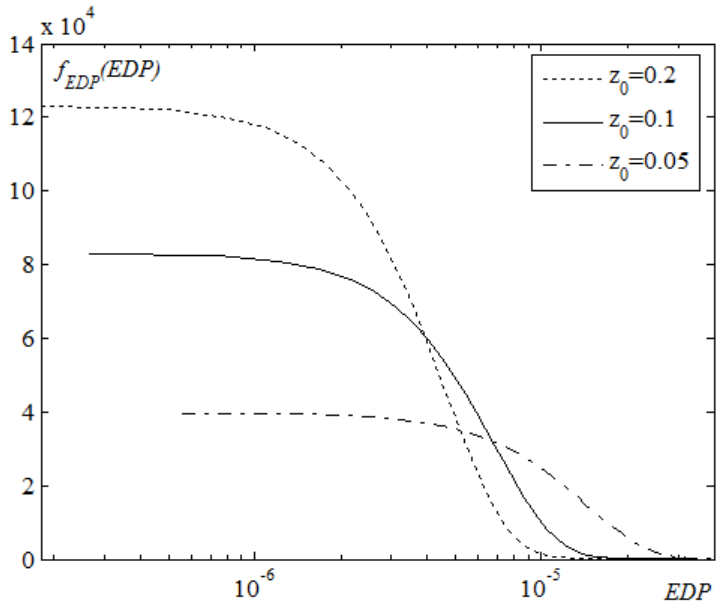

Figure 5.29. EDP Probability density functions corresponding to different values of the roughness.

5.1.4.2.Importance of the Interaction Parameters (IP)

The importance of the uncertainty affecting the values of the aerodynamic polar lines has been investigated by a parametric analysis. Stability analysis have been conducted by using of static polar lines derived from a linear combinations (Eq. (5.8)) of the two type of polar lines showed before (see Fig. 5.16), here identified as polar A (Fig. 5.16a) and polar B (Fig. 5.16b). Namely:

$$\begin{aligned} c_L(\alpha) &= c_{L\_A}(\alpha)\cdot P_L + c_{L\_B}(\alpha)\cdot(1-P_L) \\ c_M(\alpha) &= c_{M\_A}(\alpha)\cdot P_M + c_{M\_B}(\alpha)\cdot(1-P_M) \end{aligned} \tag{5.8}$$

where c_{i_j} (i=L,M and j=A,B) is the aerodynamic coefficient i, corresponding to the polar type j, α is the generic angle of attack, P_L and P_M are the combination parameters, which vary between 0 and 1.

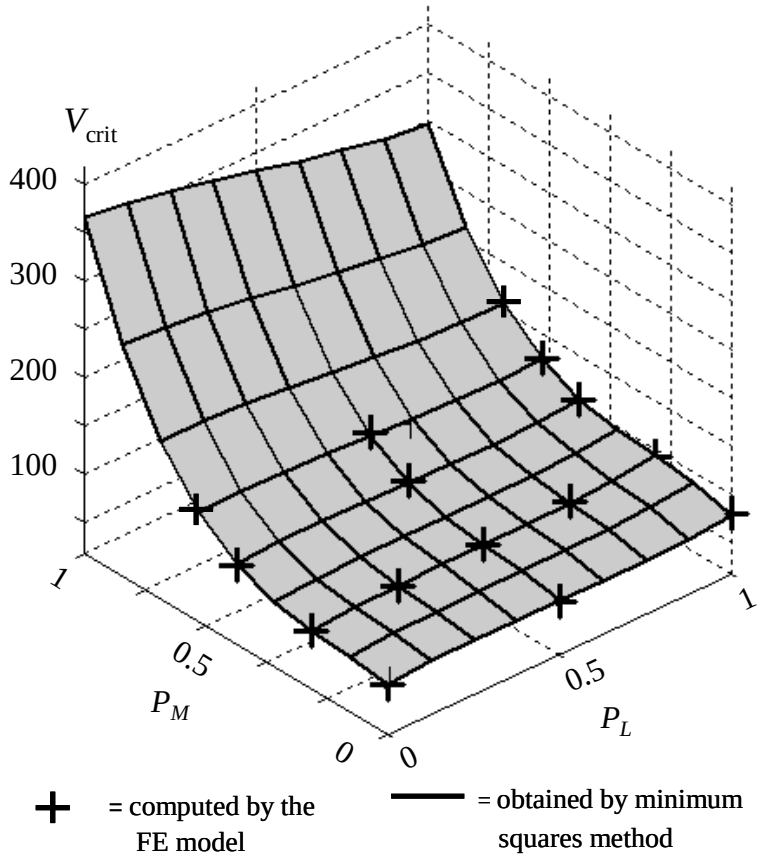

Fig. 5.30. Response surface of critic velocities in the parametric space.

Critic velocities computed by the FE model are shown in Fig. 5.30 (cross symbols); from these data, the response surface of critic velocities has been extrapolated by using of the minimum square method. The analyses show that the uncertainty affecting the IPs

(aerodynamic parameters in this case), exerts a strong influence on the bridge investigated performance.

5.2. PBWE for an offshore wind turbine

The second application of the proposed PBWE procedure, regards an Offshore Wind Turbine (OWT), in particular the performances regarding the support structure under the wind action have been investigated.

5.2.1. General aspect for offshore wind turbines

Offshore wind turbines (OWT) are the result of an evolution of the onshore plants for which the construction is a relatively widespread and consolidated practice providing a renewable power resource (Hau, 2006); in order to make the wind generated power more competitive with respect to conventional exhaustible and high environmental impact sources of energy, the attention has turned toward offshore wind power production (Breton and Moe, 2008).

Beside being characterized by a reduced visual impact as they are placed far from the coast, offshore wind turbines can take advantage from the more constant and intense wind forcing, this could increase the regularity and amount of the productive capacity and could make such a resource more cost-effective if the plant will be durable and operate with minimum stoppage through its life.

From the general point of view, an offshore wind turbine is formed by both mechanical and structural elements. As a consequence, it is not a “common” civil engineering structure; it behaves differently according to different circumstances related to functional activity (idle, power production etc), and it is subject to highly variable loads (wind, waves, sea currents etc.).

Moreover, since the structural behavior of OWTs is influenced from nonlinearities, uncertainties and interactions, they can be defined as complex in the sense of up to date facilities required today by the general public (Bontempi, 2006).

These considerations highlight that a modern approach in Structural Engineering has to evolve from the idea of “Structure”, as a simple device for channeling loads, to the idea of “Structural System”, as “a set of interrelated components which interact one with another in an organized fashion toward a common purpose” (NASA, 1995): this systemic approach includes a set of activities which lead and control the overall design, implementation and integration of the complex set of interacting components (Simon, 1998, Bontempi et al. 2008a). In the present work, the original NASA definition has been extended in such a way that the “structural system” contains also the actions; by this way the “set of interrelated components” is called simply “structure” in what follows.

The system decomposition is a fundamental tool for the design of complex structural systems. It has to be done both for the structure and for the actions, and can be carried out focusing the attention on different levels of detail: the decomposition usually starts from a macro-level vision and go on toward to the micro-level details which, in the case of the structure, regards the connections level. A typical structural decomposition of an OWT is represented from the scheme in Fig.5.31 that can be appreciated with reference to Fig.5.32, where the main parts of an offshore wind turbine structure are exposed.

Several substructure types could be adopted: the choice is related principally to water depth (h), soil characteristics and economical reasons. According to DNV-OS-J101 (2004), the following rough classification can be done: monopile, gravity and suction buckets (h<25m); tripod, jacket and lattice tower (20m<h<40÷50m); low-roll floaters and tension leg platform (h>50m). In the present study attention has been focused jacket substructure type.

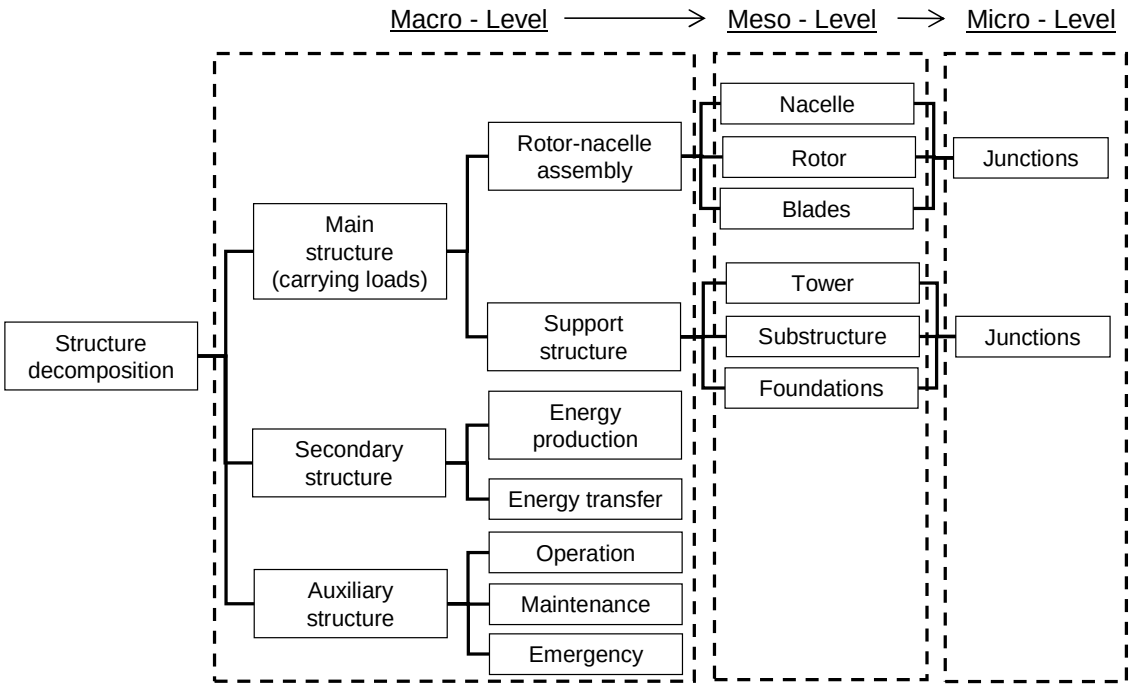

Fig. 5.31. Structural decomposition of an offshore wind turbine.

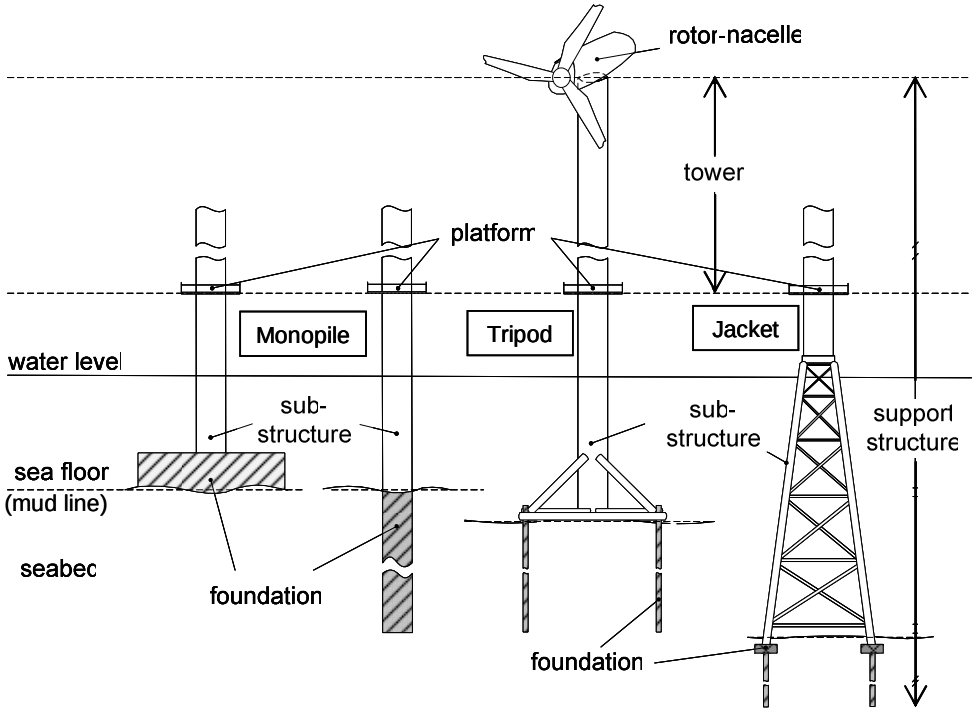

Fig. 5.32. Main parts of an offshore wind turbine structure and three different support structures (partially adapted from IEC 61400-3).

A certain amount of complexity becomes from the lack of knowledge and from the modeling of the environment in which the turbine is located; in particular, two main sources of complexity can be individuated: the stochastic nature of the environmental actions (aerodynamic and hydrodynamic actions in particular) and the possible presence of non linear interaction phenomena between the different actions and between the actions and the structure.

The generic environmental configuration is shown in Fig. 5.33, were the macro geometric parameters defining the problem are also represented. These are: the water mean depth (h), the hub height above the mean water level (H) and the pales length (or rotor radius) (R).

Generally speaking, the uncertainties can spread their selves during the various analysis phases that are developed in cascade; an alignment of uncertainty sources could produce an unacceptable level of unquantifiable risk.

In the specific case of the OWTs, the general scheme describing the uncertainties propagation reported in Fig. 3.4 (section 3.4) can be adapted as shown in the figure 5.34, in which the mutual interaction between the wind and the waves is determined by the mechanisms described in the section 1.1.5 and in the following section 5.2.4.4.

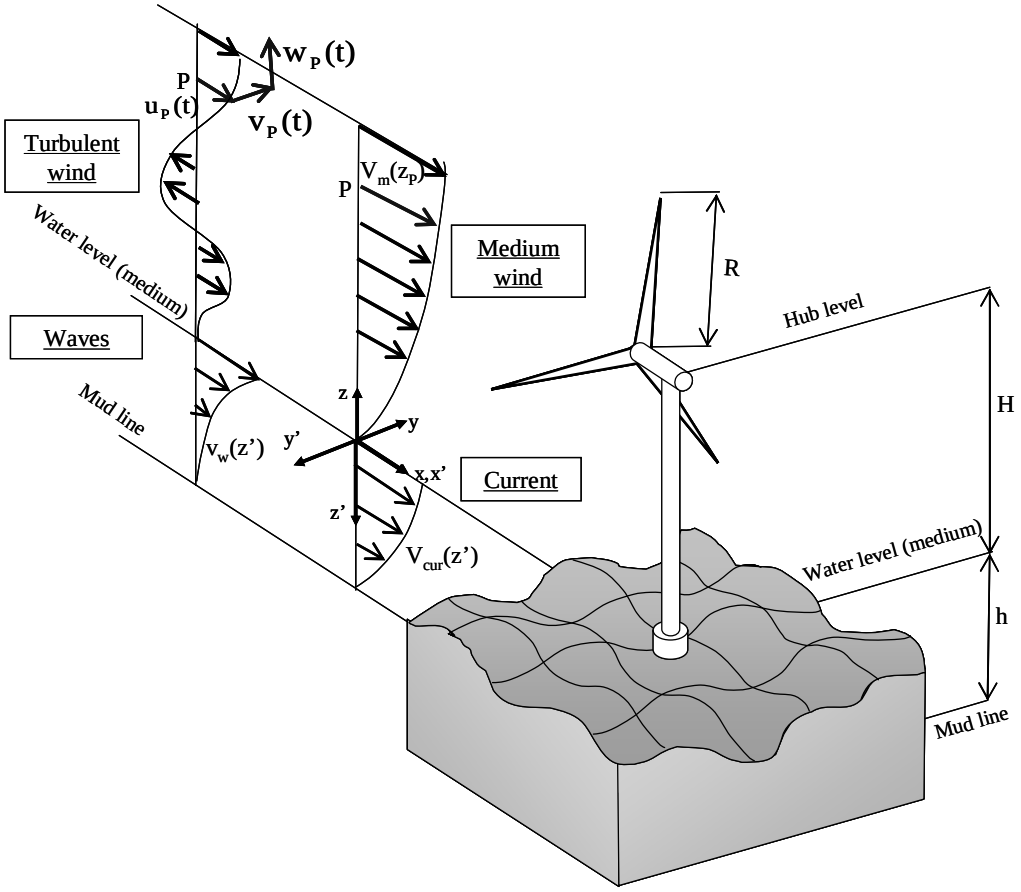

Fig. 5.33. Problem statement and actions configuration.

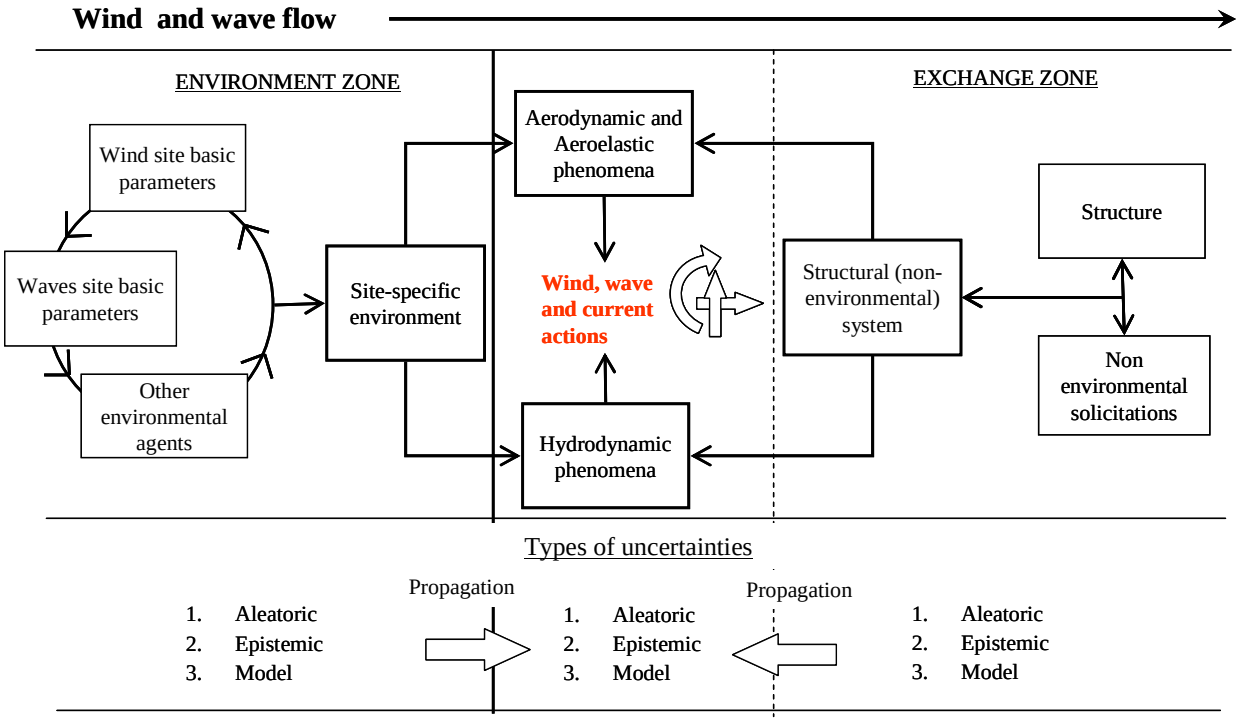

Fig. 5.34. Uncertainties in OWTs design.

5.2.2. Case study structure

As previously stated, a case study of an OWT with a Jacket support type has been investigated,. The jacket is composed from tubular beam steel members with circular section. The diagonal bars have a diameter of 0.5 m and a thickness of 0.016 m the longitudinal (vertical) bars have a diameter of 1.3 m and a thickness of 0.026 m and the horizontal bars have a diameter of 0.6 m and a thickness of 0.016 m; the tower is also a tubular beam steel members with circular section having a diameter of 5m and a thickness of 0.05 m, referring to the Fig. 5.33, the problem sizes are H (hub height over the mean sea level) equal to 100 m, h (water depth) equal to 35m and R (rotor radius) equal to 80 m. The turbine is a 3MW Vestas type (http://www.vestas.com/). The connection between the jacket and the tower is a rigid connection. The structural characteristics are resumed in Table 5.6.

Table 5.6. Main structural characteristics (in meters).

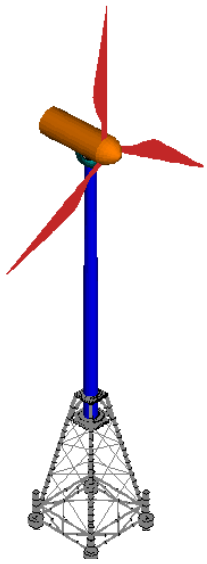	H = 100 h=35 D =5 t_w =0.05
	jacket members:
	D_{vert} =1.3 $t_{w\ vert}$ =0.026 D_{hor} =0.6 $t_{w\ hor}$ =0.016 D_{diag} =0.5 $t_{w\ diag}$ =0.016
	D = tubular tower diameter; $D_{vert, hor, diag}$ = diameter of the jacket vertical, horizontal or diagonal tubular members t_w = thickness of the tower tubular member; $t_{w\ vert, hor, diag}$ = thickness of the jacket vertical, horizontal or diagonal tubular members;

5.2.3. Hydrodynamic field and action models

Concerning the hydrodynamic actions, as previously stated, they are due to currents and waves.

For what concerns the sea currents induced by the tidal wave propagation in shallow water, in general they are characterized by a velocity field practically horizontal, while their intensity decreases slowly with the depth. Adopting a Cartesian three-dimensional coordinate system (*x'*,*y'*,*z'*) with origin at water level and the z-axis oriented downward (Fig.5.33), the velocity profile is given by

$$V_{cur}(z') = V_{tide}(z') + V_{wind}(z')$$

$$V_{tide}(z') = V_{tide0}\left(\frac{h - z'}{h}\right)^{1/7} \tag{5.9}$$

$$V_{wind}(z') = V_{wind\,0}\left(\frac{h_0 - z'}{h_0}\right)$$

where V_{tide} and V_{wind} are the sea currents generated from the tide and the wind respectively, z' indicates the depth under the sea water level, V_{tide0} and V_{wind0} are tide and wind induced the current velocities on the surface, and h_0 is a reference depth (which typically is assumed of 20 meters).

In absence of site-specific measurements the wind generated sea surface current velocity may be estimated from:

$$V_{wind\,0} = 0.01 \cdot V_{1hour}(z = 10m) \tag{5.10}$$

Waves act on the submerged structural elements and on the transition zone above the water-air interface surface; in the first case actions are the result of the alternative motion of fluid particles, induced by the fluctuating perturbation of the liquid surface; in the second case the action is the consequence of the breaking waves, which may occur in relative in shallow water conditions.

In general the water surface height, in respect to the mean sea level, is a time-dependent stochastic variable, and can be described by means of statistical parameters:

- *the significant wave height* H_S; it is defined as four times the standard deviation of the sea elevation process. It represents a statistical measure of the intensity of the wave climate as well as of the variability in the arbitrary wave heights.
- *the spectral peak period* T_P; it is related to the mean zero-crossing period of the sea elevation process.

For extreme events analysis, in general the significant wave height is defined with respect to a return period T_R as (DNV-OS-J101, 2004):

$$H_{S,T_R}(z) = F_{H_S,\max,1year}^{-1}\left(1-\frac{1}{T_R}\right) \tag{5.11}$$

where $F_{HS,max,1year}$ represents the maximum annual significant wave height, which can be deduced by means of a Weibull distribution.

The wave characteristics required in order to define the wave loading on the structure, are represented by the wave height H_S and the wave period T_P.

For particular performance investigations, like the fatigue analysis of the structure subject to the wave action, it is necessary to define an appropriate spectral density of the surface elevation. The characteristic spectral density of the specific sea-state *S(f)* can be defined by means of the parameters H_S and T_P, after selecting an appropriate mathematical model for the *S(f)* function. Usually the Jonswap spectrum is adopted for a developing sea:

$$S(f) = \frac{\alpha g^2}{(2\pi)^4} f^{-5} \exp\left[-\frac{5}{4}\left(\frac{f}{f_P}\right)^{-4}\right] \gamma^{\exp\left[-0.5\left(\frac{f-f_P}{\sigma f_P}\right)^2\right]} \tag{5.12}$$

where $f=2\pi/T$ is the frequency, $f_P=2\pi/T_P$ is the peak frequency, α and g constants, σ and γ parameters dependent on H_S and T_P.

In general, the sea state is characterized by a distribution of the energy spectral density, depending on the geographic direction of the wave components: this can be obtained by multiplying the one-dimensional spectrum *S(f)* by a function of directional spreading, symmetric to the principal direction of the wave propagation.

Finally the designer has to identify the analytical or numerical wave theories, and their range of validity, which may represent the kinematics of waves:

- *linear wave theory (Airy theory) for small-amplitude deep water waves; wave profile is represented by a sine function;*
- *Stokes wave theories for high waves;*
- *stream function theory, based on numerical methods and accurately representing the wave kinematics over a broad range of water depths;*
- *Boussinesq higher-order theory for shallow water waves;*
- *solitary wave theory for waves in very shallow water.*

For what concerns the hydrodynamic loads computation, referring on a structural slender cylindrical member (D/L<0.2, with: D member diameter normal to the fluid flow, L wave length), both wave and (stationary) current generate the following two kind of forces.

- A force per unit length acts in the direction perpendicular to the axis of the member and related to the orthogonal (with respect to the member) components of the water particle velocity (wave v_w plus current V_{cur} induced) and acceleration (wave only); it can be estimated by means of Morison equation:

$$dF(z',t) = \left(c_i \frac{\rho_{wat} \pi D^2}{4} \dot{v}_w(z',t) + \frac{1}{2} c_d \rho_{wat} D\left(v_w(z',t) + V_{cur}(z',t)\right)\left|v_w(z',t) + V_{cur}(z',t)\right| \right) dz' \quad (5.13)$$

  where ρ_{wat} is the water density c_i and c_d are the inertia (including added mass for a moving member) and drag coefficient respectively, which are related to structural geometry, flow condition and surface roughness: the dot indicates the time derivate, in the Eq. (5.13). Periodic functions are adopted for both wave velocities and accelerations (Brebbia et al. 1979).

- A non-stationary (lift) force per unit length acts in the direction perpendicular both to the axis of the slender member and to the water current. This component is induced by vortex shedding past the cylinder and inverts direction at the frequency f_l of eddies separation which is related to flow field and structural geometry through Strouhal number $St=Df_l/V_{cur}$; it should be kept far from the structure's natural frequency to avoid resonances.

The lift force has not been considered in what follow.

5.2.4. Application of the PBWE procedure

Starting from the complete equation (3.17) that has been proposed for the PBWE

$$\lambda(DV) = \int_{-\infty}^{\infty} P(DV|DM) \cdot P(DM|EDP) \cdot P(EDP|\underline{IM},\underline{IP},\underline{\gamma}) \cdot g(\underline{IP}|\underline{IM},\underline{\gamma}) \cdot g(\underline{IM}) \cdot g(\underline{\gamma}) \cdot dDM \cdot dEDP \cdot d\underline{IM} \cdot d\underline{IP} \cdot d\underline{\gamma} \quad (5.14)((3.17))$$

the following simplified hypotheses are made:

- the uncertainties affecting the "*independent parameters*" (vector $\underline{\gamma}$) are neglected;
- the "Intensity Measure parameters" (vector $\underline{IM}$) and the "Interaction Parameters" (vector $\underline{IP}$) are considered statistically independent each others;

- the damage measure *DM* and the decision variable *DV* are identified by the *EDP* magnitude;
- the performance can be expressed by a Limit State (*LS*) function that depends on the *EDP*(=*DM*);
- a deterministic relation between the *EDP*s is chosen as *LS* function, the probabilistic response can be synthesized by the probability distribution of the *EDP*s;

under these assumptions, the equation (5.14) can be reduced to the equation (5.15)

$$\lambda(EDP) = \int_{-\infty}^{\infty} P(EDP|\underline{IM},\underline{IP},\underline{\gamma}) \cdot g(\underline{IP}) \cdot g(\underline{IM}) \cdot d\underline{IM} \cdot d\underline{IP} \tag{5.15}$$

which represent a simplified PBWE procedure. The (5.15) has been adopted to evaluate the OWT performances and to conduct the sensitivity analysis with respect to the stochastic parameters.

For what concerns the $\underline{IM}$ vector, the following three component parameters have been considered:

- the 10 meters height mean wind speed (V_{10}), characterized by a Weibull (annual) probabilistic distribution;
- the roughness (z_0), characterized by a Lognormal probabilistic distribution;
- the wind mean speed direction (α), characterized by a Gaussian probabilistic distribution.

The Strouhal number (*St*) (see section 1.2.4) has been considered as the unique *IP* scalar parameter, it has been characterized by a Gaussian probabilistic distribution.

For what concerns the structural response, the following *EDPs* has been considered:

- along-wind structural mean displacement at the hub height;
- across-wind and along-wind structural peak displacement at the hub height;
- absolute structural peak displacement at the hub height (vectorial sum of the across and the along-wind displacements);

The peak displacement at the hub height has been considered as the *EDP*. This has been computed as described by the equation (4.29) (section 4.2.1) assuming T_{wind}= 3600 s.

The stochastic parameters description is synthetically shown in Table 5.7 (were “stdev” stand for “standard deviation” and “PDF” stand for “Probability Density Function”).

Table 5.6. Stochastic parameters description.

IM		***IP***	***EDP***
PDF 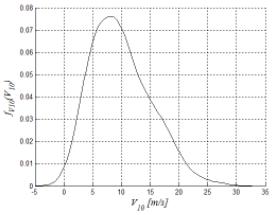 V_{10}	*Weibull* (annual) $P(V_{10}) = 1-\exp\left[-\frac{1}{2}\left(\frac{V_{10}}{\sigma}\right)^{k}\right]$ σ = 6.2 k = 2.02	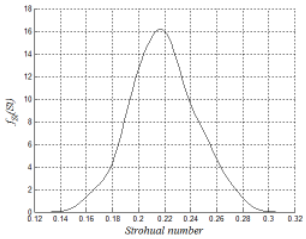 *St* *Gaussian* mean = 0.22 stdev = 0.025	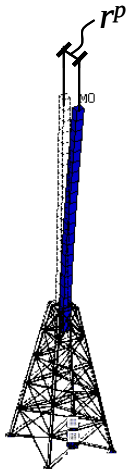 Structural displacements at the hub height: Peak displacement $r^p(h) = r_m + g_r \cdot \sigma_r(h)$ (equation (4.29)) Along-wind mean displacement Across-wind peak displacement Along-wind peak displacement
PDF 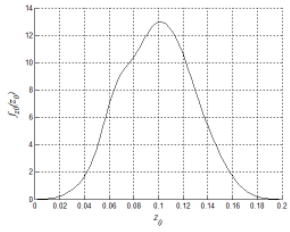 z_0	*Lognormal* mean = 0.05 m stdev = 0.03		
PDF 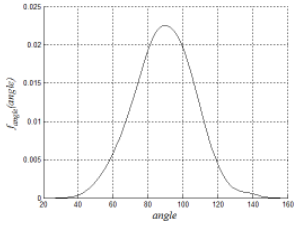 α	*Gaussian* mean = 90° (parallel to the *y* axis) stdev = 30°		

5.2.4.1.Details on the structural analysis and the vortex shedding action model

Only the configurations that do not imply the pales rotation have been considered (parked standstill or idling configurations).

The structural analyses has been conducted in the frequency domain, the probabilistic characterization of the response parameters has been made by adopting the Monte Carlo method.

The hydrodynamic actions has been modeled as a static force in order to extrapolate the influence of the wind parameters to the dynamic response without noises generated from other dynamic actions. During the sensitivity analysis, the magnitude of the hydrodynamic actions

has been initially set equal to a constant extreme value, while the wind actions parameters vary according with their PDFs (sections 5.2.4.1 and 5.2.4.2). In a subsequent application of the PBWE procedure, the magnitude of the hydrodynamic actions varies according to the wind-waves-current interaction mechanisms described in what follows.

Concerning the wind actions, the vortex shedding effect (see section 1.3.1) has been considered as an impressed maximum across-wind displacement $(r^{VS}_{across})_{\max}$ given from (Borri and Pastò, 2007)

$$\left(\frac{r^{VS}_{across}}{D}\right)_{\max} = \frac{1.29}{\left[1+0.43\cdot\left(2\pi\cdot S_t^2\cdot S_c\right)\right]} \tag{5.16}$$

were D is the diameter of the tubular section under the wind action while S_t and S_c are the Strohual and the Scruton numbers, previously defined. The displacement given from the (5.16) has applied at the node located at the hub height, when the mean wind speed at the hub height falls in a certain range of values, defined as the vortex shedding critical velocity ($V^{VS}crit$) plus or minus 0.5 m/s (critic vortex shedding range).

5.2.4.2.Sensitivity analysis for the stochastic parameters

First of all, a sensitivity analysis has been conducted in order to investigate the propagation of the uncertainties affecting the input parameters (IMs and IP) in the structural response (EDP).

The investigation has been conducted by carrying out various Monte Carlo analyses, in which only one of the previously introduced input parameters has been assumed as stochastic (having the previously specified probability distributions), while the others has been considered as deterministic and equal to their mean value.

The analysis sets are shown in Table 5.6. Each Monte Carlo analysis implies 1000 samples of the stochastic variables.

The sensitivity evaluation has been made by extracting from the each Monte Carlo analysis the following results related to the IMs and IP variations:

- trend of the considered EDPs;
- trend of both the across-wind and the along-wind variances of the structural displacement at the hub height;
- annual probability of occurrence curves λ(EDP);

Table 5.6. Stochastic parameters description.

Analyses set number	***IM***			***IP***	
	V_{10}	z_0	α	***St***	
1	***Stochastic*** (*Weibull* σ = 6.2 k = 2.02)	Deterministic 0.05 m	Deterministic 90° (parallel to the *y* axis)	Deterministic 0.22	Sensitivity analysis
2	Deterministic 15 m/s	***Stochastic*** (*Lognormal* mean = 0.05 stdev = 0.03)	Deterministic 90° (parallel to the *y* axis)	Deterministic 0.22	
3	Deterministic 15 m/s	Deterministic 0.05 m	***Stochastic*** (*Gaussian* mean = 90° stdev = 30°)	Deterministic 0.22	
4	***Stochastic*** (*Weibull* σ = 6.2 k = 2.02)	Deterministic 0.05 m	Deterministic 90° (parallel to the *y* axis)	***Stochastic*** (*Gaussian* mean = 0.22 stdev = 0.025)	
5	***Stochastic*** (*Weibull* σ = 6.2 k = 2.02)	***Stochastic*** (*Lognormal* mean = 0.05 stdev = 0.03)	***Stochastic*** (*Gaussian* mean = 90° stdev = 30°)	***Stochastic*** (*Gaussian* mean = 0.22 stdev = 0.025)	PBWE

In the Figures 5.35, 5.36, 5.37 and 5.38 the results corresponding to the analysis sets from 1 to 4 introduced in Table 5.6 are shown.

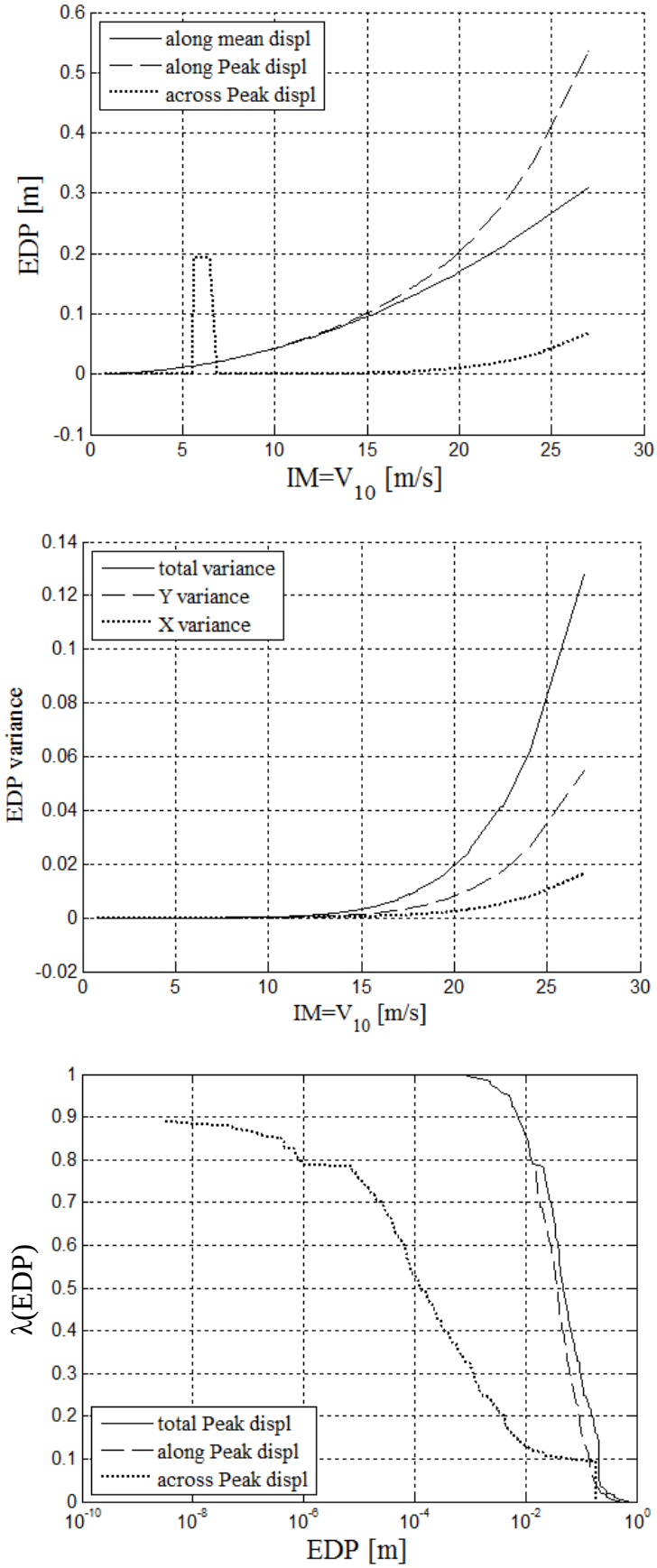

Fig. 5.35. Sensitivity study for the analysis set No.1: EDPs (upper), EDP variances (central), occurrence curves (bottom).

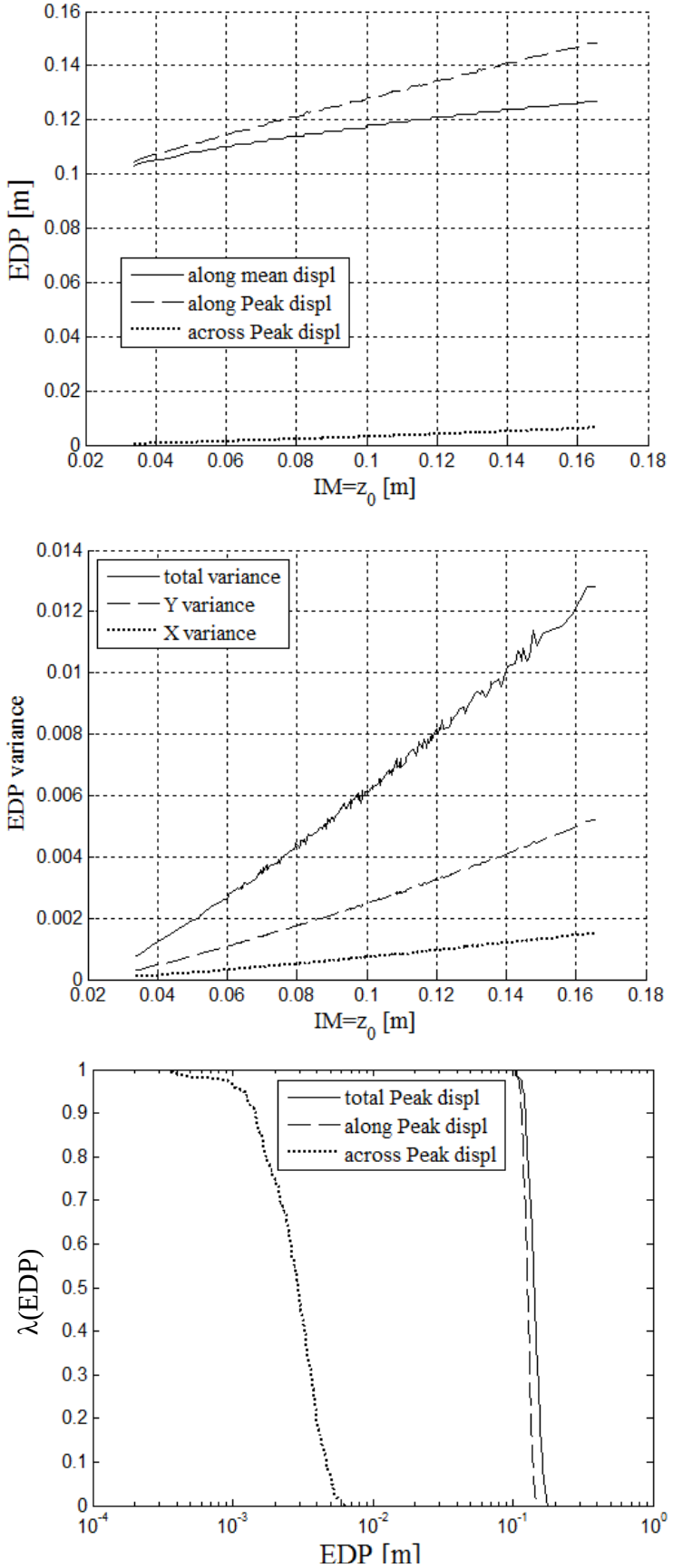

Fig. 5.36. Sensitivity study for the analysis set No.2: EDPs (upper), EDP variances (central), occurrence curves (bottom).

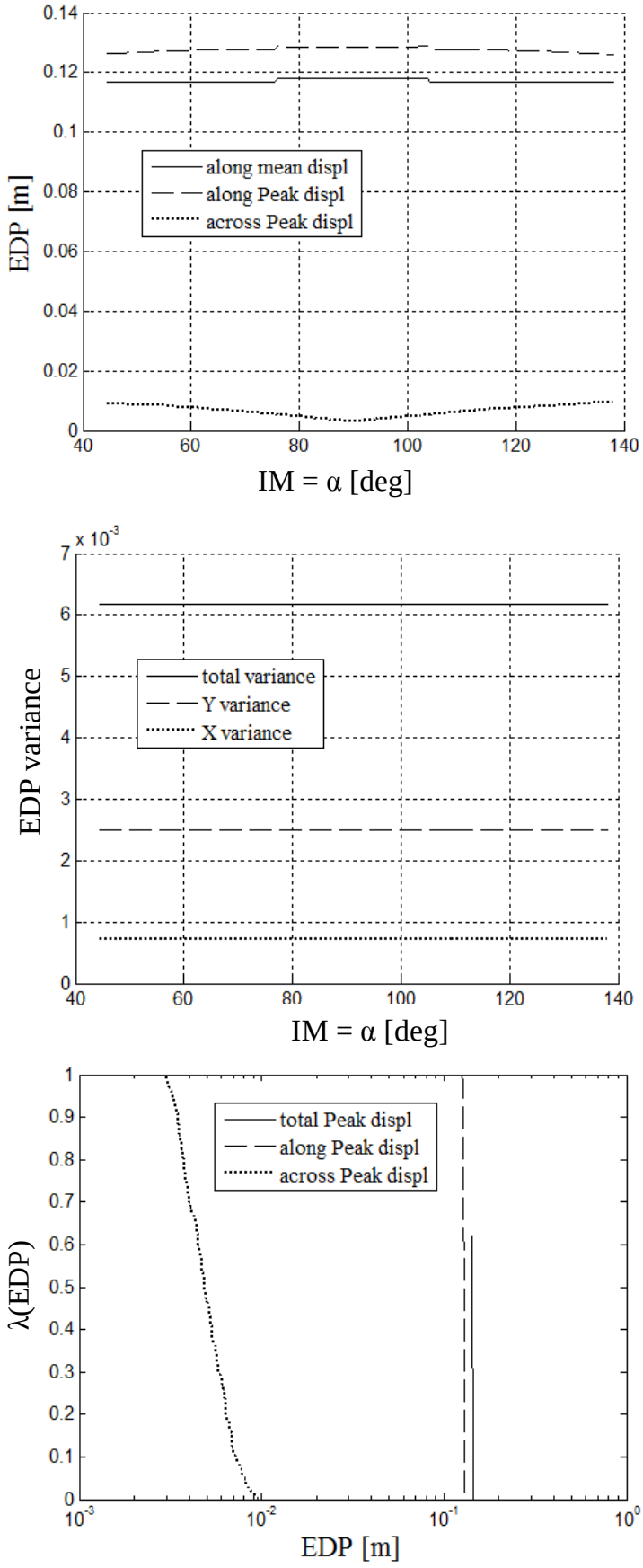

Fig. 5.37. Sensitivity study for the analysis set No.3: EDPs (upper), EDP variances (central), occurrence curves (bottom).

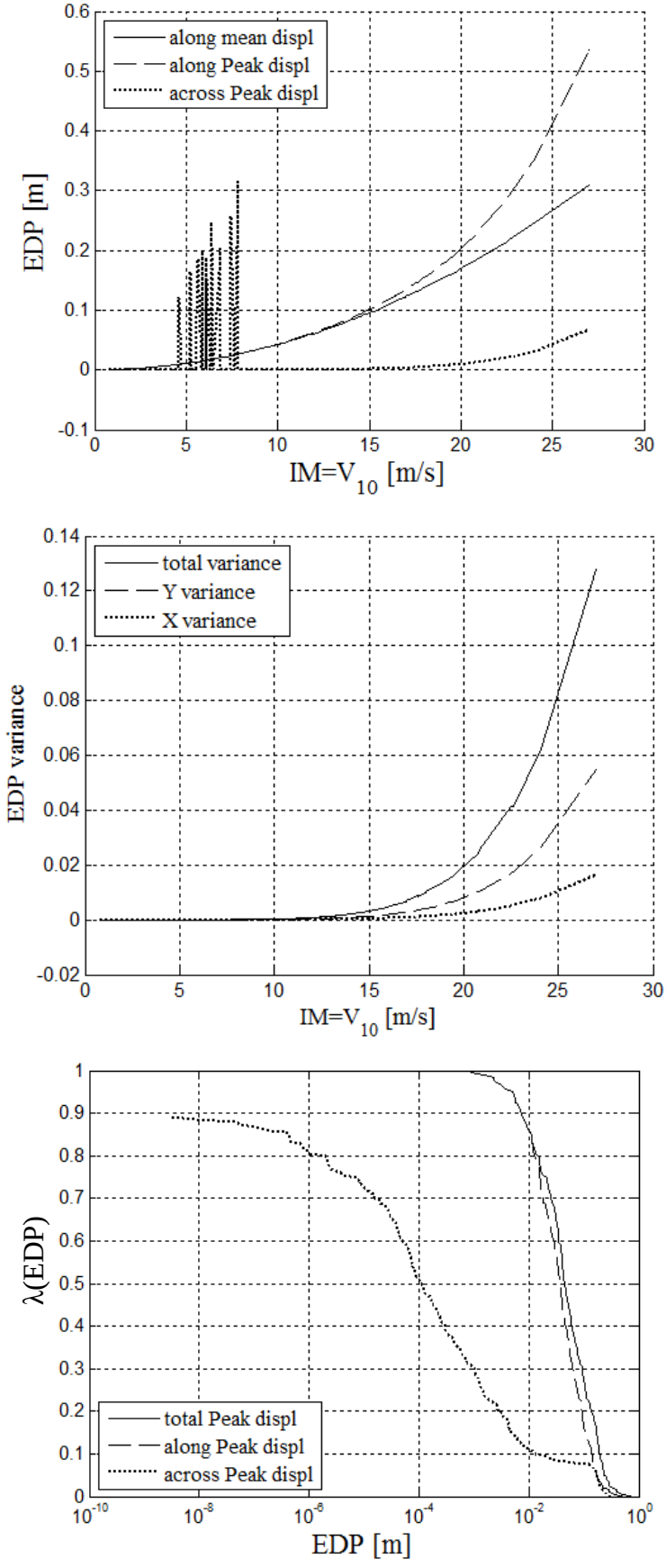

Fig. 5.38. Sensitivity study for the analysis set No.4: EDPs (upper), EDP variances (central), occurrence curves (bottom).

From the first plot of the figure 5.35, the across-wind displacements due to the vortex shedding can be appreciated when the wind speed falls in the critic vortex shedding range defined in the previous section. From the second plot it can be noted that the response variance due to the wind action turbulence increase with the V_{10} and, finally in the third plot, the annual occurrences due to the uncertainty affecting the V_{10} values can be appreciated.
In the Figures 5.36 and 5.37 the results regarding the analysis sets No. 2 and 3 are shown, in these cases the wind speed does not fall in the critic vortex shedding range. From the Fig. 5.36 can be deduced that the increasing of the roughness implies an increasing in the displacements variance. From fig. 5.37 can be deduced that the configuration in which the mean wind speed direction is parallel to the y axis (α=90°) produce the maximum along-wind displacement and the minimum across-wind displacement. This fact depends on the different stiffness of the support structure with respect to different direction for the imposed deflection.
In the Fig.5.38, the results regarding the analysis set No. 4 are shown, here the Strouhal number (*St*) has been considered as stochastic, consequently the critic vortex shedding range for the wind mean speed is not deterministic, this can be appreciated from the first plot, were the across-wind peak displacement shows to have an irregular trend inside the range.
The sensitivity analysis shown that the most important variation of the results is due to the variation of the V_{10} which is considered the principal intensity measure stochastic parameter, the uncertainty affecting the mean wind speed direction is not negligible for asymmetric structures, while the uncertainty affecting the Strouhal number determines the dispersion of the across-wind response which can be viewed as a particular aspect. The uncertainty affecting the roughness value can determines an increment in the response variance which can be greater than the 100%.

5.2.4.3.Complete PBWE procedure

After the sensitivity analysis, the PBWE procedure has been applied in the analysis set No. 5 considering all the previously introduced parameters as stochastic and considering the same previous samples for the stochastic variables. The results of the last set (No. 5) are shown in Fig.5.39, the graphs are plotted with respect to the same abscissa of the analyses sets No. 1 and No. 4: the 10 meters mean wind speed that, as previously stated, is considered the principal intensity measure stochastic parameter. Obviously both the EDPs and the EDPs variance present an irregular trend with respect to the IM, although the mean trend of the EDPs can confirm the previous results: they increase more than linear with the IM.

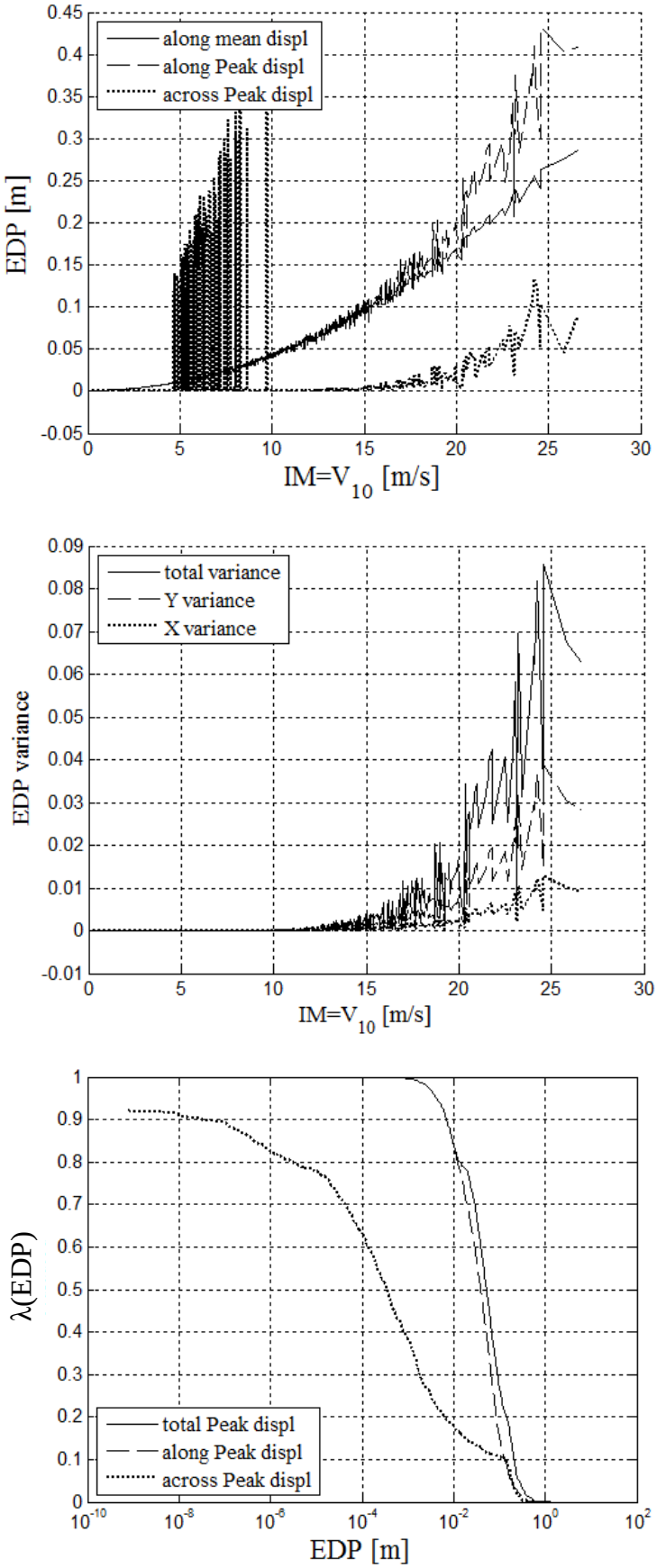

Fig. 5.39. Application of the PBWE procedure (analysis set No.5): EDPs (upper), EDPs variance (central), occurrence curves (bottom).

In order to properly understand the entity of the differences between the results obtained by adopting a reduced procedure (in which only the principal intensity measure is considered as a stochastic parameter) and the complete procedure (considering all the previously introduced parameters as stochastic), a comparison between the occurrence curves derived from the analyses sets numbers 1 and 5 is shown in Figure 5.40.

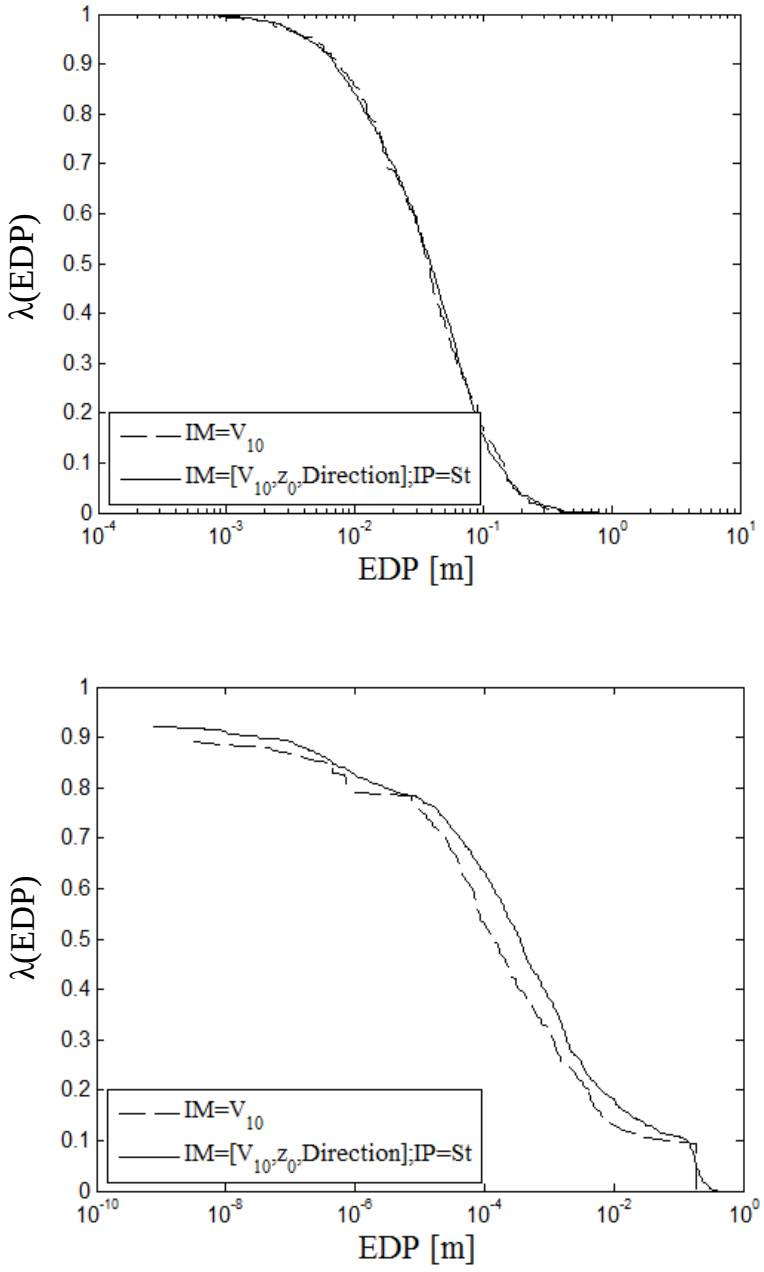

Fig. 5.40. Comparison between reduced and complete PBWE procedure. Occurrence curves: EDP = along-wind peak hub displacement (upper), EDP = across-wind peak hub displacement (bottom).

From the figure the following important conclusions can be deduced:

- there is not substantial differences between the results relative the analysis sets in the along-wind direction;
- the results relatively to the reduced or the complete procedure differ for what concerns the across-wind direction, in this case the complete PBWE procedure gives a more conservative result.

5.2.4.4.Wind-waves-current interaction

As previously stated (section 5.1), in the specific case of the OWTs, the general scheme describing the uncertainties propagation reported in Fig. 3.4 (section 3.4) can be adapted as shown in the figure 5.34, in which the mutual interaction between the wind with both currents and the waves is determined by the mechanisms introduced in the section 1.1.5.

Here the interaction phenomena have be considered as follow:

- the wind speed generates an additional sea current given from the equation (5.17)

  $$Vcurr_{wind} = 0.01 \cdot V_{1hour}(z = 10m) \quad (5.17)$$

  where V1hour is the mean wind speed averaged over a period of T=1 hour;
- the wind and the sea current speeds are statistically correlated both in direction and in magnitude; it has been assumed that there is a perfect correlation between the wind and the current directions (the wind and the current speeds are aligned);
- the wind speed and the wave characteristic height are statistically correlated, the correlation has been modeled as a deterministic relation between the mean wind speed at 10 meters of altitude (V_{10}) and the significant wave height (H_S) (see section 5.2.3) referring to the correlation data given in Zaaijer (2005). Although the wave heights have been scaled in order to consider Mediterranean waves instead of the ocean ones, the decreasing factors has been calibrated by the Italian Wave Atlas (APAT 2004). In conclusion the relation between V_{10} and H_S is given from:

  $$H_s = \frac{1}{2}(0.221 \cdot V_{10}{}^2 - 0.0291 \cdot V_{10} + 0.164) \quad (5.18)$$

In order to evaluate the environmental interactions effects on the results, the occurrence curves derived from three sets of analyses have been considered:

- set No. 6: an analysis set in which the V_{10} has been considered the only stochastic IM, while both z_0 and H_S has been considered as constant and equal to 0.05 m and 5.5 m respectively (their mean values);

- set No.7: an analysis set in which the V_{10} has been considered the only stochastic IM with the same V_{10} samples of the previous set, the additional sea current due to the wind speed (equation (5.17)) and the wind-wave correlations (equation (5.18)) have been implemented while z_0 has been considered as a constant and equal to 0.05m;
- set No.8: an analysis set with the same V_{10} samples of the previous sets, but implementing all the previously described environmental interactions.

In Fig. 5.41 a comparison between the analyses sets No. 6 and No. 7 is shown.

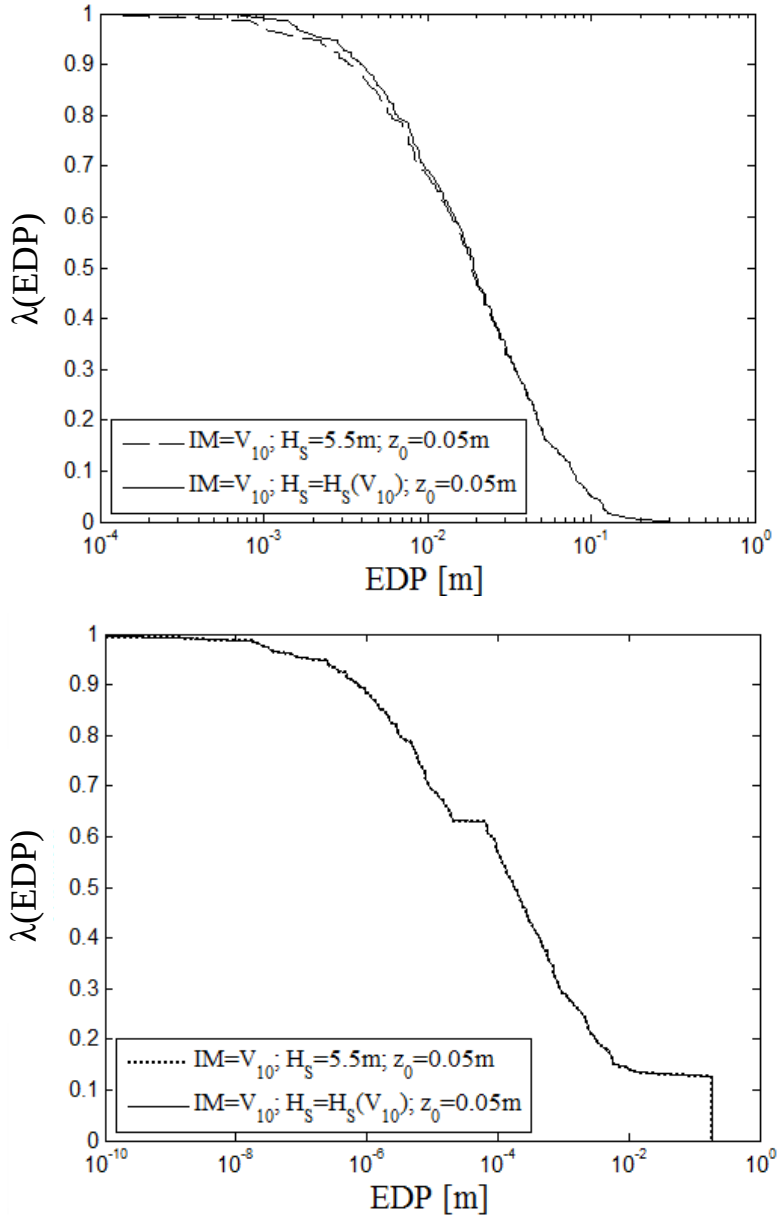

Fig. 5.42. Evaluation of the environmental interactions influence. Comparison between the occurrence curves derived from analysis sets No. 6 and No. 7. EDP = along-wind peak hub displacement (upper), EDP = across-wind peak hub displacement (bottom).

In Fig. 5.43 a comparison between the analyses sets No. 7 and No. 8 is shown.

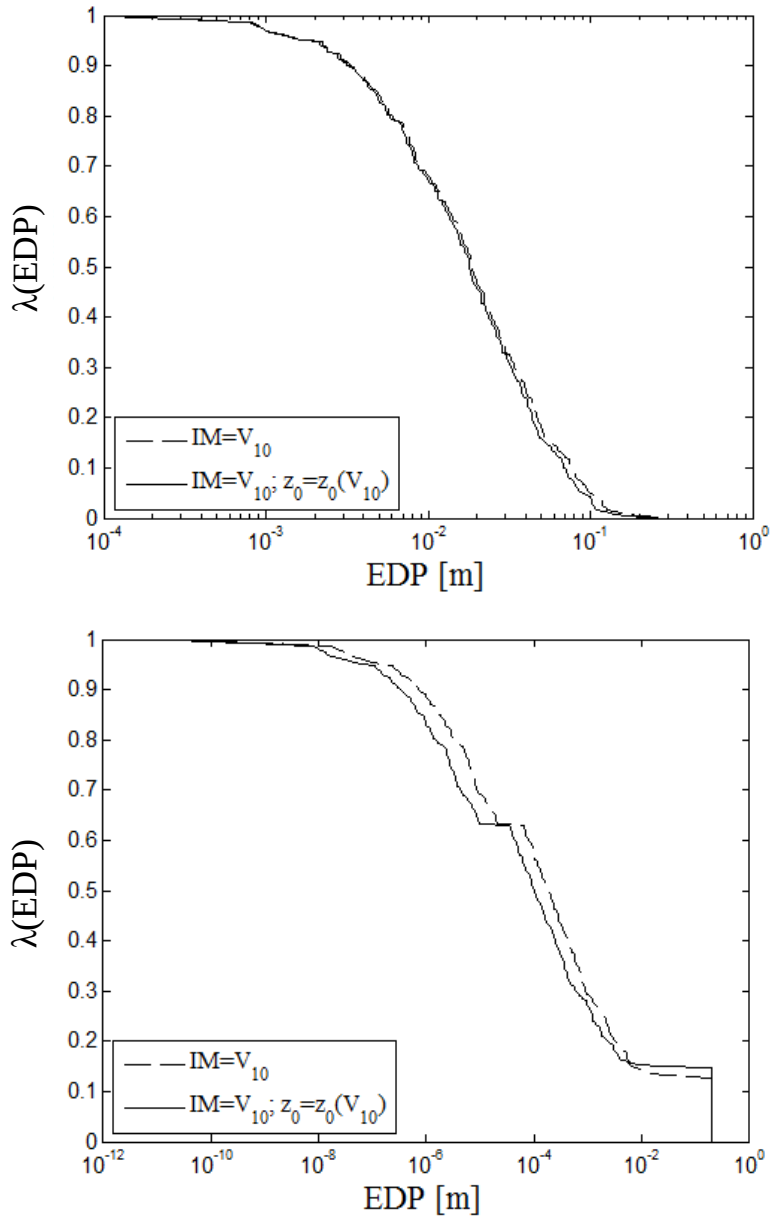

Fig. 5.43. Evaluation of the environmental interactions influence. Comparison between the occurrence curves derived from analysis sets No. 7 and No. 8. EDP = along-wind peak hub displacement (upper), EDP = across-wind peak hub displacement (bottom).

From the figure 5.42 can be deduced that the consideration of the wind-wave correlation produces an insignificant deviation of the results from the case in which the mean value is assumed for the waves significant height (*Hs*). While from the Fig. 5.43 can be deduced that considering the interaction generating the wind-induced roughness, the results can be change, especially with regard to the across-wind displacement.

5.3. References

Agenzia per la Protezione dell'Ambiente e per I Servizi Tecnici (APAT), 2004, Atlante delle onde nei mari italiani – Italian wave atlas, Rome, Italy (in italian).

Augusti, G., Borri, C., Neumann, H-J. (2001), "Is Aeolian risk as significant as other environmental risks?", Reliability Engineering and System Safety, (74), 227-237.

Augusti, G., Ciampoli, M., (2006), "First steps towards Performance-based Wind Engineering", in Performance of Wind Exposed Structures: Results of the PERBACCO project (G. Bartoli, F. Ricciardelli, A. Saetta, V. Sepe eds.), Firenze University Press, 13-20.

Bartoli, G., Ricciardelli, F., Saetta, A., Sepe, V. (eds.) (2006). "Performance of Wind Exposed Structures: Results of the PERBACCO Project", Firenze University Press, Italy.

Bontempi, F. (2006), "Basis of Design and expected Performances for the Messina Strait Bridge". Proc. of the International Conference on Bridge Engineering – Challenges in the 21st Century, Hong Kong, 1-3 November, 2006.

Bontempi, F., Giuliani, L., (2006b), "Engineering complexity: uncertainty modelling and structural robustness", 10. Dresdner Baustatik Seminar, Technische Universitaet Dresden, Deutschland, September 2006.

Bontempi, F., Gkoumas, K. and Arangio, S. (2008a), "Systemic approach for the maintenance of complex structural systems". Structure and infrastructure engineering, vol. 4; pp. 77-94, ISSN: 1573-2479, doi: 10.1080/15732470601155235.

Bontempi, F., Li, H., Petrini, F. and Manenti, S. (2008b), "Numerical modeling for the analysis and design of offshore wind turbines", The 4th International Conference on Advances in Structural Engineering and Mechanics (ASEM'08). 26-28 May 2008, Seoqwipo KAL Hotel, Jeju, Korea.

Bontempi, F., Li, H., Petrini, F. and Gkoumas, K. (2008c), "Basis of Design of Offshore Wind Turbines by System Decomposition", The 4th International Conference on Advances in Structural Engineering and Mechanics (ASEM'08). 26-28 May 2008, Seoqwipo KAL Hotel, Jeju, Korea.

Borri, C. and Pastò, S., Lezioni di ingegneria del vento, Firenze University Press, Firenze 2007.

Breton, S.-P. and Moe, G. (2009). "Status, plans and technologies for offshore wind turbines in Europe and North America", Renewable Energy, 34 (3), 646-654.

Carassale, L., Solari, G., (2006), "Monte Carlo simulation of wind speed field on complex structures", Journal of Wind Engineering and Industrial Aerodynamics, (94), 323-339.

CEN (European Committee for Standardization), (2003). prEN 1993-1-9: Design of steel structures – Part 1-9: Fatigue strength of steel structures, Brussels (BE), European Committee for Standardization

DNV, Det Norske Veritas (2004): DNV-OS-J101 Offshore Standard. Design of Offshore Wind Turbine Structures, June 2004.

Ellingwood, B.R. Rosowsky, D.V. and Kim, Y. Li, J. H. (2004), "Fragility Assessment of Light-Frame Wood Construction Subjected to Wind and Earthquake Hazards", Journal of Structural Engineering, 130(12), 1921-1930.

ESDU (Engineering Sciences Data Unit) (2001), Report N. 86010: "Characteristic of atmospheric turbulence near the ground. Part III: variations in space and time for strong winds (neutral atmosphere)", http:// www.esdu.com.

Garciano, L.E., Maruyama, O. and Koike, T. (2005) "Performance-based design of wind turbines for typhoons", Proc. Ninth International Conference on Structural Safety and Reliability ICOSSAR05, (G. Augusti, G.I. Schueller, M. Ciampoli eds.), Millpress, Rotterdam.

Hau, E., Wind Turbines: Fundamentals, technologies, Application, Economics, 2nd edition. Springer-Verlag Berlin Heidelberg 2006.

Khanduri, A.C. and Morrow, G.C. (2003), "Vulnerability of buildings to windstorms and insurance loss estimation", Journal of Wind Engineering and Industrial Aerodynamics, (91), 455-467.

NASA, National Aeronautics and Space Administration, Systems Engineering Handbook., 1995, Available online at: www.nasa.gov.

Norton, T.R. (2007), "Performance-Based vulnerability analysis of wind-excited tall buildings", Ph.D. Thesis, Florida Agricultural and Mechanical University FAMU-FSU, College of Engineering.

Pagnini, L. (2005), "The reliability of structures with uncertain parameters excited by the wind", Proc. Ninth International Conference on Structural Safety and Reliability ICOSSAR05, (G. Augusti, G.I. Schueller, M. Ciampoli eds.), Millpress, Rotterdam.

Pastò, S and de Grenet, E.T. (2005), "Risk-Assessment and Control of Flow-Induced Vibrations Of Structures", Proc. Ninth International Conference on Structural Safety and Reliability ICOSSAR05, (G. Augusti, G.I. Schueller, M. Ciampoli eds.), Millpress, Rotterdam.

Paulotto, C., Ciampoli, M., Augusti, G. (2004), "Some proposals for a first step towards a Performance Based Wind Engineering", IFED-International Forum in Engineering Decision Making; First Forum, Stoos; www.ifed.ethz.ch

Petrini, F., Bontempi, F. and Ciampoli, M. (2008), "Performance-based wind engineering as a tool for the design of the hangers in a suspension bridge", Proc. Fouth International ASRANet colloquium, Athens, Greece; in press.

Petrini, F. Giuliano, F. Bontempi, F., (2007), "Comparison of time domain techniques for the evaluation of the response and the stability in long span suspension bridges", Computer & Structures, (85), 1032-1048.

Porter KA (2003), "An Overview of PEER's Performance-Based Engineering Methodology", Proc of the Ninth International Conference on Applications of Statistics and Probability in Civil Engineering (ICASP9). San Francisco, CA, USA; Millpress Rotterdam.

Repetto, M.P. and Solari, G., (2002). "Dynamic crosswind fatigue of slender vertical structures", Wind and Structures, Vol. 5, No.6, 527-542.

Salvatori, L. and Borri, C. (2007), "Frequency and time-domain methods for the numerical modeling of full-bridge aerolasticity". Computer & Structures (85), 675-687.

Sibilio, E. and Ciampoli, M. (2007), "Performance-Based wind design for footbridges: evaluation of pedestrian comfort", Proc. Tenth International Conference on Applications of Statistics and Probability in Civil Engineering ICASP10, Tokyo, Japan; abstract 561-562; paper in CDRom.

Simon, H.A, The Sciences of the Artificial, The MIT Press, Cambridge, 1998.

Solari, G. Piccardo, G. (2001), "Probabilistic 3-D turbulence modeling for gust buffeting of structures", Probabilistic Engineering Mechanics, (16), 73–86.

Unanwa, C.o., McDonald, J.R., Mehta, K.C. and Smith, D.A. (2000), "The development of wind damage bands for buildings", Journal of Wind Engineering and Industrial Aerodynamics, (84), 119-149.

Zaaijer, M.B. (Editor) (2005), Design Methods for Offshore Wind Turbines at Exposed Sites (OWTES), Report No.SW-02181 Delft University of Technology, Section Wind Energy.

Zaaijer, M. B. (2006). "Foundation modeling to assess dynamic behavior of offshore wind turbines", Applied Ocean Research, (28), 45–57.

Zhang, L., Jie, L. and Peng, Y, (2008), "Dynamic response and reliability analysis of tall buildings subject to wind loading", Journal of Wind Engineering and Industrial Aerodynamics, (96), 25-40.

CONCLUSIONS AND FUTURE DEVELOPMENTS

In this work, the problem of the Aeolian risk assessment has been considered and a probabilistic approach for the performance evaluation of civil engineering structures subjected to the wind action has been proposed.

Actually the procedure is inserted in the Performance-Based Wind Engineering (PBWE) framework, which is the new engineering field having the goal of extending the PBE concepts to the field of wind engineering.

Inside this context, the present work represent, what seems a first attempt in developing a probabilistic procedure which is specifically referred to the peculiar aspects of the Aeolian risk.

The thesis starts recalling some basic concepts in the two fundamental engineering fields related with the PBWE, which are the wind engineering and the probabilistic PBE, after that the proposed formulation his presented, subsequently the numerical procedures adopted for the problem computations are introduced and tested and, finally, the procedure has been applied on a long span suspension bridge.

Several aspects can be found in the present work relatively to the Aeolian risk assessment:

1. some limit states have been qualitatively defined for different structural typologies. This topic was previously partially considered from other authors. In particular, here the performances have been divided in two main levels: low and high, the former it is related with the ultimate limit states, the second it is related with the serviceability limit states;
2. starting from consolidated approaches adopted for the Performance-Based Earthquake Engineering (PBEE), some similitude between the seismic and aeolian risks has been recognized; for this reason, first of all the PBEE techniques have been applied to the wind engineering in their original form;
3. an original classification of the wind engineering uncertainties has been proposed; this has been associated with some hypothesis on the uncertainties propagation in the wind engineering structural problem;
4. starting from the seismic risk assessment expression proposed from the Pacific Earthquake Engineering Research center (PEER):

$$\lambda(DV) = \int_{-\infty}^{+\infty} P(DV|DM) \cdot P(DM|EDP) \cdot P(EDP|IM) \cdot g(IM) \cdot dDM \cdot dEDP \cdot dIM$$

a specialized equation has been proposed for the Aeolian risk analysis. This formulation contains additional terms, specifically related to the wind effects:

$$\lambda(DV) = \int_{-\infty}^{\infty} P(DV|DM) \cdot P(DM|EDP) \cdot P(EDP|\underline{IM},\underline{IP},\underline{\gamma}) \cdot g(\underline{IP}|\underline{IM},\underline{\gamma}) \cdot g(\underline{IM}) \cdot g(\underline{\gamma}) \cdot dDM \cdot dEDP \cdot d\underline{IM} \cdot d\underline{IP} \cdot d\underline{\gamma}$$

where two main new aspects with respect to the PEER equation are introduced

a. the intensity measure (*IM*) here is a vector containing the basic parameters of the wind field characterization, while in seismic procedures *IM* it is usually a scalar entity; this purpose is specifically motivated from the need of give a probabilistic characterization of both the mean and the turbulent intensity of the wind action;
b. a new entity vector (*IP*) has been introduced, representing the stochastic interaction parameters (aerodynamic and aeroelastic parameters); this approach is specifically motivated from the fact that, in wind engineering problems, these parameters determine the mechanical exchanges between the structure and the wind flow, being this point particular relevant from the wind action magnitude; moreover, their quantification is an activity characterized from an high level of uncertainty both from the experimental (wind tunnel tests) and numerical (Computational Fluid Dynamic – CFD) point of view. This coupling of high levels of importance and uncertainty related to the *IP*s lead to the necessity to model the *IP*s as stochastic parameters.

With these positions, the differences between the PEER and PBWE procedures are immediately clear by the comparison of the two flowcharts (Fig. 3.5):

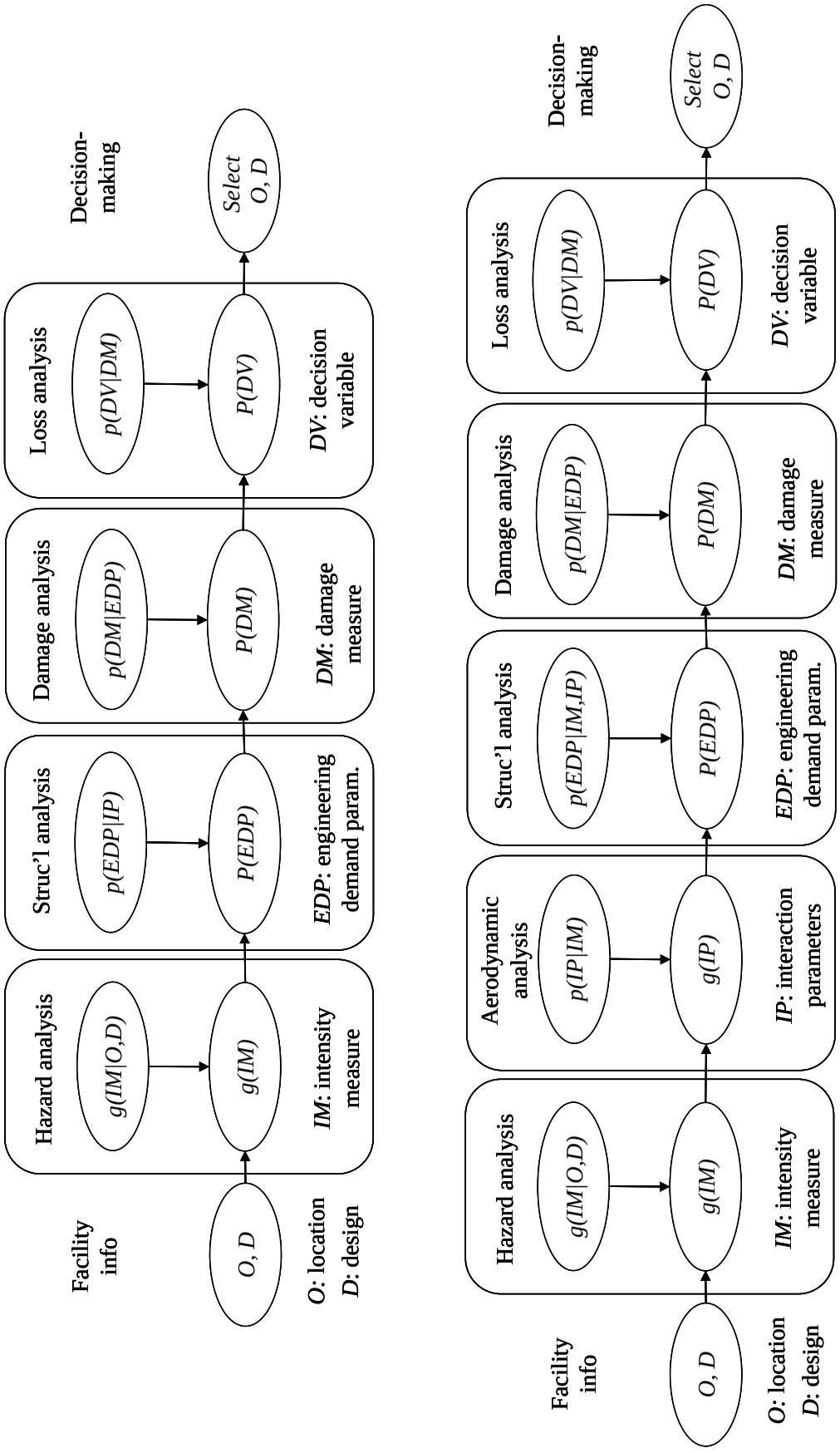

Fig. 3.5. Comparison between the PEER (left) and the PBWE (right).

the applications confirm that adopting the proposed modifications, the estimated Aeolian risk (in terms of failure probabilities) changes in a consistent manner.

Conclusions regarding the applications

The proposed PBWE procedure has been applied on a long span suspension bridge (serving both railway and roadway traffic) for which both serviceability limit states (usability of the bridge under buffeting effects – BU_SLS) and ultimate limit states (safety against the flutter – FL_ULS and fatigue damage of the secondary suspension system under buffeting effects and train transit – Ftg_ULS) have been investigated.

About this structure the following conclusion can be made:

1. Concerning the BU_SLS problem, from the computation of the *annual failure probabilities*, considerations on the different dangerous of the various failure criteria (based on different Engineering Demand Parameters - *EDP*s) can be made, for example in the case study one of the three considered *EDP*s has been revealed to be not dangerous, giving a failure probability equal to zero. This can be useful to individuate which aspect of the structural behavior can be improved to obtain the best results in the performance improving. From the *fragility curves* computation, it is possible to asses the Intensity Measure (*IM*) ranges of values where the various *EDP*s assume the primary role in determining the failure.

   The adoption of proper *non dimensional performance indicators*, leads to the comparison of the structural state relatively to the various dimensional *EDP*s in the same diagrams.

   Finally one has been proved that considering the *roughness value as a stochastic IM parameter* it is significant for the correct evaluation of the failure probabilities.
2. Concerning the FL_ULS problem, the analysis shown that the flutter critic velocity is very sensitive to the changes in the *Interaction Parameters* (*IP*s) values.
3. Concerning the Ftg_ULS problem, analyses shown that, for the case study structure the train transit constitute the main cause of fatigue damage in the hangers, nevertheless also the wind action causes a damage. The *main fatigue damage* produced from the two actions is located *in different locations along the deck*. The most relevant result is given from the analyses conducted in order to asses the *wind-train interactions effects* on the fatigue damage: these shown that the contemporaneous action of wind blowing and train transit produces a fatigue damage

which is less than the one produced from the superposition of the damages due from two actions when they act separately.

As second application, the proposed PBWE procedure has been applied on an offshore wind turbine (OWT) in order to investigate the response probabilistic distribution under the wind stochastic action with possible presence of the vortex shedding phenomenon. The displacements of the nacelle (node located at the hub height) has been assumed as the significant *EDPs*. In this second application the performance levels have not be fixed since the main goal was to asses the relative importance between the uncertainties affecting the various uncertain *IMs* and *IPs*. Another objective of this application is to investigate the effects of the wind-waves-sea current interaction effects.

About this structure the following conclusions can be made:

1. The *most important uncertainty* among these which affect the *IMs*, is the aleatoric one affecting the mean wind speed at 10 meters of height over the sea mean level V_{10}.
2. Concerning the *across-wind response*, the vortex shedding phenomenon plays a prominent role and, consequently, the *uncertainty affecting the Strouhal number St* can not be neglected.
3. The annual probability occurrence curves that have be computed by considering all the proposed stochastic *IMs* and *IPs* ($\underline{IM}=[V_{10}, z_0, \alpha]^T$ =[mean wind speed at 10 meters of height, roughness, mean wind speed direction]^T and $IP=St$= Strouhal number) gives a probabilistic results which is conservative with respect to the one obtained by considering only the V_{10} as stochastic variable, expecially for what concerns the across-wind response (see Fig.5.40). This means that the proposed modifiers to the original PEER approach are valid for this structure.
4. The consideration of the wind-waves-sea current interaction effects produces a change in the annual probability occurrence curves, especially in the case of across-wind response (see Fig.5.43) due to the effect of wind-induced roughness.

Future developments

It is important to outline that further developments can be addressed principally in three directions:

1. PBWE procedure refinement and completion:
   - outlining of methods in order to develop the follow procedure steps (see Fig.3.5): *aerodynamic analysis*, *damage analysis*, *loss analysis*.
   - specialization of the procedure for different performance assessments and structural typologies, giving indications on the parameters which have to adopted as *IM*, *IP*, *EDP*, *DM* and *DV* for specific cases.

2. Probabilistic characterization of the stochastic parameters. In particular, in the author knowledge, the scientific literature lacking in the probabilistic characterization of the roughness.

3. Numerical and analytical procedures. Further efforts have to be spent in direction of developing numerical and analytical procedures to improve the efficiency of the probabilistic analysis, in particular could be applied:
   - advanced techniques for the wind speed time histories generation;
   - advanced techniques for the reduction of the structural model degrees of freedom;
   - advanced Monte Carlo analyses.

APPENDIX A. PROBABILITY THEORY RESUMING TABLES

A.1 Single stochastic variable definitions

Name	Symbol, equation, proprieties
Cumulative distribution function (CDF)	$F_X(x) = P[X \le x]$ a) $0 \le F_X(x) \le 1$ b) $\lim_{x \longrightarrow -\infty} F_X(x) = 0 \qquad \lim_{x \longrightarrow +\infty} F_X(x) = 1$ c) $F_X(x+h) \ge F_X(x)$ con h > 0
Probability density function (PDF)	$\lim_{\Delta x \longrightarrow 0} \frac{P[x < X \le x + \Delta x]}{\Delta x} = \lim_{\Delta x \longrightarrow 0} \frac{F_X(x+\Delta x) - F_X(x)}{\Delta x} = f_X(x)$ If X is a continuous variable $F_X(x) = \int_{-\infty}^{x} f_X(\rho) d\rho \qquad f_X(x) = \frac{dF_X(x)}{dx}$ a) $f_X(x) \ge 0$, being $F_X(x)$ not decreasing; b) $\int_{-\infty}^{+\infty} f_X(x) dx = 1$, being $\lim_{x \longrightarrow +\infty} F_X(x) = 1$; c) $P[X \le a] = \int_{-\infty}^{a} f_X(x) dx$; d) $P[a < X \le b] = \int_{a}^{b} f_X(x) dx$, being $P[a < X \le b] = F_X(b) - F_X(a)$
Mean Value	If X is a discrete variable $\bar{x}_N = \frac{1}{N} \sum_{i=1}^{n} N_i x_i$ If X is a continuous variable $\mu_X = \int_{-\infty}^{+\infty} x f_X(x) dx$
Quadratic mean value	$\varphi_X^2 = \int_{-\infty}^{+\infty} x^2 f_X(x) dx$
Variance	If X is a discrete variable $\bar{x}_N = \frac{1}{N} \sum_{i=1}^{n} (x_i - \mu_X)^2$ If X is a continuous variable $\sigma_X^2 = \varphi_X^2 - \mu_X^2 = \int_{-\infty}^{+\infty} (x - \mu_X)^2 f_X(x) dx$
Standard deviation (scarto quadratico medio)	If X is a discrete variable $\delta_X = \sigma_X = \sqrt{\frac{1}{N} \sum_{i=1}^{n} x_i - \bar{x}} = \sqrt{\sigma_X^2}$ If X is a continuous variable $\delta_X = \sigma_X = \sqrt{\int_{-\infty}^{+\infty} (x - \mu_X)^2 f_X(x) dx} = \sqrt{\sigma_X^2}$

Coefficient of variation	$C_X = \dfrac{\delta_X}{\mu_X}$
Stochastic mean linear operator	In Y is a stochastic function of X, namely Y=f(X): $E[Y] = E[f(X)] = \int_{-\infty}^{+\infty} f(x) f_X(x) dx$

Name	**Symbol, equation, proprieties**
Stochastic moments for a stochastic variable X	Stochastic moment of order k $m_k[X] = E[X^k] = \int_{-\infty}^{+\infty} x^k f_X(x) dx$ $m_0[X] = \int_{-\infty}^{+\infty} f_X(x) dx = 1$ zero-order moment $m_1[X] = E[X] = \int_{-\infty}^{+\infty} x f_X(x) dx = \mu_X$ first-order moment $m_2[X^2] = E[X] = \int_{-\infty}^{+\infty} x^2 f_X(x) dx = \varphi_X^2$ second-order moment
Characteristic function of the stochastic variable X	$M_X(\vartheta) = E[\exp(-i\vartheta X)] = \int_{-\infty}^{+\infty} e^{-i\vartheta x} f_X(x) dx \qquad \vartheta \in \mathrm{Re}$ By operating a Taylor's transformation $\left[\dfrac{d^k M_X(\vartheta)}{d\vartheta^k}\right]_{\vartheta=0} = (-i)^k \int_{-\infty}^{+\infty} x^k f_X(x) dx = (-i)^k E[X^k] = (-i)^k m_k[X]$ $M_X(\vartheta) = \sum_{j=0}^{\infty} \dfrac{(-i)^j}{j!} m_j[X] \theta^j$ Subsequent steps for the derivation of the PDF from the stochastic moments Momenti statistici → Funzione caratteristica → Trasformata inversa di Fourier → Densità di probabilità
Log-characteristic function of the stochastic variable X	$\ln M_X(\vartheta) = \sum_{j=1}^{\infty} \dfrac{(-i)^j}{j!} k_j[X] \theta^j$ Con $k_j[X] = \ln m_j[X]$ cumulants of the stochastic variable X

Gaussian stochastic variable

The Gaussian (or normal) stochastic variables are completely characterized from the first two stochastic moments (mean value and variance).

Central limit Theorem, if a stochastic variable X is given from the sum of a great number of unconditioned mutually independent stochastic variables, then the variable X will have a normal distribution, whatever was the original variables distribution. (Freeman, 1963)

Characteristic function	$$M_X(\vartheta) = \exp\left[\sum_{j=1}^{\infty} \frac{(-i)^j}{j!} k_j \theta^j\right] = \exp\left[-ik_1 - \frac{1}{2}k_2\vartheta^2\right]$$
Gaussian PDF and CDF	$$f_X(x) = \frac{1}{\sqrt{2\pi k_2}} \exp\left[-\frac{1}{2}\frac{(x-k_1)^2}{k_2}\right] = \frac{1}{\sigma_X\sqrt{2\pi}} \exp\left[-\frac{1}{2}\left(\frac{x-\mu_X}{\sigma_X}\right)^2\right]$$ 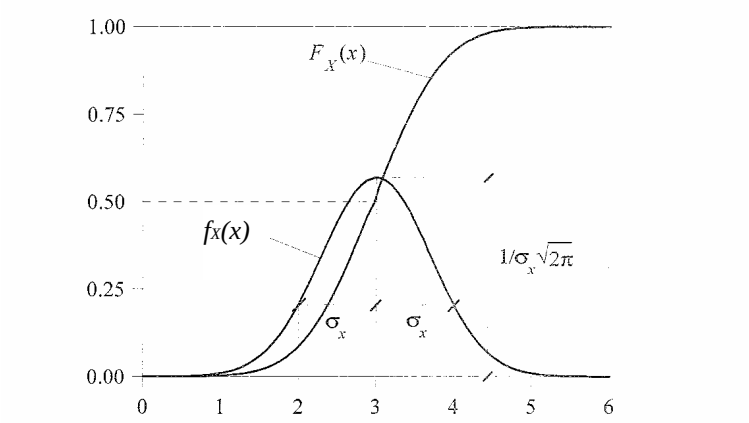

A.2 Bi-dimensional stochastic variable definitions

Name	Symbol, equation, proprieties
Joined cumulative probability function of the two stochastic variables X_1 and X_2	$F_{X_1X_2}(x_1,x_2)=P\left[X_1\le x_1\cap X_2\le x_2\right]=\int_{-\infty-\infty}^{x_1\,x_2} f_{X_1X_2}(\rho_1\rho_2)d\rho_1 d\rho_2$
Joined probability density function of the two stochastic variables X_1 and X_2	$f_{X_1X_2}(x_1,x_2)=\frac{\partial^2}{\partial x_1\partial x_2}F_{X_1X_2}(x_1x_2)$ If X is a continuous variable $F_{X_1X_2}(x_1,x_2)=\int_{-\infty-\infty}^{x_1\,x_2} f_{X_1X_2}(\rho_1\rho_2)d\rho_1 d\rho_2$ The probability functions defined in the case of the one-dimensional stochastic variables, can be defined for two-dimensional stochastic variables too
Marginal probability density function of a stochastic variable X_1	$f_{X_1}(x_1)=\int_{-\infty-\infty}^{+\infty+\infty} f_{X_1X_2}(x_1x_2)dx_2$
Conditional probability density function	$f_{X_1\mid X_2=\bar{X}}(x_1)=f_{X_1}(x_1\mid x_2=\bar{x})=\frac{f_{X_1X_2}(x_1,\bar{x})}{f_{X_2}(\bar{x})}$
Stochastic moments for a stochastic variable X	momento di ordine k $m_K\left[X_1X_2\right]=E\left[X_1^{\,r}X_2^{\,s}\right]=\int_{-\infty-\infty}^{+\infty+\infty} x_1^r x_2^s f_{X_1X_2}(x_1x_2)dx_1dx_2$ con r + s = k I ord $E\left[X_1\right],E\left[X_2\right]$ medie marginali II ord $E\left[X_1^2\right],E\left[X_1X_2\right],E\left[X_2^2\right]$ valori quadratici medi delle singole componenti III ord $E\left[X_1^3\right],E\left[X_1^2X_2\right],E\left[X_1X_2^2\right],E\left[X_2^3\right]$
Marginal variances	$\sigma_{X_1}^2=\varphi_{X_1}^2-\mu_{X_1}^2$ $\sigma_{X_2}^2=\varphi_{X_2}^2-\mu_{X_2}^2$
Covariance between X_1 and X_2	$\sigma_{X_1X_2}=E\left[X_1X_2\right]-E\left[X_1\right]E\left[X_2\right]=\varphi_{X_1X_2}-\mu_{X_1X_2}$
Correlation coefficient between X_1 and X_2	$\rho_{X_1X_2}=\frac{\sigma_{X_1X_1}}{\sigma_{X_1}\sigma_{X_2}}$; con $0<\rho_{X_1X_2}<1$

Gaussian stochastic variables	
Name	**Symbol, equation, proprieties**
Gaussian PDF	$$f_{X_1X_2}(x_1,x_2)=\frac{1}{\sigma_{X_1}\sigma_{X_2}2\pi\sqrt{1-\rho_{X_1X_2}^2}}\cdot$$ $$\cdot\exp\left\{-\frac{1}{2\left(1-\rho_{X_1X_2}^2\right)}\times\left[\frac{\left(x_1-\mu_{X_1}\right)^2}{\sigma_{X_1}^2}-\frac{2\rho_{X_1X_2}\left(x_1-\mu_{X_1}\right)\left(x_2-\mu_{X_2}\right)}{\sigma_{X_1}\sigma_{X_2}}+\frac{\left(x_2-\mu_{X_2}\right)^2}{\sigma_{X_2}^2}\right]\right\}$$ The Gaussian PDF is univocally determined by the knowledge of the , μ_{X1}, μ_{X2}, $\sigma_{X_1}^2$ e $\sigma_{X_2}^2$ and $\sigma_{X_1X_2}$ Two Gaussian stochastic variable are uncorrelated since they are independent; this can be easly deduced from the previous expression, by assuming $\rho_{X_1X_2}=0$, can be obtained: $$f_{X_1X_2}(x_1,x_2)=$$ $$\frac{1}{\sigma_{X_1}\sqrt{2\pi}}\exp\left[-\frac{1}{2}\left(\frac{x_1-\mu_{X_1}}{\sigma_{X_1}}\right)^2\right]\times\frac{1}{\sigma_{X_2}\sqrt{2\pi}}\exp\left[-\frac{1}{2}\left(\frac{x_2-\mu_{X_2}}{\sigma_{X_2}}\right)^2\right]=p_{X_1}(x_1)p_{X_2}(x_2)$$

APPENDIX B. COMPUTER CODES

In what follow, two of the codes created in order to develop the numerical procedure adopted in the thesis are reported.

B.1. MATLAB code for the numerical generation of wind turbulent velocity time histories

```
%%%%%%%%%%%%%%%%%%%%%%%%%%%%%%%%%%%%%%%%%%%%%%%%%%%%%%%%%%%%%%%%%%
% GENERAZIONE DI DUE COMPONENTI DI VELOCITA' TURBOLENTA ORTOGONALI TRA
% LORO (u E w NEL CASO DI PONTI) CON ESPANSIONE BILINEARE, CIOE'
% PER PUNTI DISTRIBUITI SU UNA SUPERFICIE
%
% AUTORE: FRANCESCO PETRINI
%
%ATTENZIONE: ALLO STATO ATTUALE LE COMPONENTI SONO SCORRELATE
%
%  ROMA OTTOBRE-2008
%%%%%%%%%%%%%%%%%%%%%%%%%%%%%%%%%%%%%%%%%%%%%%%%%%%%%%%%%%%%%%%%%%%

numgirate=1;  %numero di girate di generazione storie; i dati riportati in un eventuale
            %diverso da 1 solo se si vogliono generare piu campi di
            %velocità in serie

AnalisTime_vector=zeros(numgirate,2); %vettore in cui appunto i tempi delle analisi

for run=1:1:numgirate    %ciclo globale: ripeto la generazione di storie
                      %per "numgirate" volte


UUU=1; %immettere 1 se si vuole generare la componente di turbolenza u,
     %immettere 0 se non si vuole generare la componente di turbolenza u

VVV=0; %immettere 1 se si vuole generare la componente di turbolenza v,
     %immettere 0 se non si vuole generare la componente di turbolenza v

WWW=1; %immettere 1 se si vuole generare la componente di turbolenza w,
     %immettere 0 se non si vuole generare la componente di turbolenza w

%intervalli di campionamento
T=3600; %durata del segnale

dt=0.1; %discretizzazione nel dominio del tempo, deve rispettare la
        %condizione dt<=pi/(4*omegamax)


omegamax=pi/dt; %frequenza di cut-off
dw=omegamax/(T/dt); %intervallo di campionamento dello spettro, deve rispettare la
        %condizione dw<=4*pi/T (altri riportano dw<=pi/T)

a=(omegamax/dw); %n° di frequenze di campionamento

b=T/dt;   %n° elementi del vettore tempo

t0=0;
t=zeros(b,1); %vettore tempo
for j=1:1:b
   t(j)=t0;
   t0=t0+dt;
end
w=[dw:dw:omegamax]; %vettore frequenza circolare
f=w/(2*pi) ;        %vettore frequenza

load 'coord2.txt'      %carica le coordinate per confronto generazioni
x=coord2(:,2);
y=coord2(:,3);
z=coord2(:,4);
```

```
nnodi=length(z);
nquote=length(z);

save('PASSI.dat','b','-ascii')
save('nnodi.dat','nnodi','-ascii')

h=500; %altezza strato limite atmosferico


% MICROZONAZIONE (GENERALE)
z0=0.2;   %lunghezza di rugosita'
z02=0.05;
zmin=10;   %quote min e max della generazione
zmax=200;

%ufri=friction velocity =(tau0/rò)^0,5  (vedi ESDU 82026e) con rò=densità aria e
%tau0=sforzo di taglio alla base
%Comunque fissando U10=(velovità media del vento a 10 metri di quota), si
%può ricavare ufri invertendo la  Uz=2.5*ufri.*(log(z/z0))

ufri=2.04497;      %per confronto con articolo Lazzari 2004
              %(ricavato invertendo la Uz=2.5*ufri.*(log(z/z0)))
ut=ufri;

Uz=2.5*ufri.*(log(z/z0)); %profilo delle velocità medie (vedi Carassale ICOSSAR 2005)

sigmaqu=[6-1.1*atan(log(z0)+1.75)]*ut^2; %deviazione standard ricavata da:
                                %G. Solari, G. Piccardo,
                                %Probabilistic 3D turbulence
                                %modeling for gust buffeting of
                                %structures,
                                %Prob. Eng.Mech. 16 (2001) 73–86

sigmaqv=zeros(nnodi,1);
for i=1:1:nnodi
sigmaqv(i,1)=sigmaqu*[1-0.22*(cos(pi*z(i,1)/(20*zmax)))^4]; %deviazione standard
                                    %(ESDU 85020 pag10:
end

for i=1:1:nnodi
sigmaqw(i,1)=sigmaqu*[1-0.45*(cos(pi*z(i,1)/(20*zmax)))^4]; %deviazione standard
                                    %(ESDU 85020 pag10:
end

%matrice delle scale integrali della componente longitudinale
Lux=zeros(nnodi,nnodi);
for i=1:1:nnodi
   Lux(i,i)=300*(z(i,1)/200)^(0.67+0.05*log(z0)); %ho tolto beta
end
for i=1:1:nnodi
   for j=(i+1):1:nnodi
 Lux(i,j)=300*(((z(i,1)+z(j,1))/2)/200)^(0.67+0.05*log(z0));
 Lux(j,i)=Lux(i,j);
   end
end

LuzLux=zeros(nnodi,nnodi);
for i=1:1:nnodi
   LuzLux(i,i)=0.5-0.34*exp(-35*(z(i,1)/h)^1.7);
end
for i=1:1:nnodi
   for j=(i+1):1:nnodi
   LuzLux(i,j)=0.5-0.34*exp(-35*(((z(i,1)+z(j,1))/2)/h)^1.7);
   LuzLux(j,i)=LuzLux(i,j);
   end
end

%scala integrale laterale della componente longitudinale
Luz=zeros(nnodi,nnodi);
for i=1:1:nnodi
   Luz(i,i)=LuzLux(i,i)*Lux(i,i);
end
for i=1:1:nnodi
   for j=(i+1):1:nnodi
   Luz(i,j)=LuzLux(i,j)*Lux(i,j);
```

```
   Luz(j,i)=Luz(i,j);
   end
end

%scala integrale laterale della componente longitudinale
Luy=zeros(nnodi,nnodi);
for i=1:1:nnodi
   Luy(i,i)=0.16*Lux(i,i)+0.68*Luz(i,i);
end
for i=1:1:nnodi
   for j=(i+1):1:nnodi
   Luy(i,j)=0.16*Lux(i,j)+0.68*Luz(i,j);
   Luy(j,i)=Luy(i,j);
   end
end


%Altre scale integrali per simulare le altre componenti di turbolenza
%(componenti v e w)

if VVV>0

%-------------------------------------------------------------------------
%componente v
%-------------------------------------------------------------------------

Lvy=zeros(nnodi,nnodi);
for i=1:1:nnodi
   Lvy(i,i)=Lux(i,i)*(2*Luy(i,i)/Lux(i,i))*(sigmaqv(i,1)/sigmaqu)^3; %ESDU 8610 pag 10
end
for i=1:1:nnodi
   for j=(i+1):1:nnodi

 Lvy(i,j)=Lux(i,j)*(2*Luy(i,j)/Lux(i,j))*(sigmaqv(i,1)/sigmaqu)^3; %ESDU 8610 pag 10
 Lvy(j,i)=Lvy(i,j);
   end
end

%scala integrale longitudinale della componente laterale
Lvx=zeros(nnodi,nnodi);
for i=1:1:nnodi
   Lvx(i,i)=1/2*Lux(i,i)*(sigmaqv(i,1)/sigmaqu)^3; %ESDU 8610 pag 10
end
for i=1:1:nnodi
   for j=(i+1):1:nnodi
   Lvx(i,j)=1/2*Lux(i,j)*(sigmaqv(i,1)/sigmaqu)^3; %ESDU 8610 pag 10
   Lvx(j,i)=Lvx(i,j);
   end
end

%scala integrale verticale della componente laterale
Lvz=zeros(nnodi,nnodi);
for i=1:1:nnodi
   Lvz(i,i)=1/2*Lux(i,i)*(2*Luz(i,i)/Lux(i,i))*(sigmaqv(i,1)/sigmaqu)^3; %ESDU 8610 pag 10;
end

for i=1:1:nnodi
   for j=(i+1):1:nnodi
   Lvz(i,j)=1/2*Lux(i,j)*(2*Luz(i,j)/Lux(i,j))*(sigmaqv(i,1)/sigmaqu)^3; %ESDU 8610 pag 10;
   Lvz(j,i)=Lvz(i,j);
   end
end

end

%-------------------------------------------------------------------------
%componente w
%-------------------------------------------------------------------------

if WWW>0

Lwz=zeros(nnodi,nnodi);
for i=1:1:nnodi
   Lwz(i,i)=Lux(i,i)*(2*Luz(i,i)/Lux(i,i))*(sigmaqw(i,1)/sigmaqu)^3; %ESDU 8610 pag 10
end
for i=1:1:nnodi
```

```
    for j=(i+1):1:nnodi

 Lwz(i,j)=Lux(i,j)*(2*Luz(i,j)/Lux(i,j))*(sigmaqw(i,1)/sigmaqu)^3; %ESDU 8610 pag 10
 Lwz(j,i)=Lwz(i,j);
    end
end


%scala integrale longitudinale della componente laterale
Lwx=zeros(nnodi,nnodi);
for i=1:1:nnodi
    Lwx(i,i)=1/2*Lux(i,i)*(sigmaqw(i,1)/sigmaqu)^3; %ESDU 8610 pag 10
end
for i=1:1:nnodi
    for j=(i+1):1:nnodi
    Lwx(i,j)=1/2*Lux(i,j)*(sigmaqw(i,1)/sigmaqu)^3; %ESDU 8610 pag 10
    Lwx(j,i)=Lwx(i,j);
    end
end

%scala integrale verticale della componente laterale

Lwy=zeros(nnodi,nnodi);
for i=1:1:nnodi
    Lwy(i,i)=1/2*Lux(i,i)*(2*Luy(i,i)/Lux(i,i))*(sigmaqw(i,1)/sigmaqu)^3; %ESDU 8610 pag 10;
end

for i=1:1:nnodi
    for j=(i+1):1:nnodi
    Lwy(i,j)=1/2*Lux(i,j)*(2*Luy(i,j)/Lux(i,j))*(sigmaqw(i,1)/sigmaqu)^3; %ESDU 8610 pag 10;
    Lwy(j,i)=Lwy(i,j);
    end
end

end

%inizializzazione delle matrici di densità spettrale
Svvu=zeros(nnodi,nnodi,a); %"a" è il n° di frequenze circolari considerate

Svvufreq=zeros(nnodi,nnodi,a);

%definizione degli autospettri

for i=1:1:nnodi
for j=1:1:a

Svvufreq(i,i,j)=(6.868*sigmaqu*Lux(i,i)/Uz(i))/((1+1.5*6.868*f(1,j)*Lux(i,i)/Uz(i))^(5/3));
%spettro di Solari (Carassale Solari 2006)

end
end


% matrice di correlazione geometrica dei nodi della struttura
% per il calcolo delle scale integrali risultanti della componente u

Dru=zeros (nnodi,nnodi);
for j=1:1:nnodi
    for l=(j+1):1:nnodi
Dru(j,l)=[(y(j,1)-y(l,1))^2+(z(j,1)-z(l,1))^2]^0.5;
Dru(l,j)=Dru(j,l);
    end
end

%inizializzazione della matrice delle scale integrali risultanti
%(ESDU 86010 (vol 1) pag 11)
rLu=zeros (nnodi,nnodi);

for j=1:1:nnodi
    for l=(j+1):1:nnodi
        rLu(j,l)=[(Luy(j,l)*(y(j,1)-y(l,1)))^2+(Luz(j,l)*(z(j,1)-z(l,1)))^2]^0.5/Dru(j,l);
        rLu(l,j)=rLu(j,l);
    end
end
```

```
%inizializzazione matrice delle distanze adimensionalizzate ortogonali
%alla componente longitudinale di turbolenza
rgu=zeros (nnodi,nnodi);

for j=1:1:nnodi
   for l=(j+1):1:nnodi
rgu(j,l)=Dru(j,l)/(2*rLu(j,l)); %(ESDU 86010 (vol 1) pag 14 formula (7.8))
rgu(l,j)=rgu(j,l);
   end
end

biu=zeros (nnodi,nnodi);

for j=1:1:nnodi
   for l=(j+1):1:nnodi
      biu(j,l)=0.35*(rgu(j,l))^0.2;%(ESDU 86010 (vol 1) pag 14 formula (7.9))
      biu(l,j)=biu(j,l);
   end
end

%inizializzazione del parametro di separazione adimensionalizzato
%(serve per il successivo calcolo delle funzioni di coerenza)
etau=zeros(nnodi,nnodi,a);
for j=1:1:nnodi
   for l=(j+1):1:nnodi
      for i=1:1:a
   etau(j,l,i)=[(0.747*rgu(j,l))^2+(w(i)*Dru(j,l)/((Uz(j)+Uz(l))/2))^2]^0.5;%ORIGINAL PADUANO (ESDU 86010 (vol 1) pag 14 formula
(7.10))
   etau(l,j,i)=etau(j,l,i);
      end
   end
end
Ciu=zeros(nnodi,nnodi);

for j=1:1:nnodi
   for l=(j+1):1:nnodi
      Ciu(j,l)=(1.6*(rgu(j,l))^0.13)/etau(j,l)^biu(j,l);
      Ciu(l,j)=Ciu(j,l);
   end
end

%funzioni di coerenza
%(ESDU 86010 (vol 1) pag 14)
gammau=zeros(nnodi,nnodi,a);
for j=1:1:nnodi
   for l=(j+1):1:nnodi
      for i=1:1:a
      gammau(j,l,i)=exp(-1.15*etau(j,l,i)^1.5);
      gammau(l,j,i)=gammau(j,l,i);
      end
   end
end

%definizione degli spettri trasversali
for j=1:1:a
for i=1:1:nnodi
   for l=(1+i):1:nnodi
Svvufreq(i,l,j)=(Svvufreq(i,i,j)*Svvufreq(l,l,j))^0.5*gammau(i,l,j);
Svvufreq(l,i,j)=Svvufreq(i,l,j);
   end
end
end

Svvuadim=zeros(nnodi,a); %matrice la cui colonna i-esima contiene gli autospettri alla frequenza "i" adimensionalizzati

for s=1:1:a
 for j=1:1:nnodi
   Svvuadim(j,s)=f(1,s)*Svvufreq(j,j,s);
 end
 end

Sviifreq=zeros(a,nnodi);
for i=1:1:nnodi
for j=1:1:a
   Sviifreq(j,i)=Svvufreq(i,i,j);
end
```

```
end

%-------------------------------------------------------------------------
%-------------------------------------------------------------------------
%nel caso si vogliano generare anche la componente turbolenta v
%VVV e WWW sono definite all'inizio del listato
%-------------------------------------------------------------------------
%-------------------------------------------------------------------------
if VVV>0

Svvv=zeros(nnodi,nnodi,a); %"a" è il n° di frequenze circolari considerate
Svvvfreq=zeros(nnodi,nnodi,a);

for i=1:1:nnodi
for j=1:1:a
Svvvfreq(i,i,j)=(6.868*sigmaqv(i,1)*Lvy(i,i)/Uz(i))/((1+1.5*6.868*f(1,j)*Lvy(i,i)/Uz(i))^(5/3));
end
end

Drv=zeros (nnodi,nnodi);
for j=1:1:nnodi
   for l=(j+1):1:nnodi
Drv(j,l)=[(x(j,1)-x(l,1))^2+(z(j,1)-z(l,1))^2]^0.5;
Drv(l,j)=Drv(j,l);
   end
end

%inizializzazione della matrice delle scale integrali risultanti
%(ESDU 86010 (vol 1) pag 11)
rLv=zeros (nnodi,nnodi);
for j=1:1:nnodi
   for l=(j+1):1:nnodi
      rLv(j,l)=[(Lvx(j,l)*(x(j,1)-x(l,1)))^2+(Lvz(j,l)*(z(j,1)-z(l,1)))^2]^0.5/Drv(j,l);
      rLv(l,j)=rLv(j,l);
   end
end

%inizializzazione matrice delle distanze adimensionalizzate ortogonali
%alla componente longitudinale di turbolenza
rgv=zeros (nnodi,nnodi);
for j=1:1:nnodi
   for l=(j+1):1:nnodi
rgv(j,l)=Drv(j,l)/(2*rLv(j,l));
rgv(l,j)=rgv(j,l);
   end
end
biv=zeros (nnodi,nnodi);
for j=1:1:nnodi
   for l=(j+1):1:nnodi
      biv(j,l)=0.35*(rgv(j,l))^0.2;
      biv(l,j)=biv(j,l);
   end
end


%inizializzazione del parametro di separazione adimensionalizzato
%(serve per il successivo calcolo delle funzioni di coerenza)
etav=zeros(nnodi,nnodi,a);
for j=1:1:nnodi
   for l=(j+1):1:nnodi
      for i=1:1:a
   etav(j,l,i)=[(0.747*rgv(j,l))^2+(w(i)*Drv(j,l)/((Uz(j)+Uz(l))/2))^2]^0.5;
   etav(l,j,i)=etav(j,l,i);
      end
   end
end

Civ=zeros(nnodi,nnodi);

for j=1:1:nnodi
   for l=(j+1):1:nnodi
      Civ(j,l)=(1.6*(rgv(j,l))^0.13)/etav(j,l)^biv(j,l);
      Civ(l,j)=Civ(j,l);
   end
end
```

```
%funzioni di coerenza
gammav=zeros(nnodi,nnodi,a);
for j=1:1:nnodi
   for l=(j+1):1:nnodi
      for i=1:1:a
      gammav(j,l,i)=exp(-0.65*etav(j,l,i)^1.3);%(ESDU 86010 (vol 1) pag 14) formula (7,14)
      gammav(l,j,i)=gammav(j,l,i);
      end
   end
end

%definizione degli spettri trasversali (componente v)
for j=1:1:a
for i=1:1:nnodi
   for l=(1+i):1:nnodi
Svvvfreq(i,l,j)=(Svvvfreq(i,i,j)*Svvvfreq(l,l,j))^0.5*gammav(i,l,j);
Svvvfreq(l,i,j)=Svvvfreq(i,l,j);
   end
end
end



end

%-------------------------------------------------------------------------
%-------------------------------------------------------------------------
%nel caso si vogliano generare anche la componente turbolenta v
%VVV e WWW sono definite all'inizio del listato
%-------------------------------------------------------------------------
%-------------------------------------------------------------------------

if WWW>0
Svvw=zeros(nnodi,nnodi,a); %"a" è il n° di frequenze circolari considerate
Svvwfreq=zeros(nnodi,nnodi,a);

for i=1:1:nnodi
for j=1:1:a
   Svvwfreq(i,i,j)=(6.868*sigmaqw(i,1)*Lwz(i,i)/Uz(i))/((1+1.5*6.868*f(1,j)*Lwz(i,i)/Uz(i))^(5/3));
%spettro di Solari (Carassale Solari 2006)
end
end

Drw=zeros (nnodi,nnodi);
for j=1:1:nnodi
   for l=(j+1):1:nnodi
Drw(j,l)=[(x(j,1)-x(l,1))^2+(y(j,1)-y(l,1))^2]^0.5;
if Drw(j,l)==0
   Drw(j,l)=1;
end
Drw(l,j)=Drw(j,l);
   end
end

%inizializzazione della matrice delle scale integrali risultanti
%(ESDU 86010 (vol 1) pag 11)
rLw=zeros (nnodi,nnodi);
for j=1:1:nnodi
   for l=(j+1):1:nnodi
      rLw(j,l)=[(Lwx(j,l)*(x(j,1)-x(l,1)))^2+(Lwy(j,l)*(y(j,1)-y(l,1)))^2]^0.5/Drw(j,l);
     if rLw(j,l)==0

      rLw(j,l)=Lwz(j,l);
     end
      rLw(l,j)=rLw(j,l);
   end
end

%inizializzazione matrice delle distanze adimensionalizzate ortogonali
%alla componente longitudinale di turbolenza
rgw=zeros (nnodi,nnodi);
for j=1:1:nnodi
   for l=(j+1):1:nnodi
rgw(j,l)=Drw(j,l)/(2*rLw(j,l));
rgw(l,j)=rgw(j,l);
   end
end
```

```
biw=zeros (nnodi,nnodi);

for j=1:1:nnodi
    for l=(j+1):1:nnodi
        biw(j,l)=0.35*(rgw(j,l))^0.2;
        biw(l,j)=biw(j,l);
    end
end


%inizializzazione del parametro di separazione adimensionalizzato
%(serve per il successivo calcolo delle funzioni di coerenza)
etaw=zeros(nnodi,nnodi,a);
for j=1:1:nnodi
    for l=(j+1):1:nnodi
        for i=1:1:a
    etaw(j,l,i)=[(0.747*(rgw(j,l)))+(w(i)*Drw(j,l)/((Uz(j)+Uz(l))/2))^2]^0.5;
    etaw(l,j,i)=etaw(j,l,i);
        end
    end
end

Ciw=zeros(nnodi,nnodi);

for j=1:1:nnodi
    for l=(j+1):1:nnodi
        Ciw(j,l)=(1.6*(rgw(j,l))^0.13)/etaw(j,l)^biw(j,l);
        Ciw(l,j)=Ciw(j,l);
    end
end

%funzioni di coerenza
gammaw=zeros(nnodi,nnodi,a);
for j=1:1:nnodi
    for l=(j+1):1:nnodi
        for i=1:1:a
        gammaw(j,l,i)=exp(-0.65*etaw(j,l,i)^1.3); %(ESDU 86010 (vol 1) pag 14) formula (7,14)
        gammaw(l,j,i)=gammaw(j,l,i);
        end
    end
end

%definizione degli spettri trasversali (componente w)
for j=1:1:a
for i=1:1:nnodi
    for l=(1+i):1:nnodi
Svvwfreq(i,l,j)=(Svvwfreq(i,i,j)*Svvwfreq(l,l,j))^0.5*gammaw(i,l,j);
Svvwfreq(l,i,j)=Svvwfreq(i,l,j);
    end
end
end


end  %chiude la proposizione if WWW>1

Matrix_Time=cputime

%%%%%%%%%%%%%%%%%%%%%%%%%%%%%%%%%%%%%%%%%%%%%%%%%%%%%%%%%%%%%%%%%%%%%%%%%%%%
% Scomposizione POD
%%%%%%%%%%%%%%%%%%%%%%%%%%%%%%%%%%%%%%%%%%%%%%%%%%%%%%%%%%%%%%%%%%%%%%%%%%%%

if UUU>0
%%%%%%%%%%%%%%%%%%%%%%%%%%%%%%%%%%%%%%%%%%%%%%%%%%%%%%%%%%%%%%%%%%%%%%%%%%%%
%calcolo degli autovalori e degli autovettori
%%%%%%%%%%%%%%%%%%%%%%%%%%%%%%%%%%%%%%%%%%%%%%%%%%%%%%%%%%%%%%%%%%%%%%%%%%%%

num=nnodi; %n° di autovettori che voglio calcolare
autovettori=zeros(nnodi,nnodi,a);
autovalori=zeros(nnodi,nnodi,a);


for j=1:1:a
 [autovettori(:,:,j),autovalori(:,:,j)]=eig(Svvufreq(:,:,j));
end
```

```
%generazione di numeri random con media nulla e varianza=0.5
R= zeros (1,nnodi,a);
R = normrnd(0,0.5,1,nnodi,a);
I= zeros (1,nnodi,a);
I = normrnd(0,0.5,1,nnodi,a);
%%%%%%%%%%%%%%%%%%%%%%%%%%%%%%%%%%%%%%%%%%%%%%%%%%%%%%%%%%%%%%%%%%%%%%%%%%%%%%%%%%%%%%

%generazione delle storie di vento
Y=zeros(nnodi,nnodi,a);  %num è il numero di autovettori calcolati
Y2=zeros(nnodi,a);     %SE VOGLIO UTILIZZARE FFT TECHNIQUE

%Matrici delle time history di vento Vx
Uvel0=zeros(nnodi,2*b);   %SE VOGLIO UTILIZZARE FFT TECHNIQUE
Uvel=zeros(nnodi,b); %matrice delle velocità turbolente
Uvel1=zeros(nnodi,b);%matrice delle velocità totali
Uvel2=zeros(nnodi,b+1); %per mettere matrice delle velocità turbolente in formato ANSYS

for s=1:1:b
for i=1:1:num    %num è il numero di autovettori calcolati
for j=1:1:a
    Y(:,i,j)=2*(autovalori(i,i,j)*dw)^0.5*((autovettori(:,i,j)*(R(1,i,j)+I(1,i,j)))); %SE VOGLIO UTILIZZARE FFT TECHNIQUE
end
end

 for i=1:1:num    %num è il numero di autovettori calcolati
for j=1:1:nnodi
Y2(j,:)=sum(Y(j,:,:));  %SE VOGLIO UTILIZZARE FFT TECHNIQUE
end
end
c=s/b*100; %contatore del processo
end

for s=1:1:b
for j=1:1:nnodi
    Uvel0(j,:)=real(fft(Y2(j,:),2*b)); %SE VOGLIO UTILIZZARE FFT TECHNIQUE%mi faccio la sommatoria degli autovettori da Uvel0
(e perciò degli Y) all'istante s
end
end

% %%%%%%%%%%%%%%%%%%%%%%%%%%%%%%%%%%%%%%%%%%%%%%%
% %SE VOGLIO UTILIZZARE FFT TECHNIQUE
 for j=1:1:nnodi
     for s=1:1:2*b
     if s>b
 Uvel(j,s-b)=Uvel0(j,s);
     end
     end
 end
% %%%%%%%%%%%%%%%%%%%%%%%%%%%%%%%%%%%%%%%%%%%%%%%

for s=1:1:b
for j=1:1:nnodi
    Uvel1(j,s)=Uz(j,1)+Uvel(j,s);
end
end

for n=1:nnodi
    Uvel2(n,1)=n;
  for s=2:1:b+1
    Uvel2(n,s)=Uvel(n,s-1);  %per mettere matrice delle velocità turbolente in formato ANSYS
end
end

Uvel3=zeros((nnodi+1)*(b+1),1); %matrice delle velocità turbolente in formato ANSYS

for s=2:1:b+1
    Uvel3(s,1)=t(s-1,1);
end




for j=2:1:nnodi+1
for s=1:1:b+1
Uvel3(s+(j-1)*b+j,1)=Uvel2(j-1,s)+Uz(j-1,1);
end
```

```
end

llll=1;
for j=1:b+1:(b+2)*nnodi
    Uvel3(j,1)=llll;
    llll=llll+1;
end

%save('Vvel.dat','Uvel1_Cho','-ascii')
save('Vvel.dat','Uvel3','-ascii')


midpoint=(nnodi+1)/2;
MeanU=zeros(numgirate,1);
MeanU_Teoric=zeros(numgirate,1);

MeanU_Teoric(run,1)=Uz(midpoint,1);
MeanU(run,1)=mean(Uvel1(midpoint,:));


end  %fine del ciclo if UUU>0


%%%%%%%%%%%%%%%%%%%%%%%%%%%%%%%%%%%%%%%%%%%%%%%%%%%%%%%%%%%%%%%%%%%%%%%%
%GENERAZIONE COMPONENTE VERTICALE  w
%%%%%%%%%%%%%%%%%%%%%%%%%%%%%%%%%%%%%%%%%%%%%%%%%%%%%%%%%%%%%%%%%%%%%%%%%
if WWW>0

%%%%%%%%%%%%%%%%%%%%%%%%%%%%%%%%%%%%%%%%%%%%%%%%%%%%%%%%%%%%%%%%%%%%%%%
%calcolo degli autovalori e degli autovettori

autovettori=zeros(nnodi,nnodi,a);
autovalori=zeros(nnodi,nnodi,a);
for j=1:1:a
[autovettori(:,:,j),autovalori(:,:,j)]=eig(Svvwfreq(:,:,j));
end

%generazione di numeri random con media nulla e varianza=0.5
R= zeros (1,nnodi,a);
R = normrnd(0,0.5,1,nnodi,a);

%%%%%%%%%%%%%%%%%%%%%%%%%%%%%%%%%%%%%%%%%%%%%%%%%%%%%%%%%%%%%%%%%%%%%%%%

%generazione delle storie di vento
Y=zeros(nnodi,nnodi,a);

%Matrici delle time history di vento Vx
Wvel0=zeros(b,nnodi,nnodi);%matrice dei processi somma degli Y (vedi Di Paola)


Wvel=zeros(nnodi,b); %matrice delle velocità turbolente
Wvel1=zeros(nnodi,b);%matrice delle velocità totali
Wvel2=zeros(nnodi,b+1); %per mettere matrice delle velocità turbolente in formato ANSYS

for s=1:1:b
for i=1:1:nnodi
for j=1:1:a
    Y(:,i,j)=2*(autovalori(i,i,j)*dw)^0.5*((autovettori(:,i,j)*R(1,i,j)))*cos(w(j)*dt*s);
end
end

for i=1:1:nnodi
for j=1:1:nnodi
  Wvel0(s,i,j)=sum(Y(j,i,:));
end
end
c=s/b*100; %contatore del processo
end

for s=1:1:b
for j=1:1:nnodi
    Wvel(j,s)=sum(Wvel0(s,:,j));
end
end

for n=1:nnodi
```

```
    Wvel2(n,1)=n;
  for s=2:1:b+1

    Wvel2(n,s)=Wvel(n,s-1);  %per mettere matrice delle velocità turbolente in formato ANSYS
end
end

Wvel3=zeros((nnodi+1)*(b+1),1); %matrice delle velocità turbolente in formato ANSYS

for s=2:1:b
    Wvel3(s,1)=t(s-1,1);
End

for j=2:1:nnodi+1
for s=1:1:b+1
Wvel3(s+(j-1)*b+j,1)=Wvel2(j-1,s);
end
end

llll=1;
for j=1:b+1:(b+2)*nnodi
    Wvel3(j,1)=llll;
    llll=llll+1;
end

MeanW=zeros(numgirate,1);
MeanW(run,1)=mean(Wvel(midpoint,:));

save('Wvel.dat','Wvel3','-ascii')

Svvwadim=zeros(nnodi,a); %matrice la cui colonna i-esima contiene gli autospettri alla frequenza "i" adimensionalizzati

for s=1:1:a
 for j=1:1:nnodi
   Svvwadim(j,s)=f(1,s)*Svvwfreq(j,j,s);
 end
 end

%PSD di Wvel1
[Pw1w1,freq]=periodogram(Wvel(1,:),[]);%PSD calcolato con periodogramma di u1_POD

 for j=1:1:length(Pw1w1)
   Pw1w1adim(j,1)=freq(j,1)*Pw1w1(j,1);
 end

end %fine ciclo GLOBALE (numgirate)
```

B.2.ANSYS code for the Finite Element analysis of a long span suspension bridge under turbulent wind action.

I what follow, the ASYS code of the case study bridge Finite Element Analysis is reported. It is important to outline that the model has been written and refined from various authors, during the researches conducted on this bridge between the years from 2003 to 2008 from the Professor Franco Bontempi research group. The main contribute of the present author to the code concerns only a short part regarding the aeroelastic forces computation. This part has been outlined by using the bold style and has been evidenced in the following code.

```
!Modello per l'analisi del Ponte sullo Stretto di Messina sotto l'azione del vento

Autori: Prof. Franco Bontempi e collaboratori


!Caratteristiche del modello:
!Peso proprio definito con densità dei materiali
!Carichi permanenti assegnati con comando "ADDMASS"
!carichi permanenti sui traversi assegnati come masse concentrate alle estremità (MASS21)

/CONFIG,NRES,100000
/NERR,,1000000

/TITLE,ANALISI DINAMICA VENTO MEDIO 45 m/s SOLO CASSONE FERROVIARIO (Modello PG04_CL)
/PREP7

---------------------------------------
!Definizione dei TEMPI--
!---------------------------------
T_TI=400    !Durata del Transitorio Iniziale
T_VENTO=3000        !Durata della raffica di Vento
T_incs=0.05         !Passo di integrazione durante la raffica di Vento
T_inc=2         !Passo di integrazione prima della raffica di Vento
T_TIV=180           !Durata del transitorio iniziale del vento

FRT=2           !Frequenza scrittura risultati transitorio iniziale (in passi)
FRV=10              !Frequenza scrittura risultati raffica vento (in passi)

!-----------------------------------------------------
!Grandezza caratteristica d'impalcato--------
!-----------------------------------------------------

B=60.4
!-----------------------------------------------------
!Definizione dello SMORZAMENTO ALLA RAYLAYGH-
!-----------------------------------------------------
!fase transitotia iniziale Smorzamento alla struttura del 95 %

BTI=3.051412253     !Smorzamento alla matrice di rigidezza (I e II modo di vibrare)
```

```
ATI=0.268235302     !Smorzamento alla matrice delle masse (I e II modo di vibrare)

!-----------------------------------------------------
!fase dinamica Smorzamento alla struttura del 0.5 %

BD=0.013174784      !Smorzamento alla matrice di rigidezza (I e III modo di vibrare)
AD=0.001546814      !Smorzamento alla matrice delle masse (I e III modo di vibrare)

!-----------------------------------------------------
!Definizione dello Spessore gamba torre (Calcolo del Drag)----------
!-----------------------------------------------------
SG=16

!-----------------------------------------------------
!DEFINIZIONE DELL'ELEMENTO FRAME TRIDIMENSIONALE:

ET,1,BEAM4,,1
ET,2,MASS21,,,2
ET,3,LINK10
ET,4,CONTAC52

!-----------------------------------------------------
!MATERIALI

!PROPRIETA'DEL MATERIALE NUMERO 1 (Cassoni, Traversi, Gambe)
MP,EX,1,2.059e11,
MP,NUXY,1,0.25,
MP,ALPX,1,1.17E-5,
MP,DENS,1,7980,


!PROPRIETA'DEL MATERIALE NUMERO 2 (Cavi, Pendini)
MP,EX,2,1.863e11,
MP,NUXY,2,0.25,
MP,ALPX,2,1.17E-5,
MP,DENS,2,7980,

!-----------------------------------------------------

!DEFINIZIONE DELLE MASSE DEI CARICHI PERMANENTI SUI CASSONI STRADALI E FERROVIARI

PERMSTR=48900/30   !KG MASSA AL METRO LINEARE
PERMFERR=81000/30 !KG MASSA AL METRO LINEARE
```

```
!-----------------------------------------------------

!DESCRIZIONE DELLE CARATTERISTICHE DELLE SEZIONI (REAL):

! 1)SEZIONE DEL CAVO
R,1,2.02,1E-8
!---------------------------------------
! 2)SEZIONE PEAL(PENDINI)
R,2,0.0327,1E-8
!---------------------------------------
! 3)SEZIONE PEME (PENDINI)
R,3,0.0137,1E-8
!---------------------------------------
! 4)SEZIONE PECO(PENDINI)
R,4,0.0117,1E-8
!---------------------------------------
! 5)SEZIONE CASSTR (CASSONE STRADALE)
R,5,0.45,8.0787,0.3589,1 ,1 , ,

RMORE, ,1.1642, , , ,PERMSTR
!---------------------------------------
! 6)SEZIONE CASFER (CASSONE FERROVIARIO)
R,6,0.2996,2.4394,0.2245, 1,1 , ,

RMORE, ,0.6877 , , , ,PERMFERR
!---------------------------------------
! 7)SEZIONE TRAS (TRASVERSI)
R,7,0.3233,0.7629,0.6336, 1,1 , ,

RMORE, ,1.1344 , , , ,
!---------------------------------------
! 8)SEZIONE GAMBE (PILE)
R,8,8.4252,222.3904,131.5288,1,1 , ,

RMORE, ,52.941 , , , ,
!---------------------------------------
! 9)SEZIONE ORTORRI (TRASVERSI DELLE PILE)
R,9,1.9792,6.1036,67.2698,1,1 , ,

RMORE, ,13.9804 , , , ,
!---------------------------------------
! 11)SEZIONE FS1 (CAVALLETTO IN PROSSIMITA' DELL'ANCORAGGIO)
R,11,5,1.99,1.99,1 ,1 , ,

RMORE, ,3.98,0,0, ,
!---------------------------------
! 14)MASSE CONCENTRATE ALLE ESTREMITA' DEI TRAVERSI
R,14,1830
!---------------------------------
```

```
! 1111)SEZIONE GAP LONGITUDINALE DI 0.5m
R,1111,2E9,0.5
!----------------------------------
! 1112)SEZIONE GAP TRASVERSALE DI 0.3m
R,1112,2E9,0.3


!-----------------------------------------------------
! GEOMETRIA ------------------------------
!-----------------------------------------------------

!A)DEFINIZIONE DEI NODI NELLO SPAZIO DEL MODELLO (X;Y;Z):

N,1,-980.18,0,40.397                    ! Nodi cavo di destra
N,3,-960,0,53.5
N,7,-930,0,61.737
N,9,-900,0,70.094
N,11,-870,0,78.572
N,13,-840,0,87.17
N,15,-810,0,95.888
N,17,-780,0,104.73
N,19,-750,0,113.69
N,21,-720,0,122.77
N,23,-690,0,131.97
N,25,-660,0,141.29
N,27,-630,0,150.73
N,29,-600,0,160.3
N,31,-570,0,169.98
N,33,-540,0,179.79
N,35,-510,0,189.72
N,37,-480,0,199.77
N,39,-450,0,209.94
N,41,-420,0,220.24
N,43,-390,0,230.66
N,45,-360,0,241.2
N,47,-330,0,251.86
N,49,-300,0,262.65
N,51,-270,0,273.56
N,53,-240,0,284.59
N,55,-210,0,295.75
N,60,-180,0,306.9
N,65,-150,0,318.7
N,72,-120,0,330.48
N,79,-90,0,342.51
N,86,-60,0,354.76
N,88,-30,0,367
N,97,-8,0,376.59
N,167,0,0,380
N,169,8,0,377.05
N,178,30,0,369.2
N,185,60,0,358.76
N,192,90,0,348.44
N,199,120,0,338.31
N,206,150,0,328.39
N,213,180,0,318.65
N,220,210,0,309.12
N,227,240,0,299.78
N,234,270,0,290.63
N,241,300,0,281.69
N,248,330,0,272.94
N,255,360,0,264.38
N,262,390,0,256.03
N,269,420,0,247.87
N,276,450,0,239.9
N,283,480,0,232.14
N,290,510,0,224.57
N,297,540,0,217.19
N,304,570,0,210.01
N,311,600,0,203.03
N,318,630,0,196.25
N,325,660,0,189.66
N,332,690,0,183.27
N,339,720,0,177.08
N,346,750,0,171.08
N,353,780,0,165.28
N,360,810,0,159.68
N,367,840,0,154.27
N,374,870,0,149.06
N,381,900,0,144.05
N,388,930,0,139.23
N,395,960,0,134.61
N,402,990,0,130.18
N,409,1020,0,125.96
N,416,1050,0,121.93
N,423,1080,0,118.09
N,430,1110,0,114.45
N,437,1140,0,111.01
N,444,1170,0,107.77
N,451,1200,0,104.72
N,458,1230,0,101.87
N,465,1260,0,99.215
N,472,1290,0,96.757
N,479,1320,0,94.496
N,486,1350,0,92.431
N,493,1380,0,90.563
N,500,1410,0,88.892
N,507,1440,0,87.417
N,514,1470,0,86.139
N,521,1500,0,85.058
N,528,1530,0,84.173
N,535,1560,0,83.485
N,542,1590,0,82.993
N,549,1620,0,82.698
N,556,1650,0,82.6
N,563,1680,0,82.698
N,570,1710,0,82.993
N,577,1740,0,83.485
N,584,1770,0,84.173
N,591,1800,0,85.058
N,598,1830,0,86.139
N,605,1860,0,87.417
N,612,1890,0,88.892
N,619,1920,0,90.563
N,626,1950,0,92.431
N,633,1980,0,94.496
N,640,2010,0,96.757
N,647,2040,0,99.215
N,654,2070,0,101.87
N,661,2100,0,104.72
N,668,2130,0,107.77
N,675,2160,0,111.01
N,682,2190,0,114.45
N,689,2220,0,118.09
N,696,2250,0,121.93
N,703,2280,0,125.96
N,710,2310,0,130.18
N,717,2340,0,134.61
N,724,2370,0,139.23
N,731,2400,0,144.05
N,738,2430,0,149.06
N,745,2460,0,154.27
N,752,2490,0,159.68
N,759,2520,0,165.28
N,766,2550,0,171.08
N,773,2580,0,177.08
N,780,2610,0,183.27
N,787,2640,0,189.66
N,794,2670,0,196.25
N,801,2700,0,203.03
N,808,2730,0,210.01
N,815,2760,0,217.19
N,822,2790,0,224.57
N,829,2820,0,232.14
N,836,2850,0,239.9
N,843,2880,0,247.87
N,850,2910,0,256.03
N,857,2940,0,264.38
N,864,2970,0,272.94
N,871,3000,0,281.69
N,878,3030,0,290.63
N,885,3060,0,299.78
N,892,3090,0,309.12
N,899,3120,0,318.65
N,906,3150,0,328.39
N,913,3180,0,338.31
N,920,3210,0,348.44
N,927,3240,0,358.76
N,929,3270,0,369.2
N,938,3292,0,377.05
N,1008,3300,0,380
N,1010,3308,0,376.81
N,1019,3330,0,368.1
N,1026,3360,0,356.46
N,1033,3390,0,345.05
N,1040,3420,0,333.85
N,1042,3450,0,322.92
N,1049,3480,0,312
N,1052,3510,0,301.63
N,1054,3540,0,291.31
N,1056,3570,0,281.11
N,1058,3600,0,271.02
N,1060,3630,0,261.06
N,1062,3660,0,251.22
N,1064,3690,0,241.5
N,1066,3720,0,231.91
N,1068,3750,0,222.43
N,1070,3780,0,213.07
N,1072,3810,0,203.83
N,1074,3840,0,194.71
N,1076,3870,0,185.71
N,1078,3900,0,176.83
N,1080,3930,0,168.07
N,1082,3960,0,159.42
N,1084,3990,0,150.9
N,1086,4020,0,142.5
N,1088,4050,0,134.21
N,1090,4080,0,126.05
N,1094,4110,0,118
N,1096,4130.1,0,105.03
N,2,-980.18,52,40.397                   ! Nodi cavo sinistra
N,4,-960,52,53.5
N,8,-930,52,61.737
N,10,-900,52,70.094
N,12,-870,52,78.572
N,14,-840,52,87.17
N,16,-810,52,95.888
N,18,-780,52,104.73
N,20,-750,52,113.69
N,22,-720,52,122.77
N,24,-690,52,131.97
N,26,-660,52,141.29
N,28,-630,52,150.73
N,30,-600,52,160.3
N,32,-570,52,169.98
N,34,-540,52,179.79
N,36,-510,52,189.72
N,38,-480,52,199.77
N,40,-450,52,209.94
N,42,-420,52,220.24
N,44,-390,52,230.66
N,46,-360,52,241.2
N,48,-330,52,251.86
N,50,-300,52,262.65
N,52,-270,52,273.56
N,54,-240,52,284.59
N,56,-210,52,295.75
N,61,-180,52,306.9
N,66,-150,52,318.7
N,73,-120,52,330.48
N,80,-90,52,342.51
N,87,-60,52,354.76
N,89,-30,52,367
N,98,-8,52,376.59
```

N,168,0,52,380
N,170,8,52,377.05
N,179,30,52,369.2
N,186,60,52,358.76
N,193,90,52,348.44
N,200,120,52,338.31
N,207,150,52,328.39
N,214,180,52,318.65
N,221,210,52,309.12
N,228,240,52,299.78
N,235,270,52,290.63
N,242,300,52,281.69
N,249,330,52,272.94
N,256,360,52,264.38
N,263,390,52,256.03
N,270,420,52,247.87
N,277,450,52,239.9
N,284,480,52,232.14
N,291,510,52,224.57
N,298,540,52,217.19
N,305,570,52,210.01
N,312,600,52,203.03
N,319,630,52,196.25
N,326,660,52,189.66
N,333,690,52,183.27
N,340,720,52,177.08
N,347,750,52,171.08
N,354,780,52,165.28
N,361,810,52,159.68
N,368,840,52,154.27
N,375,870,52,149.06
N,382,900,52,144.05
N,389,930,52,139.23
N,396,960,52,134.61
N,403,990,52,130.18
N,410,1020,52,125.96
N,417,1050,52,121.93
N,424,1080,52,118.09
N,431,1110,52,114.45
N,438,1140,52,111.01
N,445,1170,52,107.77
N,452,1200,52,104.72
N,459,1230,52,101.87
N,466,1260,52,99.215
N,473,1290,52,96.757
N,480,1320,52,94.496
N,487,1350,52,92.431
N,494,1380,52,90.563
N,501,1410,52,88.892
N,508,1440,52,87.41
N,515,1470,52,86.139
N,522,1500,52,85.058
N,529,1530,52,84.173
N,536,1560,52,83.485
N,543,1590,52,82.993
N,550,1620,52,82.698
N,557,1650,52,82.6
N,564,1680,52,82.698
N,571,1710,52,82.993
N,578,1740,52,83.485
N,585,1770,52,84.173
N,592,1800,52,85.058
N,599,1830,52,86.139
N,606,1860,52,87.417
N,613,1890,52,88.892
N,620,1920,52,90.563
N,627,1950,52,92.431
N,634,1980,52,94.496
N,641,2010,52,96.757
N,648,2040,52,99.215
N,655,2070,52,101.87
N,662,2100,52,104.72
N,669,2130,52,107.77
N,676,2160,52,111.01
N,683,2190,52,114.45
N,690,2220,52,118.09
N,697,2250,52,121.93
N,704,2280,52,125.96
N,711,2310,52,130.18
N,718,2340,52,134.61
N,725,2370,52,139.23
N,732,2400,52,144.05
N,739,2430,52,149.06
N,746,2460,52,154.27
N,753,2490,52,159.68
N,760,2520,52,165.28
N,767,2550,52,171.08
N,774,2580,52,177.08
N,781,2610,52,183.27
N,788,2640,52,189.66
N,795,2670,52,196.25
N,802,2700,52,203.03
N,809,2730,52,210.01
N,816,2760,52,217.19
N,823,2790,52,224.57
N,830,2820,52,232.14
N,837,2850,52,239.9
N,844,2880,52,247.87
N,851,2910,52,256.03
N,858,2940,52,264.38
N,865,2970,52,272.94
N,872,3000,52,281.69
N,879,3030,52,290.63
N,886,3060,52,299.78
N,893,3090,52,309.12
N,900,3120,52,318.65
N,907,3150,52,328.39
N,914,3180,52,338.31
N,921,3210,52,348.44
N,928,3240,52,358.76
N,930,3270,52,369.2
N,939,3292,52,377.05
N,1009,3300,52,380
N,1011,3308,52,376.81
N,1020,3330,52,368.1
N,1027,3360,52,356.46
N,1034,3390,52,345.05
N,1041,3420,52,333.85
N,1043,3450,52,322.92
N,1050,3480,52,312
N,1053,3510,52,301.63
N,1055,3540,52,291.31
N,1057,3570,52,281.11
N,1059,3600,52,271.02
N,1061,3630,52,261.06
N,1063,3660,52,251.22
N,1065,3690,52,241.5
N,1067,3720,52,231.91
N,1069,3750,52,222.43
N,1071,3780,52,213.07
N,1073,3810,52,203.83
N,1075,3840,52,194.71
N,1077,3870,52,185.71
N,1079,3900,52,176.83
N,1081,3930,52,168.07
N,1083,3960,52,159.42
N,1085,3990,52,150.9
N,1087,4020,52,142.5
N,1089,4050,52,134.21
N,1091,4080,52,126.05
N,1095,4110,52,118
N,1097,4130.1,52,105.03
N,62,-167.1,6.575,52.65 !
Nodi cassone stradale di destra
N,68,-120,6.575,53.45
N,75,-90,6.575,53.795
N,82,-60,6.575,54.3
N,93,-30,6.575,54.824
N,116,0,6.575,55.4
N,174,30,6.575,56.047
N,181,60,6.575,56.763
N,188,90,6.575,57.427
N,195,120,6.575,58.081
N,202,150,6.575,58.724
N,209,180,6.575,59.355
N,216,210,6.575,59.976
N,223,240,6.575,60.585
N,230,270,6.575,61.184
N,237,300,6.575,61.771
N,244,330,6.575,62.347
N,251,360,6.575,62.912
N,258,390,6.575,63.467
N,265,420,6.575,64.01
N,272,450,6.575,64.542
N,279,480,6.575,65.063
N,286,510,6.575,65.573
N,293,540,6.575,66.072
N,300,570,6.575,66.56
N,307,600,6.575,67.036
N,314,630,6.575,67.502
N,321,660,6.575,67.957
N,328,690,6.575,68.4
N,335,720,6.575,68.833
N,342,750,6.575,69.255
N,349,780,6.575,69.665
N,356,810,6.575,70.064
N,363,840,6.575,70.453
N,370,870,6.575,70.83
N,377,900,6.575,71.196
N,384,930,6.575,71.552
N,391,960,6.575,71.896
N,398,990,6.575,72.229
N,405,1020,6.575,72.551
N,412,1050,6.575,72.862
N,419,1080,6.575,73.162
N,426,1110,6.575,73.451
N,433,1140,6.575,73.728
N,440,1170,6.575,73.995
N,447,1200,6.575,74.251
N,454,1230,6.575,74.496
N,461,1260,6.575,74.729
N,468,1290,6.575,74.952
N,475,1320,6.575,75.163
N,482,1350,6.575,75.364
N,489,1380,6.575,75.553
N,496,1410,6.575,75.731
N,503,1440,6.575,75.899
N,510,1470,6.575,76.055
N,517,1500,6.575,76.2
N,524,1530,6.575,76.334
N,531,1560,6.575,76.457
N,538,1590,6.575,76.569
N,545,1620,6.575,76.67
N,552,1650,6.575,76.76
N,559,1680,6.575,76.839
N,566,1710,6.575,76.907
N,573,1740,6.575,76.963
N,580,1770,6.575,77.009
N,587,1800,6.575,77.044
N,594,1830,6.575,77.067
N,601,1860,6.575,77.08
N,608,1890,6.575,77.081
N,615,1920,6.575,77.072
N,622,1950,6.575,77.051
N,629,1980,6.575,77.019
N,636,2010,6.575,76.976
N,643,2040,6.575,76.923
N,650,2070,6.575,76.858
N,657,2100,6.575,76.782
N,664,2130,6.575,76.695
N,671,2160,6.575,76.597
N,678,2190,6.575,76.488
N,685,2220,6.575,76.368
N,692,2250,6.575,76.236
N,699,2280,6.575,76.094
N,706,2310,6.575,75.941
N,713,2340,6.575,75.776
N,720,2370,6.575,75.601

```
N,727,2400,6.575,75.415
N,734,2430,6.575,75.217
N,741,2460,6.575,75.008
N,748,2490,6.575,74.789
N,755,2520,6.575,74.558
N,762,2550,6.575,74.316
N,769,2580,6.575,74.064
N,776,2610,6.575,73.8
N,783,2640,6.575,73.525
N,790,2670,6.575,73.239
N,797,2700,6.575,72.942
N,804,2730,6.575,72.634
N,811,2760,6.575,72.315
N,818,2790,6.575,71.984
N,825,2820,6.575,71.643
N,832,2850,6.575,71.291
N,839,2880,6.575,70.928
N,846,2910,6.575,70.553
N,853,2940,6.575,70.168
N,860,2970,6.575,69.771
N,867,3000,6.575,69.364
N,874,3030,6.575,68.945
N,881,3060,6.575,68.515
N,888,3090,6.575,68.075
N,895,3120,6.575,67.623
N,902,3150,6.575,67.16
N,909,3180,6.575,66.686
N,916,3210,6.575,66.201
N,923,3240,6.575,65.705
N,934,3270,6.575,65.173
N,957,3300,6.575,64.68
N,1015,3330,6.575,64.294
N,1022,3360,6.575,63.9
N,1029,3390,6.575,63.675
N,1036,3420,6.575,63.35
N,1044,3467.1,6.575,62.86
N,64,-167.1,45.425,52.65
!Nodi cassone stradale di sinistra
N,70,-120,45.425,53.45
N,77,-90,45.425,53.795
N,84,-60,45.425,54.3
N,95,-30,45.425,54.824
N,118,0,45.425,55.4
N,176,30,45.425,56.047
N,183,60,45.425,56.763
N,190,90,45.425,57.427
N,197,120,45.425,58.081
N,204,150,45.425,58.724
N,211,180,45.425,59.355
N,218,210,45.425,59.976
N,225,240,45.425,60.585
N,232,270,45.425,61.184
N,239,300,45.425,61.771
N,246,330,45.425,62.347
N,253,360,45.425,62.912
N,260,390,45.425,63.467
N,267,420,45.425,64.01
N,274,450,45.425,64.542
N,281,480,45.425,65.063
N,288,510,45.425,65.573
N,295,540,45.425,66.072
N,302,570,45.425,66.56
N,309,600,45.425,67.036
N,316,630,45.425,67.502
N,323,660,45.425,67.957
N,330,690,45.425,68.4
N,337,720,45.425,68.833
N,344,750,45.425,69.255
N,351,780,45.425,69.665
N,358,810,45.425,70.064
N,365,840,45.425,70.453
N,372,870,45.425,70.83
N,379,900,45.425,71.196
N,386,930,45.425,71.552
N,393,960,45.425,71.896
N,400,990,45.425,72.229
N,407,1020,45.425,72.551
N,414,1050,45.425,72.862
N,421,1080,45.425,73.162
N,428,1110,45.425,73.451
N,435,1140,45.425,73.728
N,442,1170,45.425,73.995
N,449,1200,45.425,74.251
N,456,1230,45.425,74.496
N,463,1260,45.425,74.729
N,470,1290,45.425,74.952
N,477,1320,45.425,75.163
N,484,1350,45.425,75.364
N,491,1380,45.425,75.553
N,498,1410,45.425,75.731
N,505,1440,45.425,75.899
N,512,1470,45.425,76.055
N,519,1500,45.425,76.2
N,526,1530,45.425,76.334
N,533,1560,45.425,76.457
N,540,1590,45.425,76.569
N,547,1620,45.425,76.67
N,554,1650,45.425,76.76
N,561,1680,45.425,76.839
N,568,1710,45.425,76.907
N,575,1740,45.425,76.963
N,582,1770,45.425,77.009
N,589,1800,45.425,77.044
N,596,1830,45.425,77.067
N,603,1860,45.425,77.08
N,610,1890,45.425,77.081
N,617,1920,45.425,77.072
N,624,1950,45.425,77.051
N,631,1980,45.425,77.019
N,638,2010,45.425,76.976
N,645,2040,45.425,76.923
N,652,2070,45.425,76.858
N,659,2100,45.425,76.782
N,666,2130,45.425,76.695
N,673,2160,45.425,76.597
N,680,2190,45.425,76.488
N,687,2220,45.425,76.368
N,694,2250,45.425,76.236
N,701,2280,45.425,76.094
N,708,2310,45.425,75.941
N,715,2340,45.425,75.776
N,722,2370,45.425,75.601
N,729,2400,45.425,75.415
N,736,2430,45.425,75.217
N,743,2460,45.425,75.008
N,750,2490,45.425,74.789
N,757,2520,45.425,74.558
N,764,2550,45.425,74.316
N,771,2580,45.425,74.064
N,778,2610,45.425,73.8
N,785,2640,45.425,73.525
N,792,2670,45.425,73.239
N,799,2700,45.425,72.942
N,806,2730,45.425,72.634
N,813,2760,45.425,72.315
N,820,2790,45.425,71.984
N,827,2820,45.425,71.643
N,834,2850,45.425,71.291
N,841,2880,45.425,70.928
N,848,2910,45.425,70.553
N,855,2940,45.425,70.168
N,862,2970,45.425,69.771
N,869,3000,45.425,69.364
N,876,3030,45.425,68.945
N,883,3060,45.425,68.515
N,890,3090,45.425,68.075
N,897,3120,45.425,67.623
N,904,3150,45.425,67.16
N,911,3180,45.425,66.686
N,918,3210,45.425,66.201
N,925,3240,45.425,65.705
N,936,3270,45.425,65.173
N,959,3300,45.425,64.68
N,1017,3330,45.425,64.294
N,1024,3360,45.425,63.9
N,1031,3390,45.425,63.675
N,1038,3420,45.425,63.35
N,1046,3467.1,45.425,62.86
N,57,-192.25,26,52.65
! Nodi cassone ferroviario
N,63,-167.1,26,52.65
N,69,-120,26,53.45
N,76,-90,26,53.795
N,83,-60,26,54.3
N,94,-30,26,54.824
N,117,0,26,55.4
N,175,30,26,56.047
N,182,60,26,56.763
N,189,90,26,57.427
N,196,120,26,58.081
N,203,150,26,58.724
N,210,180,26,59.355
N,217,210,26,59.976
N,224,240,26,60.585
N,231,270,26,61.184
N,238,300,26,61.771
N,245,330,26,62.347
N,252,360,26,62.912
N,259,390,26,63.467
N,266,420,26,64.01
N,273,450,26,64.542
N,280,480,26,65.063
N,287,510,26,65.573
N,294,540,26,66.072
N,301,570,26,66.56
N,308,600,26,67.036
N,315,630,26,67.502
N,322,660,26,67.957
N,329,690,26,68.4
N,336,720,26,68.833
N,343,750,26,69.255
N,350,780,26,69.665
N,357,810,26,70.064
N,364,840,26,70.453
N,371,870,26,70.83
N,378,900,26,71.196
N,385,930,26,71.552
N,392,960,26,71.896
N,399,990,26,72.229
N,406,1020,26,72.551
N,413,1050,26,72.862
N,420,1080,26,73.162
N,427,1110,26,73.451
N,434,1140,26,73.728
N,441,1170,26,73.995
N,448,1200,26,74.251
N,455,1230,26,74.496
N,462,1260,26,74.729
N,469,1290,26,74.952
N,476,1320,26,75.163
N,483,1350,26,75.364
N,490,1380,26,75.553
N,497,1410,26,75.731
N,504,1440,26,75.899
N,511,1470,26,76.055
N,518,1500,26,76.2
N,525,1530,26,76.334
N,532,1560,26,76.457
N,539,1590,26,76.569
N,546,1620,26,76.67
N,553,1650,26,76.76
N,560,1680,26,76.839
N,567,1710,26,76.907
N,574,1740,26,76.963
N,581,1770,26,77.009
N,588,1800,26,77.044
N,595,1830,26,77.067
N,602,1860,26,77.08
```

```
N,609,1890,26,77.081
N,616,1920,26,77.072
N,623,1950,26,77.051
N,630,1980,26,77.019
N,637,2010,26,76.976
N,644,2040,26,76.923
N,651,2070,26,76.858
N,658,2100,26,76.782
N,665,2130,26,76.695
N,672,2160,26,76.597
N,679,2190,26,76.488
N,686,2220,26,76.368
N,693,2250,26,76.236
N,700,2280,26,76.094
N,707,2310,26,75.941
N,714,2340,26,75.776
N,721,2370,26,75.601
N,728,2400,26,75.415
N,735,2430,26,75.217
N,742,2460,26,75.008
N,749,2490,26,74.789
N,756,2520,26,74.558
N,763,2550,26,74.316
N,770,2580,26,74.064
N,777,2610,26,73.8
N,784,2640,26,73.525
N,791,2670,26,73.239
N,798,2700,26,72.942
N,805,2730,26,72.634
N,812,2760,26,72.315
N,819,2790,26,71.984
N,826,2820,26,71.643
N,833,2850,26,71.291
N,840,2880,26,70.928
N,847,2910,26,70.553
N,854,2940,26,70.168
N,861,2970,26,69.771
N,868,3000,26,69.364
N,875,3030,26,68.945
N,882,3060,26,68.515
N,889,3090,26,68.075
N,896,3120,26,67.623
N,903,3150,26,67.16
N,910,3180,26,66.686
N,917,3210,26,66.201
N,924,3240,26,65.705
N,935,3270,26,65.173
N,958,3300,26,64.68
N,1016,3330,26,64.294
N,1023,3360,26,63.9
N,1030,3390,26,63.675
N,1037,3420,26,63.35
N,1045,3467.1,26,62.86
N,1051,3492.3,26,62.86
N,99,0,-13,0
 ! Nodi pila destra Sicilia
N,101,0,-12.793,6
N,103,0,-12.208,19.9
N,105,0,-11.624,30.55
N,107,0,-11.332,39
  N,111,0,-10.655,55.4
N,119,0,-10.455,70.6
N,121,0,-9.871,90.5
N,123,0,-9.2867,107.4
N,125,0,-8.7024,124.3
N,127,0,-8.1181,137.05
N,129,0,-7.8259,145.5
N,133,0,-7.5338,153.95
N,135,0,-6.9495,175
N,137,0,-6.3652,191.9
N,139,0,-5.7809,208.8
N,141,0,-5.1965,225.7
N,143,0,-4.6122,243.4
N,145,0,-4.3201,251.85
N,149,0,-4.0279,260.3
N,151,0,-3.4436,276.4
N,153,0,-2.8593,293.3
N,155,0,-2.275,310.2
N,157,0,-1.6907,327.1
N,159,0,-1.1064,349.8
N,161,0,-0.81423,358.25
N,165,0,-0.52207,366.7
N,100,0,65,0
 ! Nodi pila sinistra Sicilia
N,102,0,64.793,6
N,104,0,64.208,19.9
N,106,0,63.624,30.55
N,110,0,63.332,39
  N,112,0,62.655,55.4
N,120,0,62.455,70.6
N,122,0,61.871,90.5
N,124,0,61.287,107.4
N,126,0,60.702,124.3
N,128,0,60.118,137.05
N,132,0,59.824,145.5
N,134,0,59.534,153.95
N,136,0,58.949,175
N,138,0,58.365,191.9
N,140,0,57.781,208.8
N,142,0,57.197,225.7
N,144,0,56.612,243.4
N,148,0,56.32,251.85
N,150,0,56.028,260.3
N,152,0,55.444,276.4
N,154,0,54.859,293.3
N,156,0,54.275,310.2
N,158,0,53.691,327.1
N,160,0,53.106,349.8
N,164,0,52.814,358.25
N,166,0,52.522,366.7
N,940,3300,-13,0
 ! Nodi pila destra Calabria
N,942,3300,-12.793,6
N,944,3300,-12.208,22.9
N,946,3300,-11.624,39.8
N,948,3300,-11.332,48.25
  N,952,3300,-10.6804,64.68
N,960,3300,-10.455,73.6
N,962,3300,-9.871,90.5
N,964,3300,-9.2867,107.4
N,966,3300,-8.7024,124.3
N,968,3300,-8.1181,137.05
N,970,3300,-7.8259,145.5
N,974,3300,-7.5338,153.95
N,976,3300,-6.9495,175
N,978,3300,-6.3652,191.9
N,980,3300,-5.7809,208.8
N,982,3300,-5.1965,225.7
N,984,3300,-4.6122,243.4
N,986,3300,-4.3201,251.85
N,990,3300,-4.0279,260.3
N,992,3300,-3.4436,276.4
N,994,3300,-2.8593,293.3
N,996,3300,-2.275,310.2
N,998,3300,-1.6907,327.1
N,1000,3300,-1.1064,349.8
N,1002,3300,-0.81423,358.25
N,1006,3300,-0.52207,366.7
N,941,3300,65,0
 ! Nodi pila sinistra Calabria
N,943,3300,64.793,6
N,945,3300,64.208,22.9
N,947,3300,63.624,39.8
N,951,3300,63.332,48.25
  N,953,3300,62.8146,64.68
N,961,3300,62.455,73.6
N,963,3300,61.871,90.5
N,965,3300,61.287,107.4
N,967,3300,60.702,124.3
N,969,3300,60.118,137.05
N,973,3300,59.824,145.5
N,975,3300,59.534,153.95
N,977,3300,58.949,175
N,979,3300,58.365,191.9
N,981,3300,57.781,208.8
N,983,3300,57.197,225.7
N,985,3300,56.612,243.4
N,989,3300,56.32,251.85
N,991,3300,56.028,260.3
N,993,3300,55.444,276.4
N,995,3300,54.859,293.3
N,997,3300,54.275,310.2
N,999,3300,53.691,327.1
N,1001,3300,53.106,349.8
N,1005,3300,52.814,358.25
N,1007,3300,52.522,366.7
N,67,-120,0,53.45
 ! Nodi trasversi destra
N,74,-90,0,53.795
N,81,-60,0,54.3
N,92,-30,0,54.824
N,90,0,0,55.4
N,173,30,0,56.047
N,180,60,0,56.763
N,187,90,0,57.427
N,194,120,0,58.081
N,201,150,0,58.724
N,208,180,0,59.355
N,215,210,0,59.976
N,222,240,0,60.585
N,229,270,0,61.184
N,236,300,0,61.771
N,243,330,0,62.347
N,250,360,0,62.912
N,257,390,0,63.467
N,264,420,0,64.01
N,271,450,0,64.542
N,278,480,0,65.063
N,285,510,0,65.573
N,292,540,0,66.072
N,299,570,0,66.56
N,306,600,0,67.036
N,313,630,0,67.502
N,320,660,0,67.957
N,327,690,0,68.4
N,334,720,0,68.833
N,341,750,0,69.255
N,348,780,0,69.665
N,355,810,0,70.064
N,362,840,0,70.453
N,369,870,0,70.83
N,376,900,0,71.196
N,383,930,0,71.552
N,390,960,0,71.896
N,397,990,0,72.229
N,404,1020,0,72.551
N,411,1050,0,72.862
N,418,1080,0,73.162
N,425,1110,0,73.451
N,432,1140,0,73.728
N,439,1170,0,73.995
N,446,1200,0,74.251
N,453,1230,0,74.496
N,460,1260,0,74.729
N,467,1290,0,74.952
N,474,1320,0,75.163
N,481,1350,0,75.364
N,488,1380,0,75.553
N,495,1410,0,75.731
N,502,1440,0,75.899
N,509,1470,0,76.055
N,516,1500,0,76.2
N,523,1530,0,76.334
N,530,1560,0,76.457
N,537,1590,0,76.569
N,544,1620,0,76.67
N,551,1650,0,76.76
N,558,1680,0,76.839
```

```
N,565,1710,0,76.907
N,572,1740,0,76.963
N,579,1770,0,77.009
N,586,1800,0,77.044
N,593,1830,0,77.067
N,600,1860,0,77.08
N,607,1890,0,77.081
N,614,1920,0,77.072
N,621,1950,0,77.051
N,628,1980,0,77.019
N,635,2010,0,76.976
N,642,2040,0,76.923
N,649,2070,0,76.858
N,656,2100,0,76.782
N,663,2130,0,76.695
N,670,2160,0,76.597
N,677,2190,0,76.488
N,684,2220,0,76.368
N,691,2250,0,76.236
N,698,2280,0,76.094
N,705,2310,0,75.941
N,712,2340,0,75.776
N,719,2370,0,75.601
N,726,2400,0,75.415
N,733,2430,0,75.217
N,740,2460,0,75.008
N,747,2490,0,74.789
N,754,2520,0,74.558
N,761,2550,0,74.316
N,768,2580,0,74.064
N,775,2610,0,73.8
N,782,2640,0,73.525
N,789,2670,0,73.239
N,796,2700,0,72.942
N,803,2730,0,72.634
N,810,2760,0,72.315
N,817,2790,0,71.984
N,824,2820,0,71.643
N,831,2850,0,71.291
N,838,2880,0,70.928
N,845,2910,0,70.553
N,852,2940,0,70.168
N,859,2970,0,69.771
N,866,3000,0,69.364
N,873,3030,0,68.945
N,880,3060,0,68.515
N,887,3090,0,68.075
N,894,3120,0,67.623
N,901,3150,0,67.16
N,908,3180,0,66.686
N,915,3210,0,66.201
N,922,3240,0,65.705
N,933,3270,0,65.173
N,931,3300,0,64.68
N,1014,3330,0,64.294
N,1021,3360,0,63.9
N,1028,3390,0,63.675
N,1035,3420,0,63.35
N,71,-120,52,53.45
! Nodi trasversi sinistra
N,78,-90,52,53.795
N,85,-60,52,54.3
N,96,-30,52,54.824
N,91,0,52,55.4
N,177,30,52,56.047
N,184,60,52,56.763
N,191,90,52,57.427
N,198,120,52,58.081
N,205,150,52,58.724
N,212,180,52,59.355
N,219,210,52,59.976
N,226,240,52,60.585
N,233,270,52,61.184
N,240,300,52,61.771
N,247,330,52,62.347
N,254,360,52,62.912
```

```
N,261,390,52,63.467
N,268,420,52,64.01
N,275,450,52,64.542
N,282,480,52,65.063
N,289,510,52,65.573
N,296,540,52,66.072
N,303,570,52,66.56
N,310,600,52,67.036
N,317,630,52,67.502
N,324,660,52,67.957
N,331,690,52,68.4
N,338,720,52,68.833
N,345,750,52,69.255
N,352,780,52,69.665
N,359,810,52,70.064
N,366,840,52,70.453
N,373,870,52,70.83
N,380,900,52,71.196
N,387,930,52,71.552
N,394,960,52,71.896
N,401,990,52,72.229
N,408,1020,52,72.551
N,415,1050,52,72.862
N,422,1080,52,73.162
N,429,1110,52,73.451
N,436,1140,52,73.728
N,443,1170,52,73.995
N,450,1200,52,74.251
N,457,1230,52,74.496
N,464,1260,52,74.729
N,471,1290,52,74.952
N,478,1320,52,75.163
N,485,1350,52,75.364
N,492,1380,52,75.553
N,499,1410,52,75.731
N,506,1440,52,75.899
N,513,1470,52,76.055
N,520,1500,52,76.2
N,527,1530,52,76.334
N,534,1560,52,76.457
N,541,1590,52,76.569
N,548,1620,52,76.67
N,555,1650,52,76.76
N,562,1680,52,76.839
N,569,1710,52,76.907
N,576,1740,52,76.963
N,583,1770,52,77.009
N,590,1800,52,77.044
N,597,1830,52,77.067
N,604,1860,52,77.08
N,611,1890,52,77.081
N,618,1920,52,77.072
N,625,1950,52,77.051
N,632,1980,52,77.019
N,639,2010,52,76.976
N,646,2040,52,76.923
N,653,2070,52,76.858
N,660,2100,52,76.782
N,667,2130,52,76.695
N,674,2160,52,76.597
N,681,2190,52,76.488
N,688,2220,52,76.368
N,695,2250,52,76.236
N,702,2280,52,76.094
N,709,2310,52,75.941
N,716,2340,52,75.776
N,723,2370,52,75.601
N,730,2400,52,75.415
N,737,2430,52,75.217
N,744,2460,52,75.008
N,751,2490,52,74.789
N,758,2520,52,74.558
N,765,2550,52,74.316
N,772,2580,52,74.064
N,779,2610,52,73.8
N,786,2640,52,73.525
```

```
N,793,2670,52,73.239
N,800,2700,52,72.942
N,807,2730,52,72.634
N,814,2760,52,72.315
N,821,2790,52,71.984
N,828,2820,52,71.643
N,835,2850,52,71.291
N,842,2880,52,70.928
N,849,2910,52,70.553
N,856,2940,52,70.168
N,863,2970,52,69.771
N,870,3000,52,69.364
N,877,3030,52,68.945
N,884,3060,52,68.515
N,891,3090,52,68.075
N,898,3120,52,67.623
N,905,3150,52,67.16
N,912,3180,52,66.686
N,919,3210,52,66.201
N,926,3240,52,65.705
N,937,3270,52,65.173
N,932,3300,52,64.68
N,1018,3330,52,64.294
N,1025,3360,52,63.9
N,1032,3390,52,63.675
N,1039,3420,52,63.35
N,171,0,0,145.5
! Nodi traversi torri Sicilia
N,108,0,13.556,39
N,130,0,14.724,145.5
N,146,0,15.893,251.85
N,162,0,17.062,358.25
N,172,0,52,145.5
N,109,0,38.444,39
N,131,0,37.274,145.5
N,147,0,36.107,251.85
N,163,0,34.938,358.25
N,1012,3300,0,145.5
N,949,3300,13.556,48.25
! Nodi traversi torri Calabria
N,971,3300,14.724,145.5
N,987,3300,15.893,251.85
N,1003,3300,17.062,358.25
N,950,3300,38.444,48.25
N,972,3300,37.274,145.5
N,988,3300,36.107,251.85
N,1004,3300,34.938,358.25
N,1013,3300,52,145.5
N,5,-957.93,0,48.871
 ! Nodi FS1
N,6,-957.93,52,48.871
N,1092,4108.1,0,113.6
N,1093,4108.1,52,113.6
N,58,-183,0,62.977
! Nodi di attacco dei pendini a terra
N,59,-183,52,62.977
N,1047,3483,0,62.977
N,1048,3483,52,62.977

N,1102,-10,45.425,55.1335
! Nuovi Nodi sull'impalcato
N,1103,-10,26,55.1335
N,1104,-10,6.575,55.1335
N,1107,10,45.425,55.6866
N,1108,10,26,55.6866
N,1109,10,6.575,55.6866
N,1112,3290,45.425,64.9391
N,1113,3290,26,64.9391
N,1114,3290,6.575,64.9391
N,1117,3310,45.425,64.4235
N,1118,3310,26,64.4235
N,1119,3310,6.575,64.4235
N,1121,0,54,55.4
! Nuovi Nodi alla fine dei traversi
N,1122,0,-2,55.4
N,1123,3300,54,64.68
```

```
N,1124,3300,-2,64.68
N,1125,0,16.2875,39
! Nuovi Nodi per vincoli longitudinali
N,1126,-2,16.2875,39
N,1127,-2,16.2875,55.4
N,1128,0,16.2875,55.4
N,1129,0,35.7125,39
N,1130,-2,35.7125,39
N,1131,-2,35.7125,55.4
N,1132,0,35.7125,55.4
N,1133,3300,16.2875,48.25
N,1134,3302,16.2875,48.25
N,1135,3302,16.2875,64.68
N,1136,3300,16.2875,64.68
N,1137,3300,35.7125,48.25
N,1138,3302,35.7125,48.25
N,1139,3302,35.7125,64.68
N,1140,3300,35.7125,64.68

!FINE INSERIMENTO DEI NODI

!------------------------------------------------------
!CAMBIO VISTA ISO AL MODELLO

/VIEW,1,0,0,1
/VUP,1,Z
/REPLOT
/VIEW,1,1,1,1
/ANG,1
/REP,FAST

!------------------------------------------------------
!ASSEGNAZIONE DELLE SEZIONI E DEL MATERIALE AGLI ELEMENTI

TYPE,3      !CAVO
REAL,1
MAT,2
E,      3       ,       1
E,      4       ,       2
E,      3       ,       7
E,      4       ,       8
E,      7       ,       9
E,      8       ,       10
E,      9       ,       11
E,      10      ,       12
E,      11      ,       13
E,      12      ,       14
E,      13      ,       15
E,      14      ,       16
E,      15      ,       17
E,      16      ,       18
E,      17      ,       19
E,      18      ,       20
E,      19      ,       21
E,      20      ,       22
E,      21      ,       23
E,      22      ,       24
E,      23      ,       25
E,      24      ,       26
E,      25      ,       27
E,      26      ,       28
E,      27      ,       29
E,      28      ,       30
E,      29      ,       31
E,      30      ,       32
E,      31      ,       33
E,      32      ,       34
E,      33      ,       35
E,      34      ,       36
E,      35      ,       37
E,      36      ,       38
E,      37      ,       39
E,      38      ,       40
E,      39      ,       41
E,      40      ,       42
E,      41      ,       43
E,      42      ,       44
E,      43      ,       45
E,      44      ,       46
E,      45      ,       47
E,      46      ,       48
E,      47      ,       49
E,      48      ,       50
E,      49      ,       51
E,      50      ,       52
E,      51      ,       53
E,      52      ,       54
E,      53      ,       55
E,      54      ,       56
E,      55      ,       60
E,      56      ,       61
E,      60      ,       65
E,      61      ,       66
E,      65      ,       72
E,      66      ,       73
E,      72      ,       79
E,      73      ,       80
E,      79      ,       86
E,      80      ,       87
E,      86      ,       88
E,      87      ,       89
E,      88      ,       97
E,      89      ,       98
E,      97      ,       167
E,      98      ,       168
E,      167     ,       169
E,      168     ,       170
E,      169     ,       178
E,      170     ,       179
E,      178     ,       185
E,      179     ,       186
E,      185     ,       192
E,      186     ,       193
E,      192     ,       199
E,      193     ,       200
E,      199     ,       206
E,      200     ,       207
E,      206     ,       213
E,      207     ,       214
E,      213     ,       220
E,      214     ,       221
E,      220     ,       227
E,      221     ,       228
E,      227     ,       234
E,      228     ,       235
E,      234     ,       241
E,      235     ,       242
E,      241     ,       248
E,      242     ,       249
E,      248     ,       255
E,      249     ,       256
E,      255     ,       262
E,      256     ,       263
E,      262     ,       269
E,      263     ,       270
E,      269     ,       276
E,      270     ,       277
E,      276     ,       283
E,      277     ,       284
E,      283     ,       290
E,      284     ,       291
E,      290     ,       297
E,      291     ,       298
E,      297     ,       304
E,      298     ,       305
E,      304     ,       311
E,      305     ,       312
E,      311     ,       318
E,      312     ,       319
E,      318     ,       325
E,      319     ,       326
E,      325     ,       332
E,      326     ,       333
E,      332     ,       339
E,      333     ,       340
E,      339     ,       346
E,      340     ,       347
E,      346     ,       353
E,      347     ,       354
E,      353     ,       360
E,      354     ,       361
E,      360     ,       367
E,      361     ,       368
E,      367     ,       374
E,      368     ,       375
E,      374     ,       381
E,      375     ,       382
E,      381     ,       388
E,      382     ,       389
E,      388     ,       395
E,      389     ,       396
E,      395     ,       402
E,      396     ,       403
E,      402     ,       409
E,      403     ,       410
E,      409     ,       416
E,      410     ,       417
E,      416     ,       423
E,      417     ,       424
E,      423     ,       430
E,      424     ,       431
E,      430     ,       437
E,      431     ,       438
E,      437     ,       444
E,      438     ,       445
E,      444     ,       451
E,      445     ,       452
E,      451     ,       458
E,      452     ,       459
E,      458     ,       465
E,      459     ,       466
E,      465     ,       472
E,      466     ,       473
E,      472     ,       479
E,      473     ,       480
E,      479     ,       486
E,      480     ,       487
E,      486     ,       493
E,      487     ,       494
E,      493     ,       500
E,      494     ,       501
E,      500     ,       507
E,      501     ,       508
E,      507     ,       514
E,      508     ,       515
E,      514     ,       521
E,      515     ,       522
E,      521     ,       528
E,      522     ,       529
E,      528     ,       535
E,      529     ,       536
E,      535     ,       542
E,      536     ,       543
E,      542     ,       549
E,      543     ,       550
E,      549     ,       556
E,      550     ,       557
E,      556     ,       563
E,      557     ,       564
E,      563     ,       570
E,      564     ,       571
E,      570     ,       577
E,      571     ,       578
E,      577     ,       584
E,      578     ,       585
E,      584     ,       591
E,      585     ,       592
```

```
E,    591   ,   598
E,    592   ,   599
E,    598   ,   605
E,    599   ,   606
E,    605   ,   612
E,    606   ,   613
E,    612   ,   619
E,    613   ,   620
E,    619   ,   626
E,    620   ,   627
E,    626   ,   633
E,    627   ,   634
E,    633   ,   640
E,    634   ,   641
E,    640   ,   647
E,    641   ,   648
E,    647   ,   654
E,    648   ,   655
E,    654   ,   661
E,    655   ,   662
E,    661   ,   668
E,    662   ,   669
E,    668   ,   675
E,    669   ,   676
E,    675   ,   682
E,    676   ,   683
E,    682   ,   689
E,    683   ,   690
E,    689   ,   696
E,    690   ,   697
E,    696   ,   703
E,    697   ,   704
E,    703   ,   710
E,    704   ,   711
E,    710   ,   717
E,    711   ,   718
E,    717   ,   724
E,    718   ,   725
E,    724   ,   731
E,    725   ,   732
E,    731   ,   738
E,    732   ,   739
E,    738   ,   745
E,    739   ,   746
E,    745   ,   752
E,    746   ,   753
E,    752   ,   759
E,    753   ,   760
E,    759   ,   766
E,    760   ,   767
E,    766   ,   773
E,    767   ,   774
E,    773   ,   780
E,    774   ,   781
E,    780   ,   787
E,    781   ,   788
E,    787   ,   794
E,    788   ,   795
E,    794   ,   801
E,    795   ,   802
E,    801   ,   808
E,    802   ,   809
E,    808   ,   815
E,    809   ,   816
E,    815   ,   822
E,    816   ,   823
E,    822   ,   829
E,    823   ,   830
E,    829   ,   836
E,    830   ,   837
E,    836   ,   843
E,    837   ,   844
E,    843   ,   850
E,    844   ,   851
E,    850   ,   857
E,    851   ,   858
```

```
E,    857   ,   864
E,    858   ,   865
E,    864   ,   871
E,    865   ,   872
E,    871   ,   878
E,    872   ,   879
E,    878   ,   885
E,    879   ,   886
E,    885   ,   892
E,    886   ,   893
E,    892   ,   899
E,    893   ,   900
E,    899   ,   906
E,    900   ,   907
E,    906   ,   913
E,    907   ,   914
E,    913   ,   920
E,    914   ,   921
E,    920   ,   927
E,    921   ,   928
E,    927   ,   929
E,    928   ,   930
E,    929   ,   938
E,    930   ,   939
E,    938   ,   1008
E,    939   ,   1009
E,    1008  ,   1010
E,    1009  ,   1011
E,    1010  ,   1019
E,    1011  ,   1020
E,    1019  ,   1026
E,    1020  ,   1027
E,    1026  ,   1033
E,    1027  ,   1034
E,    1033  ,   1040
E,    1034  ,   1041
E,    1040  ,   1042
E,    1041  ,   1043
E,    1042  ,   1049
E,    1043  ,   1050
E,    1049  ,   1052
E,    1050  ,   1053
E,    1052  ,   1054
E,    1053  ,   1055
E,    1054  ,   1056
E,    1055  ,   1057
E,    1056  ,   1058
E,    1057  ,   1059
E,    1058  ,   1060
E,    1059  ,   1061
E,    1060  ,   1062
E,    1061  ,   1063
E,    1062  ,   1064
E,    1063  ,   1065
E,    1064  ,   1066
E,    1065  ,   1067
E,    1066  ,   1068
E,    1067  ,   1069
E,    1068  ,   1070
E,    1069  ,   1071
E,    1070  ,   1072
E,    1071  ,   1073
E,    1072  ,   1074
E,    1073  ,   1075
E,    1074  ,   1076
E,    1075  ,   1077
E,    1076  ,   1078
E,    1077  ,   1079
E,    1078  ,   1080
E,    1079  ,   1081
E,    1080  ,   1082
E,    1081  ,   1083
E,    1082  ,   1084
E,    1083  ,   1085
E,    1084  ,   1086
E,    1085  ,   1087
```

```
E,    1086  ,   1088
E,    1087  ,   1089
E,    1088  ,   1090
E,    1089  ,   1091
E,    1090  ,   1094
E,    1091  ,   1095
E,    1094  ,   1096
E,    1095  ,   1097

TYPE,3    !PENDINI ALTI
REAL,2
MAT,2

E,    58    ,   60
E,    59    ,   61
E,    67    ,   72
E,    71    ,   73
E,    74    ,   79
E,    78    ,   80
E,    81    ,   86
E,    85    ,   87
E,    92    ,   88
E,    96    ,   89
E,    173   ,   178
E,    177   ,   179
E,    180   ,   185
E,    184   ,   186
E,    187   ,   192
E,    191   ,   193
E,    194   ,   199
E,    198   ,   200
E,    201   ,   206
E,    205   ,   207
E,    901   ,   906
E,    905   ,   907
E,    908   ,   913
E,    912   ,   914
E,    915   ,   920
E,    919   ,   921
E,    922   ,   927
E,    926   ,   928
E,    933   ,   929
E,    937   ,   930
E,    1014  ,   1019
E,    1018  ,   1020
E,    1021  ,   1026
E,    1025  ,   1027
E,    1028  ,   1033
E,    1032  ,   1034
E,    1035  ,   1040
E,    1039  ,   1041
E,    1047  ,   1049
E,    1048  ,   1050

TYPE,3    !PENDINI MEDI
REAL,3
MAT,2

E,    208   ,   213
E,    212   ,   214
E,    215   ,   220
E,    219   ,   221
E,    222   ,   227
E,    226   ,   228
E,    229   ,   234
E,    233   ,   235
E,    236   ,   241
E,    240   ,   242
E,    243   ,   248
E,    247   ,   249
E,    250   ,   255
E,    254   ,   256
E,    257   ,   262
E,    261   ,   263
E,    264   ,   269
E,    268   ,   270
```

```
E,  271  ,  276
E,  275  ,  277
E,  278  ,  283
E,  282  ,  284
E,  285  ,  290
E,  289  ,  291
E,  817  ,  822
E,  821  ,  823
E,  824  ,  829
E,  828  ,  830
E,  831  ,  836
E,  835  ,  837
E,  838  ,  843
E,  842  ,  844
E,  845  ,  850
E,  849  ,  851
E,  852  ,  857
E,  856  ,  858
E,  859  ,  864
E,  863  ,  865
E,  866  ,  871
E,  870  ,  872
E,  873  ,  878
E,  877  ,  879
E,  880  ,  885
E,  884  ,  886
E,  887  ,  892
E,  891  ,  893
E,  894  ,  899
E,  898  ,  900

TYPE,3    !PENDINI CORTI
REAL,4
MAT,2

E,  292  ,  297
E,  296  ,  298
E,  299  ,  304
E,  303  ,  305
E,  306  ,  311
E,  310  ,  312
E,  313  ,  318
E,  317  ,  319
E,  320  ,  325
E,  324  ,  326
E,  327  ,  332
E,  331  ,  333
E,  334  ,  339
E,  338  ,  340
E,  341  ,  346
E,  345  ,  347
E,  348  ,  353
E,  352  ,  354
E,  355  ,  360
E,  359  ,  361
E,  362  ,  367
E,  366  ,  368
E,  369  ,  374
E,  373  ,  375
E,  376  ,  381
E,  380  ,  382
E,  383  ,  388
E,  387  ,  389
E,  390  ,  395
E,  394  ,  396
E,  397  ,  402
E,  401  ,  403
E,  404  ,  409
E,  408  ,  410
E,  411  ,  416
E,  415  ,  417
E,  418  ,  423
E,  422  ,  424
E,  425  ,  430
E,  429  ,  431
E,  432  ,  437
E,  436  ,  438
E,  439  ,  444
E,  443  ,  445
E,  446  ,  451
E,  450  ,  452
E,  453  ,  458
E,  457  ,  459
E,  460  ,  465
E,  464  ,  466
E,  467  ,  472
E,  471  ,  473
E,  474  ,  479
E,  478  ,  480
E,  481  ,  486
E,  485  ,  487
E,  488  ,  493
E,  492  ,  494
E,  495  ,  500
E,  499  ,  501
E,  502  ,  507
E,  506  ,  508
E,  509  ,  514
E,  513  ,  515
E,  516  ,  521
E,  520  ,  522
E,  523  ,  528
E,  527  ,  529
E,  530  ,  535
E,  534  ,  536
E,  537  ,  542
E,  541  ,  543
E,  544  ,  549
E,  548  ,  550
E,  551  ,  556
E,  555  ,  557
E,  558  ,  563
E,  562  ,  564
E,  565  ,  570
E,  569  ,  571
E,  572  ,  577
E,  576  ,  578
E,  579  ,  584
E,  583  ,  585
E,  586  ,  591
E,  590  ,  592
E,  593  ,  598
E,  597  ,  599
E,  600  ,  605
E,  604  ,  606
E,  607  ,  612
E,  611  ,  613
E,  614  ,  619
E,  618  ,  620
E,  621  ,  626
E,  625  ,  627
E,  628  ,  633
E,  632  ,  634
E,  635  ,  640
E,  639  ,  641
E,  642  ,  647
E,  646  ,  648
E,  649  ,  654
E,  653  ,  655
E,  656  ,  661
E,  660  ,  662
E,  663  ,  668
E,  667  ,  669
E,  670  ,  675
E,  674  ,  676
E,  677  ,  682
E,  681  ,  683
E,  684  ,  689
E,  688  ,  690
E,  691  ,  696
E,  695  ,  697
E,  698  ,  703
E,  702  ,  704
E,  705  ,  710
E,  709  ,  711
E,  712  ,  717
E,  716  ,  718
E,  719  ,  724
E,  723  ,  725
E,  726  ,  731
E,  730  ,  732
E,  733  ,  738
E,  737  ,  739
E,  740  ,  745
E,  744  ,  746
E,  747  ,  752
E,  751  ,  753
E,  754  ,  759
E,  758  ,  760
E,  761  ,  766
E,  765  ,  767
E,  768  ,  773
E,  772  ,  774
E,  775  ,  780
E,  779  ,  781
E,  782  ,  787
E,  786  ,  788
E,  789  ,  794
E,  793  ,  795
E,  796  ,  801
E,  800  ,  802
E,  803  ,  808
E,  807  ,  809
E,  810  ,  815
E,  814  ,  816


TYPE,1    !CASSONE STRADALE
REAL,5
MAT,1

E,  62  ,  68
E,  64  ,  70
E,  68  ,  75
E,  70  ,  77
E,  75  ,  82
E,  77  ,  84
E,  82  ,  93
E,  84  ,  95
E,  93  ,  1104
!Modifica per inserire i pistono non lineari
E,  1104  ,  116
E,  95  ,  1102
E,  1102  ,  118
E,  116  ,  1109
E,  1109  ,  174
E,  118  ,  1107
E,  1107  ,  176
E,  174  ,  181
E,  176  ,  183
E,  181  ,  188
E,  183  ,  190
E,  188  ,  195
E,  190  ,  197
E,  195  ,  202
E,  197  ,  204
E,  202  ,  209
E,  204  ,  211
E,  209  ,  216
E,  211  ,  218
E,  216  ,  223
E,  218  ,  225
E,  223  ,  230
E,  225  ,  232
E,  230  ,  237
E,  232  ,  239
E,  237  ,  244
E,  239  ,  246
```

```
E,  244  ,  251
E,  246  ,  253
E,  251  ,  258
E,  253  ,  260
E,  258  ,  265
E,  260  ,  267
E,  265  ,  272
E,  267  ,  274
E,  272  ,  279
E,  274  ,  281
E,  279  ,  286
E,  281  ,  288
E,  286  ,  293
E,  288  ,  295
E,  293  ,  300
E,  295  ,  302
E,  300  ,  307
E,  302  ,  309
E,  307  ,  314
E,  309  ,  316
E,  314  ,  321
E,  316  ,  323
E,  321  ,  328
E,  323  ,  330
E,  328  ,  335
E,  330  ,  337
E,  335  ,  342
E,  337  ,  344
E,  342  ,  349
E,  344  ,  351
E,  349  ,  356
E,  351  ,  358
E,  356  ,  363
E,  358  ,  365
E,  363  ,  370
E,  365  ,  372
E,  370  ,  377
E,  372  ,  379
E,  377  ,  384
E,  379  ,  386
E,  384  ,  391
E,  386  ,  393
E,  391  ,  398
E,  393  ,  400
E,  398  ,  405
E,  400  ,  407
E,  405  ,  412
E,  407  ,  414
E,  412  ,  419
E,  414  ,  421
E,  419  ,  426
E,  421  ,  428
E,  426  ,  433
E,  428  ,  435
E,  433  ,  440
E,  435  ,  442
E,  440  ,  447
E,  442  ,  449
E,  447  ,  454
E,  449  ,  456
E,  454  ,  461
E,  456  ,  463
E,  461  ,  468
E,  463  ,  470
E,  468  ,  475
E,  470  ,  477
E,  475  ,  482
E,  477  ,  484
E,  482  ,  489
E,  484  ,  491
E,  489  ,  496
E,  491  ,  498
E,  496  ,  503
E,  498  ,  505
E,  503  ,  510
E,  505  ,  512
```

```
E,  510  ,  517
E,  512  ,  519
E,  517  ,  524
E,  519  ,  526
E,  524  ,  531
E,  526  ,  533
E,  531  ,  538
E,  533  ,  540
E,  538  ,  545
E,  540  ,  547
E,  545  ,  552
E,  547  ,  554
E,  552  ,  559
E,  554  ,  561
E,  559  ,  566
E,  561  ,  568
E,  566  ,  573
E,  568  ,  575
E,  573  ,  580
E,  575  ,  582
E,  580  ,  587
E,  582  ,  589
E,  587  ,  594
E,  589  ,  596
E,  594  ,  601
E,  596  ,  603
E,  601  ,  608
E,  603  ,  610
E,  608  ,  615
E,  610  ,  617
E,  615  ,  622
E,  617  ,  624
E,  622  ,  629
E,  624  ,  631
E,  629  ,  636
E,  631  ,  638
E,  636  ,  643
E,  638  ,  645
E,  643  ,  650
E,  645  ,  652
E,  650  ,  657
E,  652  ,  659
E,  657  ,  664
E,  659  ,  666
E,  664  ,  671
E,  666  ,  673
E,  671  ,  678
E,  673  ,  680
E,  678  ,  685
E,  680  ,  687
E,  685  ,  692
E,  687  ,  694
E,  692  ,  699
E,  694  ,  701
E,  699  ,  706
E,  701  ,  708
E,  706  ,  713
E,  708  ,  715
E,  713  ,  720
E,  715  ,  722
E,  720  ,  727
E,  722  ,  729
E,  727  ,  734
E,  729  ,  736
E,  734  ,  741
E,  736  ,  743
E,  741  ,  748
E,  743  ,  750
E,  748  ,  755
E,  750  ,  757
E,  755  ,  762
E,  757  ,  764
E,  762  ,  769
E,  764  ,  771
E,  769  ,  776
E,  771  ,  778
```

```
E,  776  ,  783
E,  778  ,  785
E,  783  ,  790
E,  785  ,  792
E,  790  ,  797
E,  792  ,  799
E,  797  ,  804
E,  799  ,  806
E,  804  ,  811
E,  806  ,  813
E,  811  ,  818
E,  813  ,  820
E,  818  ,  825
E,  820  ,  827
E,  825  ,  832
E,  827  ,  834
E,  832  ,  839
E,  834  ,  841
E,  839  ,  846
E,  841  ,  848
E,  846  ,  853
E,  848  ,  855
E,  853  ,  860
E,  855  ,  862
E,  860  ,  867
E,  862  ,  869
E,  867  ,  874
E,  869  ,  876
E,  874  ,  881
E,  876  ,  883
E,  881  ,  888
E,  883  ,  890
E,  888  ,  895
E,  890  ,  897
E,  895  ,  902
E,  897  ,  904
E,  902  ,  909
E,  904  ,  911
E,  909  ,  916
E,  911  ,  918
E,  916  ,  923
E,  918  ,  925
E,  923  ,  934
E,  925  ,  936
E,  934  ,  1114
!Modifica per inserire i pistoni non lineari
E,  1114  ,  957
E,  936  ,  1112
E,  1112  ,  959
E,  957  ,  1119
E,  1119  ,  1015
E,  959  ,  1117
E,  1117  ,  1017
E,  1015  ,  1022
E,  1017  ,  1024
E,  1022  ,  1029
E,  1024  ,  1031
E,  1029  ,  1036
E,  1031  ,  1038
E,  1036  ,  1044
E,  1038  ,  1046


TYPE,1  !CASSONE FERROVIARIO
REAL,6
MAT,1


E,  57  ,  63
E,  63  ,  69
E,  69  ,  76
E,  76  ,  83
E,  83  ,  94
E,  94  ,  1103
E,  1103  ,  117
E,  117  ,  1108
E,  1108  ,  175
```

```
E,  175 ,  182
E,  182 ,  189
E,  189 ,  196
E,  196 ,  203
E,  203 ,  210
E,  210 ,  217
E,  217 ,  224
E,  224 ,  231
E,  231 ,  238
E,  238 ,  245
E,  245 ,  252
E,  252 ,  259
E,  259 ,  266
E,  266 ,  273
E,  273 ,  280
E,  280 ,  287
E,  287 ,  294
E,  294 ,  301
E,  301 ,  308
E,  308 ,  315
E,  315 ,  322
E,  322 ,  329
E,  329 ,  336
E,  336 ,  343
E,  343 ,  350
E,  350 ,  357
E,  357 ,  364
E,  364 ,  371
E,  371 ,  378
E,  378 ,  385
E,  385 ,  392
E,  392 ,  399
E,  399 ,  406
E,  406 ,  413
E,  413 ,  420
E,  420 ,  427
E,  427 ,  434
E,  434 ,  441
E,  441 ,  448
E,  448 ,  455
E,  455 ,  462
E,  462 ,  469
E,  469 ,  476
E,  476 ,  483
E,  483 ,  490
E,  490 ,  497
E,  497 ,  504
E,  504 ,  511
E,  511 ,  518
E,  518 ,  525
E,  525 ,  532
E,  532 ,  539
E,  539 ,  546
E,  546 ,  553
E,  553 ,  560
E,  560 ,  567
E,  567 ,  574
E,  574 ,  581
E,  581 ,  588
E,  588 ,  595
E,  595 ,  602
E,  602 ,  609
E,  609 ,  616
E,  616 ,  623
E,  623 ,  630
E,  630 ,  637
E,  637 ,  644
E,  644 ,  651
E,  651 ,  658
E,  658 ,  665
E,  665 ,  672
E,  672 ,  679
E,  679 ,  686
E,  686 ,  693
E,  693 ,  700
E,  700 ,  707
```

```
E,  707 ,  714
E,  714 ,  721
E,  721 ,  728
E,  728 ,  735
E,  735 ,  742
E,  742 ,  749
E,  749 ,  756
E,  756 ,  763
E,  763 ,  770
E,  770 ,  777
E,  777 ,  784
E,  784 ,  791
E,  791 ,  798
E,  798 ,  805
E,  805 ,  812
E,  812 ,  819
E,  819 ,  826
E,  826 ,  833
E,  833 ,  840
E,  840 ,  847
E,  847 ,  854
E,  854 ,  861
E,  861 ,  868
E,  868 ,  875
E,  875 ,  882
E,  882 ,  889
E,  889 ,  896
E,  896 ,  903
E,  903 ,  910
E,  910 ,  917
E,  917 ,  924
E,  924 ,  935
E,  935 ,  1113
E,  1113 ,  958
E,  958 ,  1118
E,  1118 ,  1016
E,  1016 ,  1023
E,  1023 ,  1030
E,  1030 ,  1037
E,  1037 ,  1045
E,  1045 ,  1051

TYPE,1   !TRAVERSI DEI CASSONI
REAL,7
MAT,1

E,  62 ,  63
E,  63 ,  64
E,  67 ,  68
E,  68 ,  69
E,  69 ,  70
E,  70 ,  71
E,  74 ,  75
E,  75 ,  76
E,  76 ,  77
E,  77 ,  78
E,  81 ,  82
E,  82 ,  83
E,  83 ,  84
E,  84 ,  85
E,  92 ,  93
E,  93 ,  94
E,  94 ,  95
E,  95 ,  96
E,  90 ,  116
E,  116 ,  1128
E,  1128 ,  117
E,  117 ,  1132
E,  1132 ,  118
E,  118 ,  91
E,  173 ,  174
E,  174 ,  175
E,  175 ,  176
E,  176 ,  177
E,  180 ,  181
E,  181 ,  182
```

```
E,  182 ,  183
E,  183 ,  184
E,  187 ,  188
E,  188 ,  189
E,  189 ,  190
E,  190 ,  191
E,  194 ,  195
E,  195 ,  196
E,  196 ,  197
E,  197 ,  198
E,  201 ,  202
E,  202 ,  203
E,  203 ,  204
E,  204 ,  205
E,  208 ,  209
E,  209 ,  210
E,  210 ,  211
E,  211 ,  212
E,  215 ,  216
E,  216 ,  217
E,  217 ,  218
E,  218 ,  219
E,  222 ,  223
E,  223 ,  224
E,  224 ,  225
E,  225 ,  226
E,  229 ,  230
E,  230 ,  231
E,  231 ,  232
E,  232 ,  233
E,  236 ,  237
E,  237 ,  238
E,  238 ,  239
E,  239 ,  240
E,  243 ,  244
E,  244 ,  245
E,  245 ,  246
E,  246 ,  247
E,  250 ,  251
E,  251 ,  252
E,  252 ,  253
E,  253 ,  254
E,  257 ,  258
E,  258 ,  259
E,  259 ,  260
E,  260 ,  261
E,  264 ,  265
E,  265 ,  266
E,  266 ,  267
E,  267 ,  268
E,  271 ,  272
E,  272 ,  273
E,  273 ,  274
E,  274 ,  275
E,  278 ,  279
E,  279 ,  280
E,  280 ,  281
E,  281 ,  282
E,  285 ,  286
E,  286 ,  287
E,  287 ,  288
E,  288 ,  289
E,  292 ,  293
E,  293 ,  294
E,  294 ,  295
E,  295 ,  296
E,  299 ,  300
E,  300 ,  301
E,  301 ,  302
E,  302 ,  303
E,  306 ,  307
E,  307 ,  308
E,  308 ,  309
E,  309 ,  310
E,  313 ,  314
E,  314 ,  315
```

```
E,  315 ,  316
E,  316 ,  317
E,  320 ,  321
E,  321 ,  322
E,  322 ,  323
E,  323 ,  324
E,  327 ,  328
E,  328 ,  329
E,  329 ,  330
E,  330 ,  331
E,  334 ,  335
E,  335 ,  336
E,  336 ,  337
E,  337 ,  338
E,  341 ,  342
E,  342 ,  343
E,  343 ,  344
E,  344 ,  345
E,  348 ,  349
E,  349 ,  350
E,  350 ,  351
E,  351 ,  352
E,  355 ,  356
E,  356 ,  357
E,  357 ,  358
E,  358 ,  359
E,  362 ,  363
E,  363 ,  364
E,  364 ,  365
E,  365 ,  366
E,  369 ,  370
E,  370 ,  371
E,  371 ,  372
E,  372 ,  373
E,  376 ,  377
E,  377 ,  378
E,  378 ,  379
E,  379 ,  380
E,  383 ,  384
E,  384 ,  385
E,  385 ,  386
E,  386 ,  387
E,  390 ,  391
E,  391 ,  392
E,  392 ,  393
E,  393 ,  394
E,  397 ,  398
E,  398 ,  399
E,  399 ,  400
E,  400 ,  401
E,  404 ,  405
E,  405 ,  406
E,  406 ,  407
E,  407 ,  408
E,  411 ,  412
E,  412 ,  413
E,  413 ,  414
E,  414 ,  415
E,  418 ,  419
E,  419 ,  420
E,  420 ,  421
E,  421 ,  422
E,  425 ,  426
E,  426 ,  427
E,  427 ,  428
E,  428 ,  429
E,  432 ,  433
E,  433 ,  434
E,  434 ,  435
E,  435 ,  436
E,  439 ,  440
E,  440 ,  441
E,  441 ,  442
E,  442 ,  443
E,  446 ,  447
E,  447 ,  448
```

```
E,  448 ,  449
E,  449 ,  450
E,  453 ,  454
E,  454 ,  455
E,  455 ,  456
E,  456 ,  457
E,  460 ,  461
E,  461 ,  462
E,  462 ,  463
E,  463 ,  464
E,  467 ,  468
E,  468 ,  469
E,  469 ,  470
E,  470 ,  471
E,  474 ,  475
E,  475 ,  476
E,  476 ,  477
E,  477 ,  478
E,  481 ,  482
E,  482 ,  483
E,  483 ,  484
E,  484 ,  485
E,  488 ,  489
E,  489 ,  490
E,  490 ,  491
E,  491 ,  492
E,  495 ,  496
E,  496 ,  497
E,  497 ,  498
E,  498 ,  499
E,  502 ,  503
E,  503 ,  504
E,  504 ,  505
E,  505 ,  506
E,  509 ,  510
E,  510 ,  511
E,  511 ,  512
E,  512 ,  513
E,  516 ,  517
E,  517 ,  518
E,  518 ,  519
E,  519 ,  520
E,  523 ,  524
E,  524 ,  525
E,  525 ,  526
E,  526 ,  527
E,  530 ,  531
E,  531 ,  532
E,  532 ,  533
E,  533 ,  534
E,  537 ,  538
E,  538 ,  539
E,  539 ,  540
E,  540 ,  541
E,  544 ,  545
E,  545 ,  546
E,  546 ,  547
E,  547 ,  548
E,  551 ,  552
E,  552 ,  553
E,  553 ,  554
E,  554 ,  555
E,  558 ,  559
E,  559 ,  560
E,  560 ,  561
E,  561 ,  562
E,  565 ,  566
E,  566 ,  567
E,  567 ,  568
E,  568 ,  569
E,  572 ,  573
E,  573 ,  574
E,  574 ,  575
E,  575 ,  576
E,  579 ,  580
E,  580 ,  581
```

```
E,  581 ,  582
E,  582 ,  583
E,  586 ,  587
E,  587 ,  588
E,  588 ,  589
E,  589 ,  590
E,  593 ,  594
E,  594 ,  595
E,  595 ,  596
E,  596 ,  597
E,  600 ,  601
E,  601 ,  602
E,  602 ,  603
E,  603 ,  604
E,  607 ,  608
E,  608 ,  609
E,  609 ,  610
E,  610 ,  611
E,  614 ,  615
E,  615 ,  616
E,  616 ,  617
E,  617 ,  618
E,  621 ,  622
E,  622 ,  623
E,  623 ,  624
E,  624 ,  625
E,  628 ,  629
E,  629 ,  630
E,  630 ,  631
E,  631 ,  632
E,  635 ,  636
E,  636 ,  637
E,  637 ,  638
E,  638 ,  639
E,  642 ,  643
E,  643 ,  644
E,  644 ,  645
E,  645 ,  646
E,  649 ,  650
E,  650 ,  651
E,  651 ,  652
E,  652 ,  653
E,  656 ,  657
E,  657 ,  658
E,  658 ,  659
E,  659 ,  660
E,  663 ,  664
E,  664 ,  665
E,  665 ,  666
E,  666 ,  667
E,  670 ,  671
E,  671 ,  672
E,  672 ,  673
E,  673 ,  674
E,  677 ,  678
E,  678 ,  679
E,  679 ,  680
E,  680 ,  681
E,  684 ,  685
E,  685 ,  686
E,  686 ,  687
E,  687 ,  688
E,  691 ,  692
E,  692 ,  693
E,  693 ,  694
E,  694 ,  695
E,  698 ,  699
E,  699 ,  700
E,  700 ,  701
E,  701 ,  702
E,  705 ,  706
E,  706 ,  707
E,  707 ,  708
E,  708 ,  709
E,  712 ,  713
E,  713 ,  714
```

```
E,    714   ,   715
E,    715   ,   716
E,    719   ,   720
E,    720   ,   721
E,    721   ,   722
E,    722   ,   723
E,    726   ,   727
E,    727   ,   728
E,    728   ,   729
E,    729   ,   730
E,    733   ,   734
E,    734   ,   735
E,    735   ,   736
E,    736   ,   737
E,    740   ,   741
E,    741   ,   742
E,    742   ,   743
E,    743   ,   744
E,    747   ,   748
E,    748   ,   749
E,    749   ,   750
E,    750   ,   751
E,    754   ,   755
E,    755   ,   756
E,    756   ,   757
E,    757   ,   758
E,    761   ,   762
E,    762   ,   763
E,    763   ,   764
E,    764   ,   765
E,    768   ,   769
E,    769   ,   770
E,    770   ,   771
E,    771   ,   772
E,    775   ,   776
E,    776   ,   777
E,    777   ,   778
E,    778   ,   779
E,    782   ,   783
E,    783   ,   784
E,    784   ,   785
E,    785   ,   786
E,    789   ,   790
E,    790   ,   791
E,    791   ,   792
E,    792   ,   793
E,    796   ,   797
E,    797   ,   798
E,    798   ,   799
E,    799   ,   800
E,    803   ,   804
E,    804   ,   805
E,    805   ,   806
E,    806   ,   807
E,    810   ,   811
E,    811   ,   812
E,    812   ,   813
E,    813   ,   814
E,    817   ,   818
E,    818   ,   819
E,    819   ,   820
E,    820   ,   821
E,    824   ,   825
E,    825   ,   826
E,    826   ,   827
E,    827   ,   828
E,    831   ,   832
E,    832   ,   833
E,    833   ,   834
E,    834   ,   835
E,    838   ,   839
E,    839   ,   840
E,    840   ,   841
E,    841   ,   842
E,    845   ,   846
E,    846   ,   847
```

```
E,    847   ,   848
E,    848   ,   849
E,    852   ,   853
E,    853   ,   854
E,    854   ,   855
E,    855   ,   856
E,    859   ,   860
E,    860   ,   861
E,    861   ,   862
E,    862   ,   863
E,    866   ,   867
E,    867   ,   868
E,    868   ,   869
E,    869   ,   870
E,    873   ,   874
E,    874   ,   875
E,    875   ,   876
E,    876   ,   877
E,    880   ,   881
E,    881   ,   882
E,    882   ,   883
E,    883   ,   884
E,    887   ,   888
E,    888   ,   889
E,    889   ,   890
E,    890   ,   891
E,    894   ,   895
E,    895   ,   896
E,    896   ,   897
E,    897   ,   898
E,    901   ,   902
E,    902   ,   903
E,    903   ,   904
E,    904   ,   905
E,    908   ,   909
E,    909   ,   910
E,    910   ,   911
E,    911   ,   912
E,    915   ,   916
E,    916   ,   917
E,    917   ,   918
E,    918   ,   919
E,    922   ,   923
E,    923   ,   924
E,    924   ,   925
E,    925   ,   926
E,    933   ,   934
E,    934   ,   935
E,    935   ,   936
E,    936   ,   937
E,    931   ,   957
!Modifica
E,    957   ,   1136
E,    1136  ,   958
E,    958   ,   1140
E,    1140  ,   959
E,    959   ,   932
E,    1014  ,   1015
E,    1015  ,   1016
E,    1016  ,   1017
E,    1017  ,   1018
E,    1021  ,   1022
E,    1022  ,   1023
E,    1023  ,   1024
E,    1024  ,   1025
E,    1028  ,   1029
E,    1029  ,   1030
E,    1030  ,   1031
E,    1031  ,   1032
E,    1035  ,   1036
E,    1036  ,   1037
E,    1037  ,   1038
E,    1038  ,   1039
E,    1044  ,   1045
E,    1045  ,   1046
```

```
TYPE,1   !PILE
REAL,8
MAT,1

E,    99    ,   101
E,    100   ,   102
E,    101   ,   103
E,    102   ,   104
E,    103   ,   105
E,    104   ,   106
E,    105   ,   107
E,    106   ,   110
E,    107   ,   111
E,    110   ,   112
E,    111   ,   119
E,    112   ,   120
E,    119   ,   121
E,    120   ,   122
E,    121   ,   123
E,    122   ,   124
E,    123   ,   125
E,    124   ,   126
E,    125   ,   127
E,    126   ,   128
E,    127   ,   129
E,    128   ,   132
E,    129   ,   133
E,    132   ,   134
E,    133   ,   135
E,    134   ,   136
E,    135   ,   137
E,    136   ,   138
E,    137   ,   139
E,    138   ,   140
E,    139   ,   141
E,    140   ,   142
E,    141   ,   143
E,    142   ,   144
E,    143   ,   145
E,    144   ,   148
E,    145   ,   149
E,    148   ,   150
E,    149   ,   151
E,    150   ,   152
E,    151   ,   153
E,    152   ,   154
E,    153   ,   155
E,    154   ,   156
E,    155   ,   157
E,    156   ,   158
E,    157   ,   159
E,    158   ,   160
E,    159   ,   161
E,    160   ,   164
E,    161   ,   165
E,    164   ,   166
E,    165   ,   167
E,    166   ,   168
E,    940   ,   942
E,    941   ,   943
E,    942   ,   944
E,    943   ,   945
E,    944   ,   946
E,    945   ,   947
E,    946   ,   948
E,    947   ,   951
E,    948   ,   952
E,    951   ,   953
E,    952   ,   960
E,    953   ,   961
E,    960   ,   962
E,    961   ,   963
E,    962   ,   964
E,    963   ,   965
E,    964   ,   966
E,    965   ,   967
```

```
E,      966     ,       968
E,      967     ,       969
E,      968     ,       970
E,      969     ,       973
E,      970     ,       974
E,      973     ,       975
E,      974     ,       976
E,      975     ,       977
E,      976     ,       978
E,      977     ,       979
E,      978     ,       980
E,      979     ,       981
E,      980     ,       982
E,      981     ,       983
E,      982     ,       984
E,      983     ,       985
E,      984     ,       986
E,      985     ,       989
E,      986     ,       990
E,      989     ,       991
E,      990     ,       992
E,      991     ,       993
E,      992     ,       994
E,      993     ,       995
E,      994     ,       996
E,      995     ,       997
E,      996     ,       998
E,      997     ,       999
E,      998     ,       1000
E,      999     ,       1001
E,      1000    ,       1002
E,      1001    ,       1005
E,      1002    ,       1006
E,      1005    ,       1007
E,      1006    ,       1008
E,      1007    ,       1009

TYPE,1  !TRAVERSI TORRI
REAL,9
MAT,1


E,      107     ,       108
E,      108     ,       1125
E,      1125    ,       1129
E,      1129    ,       109
E,      109     ,       110
E,      129     ,       171
E,      171     ,       130
E,      130     ,       131
E,      131     ,       172
E,      172     ,       132
E,      145     ,       146
E,      146     ,       147
E,      147     ,       148
E,      161     ,       162
E,      162     ,       163
E,      163     ,       164
E,      948     ,       949
E,      949     ,       1133
E,      1133    ,       1137
E,      1137    ,       950
E,      950     ,       951
E,      970     ,       1012
E,      1012    ,       971
E,      971     ,       972
E,      972     ,       1013
E,      1013    ,       973
E,      986     ,       987
E,      987     ,       988
E,      988     ,       989
E,      1002    ,       1003
E,      1003    ,       1004
E,      1004    ,       1005
E,      112     ,       1121
! Nuovi Elementi per vincoli trasversali
E,      953     ,       1123
E,      111     ,       1122
E,      952     ,       1124
E,      1125    ,       1126
E,      1126    ,       1127
E,      1133    ,       1134
E,      1134    ,       1135
E,      1129    ,       1130
E,      1130    ,       1131
E,      1137    ,       1138
E,      1138    ,       1139

TYPE,1 !CAVALLETTO ANCORAGGIO
REAL,11
MAT,2

E,      3       ,       5
E,      4       ,       6
E,      1094    ,       1092
E,      1095    ,       1093

TYPE,3      ! pendini
REAL,2
MAT,2

E,90,171
E,91,172
E,931,1012
E,932,1013

! Vincoli longitudinali rigidi GAP 0,5m
TYPE,4
REAL,1111

E,1127,1128
E,1131,1132
E,1136,1135
E,1140,1139

! Vincoli trasversali rigidi GAP 0,3m
TYPE,4
REAL,1112

E,1122,90
E,91,1121
E,1124,931
E,932,1123

!-----------------------------------------------------
!GENERAZIONE ELEMENTI MASSA

TYPE,2
REAL,14

*DO,I,67,81,7
 E,I
 E,I+4
*ENDDO

*DO,I,173,922,7
 E,I
 E,I+4
*ENDDO

*DO,I,1014,1035,7
 E,I
 E,I+4
*ENDDO

E,90
E,91
E,92
E,96
E,931
E,932
E,933
E,937


! ASSEGNAZIONE TERMINATA
!-----------------------------------------------------

!INSERIMENTO DEI VINCOLI NEL
!MODELLO(ALL=INCASTRO)

D,1,ALL
D,2,ALL
D,5,ALL
D,6,ALL
D,58,ALL
D,59,ALL
D,99,ALL
D,100,ALL
D,940,ALL
D,941,ALL
D,1096,ALL
D,1097,ALL
D,1047,ALL
D,1048,ALL
D,1093,ALL
D,1092,ALL
D,57,ROTX,0,,,,UY,UZ
D,62,ROTX,0,,,,UY,UZ
D,63,ROTX,0,,,,UY,UZ
D,64,ROTX,0,,,,UY,UZ
D,1044,ROTX,0,,,,UY,UZ
D,1045,ROTX,0,,,,UY,UZ
D,1046,ROTX,0,,,,UY,UZ
D,1051,ROTX,0,,,,UY,UZ
D,3,UY
D,1094,UY
D,4,UY
D,1095,UY
!-----------------------------------------------------
!Creazione dei gruppi di elementi per
visualizzare i risultati nel post26

ESEL,S,REAL,,1111,1112
CM,PISTONI,ELEM
ALLSEL,ALL

NSEL,S,LOC,X,-30,30
NSEL,A,LOC,X,3270,3330
ESLN,R,1
CM,TORRI,ELEM
ALLSEL,ALL

NSEL,S,LOC,X,1590,1710
ESLN,R,1
CM,MEZZERIA,ELEM
ALLSEL,ALL

NSEL,S,LOC,X,-193,-120
NSEL,A,LOC,X,3420,3495
ESLN,R,1
CM,CAVALLETTI,ELEM
ALLSEL,ALL

FLST,5,10,2,ORDE,10
FITEM,5,3
FITEM,5,-4
FITEM,5,347
FITEM,5,-348
FITEM,5,457
FITEM,5,-458
FITEM,5,513
FITEM,5,-514
FITEM,5,569
FITEM,5,-570
ESEL,S, , ,P51X
CM,FUNI,ELEM
ALLSEL,ALL
```

```
FINISH
!-----------------------------------------------------
!Creazione Matrice Vento

Passi_Vento=32768  !(0 - 32768)
NODI=175

*DIM,VentoY,TABLE,NODI,Passi_Vento
*DIM,VentoZ,TABLE,NODI,Passi_Vento

!Creazione Matrice Vento (Nodo * Tempo)

/OUTPUT,Storia,dat,,

*TREAD,VentoY,Vvel,dat,,
*TREAD,Ventoz,Wvel,dat,,

*DIM,TIME,ARRAY,175,1,1
*DO,N,1,175,1
*VFILL,TIME(N,1),DATA,T_incs
*ENDDO

SAVE

/OUTPUT,Listato_Uscita_1,txt,,



!-----------------------------------------------------
!ANALISI DINAMICA!----------------------
!-----------------------------------------------------
/SOLU
ANTYPE,TRANS
TRNOPT,FULL              ! Full

AUTOTS,ON
NSUBST,1,5,1,OFF
NCNV,0
KBC,0

LUMPM,ON
NLGEOM,ON

RESCONTROL,DEFINE,NONE

!Smorzamento alla struttura del 95% RAYLEIGH
BETAD,BTI      !Smorzamento alla matrice di rigidezza (I e II modo di vibrare)
ALPHAD,ATI          !Smorzamento alla matrice delle masse (I e II modo di vibrare)

!-----------------------------------------------------
!ASSEGNAZIONE DELLA TEMPERATURA AI CAVI PRINCIPALI--
! ELEMENTI-----------------------------------
!-----------------------------------------------------
*DO,I,1,68
          BFE,I,TEMP,1,-295, , , ,
*ENDDO

*DO,I,69,96
          BFE,I,TEMP,1,-290, , , ,
*ENDDO

*DO,I,97,122
          BFE,I,TEMP,1,-285, , , ,
*ENDDO

*DO,I,123,150
          BFE,I,TEMP,1,-280, , , ,
*ENDDO

*DO,I,151,210
          BFE,I,TEMP,1,-275, , , ,
*ENDDO

*DO,I,211,238
          BFE,I,TEMP,1,-280, , , ,
*ENDDO

*DO,I,239,264
          BFE,I,TEMP,1,-285, , , ,
*ENDDO

*DO,I,265,292
          BFE,I,TEMP,1,-290, , , ,
*ENDDO

*DO,I,293,350
          BFE,I,TEMP,1,-295, , , ,
*ENDDO

ACEL,0,0,9.81
TIME,0.02
SOLVE

!-----------------------------------------------------
!Fase TRANSITORIA INIZIALE----------
!-----------------------------------------------------
!Smorzamento alla struttura del 95% RAYLEIGH
BETAD,BTI          !Smorzamento alla matrice di rigidezza (I e II modo di vibrare)
ALPHAD,ATI          !Smorzamento alla matrice delle masse (I e II modo di vibrare)
NLGEOM,ON
KBC,0
ACEL,0,0,9.81
R=1     !Contatore dei cicli di salvataggio

*DO,TTI,T_inc,T_TI,T_inc

*IF,R,LT,FRT,THEN
 OUTRES,ALL,NONE
 R=R+1

*ELSE

 OUTRES,ALL,NONE
 OUTRES,NSOL,LAST
 OUTRES,RSOL,LAST
 OUTRES,MISC,LAST,PISTONI
 OUTRES,MISC,LAST,MEZZERIA
 OUTRES,MISC,LAST,TORRI
 OUTRES,MISC,LAST,CAVALLETTI
 OUTRES,MISC,LAST,FUNI

 R=1
*ENDIF

TIME,TTI
SOLVE
*ENDDO

!-----------------------------------------------------
!Fase RAFFICA DI VENTO----------
!-----------------------------------------------------
!Smorzamento alla struttura del 0.5 %
BETAD,BD      !Smorzamento alla matrice di rigidezza (I e III modo di vibrare)
ALPHAD,AD          !Smorzamento alla matrice delle masse (I e III modo di vibrare)
ACEL,0,0,9.81

!Ordine progressivo dei nodi Ansys di Torri Cavi e Impalcato su cui sono applicate le storie di vento
*DIM,NODO_ANSYS,ARRAY,175,1,1

NODO_ANSYS(1)=99     !TORRI
NODO_ANSYS(2)=103
NODO_ANSYS(3)=107
NODO_ANSYS(4)=119
NODO_ANSYS(5)=123
NODO_ANSYS(6)=127
NODO_ANSYS(7)=133
NODO_ANSYS(8)=137
NODO_ANSYS(9)=141
NODO_ANSYS(10)=145
NODO_ANSYS(11)=151
NODO_ANSYS(12)=155
NODO_ANSYS(13)=159
NODO_ANSYS(14)=165
NODO_ANSYS(15)=940
NODO_ANSYS(16)=944
NODO_ANSYS(17)=948
NODO_ANSYS(18)=960
NODO_ANSYS(19)=964
NODO_ANSYS(20)=968
NODO_ANSYS(21)=974
NODO_ANSYS(22)=978
NODO_ANSYS(23)=982
NODO_ANSYS(24)=986
NODO_ANSYS(25)=992
NODO_ANSYS(26)=996
NODO_ANSYS(27)=1000
NODO_ANSYS(28)=1006
NODO_ANSYS(29)=7    !CAVI
NODO_ANSYS(30)=11
NODO_ANSYS(31)=15
NODO_ANSYS(32)=19
NODO_ANSYS(33)=23
NODO_ANSYS(34)=27
NODO_ANSYS(35)=31
NODO_ANSYS(36)=35
NODO_ANSYS(37)=39
NODO_ANSYS(38)=43
NODO_ANSYS(39)=47
NODO_ANSYS(40)=51
NODO_ANSYS(41)=55
NODO_ANSYS(42)=65
NODO_ANSYS(43)=79
NODO_ANSYS(44)=88
NODO_ANSYS(45)=167
NODO_ANSYS(46)=178
NODO_ANSYS(47)=192
NODO_ANSYS(48)=206
NODO_ANSYS(49)=220
NODO_ANSYS(50)=234
NODO_ANSYS(51)=248
NODO_ANSYS(52)=262
NODO_ANSYS(53)=276
NODO_ANSYS(54)=290
NODO_ANSYS(55)=304
NODO_ANSYS(56)=318
NODO_ANSYS(57)=332
NODO_ANSYS(58)=346
NODO_ANSYS(59)=360
NODO_ANSYS(60)=374
NODO_ANSYS(61)=388
NODO_ANSYS(62)=402
NODO_ANSYS(63)=416
NODO_ANSYS(64)=430
NODO_ANSYS(65)=444
NODO_ANSYS(66)=458
NODO_ANSYS(67)=472
NODO_ANSYS(68)=486
NODO_ANSYS(69)=500
NODO_ANSYS(70)=514
NODO_ANSYS(71)=528
NODO_ANSYS(72)=542
NODO_ANSYS(73)=556
NODO_ANSYS(74)=570
NODO_ANSYS(75)=584
NODO_ANSYS(76)=598
NODO_ANSYS(77)=612
```

```
NODO_ANSYS(78)=626
NODO_ANSYS(79)=640
NODO_ANSYS(80)=654
NODO_ANSYS(81)=668
NODO_ANSYS(82)=682
NODO_ANSYS(83)=696
NODO_ANSYS(84)=710
NODO_ANSYS(85)=724
NODO_ANSYS(86)=738
NODO_ANSYS(87)=752
NODO_ANSYS(88)=766
NODO_ANSYS(89)=780
NODO_ANSYS(90)=794
NODO_ANSYS(91)=808
NODO_ANSYS(92)=822
NODO_ANSYS(93)=836
NODO_ANSYS(94)=850
NODO_ANSYS(95)=864
NODO_ANSYS(96)=878
NODO_ANSYS(97)=892
NODO_ANSYS(98)=906
NODO_ANSYS(99)=920
NODO_ANSYS(100)=929
NODO_ANSYS(101)=1008
NODO_ANSYS(102)=1019
NODO_ANSYS(103)=1033
NODO_ANSYS(104)=1042
NODO_ANSYS(105)=1052
NODO_ANSYS(106)=1056
NODO_ANSYS(107)=1060
NODO_ANSYS(108)=1064
NODO_ANSYS(109)=1068
NODO_ANSYS(110)=1072
NODO_ANSYS(111)=1076
NODO_ANSYS(112)=1080
NODO_ANSYS(113)=1084
NODO_ANSYS(114)=1088
NODO_ANSYS(115)=1096
NODO_ANSYS(116)=69    !IMPALCATO
NODO_ANSYS(117)=83
NODO_ANSYS(118)=117
NODO_ANSYS(119)=175
NODO_ANSYS(120)=189
NODO_ANSYS(121)=203
NODO_ANSYS(122)=217
NODO_ANSYS(123)=231
NODO_ANSYS(124)=245
NODO_ANSYS(125)=259
NODO_ANSYS(126)=273
NODO_ANSYS(127)=287
NODO_ANSYS(128)=301
NODO_ANSYS(129)=315
NODO_ANSYS(130)=329
NODO_ANSYS(131)=343
NODO_ANSYS(132)=357
NODO_ANSYS(133)=371
NODO_ANSYS(134)=385
NODO_ANSYS(135)=399
NODO_ANSYS(136)=413
NODO_ANSYS(137)=427
NODO_ANSYS(138)=441
NODO_ANSYS(139)=455
NODO_ANSYS(140)=469
NODO_ANSYS(141)=483
NODO_ANSYS(142)=497
NODO_ANSYS(143)=511
NODO_ANSYS(144)=525
NODO_ANSYS(145)=539
NODO_ANSYS(146)=553
NODO_ANSYS(147)=567
NODO_ANSYS(148)=581
NODO_ANSYS(149)=595
NODO_ANSYS(150)=609
NODO_ANSYS(151)=623
NODO_ANSYS(152)=637
NODO_ANSYS(153)=651
NODO_ANSYS(154)=665
NODO_ANSYS(155)=679
NODO_ANSYS(156)=693
NODO_ANSYS(157)=707
NODO_ANSYS(158)=721
NODO_ANSYS(159)=735
NODO_ANSYS(160)=749
NODO_ANSYS(161)=763
NODO_ANSYS(162)=777
NODO_ANSYS(163)=791
NODO_ANSYS(164)=805
NODO_ANSYS(165)=819
NODO_ANSYS(166)=833
NODO_ANSYS(167)=847
NODO_ANSYS(168)=861
NODO_ANSYS(169)=875
NODO_ANSYS(170)=889
NODO_ANSYS(171)=903
NODO_ANSYS(172)=917
NODO_ANSYS(173)=935
NODO_ANSYS(174)=1023
NODO_ANSYS(175)=1037
!Ordine progressivo delle storie di vento
*DIM,Storia,ARRAY,175,1,1
Storia(1)=2  !Vento su torri
Storia(2)=4
Storia(3)=6
Storia(4)=8
Storia(5)=10
Storia(6)=12
Storia(7)=14
Storia(8)=16
Storia(9)=18
Storia(10)=20
Storia(11)=22
Storia(12)=24
Storia(13)=26
Storia(14)=28
Storia(15)=30
Storia(16)=32
Storia(17)=34
Storia(18)=36
Storia(19)=38
Storia(20)=40
Storia(21)=42
Storia(22)=44
Storia(23)=46
Storia(24)=48
Storia(25)=50
Storia(26)=52
Storia(27)=54
Storia(28)=56

Storia(29)=58   !Vento su cavi
Storia(30)=60
Storia(31)=62
Storia(32)=64
Storia(33)=66
Storia(34)=68
Storia(35)=70
Storia(36)=72
Storia(37)=74
Storia(38)=76
Storia(39)=78
Storia(40)=80
Storia(41)=82
Storia(42)=84
Storia(43)=86
Storia(44)=90
Storia(45)=97
Storia(46)=100
Storia(47)=104
Storia(48)=108
Storia(49)=112
Storia(50)=116
Storia(51)=120
Storia(52)=124
Storia(53)=128
Storia(54)=132
Storia(55)=136
Storia(56)=140
Storia(57)=144
Storia(58)=148
Storia(59)=152
Storia(60)=156
Storia(61)=160
Storia(62)=164
Storia(63)=168
Storia(64)=172
Storia(65)=176
Storia(66)=180
Storia(67)=184
Storia(68)=188
Storia(69)=192
Storia(70)=196
Storia(71)=200
Storia(72)=204
Storia(73)=208
Storia(74)=212
Storia(75)=216
Storia(76)=220
Storia(77)=224
Storia(78)=228
Storia(79)=232
Storia(80)=236
Storia(81)=240
Storia(82)=244
Storia(83)=248
Storia(84)=252
Storia(85)=256
Storia(86)=260
Storia(87)=264
Storia(88)=268
Storia(89)=272
Storia(90)=276
Storia(91)=280
Storia(92)=284
Storia(93)=288
Storia(94)=292
Storia(95)=296
Storia(96)=300
Storia(97)=304
Storia(98)=308
Storia(99)=312
Storia(100)=316
Storia(101)=320
Storia(102)=323
Storia(103)=327
Storia(104)=330
Storia(105)=333
Storia(106)=335
Storia(107)=337
Storia(108)=339
Storia(109)=341
Storia(110)=343
Storia(111)=345
Storia(112)=347
Storia(113)=349
Storia(114)=351
Storia(115)=353
Storia(116)=87   !Vento su impalcato
Storia(117)=91
Storia(118)=95
Storia(119)=99
Storia(120)=103
Storia(121)=107
Storia(122)=111
Storia(123)=115
Storia(124)=119
Storia(125)=123
Storia(126)=127
Storia(127)=131
```

```
Storia(128)=135
Storia(129)=139
Storia(130)=143
Storia(131)=147
Storia(132)=151
Storia(133)=155
Storia(134)=159
Storia(135)=163
Storia(136)=167
Storia(137)=171
Storia(138)=175
Storia(139)=179
Storia(140)=183
Storia(141)=187
Storia(142)=191
Storia(143)=195
Storia(144)=199
Storia(145)=203
Storia(146)=207
Storia(147)=211
Storia(148)=215
Storia(149)=219
Storia(150)=223
Storia(151)=227
Storia(152)=231
Storia(153)=235
Storia(154)=239
Storia(155)=243
Storia(156)=247
Storia(157)=251
Storia(158)=255
Storia(159)=259
Storia(160)=263
Storia(161)=267
Storia(162)=271
Storia(163)=275
Storia(164)=279
Storia(165)=283
Storia(166)=287
Storia(167)=291
Storia(168)=295
Storia(169)=299
Storia(170)=303
Storia(171)=307
Storia(172)=311
Storia(173)=315
Storia(174)=324
Storia(175)=328

R=1   !PER LA SCRITTURA DEL FILE RISULTATI
T=1   !PER LA SCRITTURA DELLA MATRICE FORZE

!-----------------------------------------------
!DEFINIZIONE DEI PARAMETRI DI ANLISI
!-----------------------------------------------
U=45   !Velocita media orizzontale del vento

*DIM,FORZAY,ARRAY,175,65000,1
!ARRAY PER IL PLOTTAGGIO DELLE FORZE AGENTI
*DIM,FORZAZ,ARRAY,175,65000,1
!ARRAY PER IL PLOTTAGGIO DELLE FORZE AGENTI
*DIM,MOMENT,ARRAY,175,65000,1
!ARRAY PER IL PLOTTAGGIO DELLE FORZE AGENTI


*DIM,AERH1,ARRAY,175,1,1
!funzione aeroelastica h1 (ZASSO)
*DIM,AERH2,ARRAY,175,1,1
!funzione aeroelastica h2 (ZASSO)
*DIM,AERH3,ARRAY,175,1,1
!funzione aeroelastica h3 (ZASSO)
*DIM,AERA1,ARRAY,175,1,1
!funzione aeroelastica a1 (ZASSO)
*DIM,AERA2,ARRAY,175,1,1
!funzione aeroelastica a2 (ZASSO)
*DIM,AERA3,ARRAY,175,1,1
!funzione aeroelastica a3 (ZASSO)

*DIM,AERH11,ARRAY,175,1,1
!per accorciare l'espressione di h1
*DIM,AERH12,ARRAY,175,1,1
 !per accorciare l'espressione di h1
*DIM,AERH21,ARRAY,175,1,1
 !per accorciare l'espressione di h2
*DIM,AERH22,ARRAY,175,1,1
 !per accorciare l'espressione di h2

*DIM,TETA0,ARRAY,175,1,1
!!posizione di equilibrio stazionario sotto vento con velocità U costante
*DIM,KD0,ARRAY,175,1,1   !!Derivata angolare del Cd statico calcolata in TETA=TETA0 (posizione di equilibrio stazionario sotto vento con velocità U)
*DIM,KL0,ARRAY,175,1,1   !!Derivata angolare del Cl statico calcolata in TETA=TETA0 (posizione di equilibrio stazionario sotto vento con velocità U)
*DIM,KM0,ARRAY,175,1,1   !!Derivata angolare del Cm statico calcolata in TETA=TETA0 (posizione di equilibrio stazionario sotto vento con velocità U)

TETA0(1,1)=0.000000
TETA0(2,1)=0.000000
TETA0(3,1)=0.000000
TETA0(4,1)=0.000000
TETA0(5,1)=0.000000
TETA0(6,1)=0.000000
TETA0(7,1)=0.000000
TETA0(8,1)=0.000000
TETA0(9,1)=0.000000
TETA0(10,1)=0.000000
TETA0(11,1)=0.000000
TETA0(12,1)=0.000000
TETA0(13,1)=0.000000
TETA0(14,1)=0.000000
TETA0(15,1)=0.000000
TETA0(16,1)=0.000000
TETA0(17,1)=0.000000
TETA0(18,1)=0.000000
TETA0(19,1)=0.000000
TETA0(20,1)=0.000000
TETA0(21,1)=0.000000
TETA0(22,1)=0.000000
TETA0(23,1)=0.000000
TETA0(24,1)=0.000000
TETA0(25,1)=0.000000
TETA0(26,1)=0.000000
TETA0(27,1)=0.000000
TETA0(28,1)=0.000000
TETA0(29,1)=0.000000
TETA0(30,1)=0.000000
TETA0(31,1)=0.000000
TETA0(32,1)=0.000000
TETA0(33,1)=0.000000
TETA0(34,1)=0.000000
TETA0(35,1)=0.000000
TETA0(36,1)=0.000000
TETA0(37,1)=0.000000
TETA0(38,1)=0.000000
TETA0(39,1)=0.000000
TETA0(40,1)=0.000000
TETA0(41,1)=0.000000
TETA0(42,1)=0.000000
TETA0(43,1)=0.000000
TETA0(44,1)=0.000000
TETA0(45,1)=0.000000
TETA0(46,1)=0.000000
TETA0(47,1)=0.000000
TETA0(48,1)=0.000000
TETA0(49,1)=0.000000
TETA0(50,1)=0.000000
TETA0(51,1)=0.000000
TETA0(52,1)=0.000000
TETA0(53,1)=0.000000
TETA0(54,1)=0.000000
TETA0(55,1)=0.000000
TETA0(56,1)=-0.000065
TETA0(57,1)=-0.000065
TETA0(58,1)=0.000099
TETA0(59,1)=0.000338
TETA0(60,1)=0.000681
TETA0(61,1)=0.000877
TETA0(62,1)=0.001220
TETA0(63,1)=0.001690
TETA0(64,1)=0.002170
TETA0(65,1)=0.002660
TETA0(66,1)=0.003160
TETA0(67,1)=0.003640
TETA0(68,1)=0.004090
TETA0(69,1)=0.004520
TETA0(70,1)=0.004950
TETA0(71,1)=0.005360
TETA0(72,1)=0.005770
TETA0(73,1)=0.006170
TETA0(74,1)=0.006570
TETA0(75,1)=0.006960
TETA0(76,1)=0.007340
TETA0(77,1)=0.007720
TETA0(78,1)=0.008100
TETA0(79,1)=0.008470
TETA0(80,1)=0.008820
TETA0(81,1)=0.009160
TETA0(82,1)=0.009500
TETA0(83,1)=0.009830
TETA0(84,1)=0.010200
TETA0(85,1)=0.010500
TETA0(86,1)=0.010800
TETA0(87,1)=0.011100
TETA0(88,1)=0.011400
TETA0(89,1)=0.011700
TETA0(90,1)=0.011900
TETA0(91,1)=0.012200
TETA0(92,1)=0.012500
TETA0(93,1)=0.012700
TETA0(94,1)=0.013000
TETA0(95,1)=0.013200
TETA0(96,1)=0.013500
TETA0(97,1)=0.013700
TETA0(98,1)=0.013900
TETA0(99,1)=0.014100
TETA0(100,1)=0.014300
TETA0(101,1)=0.014500
TETA0(102,1)=0.014700
TETA0(103,1)=0.014800
TETA0(104,1)=0.015000
TETA0(105,1)=0.015100
TETA0(106,1)=0.015300
TETA0(107,1)=0.015400
TETA0(108,1)=0.015500
TETA0(109,1)=0.015600
TETA0(110,1)=0.015700
TETA0(111,1)=0.015700
TETA0(112,1)=0.015800
TETA0(113,1)=0.015800
TETA0(114,1)=0.015800
TETA0(115,1)=0.015800
TETA0(116,1)=0.015800
TETA0(117,1)=0.015800
TETA0(118,1)=0.015800
```

```
TETA0(119,1)=0.015700
TETA0(120,1)=0.015600
TETA0(121,1)=0.015600
TETA0(122,1)=0.015500
TETA0(123,1)=0.015400
TETA0(124,1)=0.015200
TETA0(125,1)=0.015100
TETA0(126,1)=0.015000
TETA0(127,1)=0.014800
TETA0(128,1)=0.014600
TETA0(129,1)=0.014400
TETA0(130,1)=0.014300
TETA0(131,1)=0.014100
TETA0(132,1)=0.013800
TETA0(133,1)=0.013600
TETA0(134,1)=0.013400
TETA0(135,1)=0.013200
TETA0(136,1)=0.012900
TETA0(137,1)=0.012700
TETA0(138,1)=0.012400
TETA0(139,1)=0.012100
TETA0(140,1)=0.011900
TETA0(141,1)=0.011600
TETA0(142,1)=0.011300
TETA0(143,1)=0.011000
TETA0(144,1)=0.010700
TETA0(145,1)=0.010400
TETA0(146,1)=0.010100
TETA0(147,1)=0.009750
TETA0(148,1)=0.009420
TETA0(149,1)=0.009080
TETA0(150,1)=0.008740
TETA0(151,1)=0.008390
TETA0(152,1)=0.008030
TETA0(153,1)=0.007650
TETA0(154,1)=0.007270
TETA0(155,1)=0.006890
TETA0(156,1)=0.006500
TETA0(157,1)=0.006110
TETA0(158,1)=0.005710
TETA0(159,1)=0.005310
TETA0(160,1)=0.004900
TETA0(161,1)=0.004480
TETA0(162,1)=0.004040
TETA0(163,1)=0.003600
TETA0(164,1)=0.003130
TETA0(165,1)=0.002630
TETA0(166,1)=0.002150
TETA0(167,1)=0.001670
TETA0(168,1)=0.001220
TETA0(169,1)=0.000904
TETA0(170,1)=0.000650
TETA0(171,1)=0.000275
TETA0(172,1)=0.000070
TETA0(173,1)=0.000029
TETA0(174,1)=-0.000026
TETA0(175,1)=0.000000


*DIM,VQAI,ARRAY,175,2,1
!Definizione Tavola delle velocità al quadrato e dell'angolo di incidenza del vento
*DIM,CDLM,ARRAY,175,3,1
!Definizione Tavola dei coefficienti aerodinamici di Drag,Lift e Moment dell'Impalcato

*DIM,USPUNTO,ARRAY,175,1,1
!Definizione Tavola delle velocità orizzontali relative del vento U-SPUNTO
*DIM,VQUADROL,ARRAY,175,1,1
!Definizione Tavola dei quadrati del modulo delle velocità relative impalcato-vento (Per Lift)
*DIM,VQUADROM,ARRAY,175,1,1
!Definizione Tavola dei quadrati del modulo delle velocità relative impalcato-vento (Per Moment)

*DIM,COSTL,ARRAY,175,1,1
*DIM,COSTM,ARRAY,175,1,1


!*DIM,TETA,ARRAY,175,1,1
!Definizione vettore degli angoli di rotazione dell'Impalcato (per analisi quasi-staz)
!*DIM,GAMMA,ARRAY,175,1,1
!Definizione vettore degli angoli differenza(o somma)TETA+-VQAI (per analisi quasi-staz)


*DIM,S0,ARRAY,175,1,1 !Definizione vettore degli spostamenti orizzontali iniziali dell'Impalcato (per analisi quasi-staz)!!
*DIM,H0,ARRAY,175,1,1 !Definizione vettore degli spostamenti verticali iniziali dell'Impalcato (per analisi quasi-staz) !! per calcolo derivate
*DIM,T0,ARRAY,175,1,1 !Definizione vettore degli rotazioni iniziali dell'Impalcato (per analisi quasi-staz) !!

*DIM,S,ARRAY,175,1,1 !Definizione vettore degli spostamenti orizzontali dell'Impalcato (per analisi quasi-staz)
*DIM,SPUNTO,ARRAY,175,1,1
!Definizione vettore delle veloctà orizzontali dell'Impalcato (per analisi quasi-staz)
*DIM,H,ARRAY,175,1,1 !Definizione vettore degli spostamenti verticali dell'Impalcato (per analisi quasi-staz)
*DIM,HPUNTO,ARRAY,175,1,1
!Definizione vettore delle veloctà verticali dell'Impalcato (per analisi quasi-staz)
*DIM,TETA,ARRAY,175,1,1
!Definizione vettore degli angoli di rotazione dell'Impalcato (per analisi quasi-staz)
*DIM,TETAPUNTO,ARRAY,175,1,1
!Definizione vettore delle veloctà di rotazione dell'Impalcato (per analisi quasi-staz)

*DIM,BETAL,ARRAY,175,1,1
!Definizione vettore degli angoli di inclinazione relativa velocità (senza calcolare rotazione impalcato)(per analisi quasi-staz)(Per Lift)
*DIM,BETAM,ARRAY,175,1,1
!Definizione vettore degli angoli di inclinazione relativa velocità (senza calcolare rotazione impalcato)(per analisi quasi-staz)(Per Moment)

*DIM,GAMMAL,ARRAY,175,1,1
!Definizione vettore degli angoli differenza(o somma)TETA+-BETA (per analisi quasi-staz)(Per Lift)
*DIM,GAMMAM,ARRAY,175,1,1
!Definizione vettore degli angoli differenza(o somma)TETA+-BETA (per analisi quasi-staz)(Per Moment)

*DIM,BL,ARRAY,175,1,1 !Definizione parametro BL(per analisi quasi-staz)(Per Lift)
*DIM,BM,ARRAY,175,1,1 !Definizione parametro BM(per analisi quasi-staz)(Per Moment)

*DIM,CDR0,ARRAY,175,1,1 !!
*DIM,CL0,ARRAY,175,1,1
!!Definizione DEI parametri costanti di integrazione integrale(per analisi quasi-staz)
*DIM,CM0,ARRAY,175,1,1 !!

*DIM,CDR,ARRAY,175,1,1 !!
*DIM,CL,ARRAY,175,1,1
!!Definizione DEI parametri costanti di integrazione integrale(per analisi quasi-staz)
*DIM,CM,ARRAY,175,1,1 !!


*DIM,DRAG,ARRAY,175,1,1 !!
*DIM,LIFT,ARRAY,175,1,1
!!Definizione DEI parametri forze di Drag,lift e moment(per analisi quasi-staz)
*DIM,MOM,ARRAY,175,1,1 !!


*AFUN,RAD !Uso dei radianti come unità di misura degli angoli

!Riempie gli spostamenti iniziali dell'Impalcato con tutti zero
 *DO,N,1,175,1
 S0(N,1)=0
 H0(N,1)=0
 T0(N,1)=TETA0(N,1)
 *ENDDO


*DO,N,116,175
!! COSTANTI DI INTEGRAZIONE
TETA0(N,1))**2+1.415206*(-TETA0(N,1))-0.0174
CDR0(N,1)=3.2936*(-TETA0(N,1))**2+0.0787*(-TETA0(N,1))+0.0997
 CL0(N,1)=0.1626*(-TETA0(N,1))**2+0.8985*(-TETA0(N,1))-0.0486
 CM0(N,1)=0.5115*(-TETA0(N,1))**3 -0.2219*(-TETA0(N,1))**2 +0.1353*(-TETA0(N,1))+0.0186
*ENDDO

*DO,N,116,175
 KD0(N,1)=2*(3.2936*(-TETA0(N,1)))+0.0787
 KL0(N,1)=2*(0.1626*(-TETA0(N,1)))+0.8985
 KM0(N,1)=3*(0.5115*(-TETA0(N,1))**2)-2*(0.2219*(-TETA0(N,1))) +0.1353
*ENDDO


!-----------------------------------------------
!INIZIO CICLO TEMPO
!-----------------------------------------------

*DO,TV,T_incS,T_VENTO,T_incs

FDELE,ALL,ALL


*IF,TV,LT,T_TIV,THEN
 !Fattore di riduzione dell'azione del vento (varia tra 0 e 1)
FR=TV/T_TIV
*ELSE
```

```
 FR=1
*ENDIF

!Per ogni passo temporale (TV: Tempo vento)

!Riempie il vettore TETA con gli angoli di rotazione dell'impalcato
 *DO,N,116,175,1

*GET,ROT_X,NODE,NODO_ANSYS(N),ROT,X
  *VFILL,TETA(N,1),DATA,ROT_X

 *ENDDO

!Riempie il vettore S con gli spostamenti orizzontali dell'impalcato
 *DO,N,116,175,1

*GET,SPOST_Y,NODE,NODO_ANSYS(N),U,Y
  *VFILL,S(N,1),DATA,SPOST_Y

 *ENDDO

!Riempie il vettore H con gli spostamenti verticali dell'impalcato
 *DO,N,116,175,1

*GET,SPOST_Z,NODE,NODO_ANSYS(N),U,Z
  *VFILL,H(N,1),DATA,SPOST_Z

 *ENDDO

!Riempie il vettore TETA con gli angoli di rotazione dell'impalcato
 *DO,N,116,175,1

*GET,ROT_X,NODE,NODO_ANSYS(N),ROT,X
  *VFILL,TETA(N,1),DATA,ROT_X

 *ENDDO

!Riempie il vettore SPUNTO derivando il vettore S
 *DO,N,116,175,1
   SPUNTO(N,1)=(S(N,1)-S0(N,1))/T_incs
 *ENDDO

!Riempie il vettore HPUNTO derivando il vettore H
 *DO,N,116,175,1
   HPUNTO(N,1)=(H(N,1)-H0(N,1))/T_incs

 *ENDDO

!Riempie il vettore TETAPUNTO derivando il vettore TETA
 *DO,N,116,175,1
   TETAPUNTO(N,1)=(TETA(N,1)-T0(N,1))/T_incs

 *ENDDO

*DO,N,116,175

AERH11(N,1)=-5874*(-TETA(N,1))**4-94.945*(-TETA(N,1))**3
AERH12(N,1)=117.43*(-TETA(N,1))**2+0.4967*(-TETA(N,1))+0.9648
AERH21(N,1)=9756.7*(-TETA(N,1))**4+26.978*(-TETA(N,1))**3
AERH22(N,1)=-175.02*(-TETA(N,1))**2+4.4827*(-TETA(N,1))-1.6038

AERH1(N,1)=AERH11(N,1)+AERH12(N,1)
AERH2(N,1)=AERH21(N,1)+AERH22(N,1)
AERH3(N,1)=-792.16*(-TETA(N,1))**3-84.991*(-TETA(N,1))**2+5.4996*(-TETA(N,1))+1.1145

AERA1(N,1)=1384.1*(-TETA(N,1))**3-118.37*(-TETA(N,1))**2-12.513*(-TETA(N,1))+1.336
AERA2(N,1)=1101.8*(-TETA(N,1))**3-30.729*(-TETA(N,1))**2-11.831*(-TETA(N,1))+1.4752
AERA3(N,1)=1626.2*(-TETA(N,1))**3-101.22*(-TETA(N,1))**2-14.446*(-TETA(N,1))+1.2636

*ENDDO

*DO,N,116,175

 BL(N,1)=(AERH2(N,1)/AERH1(N,1))*B
 BM(N,1)=(AERA2(N,1)/AERA1(N,1))*B
*ENDDO

!CALCOLO VELOCITA' AL QUADRATO E ANGOLI DI INCIDENZA DEL VENTO
*DO,N,1,175

VQAI(N,1)=((VentoY(Storia(N),TV))**2)+((VentoZ(Storia(N),TV))**2)  !Velocità al quadrato

VQAI(N,2)=ATAN((VentoZ(Storia(N),TV))/(VentoY(Storia(N),TV)))
                !Angolo di incidenza del vento
*ENDDO

!CALCOLO VELOCITA' RELATIVA ORIZZONTALE e VELOCITA' AL QUADRATO
*DO,N,1,175

USPUNTO(N,1)=(VentoY(Storia(N),TV)-SPUNTO(N,1))
!velocità orizzontali relative del vento U-SPUNTO

VQUADROL(N,1)=(USPUNTO(N,1))**2+(VentoZ(Storia(N),TV)-HPUNTO(N,1)+TETAPUNTO(N,1)*BL(N,1))**2  !Angolo di incidenza del vento

VQUADROM(N,1)=(USPUNTO(N,1))**2+(VentoZ(Storia(N),TV)-HPUNTO(N,1)+TETAPUNTO(N,1)*BM(N,1))**2  !Angolo di incidenza del vento
*ENDDO

!CALCOLO DELL'ANGOLO DI INCIDENZA DEL VENTO BETA
*DO,N,1,175
 BETAL(N,1)=((VentoZ(Storia(N),TV)-HPUNTO(N,1)+BL(N,1)*TETAPUNTO(N,1))/(USPUNTO(N,1)))
 BETAM(N,1)=((VentoZ(Storia(N),TV)-HPUNTO(N,1)+BM(N,1)*TETAPUNTO(N,1))/(USPUNTO(N,1)))
*ENDDO

!CALCOLO DELL'ANGOLO DI INCIDENZA DEL VENTO GAMMA
*DO,N,1,175
 GAMMAL(N,1)=(-TETA(N,1)+BETAL(N,1))
 GAMMAM(N,1)=(-TETA(N,1)+BETAM(N,1))
*ENDDO

*DO,N,116,175

CDR(N,1)=CDR0(N,1)+KD0(N,1)*(GAMMAL(N,1)-TETA0(N,1))

CL(N,1)=CL0(N,1)+KL0(N,1)*(GAMMAL(N,1)-TETA0(N,1))
COSTANTI DI INTEGRAZIONE

CM(N,1)=CM0(N,1)+KM0(N,1)*(GAMMAM(N,1)-TETA0(N,1))
*ENDDO
!-----------------------------------------------------
!CALCOLO DEI COEFFICIENTI AERODINAMICI
!-----------------------------------------------------
!Coefficiente di Drag del CAVO
*DO,N,29,115
 CDLM(N,1)=0.6
*ENDDO

!Coefficienti di Drag Lift e Moment dell'impalcato (funzioni dell'angolo di incidenza del vento)
*DO,N,116,175

 CDLM(N,1)=3.2936*(-TETA0(N,1))**2+0.0787*(-TETA0(N,1))+0.0997
 CDLM(N,2)=0.1626*(-TETA0(N,1))**2+0.8985*(-TETA0(N,1))-0.0486
 CDLM(N,3)=0.5115*(-TETA0(N,1))**3 -0.2219*(-TETA0(N,1))**2+0.1353*(-TETA0(N,1))+0.0186
*ENDDO

!APPLICAZIONE DELLE FORZE AI NODI

!Applicazione delle forzanti al cavo
*DO,N,29,115

F,NODO_ANSYS(N),FY,(0.5*1.25*1.22*VQAI(N,1)*CDLM(N,1)*COS(VQAI(N,2)))*60*FR   !CAVO DESTRO

F,NODO_ANSYS(N),FZ,(0.5*1.25*1.22*VQAI(N,1)*CDLM(N,1)*SIN(VQAI(N,2)))*60*FR

F,NODO_ANSYS(N)+1,FY,(0.5*1.25*1.22*VQAI(N,1)*CDLM(N,1)*COS(VQAI(N,2)))*60*FR  !CAVO SINISTRA

F,NODO_ANSYS(N)+1,FZ,(0.5*1.25*1.22*VQAI(N,1)*CDLM(N,1)*SIN(VQAI(N,2)))*60*FR
*ENDDO

!Applicazione delle forzanti all'impalcato
*DO,N,116,175

COSTL(N,1)=0.5*1.25*60.4*VQUADRO
```

```
L(N,1)
COSTM(N,1)=0.5*1.25*3648.16*VQUAD
ROM(N,1)

DRAG(N,1)=COSTL(N,1)*CDR(N,1)
LIFT(N,1)=COSTL(N,1)*CL(N,1)
MOM(N,1)=COSTM(N,1)*CM(N,1)

FORZAY(N,T)=((DRAG(N,1)-
LIFT(N,1)*SIN(VQAI(N,2)))*60*FR)
FORZAZ(N,T)=((LIFT(N,1)+DRAG(N,1)
*SIN(VQAI(N,2)))*60*FR)
MOMENT(N,T)=(-MOM(N,1)*60*FR)


F,NODO_ANSYS(N),FY,((DRAG(N,1)-
LIFT(N,1)*SIN(VQAI(N,2)))*60*FR)
F,NODO_ANSYS(N),FZ,((LIFT(N,1)+D
RAG(N,1)*SIN(VQAI(N,2)))*60*FR)
F,NODO_ANSYS(N),MX,(-
MOM(N,1)*60*FR)
*ENDDO

!Aggiorna i vettori iniziali dell'Impalcato

*DO,N,1,175,1
  S0(N,1)=S(N,1)
  H0(N,1)=H(N,1)
  T0(N,1)=TETA(N,1)
*ENDDO
T=T+1

*IF,R,LT,FRV,THEN
 OUTRES,ALL,NONE
 R=R+1

*ELSE

 OUTRES,ALL,NONE
 OUTRES,NSOL,LAST
 OUTRES,RSOL,LAST
 OUTRES,MISC,LAST,PISTONI
 OUTRES,MISC,LAST,MEZZERIA
 OUTRES,MISC,LAST,TORRI
 OUTRES,MISC,LAST,CAVALLETTI
 OUTRES,MISC,LAST,FUNI

 R=1
*ENDIF

FINISH
SAVE
```

APPENDIX C. COMPLETE REFERENCES LIST

COMPLETE REFERENCES LIST

Books

Augusti, G. Baratta, A., Casciati, F., Probabilistic Methods in Structural Engineering, Chapman and Hall, 1984.

Bathe, K.J. Finite Element Procedures, Prentice-Hall, 1996.

Borri, C. and Pastò, S., Lezioni di ingegneria del vento, Firenze University Press, Firenze 2007 (in Italian)..

Brebbia, C.A. Walker, S., Dynamic analysis of offshore structures, Nwenes-Butterworths, 1979.

Ditevslen, O. and Madsen, H.O., Structural Reliability Methods, John Wiley & Sons Ltd, Chichester, 1996.

Faravelli, L. , Sicurezza strutturale, Ed. Pitagora, 1988 (in Italian).

Hau, E., Wind Turbines: Fundamentals, technologies, Application, Economics, 2nd edition. Springer-Verlag Berlin Heidelberg 2006.

Holmes, J.D.. Wind loading of structures, Spoon Press, 2001.

Lewis, E.E., Introduction to Reliability Engineering, John Wiley & Sons Ltd, New York, 1994 (2nd ed.)

Morgan, M. G. and Henrion, M., Uncertainty, Cambridge University Press, 1998.

NASA, National Aeronautics and Space Administration, Systems Engineering Handbook., 1995, Available online at: www.nasa.gov.

Pinto, P.E., Giannini, R. and Franchin, P., Seismic reliability analysis methods, IUSS Press, Pavia, Italy, 2004.

Robert, C.P. and Casella, G., Monte Carlo statistical methods, Springer, New York, 2004.

Simiu, E., Scanlan, R.H. Wind effects on structures, John Wiley e sons Inc., third edition 1996.

Simiu, E., Miyata, T., Design of Buildings and Bridges for Wind, John Wiley e sons Inc., 2006.

Simon, H.A, The Sciences of the Artificial, The MIT Press, Cambridge, 1998.

Stømmer, E., Theory of Bridge Aerodynamics, Springer, New York, 2006.

Papers, technical reports and standards

Agenzia per la Protezione dell'Ambiente e per I Servizi Tecnici (APAT), 2004, Atlante delle onde nei mari italiani – Italian wave atlas, Rome, Italy (in italian).

Aprile, A. & Benedetti, A. 2000. "Damage evaluation and control for fatigue under stochastic excitation", Proceedings of 8th ASCE Probabilistic Mechanics and Structural Reliability Conference (PCM2000), Notre Dame, USA (2000).

Ang, G.K.I. and Wyatt, D.P. (1998). "The role of performance specification in the design agenda", Proceedings of the Design Agenda Conference, Brighton, UK, September 1-18.

Augusti, G. Borri, C. and Neumann, H.J. (2001). "Is Aeloian risk as significant as other environmental risks?", Reliability Engineering and System safety, Vol. 74, pp. 227-237.

Augusti, G., Ciampoli, M., (2006), "First steps towards Performance-based Wind Engineering", Performance of Wind Exposed Structures: Results of the PERBACCO project (G. Bartoli, F. Ricciardelli, A. Saetta, V. Sepe eds.), Firenze University Press, 13-20.

Augusti, G., Ciampoli, M., (2008), "Performance-Based Design in risk assessment and reduction", Probabilistic Engineering Mechanics, 23, 496-508.

Bartoli, G., Ricciardelli, F., Saetta, A., Sepe, V. (eds.) (2006). "Performance of Wind Exposed Structures: Results of the PERBACCO Project", Firenze University Press, Italy.

Baker, J. W., and C. A. Cornell., (2004). "Choice of a vector of ground motion intensity measures for seismic demand hazard analysis", Proceedings of the 13th World Conference on Earthquake Engineering, Vancouver, Canada.

Baker, J. W., and C. A. Cornell., (2006). Vector-Valued Ground Motion Intensity Measures for Probabilistic Seismic Demand Analysis, Report 2006-08, Pasadena, California, United States. Available on line at http://peer.berkeley.edu/publications/peer_reports.html.

Bathe, K.J. and Baig, M.M.I. (2005). "On a composite implicit time integration procedure for nonlinear dynamics", Comput. and Struct. 83, 2513–2524.

Bontempi, F. and Giuliano, F. (2005). "Multilevel approach for the analysis and synthesis of the serviceability performances of a long span suspension bridge", Proceedings of the Tenth International Conference on Civil, Structural and Environmental Engineering Computing, 30 August - 2 September 2005, Rome – Italy.

Bontempi, F., Malerba, P. and Giudici, M. (2000). "La Formulazione matriciale dei problemi aeroelastici di ponti sospesi e strallati" (in Italian), Studi e Ricerche-Politecnico di Milano 21.

Bontempi, F. (2006), "Basis of Design and expected Performances for the Messina Strait Bridge". Proc. of the International Conference on Bridge Engineering – Challenges in the 21st Century, Hong Kong, 1-3 November, 2006.

Bontempi, F., Giuliani, L., (2006b), "Engineering complexity: uncertainty modelling and structural robustness", 10. Dresdner Baustatik Seminar, Technische Universitaet Dresden, Deutschland, September 2006.

Bontempi F., Giuliani L., Gkoumas K., (2007) "Handling the exceptions: dependability of systems and structural robustness"(invited lecture), 3rd international conference on structural engineering, mechanics and computation (SEMC 2007), Cape Town, South Africa, 10-12 September 2007.

Bontempi, F., Gkoumas, K. and Arangio, S. (2008a), "Systemic approach for the maintenance of complex structural systems". Structure and infrastructure engineering, vol. 4; pp. 77-94, ISSN: 1573-2479, doi: 10.1080/15732470601155235.

Bontempi, F., Li, H., Petrini, F. and Manenti, S. (2008b), "Numerical modeling for the analysis and design of offshore wind turbines", The 4th International Conference on Advances in Structural Engineering and Mechanics (ASEM'08). 26-28 May 2008, Seoqwipo KAL Hotel, Jeju, Korea.

Bontempi, F., Li, H., Petrini, F. and Gkoumas, K. (2008c), "Basis of Design of Offshore Wind Turbines by System Decomposition", The 4th International Conference on Advances in Structural Engineering and Mechanics (ASEM'08). 26-28 May 2008, Seoqwipo KAL Hotel, Jeju, Korea.

Bontempi, F., Giuliani, L., (2008d). "Robustness investigation of long suspension bridges", Proceedings of the 4th international conference on bridge maintenance, safety and management, Seoul, Korea, 13-17 July 2008.

Bontempi, F., Giuliani, L., (2008e), "Nonlinear dynamic analysis for the structural robustness assessment of a complex structural system", 2008 Structures Congress – Crossing Borders, Vancouver, Canada, 24-26 April 2008.

Borri, C. and Costa, C., (2004). "Quasi-steady analysis of a two-dimensional bridge deck element", Computer & Structures, (82), 993-1006.

Breton, S.-P. and Moe, G. (2009). "Status, plans and technologies for offshore wind turbines in Europe and North America", Renewable Energy, 34 (3), 646-654.

Bruno, L. and Khris, S. (2003). "The validity of 2D numerical simulations of vortical structures around a bridge deck", Mathematical and Computer Modeling 37, 795- 828.

Cao ,Y., Xiang, H. and Zhou, Y., (2000). "Simulation of Stochastic Wind Velocity Field on Long-Span Bridges", Journal of Engineering Mechanics 126(1): 1-6.

Caracoglia, L., Jones, N.P. (2003). "Time domain vs. frequency domain characterization of aeroelastic forces for bridge deck section", J Wind Eng. Ind. Aerodyn. 91, 371-402.

Carassale, L. and Solari, G. (2006). “Monte Carlo simulation of wind velocity field on complex structures”, J Wind Eng. Ind. Aerodyn. 94 (1) 323-339.

CEN (European Committee for Standardization) (2002): EN 1990 - Basis for Structural Design. Brussels, Belgium; 2002.

CEN (European Committee for Standardization) (2004). EN 1991-1-4: Actions on structures: Part 1-4: Wind actions. Brussels, BE.

CEN (European Committee for Standardization), (2003). prEN 1993-1-9: Design of steel structures – Part 1-9: Fatigue strength of steel structures, Brussels (BE), European Committee for Standardization

Chen, X., Matsumoto, M. and Kareem, A. (2000). “Time domain flutter and buffeting response analysis of bridges”, J. of Eng. Mechanics (January) 7- 16.

Ching, J., Porter, A.K. and Beck, J., (2004). Uncertainty propagation and feature selection for loss estimation in performance-based earthquake engineering, Report EERL 2004-02, Pasadena, California, United States. Available on line at http://peer.berkeley.edu/publications/peer_reports.html.

Cluni, F., Gusella, V. & Ubertini, F. 2007. “A parametric investigation of wind-induced cable fatigue”, Engineering Structures 29(11): 3094-3105

CNR (Consiglio Nazionale delle Ricerche) (2008). CNR-DT 207/2008: Istruzioni per la valutazione delle azioni e degli effetti del vento sulle costruzioni. Roma, IT; (in italian).

Davenport, A.G. (1995). “How we can simplify and generalize wind load?”, J Wind Eng. Ind. Aerodyn. 54/55, 657-669.

Davenport, A.G. (1998). “Probabilistic methods in wind engineering for long span bridges”, Proc. of the Int. Symp. on Advances in Bridge Aerodynamics, May 1998, Copenhagen, Denmark.

Davenport, A.G. (2002). “Past, present and future of wind engineering”, J Wind Eng. Ind. Aerodyn. 90, 1371-1380.

Deodatis G. (1996). "Simulation of ergodic multivariate stochastic processes", Journal of Engineering Mechanics, vol. 122, 778-787.

Der Kiureghian, A., (1996). “Structural reliability methods for seismic safety assessment: a review”, Engineering Structures, 18(6), 412-424.

Der Kiureghian, A., (2008). “Analysis of structural reliability under parameter uncertainties”, Probabilistic Engineering Mechanics, 23, 351-358.

Diana, G., Bruni, S., Cigada, A. and Collina, A. (1993). “Turbulence effect on flutter velocity in long span suspended bridges”, J Wind Eng. Ind. Aerodyn. 48, 329-342.

Diana, G., Falco, M., Bruni, S.,Cigada, A., Larose, G.L., Damsgaard, A. and Collina, A. (1995). “Comparison between wind tunnel tests on a full aeroelastic model of the proposed bridge over Stretto di Messina and numerical results”, J Wind Eng. Ind. Aerodyn. 54/55, 101-113.

Di Paola M. (1998). "Digital simulation of wind field velocity", Journal of Wind Engineering and Industrial Aerodynamics, vol. 74-76, 91-109.

Di Paola M., Gullo I. (2001). "Digital generation of multivariate wind field processes", Probabilistic Engineering Mechanics, vol. 16, 1-10.

DNV, Det Norske Veritas (2004): DNV-OS-J101 Offshore Standard. Design of Offshore Wind Turbine Structures, June 2004.

Ellingwood, B.R. Rosowsky, D.V., Li, Y. and Kim, J. H. (2004), “Fragility Assessment of Light-Frame Wood Construction Subjected to Wind and Earthquake Hazards”, Journal of Structural Engineering, 130(12), 1921-1930.

Ellingwood, B.R. (2001). “Acceptable risk bases for design of structures” Prog. Struct. Eng. Mater., 3, 170-179.

Ellingwood, B.R. (2001). “Earthquake risk assessment of buildings structures”, Reliability Engineering and System Safety, 74, 251-262.

Ellingwood B.R. and Tekie P. B. (1999). “Wind load statistics for probability-based structural design”, J. Structural Engineering, Vol. 125, No. 4, pp. 453-463.

ESDU (Engineering Sciences Data Unit) (2001), Report N. 86010: “Characteristic of atmospheric turbulence near the ground. Part III: variations in space and time for strong winds (neutral atmosphere)”, http:// www.esdu.com.

Foliente, G.C. (2000), “Developments in performance-based building codes and standards”, Forest Products Journal, 50 (7/8), 91-109.

Franchin, P., Ditlevsen, O. and Der Kiureghian, A. (2002a), "Model correction factor method for reliability problems involving integrals of non-Gaussian random fields", Probabilistic Engineering Mechanics, Elsevier, Vol 17(2): 109-122.

Franchin, P., Lupoi, A. and Pinto P.E., (2002b), "Methods of seismic risk analysis: State-of-the-Art versus advanced State-of-the-Practice", Journal of Earthquake Engineering, Imperial College Press, Vol.(6) Special Issue 1: 131-155.

Franchin, P. (2004) "Reliability of uncertain inelastic structures under earthquake excitation" ASCE Journal of Engineering Mechanics Vol 130(2): 180-191.

Franchin, P., Pinto, P.E. and Schotanus, M.I.J., (2006) "Seismic loss estimation by efficient simulation", Journal of Earthquake Engineering, Imperial College Press, Vol.10(Special Issue 1): 31-44.

Franchin, P. and Pinto, P.E. (2007),"Transitability of mainshock-damaged bridges", Proceedings of the 1st US-Italy Seismic Bridge Workshop, April 19-20, 2007, Pavia, Italy.

Garciano, L.E., Maruyama, O. and Koike, T. (2005) “Performance-based design of wind turbines for typhoons”, Proc. Ninth International Conference on Structural Safety and Reliability ICOSSAR05, (G. Augusti, G.I. Schueller, M. Ciampoli eds.), Millpress, Rotterdam.

Giuliano F. (2007). Performance based design by structural control for suspension bridges. PhD Dissertation, University of Pavia.

International Code Council, (2000). International Building Code 2000, International Conference of Building Officials, Whittier, CA.

Lazzari, M., Vitalini, R. V. and Saetta, A. V. (2004). “Aeroelastic forces and dynamic response of long-span bridges”, Int. J. Numer. Meth. Engng 60, 1011- 1048.

Lazzari, M. (2005). “Time domain modelling of aeroelastic bridge decks: a comparative study and an application”, Int. J. Numer. Meth. Engng., 62, 1064- 1104.

Lungu, D., Rackwitz, R., (2001), “Joint Committee on Structural Safety – Probabilistic Model Code, Part 2: Loads”, http://www.jcss.ethz.ch/.

Jain, A., Jones, N.P. and Scanlan, R.H. (1996). “Coupled flutter and buffeting analysis of long-span bridges”, J. of Structural Engineering , ASCE, 122(7): 716-725.

Jalayer, F., Franchin, P. and Pinto, P.E. (2007). “A scalar damage measure for seismic reliability analysis of RC frames”, Earthquake Engng. and Struct. Dyn., 36: 2059-2079.

Kareem, A., (1987). “Wind effects on structures: a probabilistic viewpoint”, Probabilistic Engineering Mechanics, 4(2), 166-200.

Khanduri, A.C. and Morrow, G.C. (2003), “Vulnerability of buildings to windstorms and insurance loss estimation”, Journal of Wind Engineering and Industrial Aerodynamics, (91), 455-467.

Kunnath, S.K., (2007). Application of the PEER PBEE Methodology to the I-880 Viaduct, PEER Report 2006/10 (I-880 testbed committee). Available on line at http://peer.berkeley.edu/publications/peer_reports.html.

Mann, J., Kristensen, L. and Jensen, N.O., (1998). “Uncertainties of extreme winds, spectra and coherence”, Proc. of the Int. Symp. on Advances in Bridge Aerodynamics, May 1998, Copenhagen, Denmark.

Minciarelli, F., Gioffrè, M., Mircea, G. and Simiu, E., (2001). “Estimates of extreme wind effects and wind load factors: influence of knowledge uncertainties”, Probabilistic Engineering Mechanics, 16, 331-340.

Mitrani-Reiser, J. (2007). An ounce of prevention: probabilistic loss estimation for performance - based earthquake engineering, Report EERL 2007-01, Pasadena, California, United States. Available on line at http://peer.berkeley.edu/publications/peer_reports.html.

Nielsen, M., Larsen, G. C., Mann, J., Ott, S., Hansen, K. S. and Pedersen, B. J., (2004). Wind Simulation for Extreme and Fatigue Loads, Risø Report 1437(EN), Risø National Laboratory, Roskilde, Denmark.

Norton, T.R. (2007), "Performance-Based vulnerability analysis of wind-excited tall buildings", Ph.D. Thesis, Florida Agricultural and Mechanical University FAMU-FSU, College of Engineering.

Pagnini, L. (2005), "The reliability of structures with uncertain parameters excited by the wind", Proceedings of the ninth International Conference on Structural Safety And Reliability, ICOSSAR '05, Rome, Italy.

Paulotto, C., Ciampoli, M. and Augusti, G., (2006). "Wind-Tunnel Evaluation of Wind Pressure on a Frame-Type Signboard", J. Wind Eng. & Ind. Aerodyn., vol. 94 No.5 pp. 397-413 ISSN:0167-6105

Paulotto, C., Augusti, G. and Ciampoli, M. (2004). "Some proposals for a first step towards a Performance Based Wind Engineering", Proc. IFED-International Forum in Engineering Decision Making, Stoos, CH. www.ifed.ethz.ch

Pastò, S and de Grenet, E.T. (2005), "Risk-Assessment and Control Of Flow-Induced Vibrations Of Structures", Proc. Ninth International Conference on Structural Safety and Reliability ICOSSAR05, (G. Augusti, G.I. Schueller, M. Ciampoli eds.), Millpress, Rotterdam.

Pecora, M., Lecce, L., Marulo, F. and Corio, D.P. (1993). "Aeroelastic behaviour of long span bridges with "multibox" type deck sections", J Wind Eng. Ind. Aerodyn. 18, 343-358.

Petrini, F., Giuliano, F. and Bontempi, F., (2005). "Modeling and simulations of aerodynamic in a long span suspension bridge", Proceedings of the ninth International Conference on Structural Safety And Reliability, ICOSSAR '05, Rome, Italy.

Petrini, F., Giuliano, F. and Bontempi, F., (2007). "Comparison of time domain techniques for the evaluation of the response and the stability in long span suspension bridges", Computer & Structures, (85), 1032-1048.

Petrini, F. and Bontempi, F. (2008), 'Estimation of life-cycle fatigue for long–span suspension bridge hangers', Proc. IALCCE'08, Varenna, Italy.

Petrini, F., Bontempi, F. and Ciampoli, M. (2008), "Performance-based wind engineering as a tool for the design of the hangers in a suspension bridge", Proc. Fouth International ASRANet colloquium, Athens, Greece.

Pinelli, J.-P., Subramanian, C., Murphree, J., Gurley, K., Cope, A., Simiu, E., Gulati, S. and Hamid, S. (2005). "Hurricane loss prediction: model development, results, and validation". Proc. ICOSSAR'05, June 2005, Rome, Italy.

Porter KA (2003). "An Overview of PEER's Performance-Based Engineering Methodology", Proc of the Ninth International Conference on Applications of Statistics and Probability in Civil Engineering (ICASP9). San Francisco, CA, USA; Millpress Rotterdam.

Porter, K.A., (2006). EDP List, Pacific Earthquake Engineering Research Center, Richmond, CA: www.peertestbeds.net/Crosscutting.htm.

Pourzeynali, S., and Datta, T.K., (2002). "Reliability analysis of suspension bridges against flutter", Journal of Sound and Vibration, 254(1),143-162.

Rajeev, P., Franchin, P. and Pinto, P.E. (2008), "Increased Accuracy of Vector-IM-Based Seismic Risk Assessment?", Journal of Earthquake Engineering, 12:1-14.

Repetto, M.P. and Solari, G., (2002). "Dynamic crosswind fatigue of slender vertical structures", Wind and Structures, Vol. 5, No.6, 527-542.

Rose, A. and Lim, D., (2002). "Business interruption losses from natural hazards: conceptual and methodological issues in the case of the Northridge earthquake", Enviromental Hazards, Vol. 4, pp. 1-14.

Rosowski, D.V. and Ellingwood, B.R., (2002). "Performance-Based Engineering of wood frame housing: Fragility Analysis methodology", Journal of Structural Engineering, 128(1), 32-38.

Rossi, R., Lazzari, M. and Vitaliani R. (2003). "Wind field simulation for structural engineering purposes", International Journal of Numerical Methods in Engineering, vol. 61, 738-763.

Salvatori L., Spinelli P. (2006). "Effects of structural nonlinearity and a long span coherence on suspension bridge aerodynamics: some numerical simulation results", Journal of Wind Engineering and Industrial Aerodynamics, vol. 94, 415-430.

Salvatori, L. and Borri, C. (2007), "Frequency and time-domain methods for the numerical modeling of full-bridge aerolasticity". Computer & Structures (85), 675-687.

Samaras E., Shinozuka M., Tsurui A. (1985). "ARMA representation of random processes", Journal of Engineering Mechanics, vol. 111, 449–461.

Scanlan, R.H. and Tomko, J.J., (1971). "Airfoil and bridge deck flutter derivates", J. of Eng. Mechanics Div. ASCE, Vol. 97, 1717-1737.

Schettini, E. and Solari, G., (1998). "Probability distribution and statistical moments of the maximum wind velocity", Wind and Structures, vol. 1, No. 4, 287-302.

Schüeller, G.I. (2006). "Developments in stochastic structural mechanics", Archive of Applied Mechanics vol. 75 No. 10-12/October 2006.

Schuëller G.I. (ed.) (1997). "A state-of-the-art report on computational stochastic mechanics", Probabilistic Engineering Mechanics, vol. 12, n. 4, 197-321.

SEAOC (1995). Vision 2000 - A Framework for Performance Based Design. Vol. I-III, Structural Engineers Association of California, Sacramento, CA.

Sedaghat, A., Cooper, J., Leung, A.Y.T. and Wright, J.R. (2001). "Estimation of the Hopf bifurcation point for aeroelastic systems", Journal of Sound and Vibration, 248 (1), 31-42.

Sepe, V., Augusti, G. (2001). "A "deformable section" model for the dynamics of large suspension bridges; Part I", Wind and Structures, vol. 4, No.1 pp. 1-18 ISSN: 1226-6116.

Sepe, V., Diaferio, M., Augusti, G. (2003). "A "deformable section" model for the dynamics of suspension bridges. PartII: Nonlinear analysis and large-amplitude oscillations", Wind and Structures, vol. 6 (No.6) pp. 451-470 ISSN:1226-6116.

Shinozuka M., Deodatis G. (1997). "Simulation of stochastic processes and fields", Probabilistic Engineering Mechanics, vol. 12, no. 4, 203–207.

Sibilio, E. and Ciampoli, M. (2007), "Performance-Based wind design for footbridges: evaluation of pedestrian comfort", Proc. Tenth International Conference on Applications of Statistics and Probability in Civil Engineering ICASP10, Tokyo, Japan; abstract 561-562; paper in CDRom.

Solari, G. Piccardo, G. (2001). "Probabilistic 3-D turbulence modeling for gust buffeting of structures", Probabilistic Engineering Mechanics, (16), 73–86.

Solari, G. and Augusti, G. (1998). "Wind engineering: a short introduction", Meccanica, 33: 215-217.

Solari, G. (1997). "Wind-excited response of structures with uncertain parameters", Probabilistic Engineering Mechanics,12 (2), 75–87.

Szigeti, F. and Davis, G. (2005). Performance Based Building: Conceptual Framework. EUR21990 Final Report, available online at http://www.pebbu.nl.

Theodorsen, T., (1931 a). On the theory of wing section with particular reference to the lift distribution", NACA Report No. 383.

Theodorsen, T., (1931 b). Theory of wing section of arbitrary shape, NACA Report No. 411.

Theodorsen, T., (1935). General theory of aerodynamic instability and the mechanism of flutter, NACA Report No. 496.

Khanduri, A.C. and Morrow, G.C. (2003). "Vulnerability of buildings to windstorms and insurance loss estimation", Journal of Wind Engineering and Industrial Aerodynamics Vol. 91, pp. 455-467.

Koss, H.H. (2004), “On differences and similarities of applied wind comfort criteria”, Proc. the Int. Conf. Urban Wind Engineering and Building Aerodynamics, von Karman Inst., Rhode-Saint-Genese, BE

Unanwa, C.O., McDonald, J.R., Mehtab, K.C. and Smith, D.A. (2000), “The development of wind damage bands for buildings” Journal of Wind Engineering and Industrial Aerodynamics, Vol. 84, pp. 119-149.

Moehle J. and Deierlen, G.G. (2004). “A framework methodology for Performance-Based Earthquake Engineering", Proc. Of International Workshop on Performance-Based Design, 28 Giugno - 2 Luglio, Bled, Slovenia.

Moehle, J., (2003). “A Framework for Performance-Based Earthquake Engineering”, Proc. Tenth U.S.-Japan Workshop on Improvement of Building Seismic Design and Construction Practices, Report ATC-15-9, Applied Technology Council, Redwood City,

Ubertini F., Giuliano F. (submitted). "A comparative study on efficiency and accuracy of Gaussian wind simulation methods", Journal of Wind Engineering and Industrial Aerodynamics, submitted for publication.

Ubertini, F. and Bontempi, F. 2008. Wind-induced fatigue assessment in main cables and hangers of suspension bridges. Proceedings of the fourth International Conference on Bridge Maintenance, Safety and Management (IABMAS’08)

Unanwa, C.O., McDonald, J.R., Mehta, K.C. and Smith, D.A. (2000), “The development of wind damage bands for buildings”, Journal of Wind Engineering and Industrial Aerodynamics, (84), 119-149.

van de Lindt, J. W. and Dao, T. N. (2009), “Performance-Based Wind Engineering for Wood-Frame Buildings”, Journal of Structural Engineering, 135(2), 169-177.

Zaaijer, M.B. (Editor) (2005), Design Methods for Offshore Wind Turbines at Exposed Sites (OWTES), Report No.SW-02181 Delft University of Technology, Section Wind Energy.

Zaaijer, M. B. (2006). “Foundation modeling to assess dynamic behavior of offshore wind turbines”, Applied Ocean Research, (28), 45–57.

Zasso, A. (1996). “Flutter derivates: Advantantages of a new representation convetion”, Journal of Wind Engineering and Industrial Aerodynamics, 60, 35-47.

Zhang, X. and Zhang, R.R. (2001). “Actual ground-exposure determination and its influences in structural analysis and design”, Journal of Wind Engineering and Industrial Aerodynamics, Vol. 89, pp. 973-985.

Zhang, L., Jie, L. and Peng, Y, (2008), “Dynamic response and reliability analysis of tall buildings subject to wind loading”, Journal of Wind Engineering and Industrial Aerodynamics, (96), 25-40.